Hydrochemical and isotopic characterization of groundwater reservoirs of Hasouna Waterfields in the Sahara Desert, Libya

DOCTORAL THESIS

For obtaining the academic degree of

Doktor der Naturwissenschaften

Rashid A. Abdalla

Graz University of Technology

Institute of Applied Geosciences

Graz University of Technology, Austria

Supervisor: Univ.-Prof. Dipl.-Min. Dr. rer. nat. Martin Dietzel

Co-Supervisors: Dr. Albrecht Leis

PhD. Dr. Stephan J. Köhler

Graz, December 2012

DEDICATION

To my wife Ruth

My parents

Brothers and sisters

My nephew Tarek

And my children, Karim, Akram, Said

and Hanin for their love!

ACKNOWLEDGMENTS

First, I would like to express my deep thanks and gratitude to my supervisor Prof. Dr. Martin Dietzel (Institute of Applied Geosciences, Graz University of Technology) for providing me the opportunity to work on and finish my PhD Thesis. I appreciate all his contributions of time for advice, support, ideas, helpful discussions, and reviewing.

Special thanks is given to the Joanneum Research Center in Graz/Austria, who gave me the opportunity to conduct this project and provided the funding for isotopes analysis. I wish to thank Dr. Albrecht Leis (Water Resources Management, Joanneum Research Center in Graz/Austria) for his help with isotopes analysis. My thanks go to Dr. Stephan Köhler for his assistance during hydrochemical laboratory analysis.

I am grateful to Dr. Ralf Benischke (Water Resources Management, Joanneum Research Center, Graz/Austria), for his assistance, and for reviewing the hydrogeology part of my thesis. I am grateful to all team members of the Institute of Applied Geosciences for their help and kind support in the laboratory analysis—in particular Prof. Dr. Dietmar Klammer, Judith Jernej, Dipl. Min. Daniel Höllen, Mag. Florian Mittermayr, Gerhard Lauk, Dr. Heike Wonisch, Dr. Andrea Niedermayr, Mag. Walter Schön and Dr. Christine Latal. My thanks also go to Peter Schreiber for his help and support providing computer issues. I wish to thank Anna Maria Pendl and Daniela Sobian for their help with various administrative and inscription issues. I am thankful to Mag. Gerald Pischinger for his support and useful discussions. I also want to thank Prof. Dr. Franz-Josef Brosch for his support and review of the geology part of my thesis. I wish to thank Dr. Thomas Rinder for support and useful discussions. I would like to thank Prof. Dr. Othmar Nestroy for his helpful comments and continuous support.

Many deepest thanks go to Joel Savarino and Samuel Morin for their support and completion of the nitrogen isotopic analysis (Laboratoire de Glaciologie et de Géophysique de l'Environnement, Université Joseph Fourier, Grenoble, France, Météo-France - CNRS, CNRM-GAME URA 1357, CEN, Grenoble, France). I would like to give thanks to Prof. Dr. Michael Böttcher (IOW, Warnemünde) for providing support for sulphur isotope analysis and to Dr. Tamer from the geology department in Graz at Karl Franzens University for motivation support and his useful scientific discussions. I greatly appreciate the scholarship financial support of Graz University of Technology (Forschungs & Technology).

Thanks to Mr. Tarek Abouaisha Ashour, Mohamed Guma El Kweldi, and Asaad Miloud Smida for their support and providing the permission for water sampling from GMRP authorities. My deepest thanks go to the General Water Authority (GWA, Tripoli), in particular to Dr. Omar Salem, for his assistance and administrative arrangements. In addition, I extend my deepest thanks to the Authority of Great Man-made Project in Tripoli and in Hasouna waterfields for their administrative cooperation and logistical support.

I express my deepest appreciation to my mother, father, brothers and sisters in Libya. This PhD research work would not have been possible without their prayers, encouragement and moral support. My special thanks go to DI (FH) Martha Bißmann for her continuous support and help during my study time. Finally big and grateful thanks to my wife Ruth and my children, Karim, Akram, Said, and Hanin for their, love, support, and care during the time of my study.

DECLARATION

I declare and confirm that this submission thesis is my own work, that I have not used other than the declared sources / resources, and that I have explicitly marked all material which has been cited either literally or by content from the used sources, except where due reference has been made.

…… ……..
(date) (signature)

ABSTRACT

Groundwater is the main source of water supply for the population of Libya, as Libya is located in an arid area with strongly limited water resources. The study area of Hasouna Water Fields is situated about 700 kilometres south of Tripoli with no groundwater recharge. The aquifer of the study area is divided in two main parts: the lower Cambro-Ordovician Sandstone Aquifer (Paleozoic), which is the most important aquifer in the Hasouna water fields, and the upper Zimam Aquifer (Upper Cretaceous), which is characterized by highly saline water. This study is focused on the origin of nitrate in this water. Therefore, groundwater compositions were analyzed within a multiproxy approach yielding hydrochemical and isotopic data sets.

High NO_3 concentrations are common features of paleo groundwater not only in North Africa but also in other arid and semi-arid areas (Edmunds, 2006). In general accumulation of nitrate in groundwater is mostly related to anthropogenic activities. However in the paleo groundwater of the Hasouna basin in the Sahara desert the origin of nitrate is far from any anthropogenic pollution and nitrate accumulation mechanisms are still under discussion.

Some of Hasouna groundwater samples are not suitable for human consumption without treatment (dilution and mixing). In particular, high concentrations of nitrate (NO_3> 50 mgL^{-1}) in the Hasouna groundwater are crucial for human health. Nitrate concentrations in this current study reach values of up to 114 mgL^{-1} and total dissolved solids of 1778 mgL^{-1}. However, groundwater quality of the transported water to Tripoli city is good with total dissolved solids value (TDS) of 1013 mgL^{-1}, chloride (256 mgL^{-1}), sulphate (157 mgL^{-1}), nitrate (38 mgL^{-1}) and sodium (171 mgL^{-1}). The water of the Hasouna area is classified as S1/S2 for sodium hazard (low and medium), and class C3/C4 for salinity hazard (high and very high). This classification shows that Hasouna groundwater is suitable for irrigation use with special management consideration to salinity values. The most frequent groundwater type of the Hasouna groundwater is Na-Ca-Cl-SO_4.

The stable isotope distribution of the water indicates - in comparison to modern meteoric water close to Tripoli - low δ^2H and $\delta^{18}O$ values in all groundwater samples. These isotope values of Hasouna groundwater discover that the groundwater of the Hasouna waterfields is of paleo origin and was recharged under ancient cooler and more humid paleoclimate conditions compared to modern climate conditions of the coastal areas of Libya. From the isotopic composition of the Hasouna groundwater a local Paleo Meteoric Water Line is estimated: δ^2H_{H2O} = 8.0 $\delta^{18}O_{H2O}$ + 6.3. From the concentrations

of dissolved ions and from $\delta^{18}O$ and $\delta^{2}H$ relationship an impact of evaporation on the chemistry of the groundwater can be excluded.

The obtained elemental and isotope data let us suggest that the groundwater of Hasouna fields receives its high salinity from the so-called Zimam aquifer by mixing along vertical hydraulic leakage caused by faulting and fracturing of lime- and dolostone. The range of ion concentrations and isotope values can be followed by a mixing approach using the lowest and highest mineralized groundwater as end-members (wells #165 and #152).

Nitrogen ($\delta^{15}N$) and oxygen isotopes ($\delta^{17}O$, $\delta^{18}O$) of dissolved nitrate indicate natural origin of nitrogen. Interestingly, all investigated samples display positive $\Delta^{17}O$ (NO_3) values ($\Delta^{17}O_{NO3}$ = $\delta^{17}O_{NO3}$ - 0.52 $\delta^{18}O_{NO3}$) which are caused by non-mass dependent isotope fractionation during the reaction of atmospheric nitrogen and ozon in the Earth´s atmosphere to finally yield nitrate. This ^{17}O anomaly in NO_3 is used as excellent tracer of atmospheric deposition of nitrate in the Hasouna groundwater reservoirs. The results of $\Delta^{17}O_{NO3}$ analyses expose up to 20 mol% of NO_3 originated from the Earth`s atmosphere besides microbial NO_3. The $\Delta^{17}O_{NO3}$ signature is a conserved tracer of atmospheric nitrate deposition and is clearly a more robust indicator for nitrate origin than commonly used $\delta^{18}O$ and $\delta^{15}N$ data. Consequently, high nitrate concentrations in the Hasouna groundwater are attributed to flooding periods of heavy precipitations and rapid infiltration during wash-out of the dry depositions of atmospheric NO_3. Individual nitrate content of groundwater in the Hasouna basin depends on ancient precipitation and wash-out rates.

ZUSAMMENFASSUNG

Grundwasser ist die wichtigste Quelle der Wasserversorgung in Libyen, einem Land mit großen Trockengebieten und stark begrenzten Wasserressourcen. Das Untersuchungsgebiet, das Hasouna-Brunnenfeld, liegt etwa 700 Kilometer südlich von Tripolis. Die Wasserressourcen in Hasouna unterliegen keiner Grundwasserneubildung. Der Grundwasserleiter des Untersuchungsgebietes ist in zwei Hauptteile unterteilt: der untere Cambro-Ordivizium Sandsteinaquifer (Paläozoikum), welcher der wichtigste Aquifer der Hasouna Brunnerfelder darstellt, sowie der obere Zimam Aquifer (Oberkreide), welcher durch stark salzhaltiges Wasser gekennzeichnet ist. Die vorliegende Studie ist auf die Herkunft des gelösten Nitrats in diesen Wässern fokussiert. Die Entstehung des Grundwassers wurde mittels hydrochemischer und isotopischer Datensätze und eines Multiproxy-Ansatzes untersucht. Hohe NO_3 Konzentrationen kennzeichnen häufig Paläo-Grundwässer nicht nur in Nordafrika, sondern auch in anderen Trocken- und Halbtrockengebieten (Edmunds, 2006). In den meisten Fällen sind hohe Gehalte an Nitrat im Grundwasser auf anthropogene Ursachen zurück zu führen. Im Paläo-Grundwasser des Hasouna-Beckens in der Sahara Wüste sind die hohen Nitrat-Gehalte offensichtlich nicht anthropogen bedingt. Einige der Hasouna Grundwasserproben eignen sich ohne Vorbehandlung (Verdünnung und Durchmischung) nicht als Trinkwasser. Insbesondere sind die hohen Konzentrationen von Nitrat (NO_3 > 50 mgL^{-1}) im Hasouna-Grundwasser gesundheitsgefährdend. Die Nitratkonzentrationen in dieser aktuellen Untersuchung erreichen Werte von bis zu 114 mgL^{-1}, und die Gesamtmenge der gelösten Feststoffe liegt bei maximal 1778 mgL^{-1}. Die Grundwasserqualität des nach Tripolis geleiteten Wassers ist jedoch gut: gelöste Feststoffe (TDS) 1013 mgL^{-1}, Chlorid (256 mgL^{-1}), Sulfat (157 mgL^{-1}), Nitrat (38 mgL^{-1}) und Natrium (171 mgL^{-1}).

Das Wasser aus dem Hasouna-Brunnenfeld wird in Klasse S1/S2 für Gefährdung durch Natrium (niedrig und mittel) und C3/C4 für die Gefährdung durch Salzgehalt (hoch und sehr hoch) eingestuft. Diese Klassifizierung zeigt, dass das Hasouna Grundwasser für den Einsatz als Bewässerungswasser geeignet ist, spezielles Management in Hinblick auf den Salzgehalt vorausgesetzt. Der häufigste Grundwassertyp des Hasouna Grundwassers entspricht einem Na-Ca-Cl-SO_4 Typ.

Die Verteilung der stabilen Isotope des Wassers zeigt niedrige δ^2H und $\delta^{18}O$ Werte in allen Grundwasserproben im Vergleich zu modernen meteorischen Wasservorkommen in der Nähe von Tripolis. Diese Isotopenwerte des Hasouna Grundwassers zeigen deutlich seinen fossilen Ursprung an und

vermitteln, dass es sich vor etlichen Jahrtausenden in einem, im Vergleich zu den heutigen klimatischen Bedingungen der Küstenregionen Libyens, kälteren und feuchteren Paläoklima gebildet hat.

Aufgrund der Isotopenzusammensetzung des Hasouna-Grundwassers wird eine lokale paläometeorische Wasserlinie ermittelt: $\delta^2H_{H2O} = 8.0\ \delta^{18}O_{H2O} + 6.3$. Die Konzentration der gelösten Ionen und die $\delta^{18}O$ - δ^2H Korrelation lässt einen Einfluss von Evaporationsprozessen (Verdunstungs-Effekt) auf die Chemie des Grundwassers praktisch ausschließen. Die erhobenen Elementgehalte und Isotopendaten lassen vermuten, dass das Grundwasser aus dem Hasouna-Feld seinen Salzgehalt vom sogenannten Zimam-Aquifer bezieht. Die Durchmischung erfolgt entlang hydraulischer Leckagen, verursacht durch Bruchzonen in den lokalen Kalk- und Dolomitengesteinen. Der Wertebereich der Ionenkonzentrationen und Isotopenwerte kann durch einen Mischungs-Ansatz bestimmt werden, wobei die am höchsten und am niedrigsten mineralisierten Grundwässer als Endglieder angesetzt werden (Brunnen #165 und #152).

Die Verteilung der Stickstoff- ($\delta^{15}N$) und Sauerstoff-Isotope ($\delta^{17}O$, $\delta^{18}O$) der gelösten Nitrate indizieren einen natürlichen Ursprung des Stickstoffs. Interessanterweise zeigen alle untersuchten Proben positive $\Delta^{17}O$ (NO_3) Werte ($\Delta^{17}O_{NO3} = \delta^{17}O_{NO3} - 0.52\ \delta^{18}O_{NO3}$), die durch massenunabhängige Isotopenfraktionierung während der Reaktion von Luftstickstoff und Ozon in der Erdatmosphäre verursacht werden um, schließlich Nitrat zu ergeben. Diese ^{17}O Anomalien in NO_3 werden als exzellenter Isotopenindikator atmosphärischer Nitrat-Ablagerungen im Hasouna Grundwasserreservoir genutzt. Die Ergebnisse der $\Delta^{17}O_{NO3}$ Analysen legen offen, dass bis zu 20 mol% des NO_3 aus der Erdatmosphäre entstammen, neben mikrobiellem NO_3. Die $\Delta^{17}O_{NO3}$ Signatur ist ein konservierter Isotopentracer für atmosphärisches Nitrat und liefert somit einen eindeutigen und robusteren Indikator für die Nitrat-Herkunft als die üblicherweise verwendeten $\delta^{18}O$ und $\delta^{15}N$ Daten. Die Isotopendaten vermitteln, dass die hohen Nitratkonzentrationen im Hasouna Grundwasser zyklischen Überschwemmungsperioden mit Starkniederschlägen und schneller Infiltration und rascher Auswaschung der trockenen Ablagerung von atmosphärischem NO_3 zugeschrieben werden können. Der individuelle Nitratgehalt des Hasouna Grundwassers ist somit durch zyklische Paleo-Niederschlagereignisse und entsprechende Auswaschraten bedingt.

Arabic Abstract

الملخص

تعتبر المياة الجوفية هي المصدر الرئيسي للمياة الذي يمد ليبيا. وذلك نظرا لوقوع ليبيا في منطقة جافة قليلة المصادر المائية. تقع منطقة الدراسة (الحساونة) علي مسافة حوالي 700 كليومتر جنوب مدينة طرابلس. وتتميز منطقة الدراسة بعدم وجود تغذية جوفيه لها. يمكن تقسيم الخزان الجوفي للمنطقة الي خزان حجر رملي سفلي ينتمي الي حقب الحياة القديمة (كمبري-أوردوفيشي) ويعتبر هذا الخزان الجوفي هو الاهم في منطقة الدراسة. أما الخزان العلوي والمسمي بخزان زمزام الجوفي ينتمي لحقب الطباشيري العلوي والذي يتميز بنسبة ملوحة عالية. وتتركز هذة الدراسة حول دراسة مصدر النترات (NO_3). ولذلك تم تحليل العينات بطرق متعددة والتي اثرت الاطروحة بالعديد من النتائج الهيدروكيميائية وبالنظائر الغير مشعة.

يعتبر التركيزات العالية ل النترات (NO_3) لهو خاصية مميزة للمياة الجوفية القديمة (paleo groundwater) ليس فقط في شمال افريقيا ولكن ايضا في المناطق الجافة وشبة الجافة (Edmunds, 2006). بصفة عامة تكون تركيزات النترات مصاحبة للنشاط البشري وما يصاحبة من تلوث. و مع ذلك فان المياة الجوفية القديمة بمنطقة مياة حقول الحساونة لهي بعيدة كل البعد عن التلوثات المصاحبة للنشاط البشري ولهذا ميكانيكية التركيز العالي للنترات هو محل نقاش في الاوساط العلمية.

بعض آبار المياة الجوفية بمنطقة الحساونة غير صالحة للأستهلاك البشري (بغرض الشرب) دون معالجة بطرق التخفيف والتخليط للمياة لخفض نسبة التركيز العالي للنترات. وتعتبر التركيزات العالية للنترات (اكبر من 50 مليجرام لكل لتر) في منطقة الحساونة خطيرة علي صحة الانسان. وفي هذة الاطروحة تم رصد نسبة نترات تصل الي 114 مليجرام لكل لتر و واجمالي الأملاح المذابة (TDS) 1778 مليجرام لكل لتر. ومع ذلك فأن جودة المياة المنقولة عبر الأنابيب من منطقة حقل مياة الحساونة الي مدينة طرابلس جيدة حيث تحتوي علي نسبة املاح ذائبة بنسبة 1013 مليجرام لكل لتر وكلوريد بنسبة 256 مليجرام لكل لترو كبريتات بنسبة 157 مليجرام لكل لتر و نترات بنسبة 38 مليجرام لكل لتر وصوديوم بنسبة 171 مليجرام لكل لتر. و بهذا تم تصنيف المياة الجوفية بمنطقة الحساونة علي أنها من النوع S1 / S2 بنسبة لخطورة الصوديوم (عالية ومتوسطة التصنيف) , كذا أمكن تصنيف المنطقة من حيث خطورة الملوحة علي أنها من النوع C3 / C4(عالية وعالية جدا). هذة التصنيفات تضع المياة الجوفية لمنطقة الحساونة في تصنيف ملائم لعمليات الري ولكن بأستخدام نظام مراقبة نسبة الملوحة. تعتبر نوعية (Na-Ca-Cl-SO_4) هي الاكثر شيوعا في منطقة مياة الحساونة.

تعتبر كمية التركيب النظائري في منطقة الدراسة (δ^2H and $\delta^{18}O$) قليلة بالنسبة للمياة السطحية لمنطقة طرابلس. و لقد أشارت المحتوي النظائري لعينات منطقة الحساونة الي ان تلك المياة الجوفية يعود اصلها وعمرها الي مياة قديمة ومتجمعة في العصور الجليدية ومن البحيرات العظمي التي كانت تغطي أجزاء كبيرة من ليبيا. وقد أثبتت الدراسة بأن هذة المياة قد تكونت في ظروف باردة ورطوبة عالية بالمقارنة بالظروف البيئية الحالية لمنطقة ساحل ليبيا. اعتمادا علي المحتوي النظائري للمنطقة قد تم حساب خط المياة القديمة علي اساس العلاقة الحسابية التالية (δ^2H_{H2O} = 8.0 $\delta^{18}O_{H2O}$ + 6.3). في هذة الدراسة تم تحليل العلاقة بين تركيز الكيميائي للعينات والتركيب النظائري (δ^2H and $\delta^{18}O$) وقد أثبتت هذة المقارنة علي ان كيميائية مياة منطقة الحساونة لم تتأثر بعملية التبخر.

وتدل النتائج الكيميائية والنظائرية (δ^2H and $\delta^{18}O$) علي ان المياة الجوفية بمنطقة الحساونة تستمد ملوحتها العالية من خزان زمزام (Zimam)عن طريق الخلط الهيدروليكي العمودي في الفتحات والكسور لطبقة الحجر الجيري والدولوميتي. ولدراسة التركيز العالي للعينات تم اختيار البئرين رقم

(#152) و (#165)لأستخدامهم بطريقة الخلط للعينات قليلة التركيز والتي تمثل البئر (#165) وعالية التركيز والممثلة بالبئر (#152).

يمكن الستدلال من نتائج التركيب النظائري لمركب النترات الذائبة (النيتروجين ($\delta^{15}N$) والاكسجين ($\delta^{17}O$, $\delta^{18}O$)) علي أن النيتروجين طبيعي المصدر. والجدير بالذكر علي ان كل عينات التي تم دراستها تشير الي قيم موجبة لقيمة التركيب النظائري للاكسجين ($\Delta^{17}O_{NO3} = \delta^{17}O_{NO3} - 0.52$ $\delta^{18}O_{NO3}$) والتي تنتج من تجزئة النظائر الغير معتمدة علي الكتلة (non-mass dependent isotope fractionation) أثناء التفاعل بين نيتروجين وأوزون الغلاف الجوي. ويمكن استخدام التركيب النظائري لعنصر الاكسجين في النترات المذابة كدليل علي الاصل الجوي للتكوين. من نتائج التركيب النظائري ل($\Delta^{17}O_{NO3}$) تم حساب نسبة 20% من نسبة النترات المذابة علي اساس رجوع اصلها الي مياة من الغلاف الجوي بجانب بكتريا النترات. ولقد أوضحت الدراسة علي أن استخدام التحليل النظائري ل ($\Delta^{17}O_{NO3}$) للأستدلال علي اصل نشأة النترات من ترسبات الغلاف الجوي لهو اكثر دقة من استخدام التركيب النظائري ل ($\delta^{18}O$ and $\delta^{15}N$). وبناءا علية فأن أصل التركيز العالي للنترات في المياة الجوفية لمنطقة الحساونة يعود الي الامطار الهائلة وما صاحبها من فيضانات في الازمنه الجليدية حيث صحبها عملية فلترة وترشيح سريع مصاحب بعملية غسيل للترسبات الجافة لنترات الغلاف الجوي. تدل نسبة تركيز النترات في حوض الحساونة علي اعتمادها علي الأمطار القديمة وعلي معدلات الترشيح.

TABLE OF CONTENTS

LIST OF FIGURES

LIST OF TABLES

LIST OF SYMBOLS AND ABBREVIATIONS

Symbol/Abb.	Description
GMRP	Great Man-made river project
GMRPA	Great Man-made river project Authority
MCM	Million cubic meter
NEJHN	North East Jabal Hasouna North
NEJHS	North East Jabal Hasouna South
EJHE	East Jabal Hasouna East
EJHW	East Jabal Hasouna West
GWA	General Water Authority
WHO	World Health Guideline (standard)
WJS	Western Jamahiriya System
BP	before present
LGM	Last Glacial Maximum
CO	Cambro Ordovician
NW	North West
NE	North East
SW	South West
SE	South East
S.L	Sea Level
I.R.C	Industrial Research Centere
UC	Upper Cretaceous Aquifer
COD	Cambro Ordovician Devonian
CO-TE	Cambro Ordovician-Tertiary Aquifer
PCCP	Pre-stressed concrete pipe
δ	Delta
‰	Per mil
O	Oxygen
D	Deuterium
R	Stable isotope ratio
$R_{reference}$	Stable isotope ratio in reference (‰)
R_{sample}	Stable isotope ratio in sample (‰)
^{14}C	Radiocarbon isotope with mass no 14
^{15}N	Stable nitrogen isotope with mass no 15
^{14}N	Stable nitrogen isotope with mass no 14
^{2}H	Stable hydrogen isotope with mass no 2
^{18}O	Stable oxygen isotope with mass no 18
^{17}O	Stable oxygen isotope with mass no 17
^{16}O	Stable oxygen isotope with mass no 16
$\Delta^{17}O$	capital delta seventeen O
^{34}S	Stable sulfur isotope with mass no 34
^{32}S	Stable sulfur isotope with mass no 32
VSMOW	Vienna Standard Mean Ocean Water
VCDT	Vienna Canyon Diablo Triolite
GMWL	Global Meteoric Water Line
LMWL	Local Meteoric Water Line
E	Error
Mg	Milligram

mM	milli Mole
meq	Milli equivalent
atm	atmosphere
SI	Saturation Index
pCO_2	Partial pressure of CO_2
K_{sp}	Solubility product
IAP	Ion activity product
TDS	Total Dissolved Solids
°C	Temperature
D.O	Dissolved oxygen
NO_3^-	Nitrate
NO_2^-	Nitrite
SO_4^{2-}	Sulphate
Cl^-	Chloride
Ca^{2+}	Calcium
Mg^{2+}	Magnesium
Na^+	Sodium
Sr^{2+}	Strontium
Li^+	Lithium
Zn^{2+}	Zinc
Mn^{2+}	Manganese
F^-	Flouride
EC	Electrical conductivity
K	Potassium
pH	power of the concentration of the Hydrogen ion
T	Temperature
MH	Magnesium Hazard (%)
Na(%)	Sodium Percentage
SAR	Sodium Hazard
TH	Total Hardness
SSP	Soluble Sodium Percentage
Max.	Maximum
Min.	Minimum
SD	Standard Deviation
N (N)	Number of Samples
n.a.	Not analysed
PZ	Piezometer
Fig.	Figure
IAEA	International Atomic Energy Agency
et al.	And others
i.e.	that is
MCL	maximum contamination level
%	percent
wt. %	weight
CO_2	carbon dioxide
MIF	mass independent fractionation
bld	below limit of detection
Has 00	Hasouna (00), mixing all water wells

1 INTRODUCTION

1.1 CHALLENGES

The Libyan Arab Country with a total area of 1,759,540 km^2 as a part of Northern Africa is bordered by the Mediterranean Sea in the north. Libya has about six million citizens, the majority of which lives along the narrow Mediterranean coastal strip. This is mostly covered by Sahara Desert with a large amount of paleo groundwater stored at greater depths in the southern 7hydrogeological basins. As many other countries in arid regions, Libyan fresh water supply heavily depends on groundwater resources. Limited quantities of renewable fresh water resources are available only in the Northwest and Northeast coastal regions. These coastal aquifers have become seriously overstrained as most people live along the Mediterranean Coast and population density is high and remains growing. Groundwater exploitation in the Libyan region has increased dramatically during the last decade, mainly due to an increase of irrigated agriculture activities, tourism and industry.

In the past, the exploration and search for new oilfields in the deserts of southern Libya resulted in the discovery not only of the significant oil reserves, but also huge amounts of fresh water with good quality trapped in the subsurface sedimentary sandstone formations. After the discovery of fresh groundwater in the deserts of Southern Libya, the local authority has made great efforts to address their water shortage problems (Edmunds et al., 2006).

The world's largest and most expensive water conveyance project has been planned, designed, and implemented to bring water to from the desert to the inhabited coastal areas. This so-called Great Man-made River Project (GMRP) was initiated in 1983 to provide groundwater from desert well-fields at a daily volume of about 6.5 million cubic meters (MCM) of water. Figure 1.1 gives an overview of the GMRP project including the Jabal Hasouna well-field which is subject to the present study. The GMRP project was designed in five phases, where each one is largely separated from the others but all are combined to an integrated system (Fig. 3.1). The Jabal Hasouna well-field is a part of phase II to deliver daily 2.5 MCM from Fezzan region to the Jeffara plain and the capital Tripoli.

The well-field configuration has been optimized to minimize the impact of water level decline in the Hasouna water fields and in surrounding agricultural development projects. The well-field discharge was planned at a rate of 2.0 MCM (million cubic meters) water per day and subsequently increased to 2.5 MCM per day (Table 1.1). Individual well discharges were predetermined as 45

l/s and 56 l/s. The well spacing of 1.5 km was performed to optimise water extraction.

The Hasouna well-field is divided into four groups with 484 individual wells (Fig.1.1). The two Northern well-fields are termed North East Jabal Hasouna North (NEJHN) and North East Jabal Hasouna South (NEJHS). The two Southern well-fields are grouped into the East Jabal Hasouna East (EJHE) and the East Jabal Hasouna west (EJHW).

The overall water supply situation in Libya consists of pumped fresh water from deep paleo aquifers in central Sahara region and from shallow groundwater aquifers along the coastline in the North. Renewable aquifers exist along the Northern strip of the coastal line, whereas the deep paleo aquifers in central Sahara of Libya are not renewable. Libya has a serious water supply shortage due to an imbalance between limited water resources and its demands. The country's population has tripled since the 1950s. Water deficits of about 4.500 MCM of water have been estimated for the year 2025 (GWA, General Water Authority). In addition to population growing, there is a big hazard of deteriorating water quality. Because of pumping out of the shallow coastal water aquifers for industrial, human and agricultural demand, seawater intruded towards the inland.

1.2 OBJECTIVES

The main objectives of the present study are to characterize the (isotope) geochemical composition of the non-renewable paleo groundwater and to get insight into the evolution of the solutions and the origin of its components in the study area. A special focus is given to the origin of elevated concentrations of nitrate in the Hasouna well-field area. High nitrate concentration can be hazardous to human health.

Evolution of the groundwater as well as nitrate distribution in groundwater samples of Hasouna area and its origin in the well-field areas were investigated during three groundwater sampling campaigns in 2007 using hydrochemical and isotope data. The study was conducted in groundwaters of a Cambro-Ordovician sandstone aquifer, where the WHO-guideline value for nitrate (WHO, 2004) of 50 mgL^{-1} is exceeded and where non-agricultural and industrial activities play major roles. It was already known that the studied water-field is characterized by elevated concentration of nitrate; however, the source of nitrate is still subject to hot debates. Monitoring of groundwater quality and knowledge of its origin are essential to develop tailored resource management for the well-field. Water quality database is required for water mixing strategies to get an optimum quality of the provided mixed water.

1.3 STUDY AREA

The Hasouna-Jeffara and Ghadamis-Zwara systems together make up the Western Jamahiriya System (WJS, see sections 3 and 4). The present study concerns only the Hasouna well-fields, which supply the Hasouna-Jeffara system. The study area is located in the west-central part of Libya and is known as Jabal Al Hasouna (Jabal Fezzan). The layout of the Hasouna well-field, which is located East and Northeast of Jabal al Hasouna, is presented in Figure 1.1.

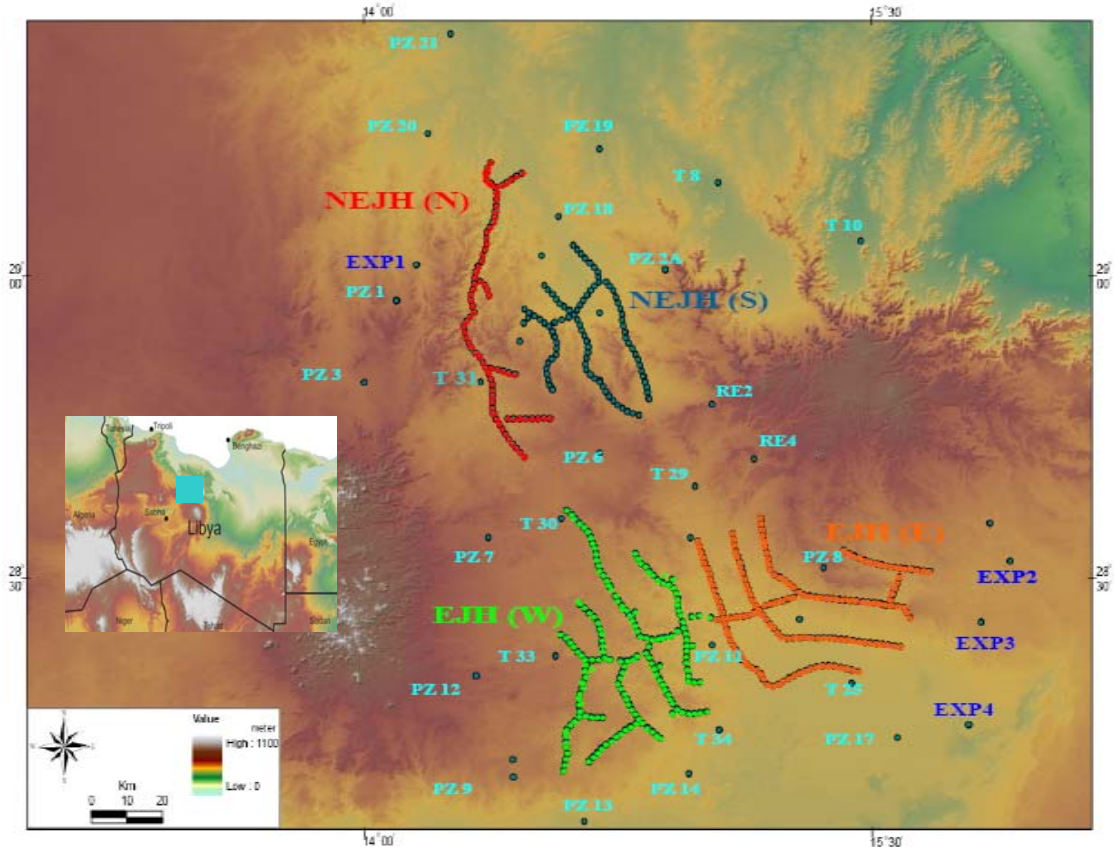

Figure 1.1: Location Map of Study Area of Hasouna wellfields, (o, o,o,o) Production wells and (T, EXP) and PZ (exploratory and piezometer wells)

The 484 production wells of the Hasouna wellfield are divided in four water fields as follows (see also Tab. 1.1): (source: GMRPA, Tripoli / Libya).

North East Jabal Hasouna South (NEJH(S)), consisting of 90 wells;

North East Jabal Hasouna North (NEJH(N)), consisting of 78 wells;

East Jabal Hasouna West (EJH(W)), consisting of 160 wells;

East Jabal Hasouna East (EJH(E)), consisting of 156 wells.

The production water wells of the Hasouna-Jeffara system supply the Tripoli and Jeffara Plain in the North (NW-Libya) with paleo water. The Hasouna-Jeffara system is the second phase of the GMRP project, which was finished in the year 2000, and completed the water supply to Tripoli city.

Table 1.1: Hasouna-Jeffara system of Great Man Made River Project (GMRP) Systems.

System	Wellfields	No of Wells	Design Production	Conveyance System	Comments
1. Hasouna-Jeffara	NEJH (S) NEJH (N) EJH (W) EJH (E)	90 78 160 156	2.5 MCMD	2,600 Km	Study Area for this PHD work

1.4 PREVIOUS STUDIES

Several groundwater studies have been performed during the initial investigation and planning of Great Man-made Water Supply Project, but most of them are unpublished and are not available within public domain. Some old hydro-geological studies have ranged from local studies on the aquifer systems of Libya by consultants to GMRP, General Water Authority and other Libyan government authorities. These studies include aspects of hydrogeology, groundwater flow and hydro-geochemistry, isotopes, recharge estimation, and groundwater modelling. Schoute (1976) published a detailed study about groundwater resources in Kufra Basin (Libya) for UNESCO. Salem et al. (1980) have studied the flow pattern in the Western Libyan Arab Jamahiriya using isotopic data of the groundwater. Moreover, Pallas (1981) reviewed earlier studies on hydrogeology and water resources assessment in Libya. Idrotechnico (1982) investigated the Western Jamahiriya System (WJS) to evaluate aquifer hydraulic parameters.

Pim and Binsariti (1994) described the general hydrogeology of Libya and the results of wellfield design and modelling studies for the GMRP wellfields, including the Jabal al Hasouna wellfields. Salem and Lloyd (1990) analysed the groundwater flow using salinity distribution and isotopes in a region of the southeastern Hamada al Hamra and northeastern Murzuq Basins, which included the EJH wellfields area. Idris (1994) studied the geology and water resources, mainly groundwater of Libya, Egypt and the Sudan. Lloyd et al. (1996) described the Groundwater assessment for the Western Jamahiriya System wellfield, Libya.

Most of former studies are focused on the basins in the east and southeast of Libya, namely Kufra, Sirte and Sarir (Edmunds and Wright, 1979; Benfield and Wright, 1981; Wright et al., 1982; Ahmad, 1983; El Maryme, 1994, who studied the hydrogeology and hydro-geochemistry of these basins).

However, Binsariti and Saeed (2000) investigated the groundwater salinity variation in the Cambro-Ordovician Aquifer of Eastern Jabal al Hasouna, the Great Man-made River Project in Libya. This investigation shows that downward vertical leakage from saline Zimam Aquifer to the underlying Cambro-Ordovician sandstone aquifer can occur through fracture zones. The salinity of the Zimam Aquifer reaches a maximum value of 4480 mgL^{-1} of TDS as measured in the shallow piezometer 29ZA/9A.

In other parts of Libya groundwater management and water quality studies are carried out by Shaki and Adeloye (2002) of an aquifer in the Murzuq Basin, southwest of the Jabal al Hasouna Wellfields. Milne-Home and Sahli (2007) applied ^{15}N isotopes to study the groundwater quality, Jabal Hasouna Wellfields, Great Man-Made River Project in Libya. The analysis of isotopes ^{15}N and ^{18}O from groundwater nitrate in the Hasouna waterfields showed values of 7.11 to 12.64 ‰ for the $\delta^{15}N$ and 12.51 to 22.35 ‰ for the $\delta^{18}O$. Therefore, these ranges suggested that soil nitrate could be the source. The groundwater hydrochemistry analysis shows the highest value with nitrate content of 133 mgL^{-1}.

1.5 THESIS OUTLINE

This study is structured into ten chapters. The present chapter gives information about the challenges, research objective and background of the study area. The second chapter provides a general review about regional aspects, climate and water situation. The third chapter gives detailed information about water supply project (Great Man-made River Project). The fourth chapter informs about the geo-hydrogeological setting of the study area, including the classification of aquifers. In chapter five the fundamentals of nitrogen, nitrate, sulphate, and application of stable isotopes are discussed. In the sixth chapter the different applied methodologies are explained. The seventh chapter comprises results and discussions of hydrochemical evolution of the groundwater chemistry in the Hasouna study area. In chapter eight the application of different stable isotopes focussing on the origin of nitrate is discussed. The ninth chapter deals with evaluation of the hydro-chemical and geophysical data of GMRP Authority. The tenth chapter focuses on the summary of the hydro-chemical and isotopes data, with a final research conclusion and recommendations. Subsequently the Table of contents and references are given.

Appendix I: .A manuscript dealing with “Tracing atmospheric nitrate in paleo groundwater of Saharan desert using ^{17}O-excess” which is submitted for publication. (Hasouna, study area).

Appendix II: Data of Groundwater chemistry and isotope results. (Hasouna Study area)

2 GENERAL OVERVIEW ABOUT LIBYAN CLIMATE, LAND AND WATER

2.1 REGIONAL ASPECTS OF LIBYA

Libya is a large country on the Mediterranean coast of North Africa, one of the smallest populations of the African continent. Libya occupies a part of Northern Africa from 20° to 34° N and 10° to 25° E (Fig. 2.1). Geographic position of Libya can be considered as a Gate to Africa, because of its long Mediterranean Sea coastline (1900 km) and central location in northern Africa. The capital city of Libya, Tripoli, is located at the Mediterranean coast in the northwestern part of the country. Tripoli has a population of 1.7 million with a high growth rate. Related to the population distribution in Libya, people concentrate in two main centres, in the northwest (Jeffara Plain) where about 60% of the Libyan population (Fig. 2.1), including Tripoli City, are living. The second centre is in northeastern Libya (Benghazi Plain). The main reasons for this concentration are productive, fertile soils and seasonable, moderate climatic conditions. More than 90 % of Libya area is desert while the area reserved for agriculture and forests account for 2 % of the Libyan territory. Libyan economy depends primarily on the oil sector, which contributes about 95 % to the export. Landforms of Libya generally consist of barren plains in the north against plateaus and depressions in the south. The Mediterranean coastland and Sahara desert are the most prominent natural features. There are several highlands with high mountains in some parts of the country, in particular in the southern desert near Chad border (Tibesti Massif).

2.2 CLIMATE

Libya is characterised by lower temperatures towards the Mediterranean Sea in the north and higher temperatures in the south. For the climate conditions in Libya, the interaction between the Mediterranean Sea and Sahara desert has to particularly be taken into account. In the coastal lowlands, where the majority of population lives, the climate is Mediterranean, which is warm and dry weather in summer and cold and rainy weather in winter. The climate in the desert is characterised by very hot summers and extreme daily temperature ranges. The highest temperature recorded in Libya was 57.8 °C at Al Azizia near Tripoli on 13 September 1922 (MARTYN, 1992:31).

Rainfall is the main source of precipitation in Libya, where the two main regions with high precipitation rates are in the northwest (Jeffara Plain & Jebal Nafussah) and in the northeast (Jebal Al Akhdar; Figure 2.2). Less than 2 % of

the country receives enough rainfall for settled agriculture. Accordingly, groundwater is the only primary source of water supply in Libya with 88 % of the water needs.

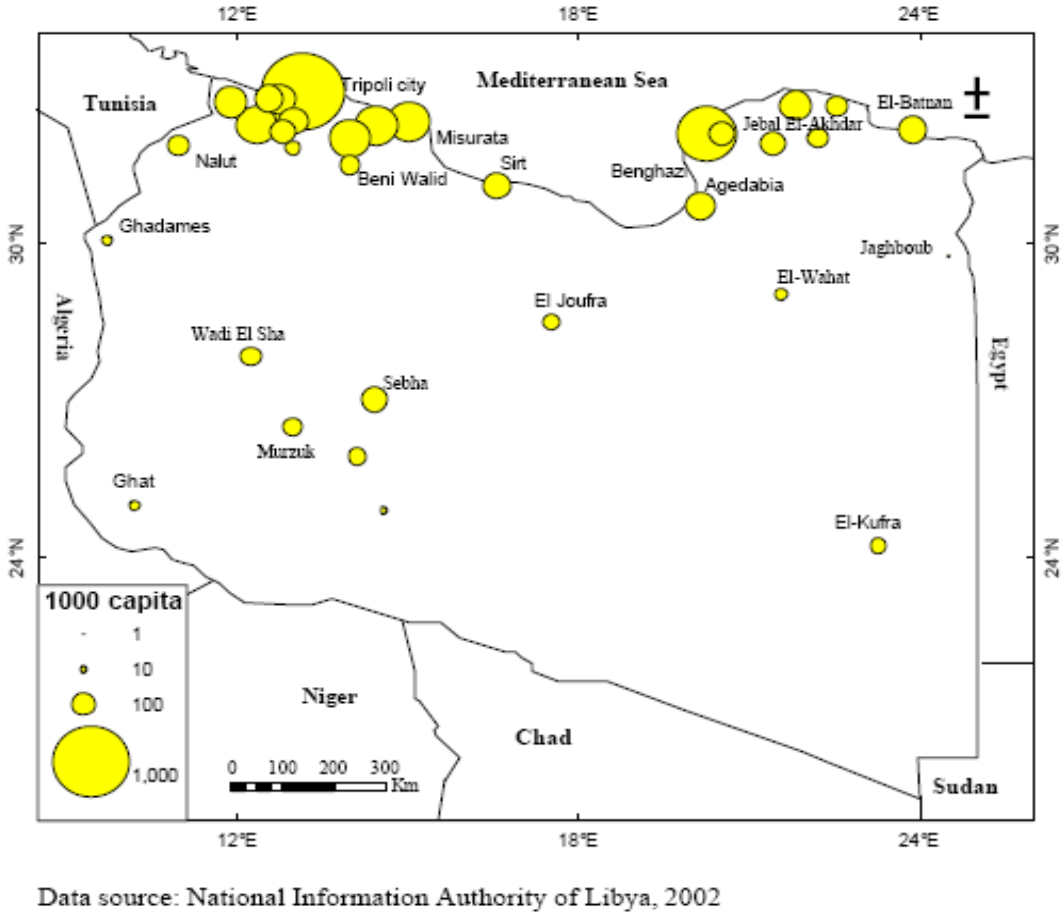

Data source: National Information Authority of Libya, 2002

Figure 2.1: Spatial distribution of population in the main cities and towns (National Information Authority of Libya), 2002.

2.3 HYDRO-GEOLOGICAL SITUATION

Libya is one of those countries that suffer from limited water resources, because most parts of the country are either semi-arid or arid, and the driest region of the world, with yearly average rainfall ranging from just 10 to 500 mm. Only about 5% of the entire area of Libya exceeds 100 mm of rainfall annually. Evaporation rates are also high, ranging from 1.700 mm in the north to 6.000 mm in the south (IMB, 1980).

Currently, aquifers are recharged only in the northern region (Jabal Nafusah and Jeffara Plain in the northwestern zone), and Jabal al Akhdar (Green Mountain) in the north-eastern zone (Fig. 2.2).

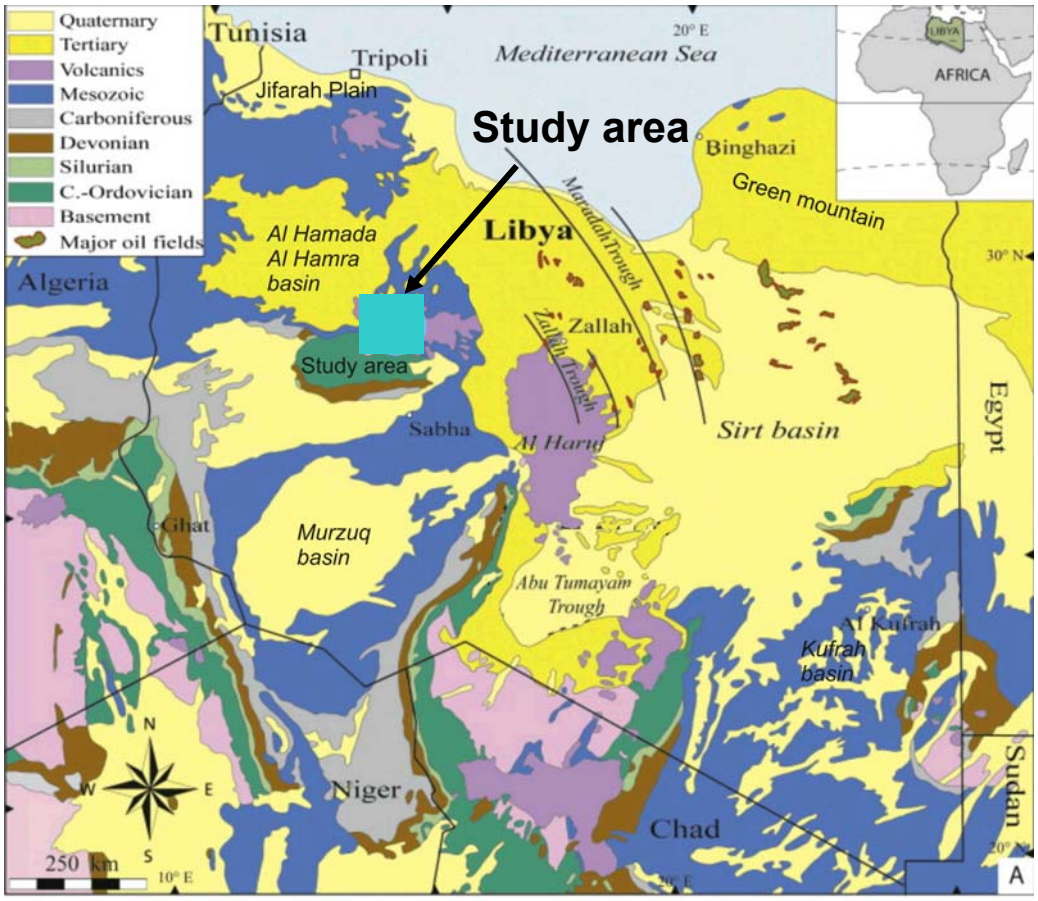

Figure 2.2: General geologic map of Libya (modified after Rubino and Blanpied, 2000).

The highlands of Jebal Naffusah (960 m) in northwestern Libya consist of massive limestones of pre-Upper Cretaceous age. Jebal El Akhdar (875 m) in northeastern Libya is composed of Paleogene limestone, Jabal El Akhdar is economically, environmentally, and agriculturally the most important highland of Libya, with highest precipitation and some snow falls in winter season. It is the wettest region with annual rainfall averages between 400 and 600 mm (Al-Idrissi et al., 1996).

The total mean annual runoff calculated or measured at the entrance of the Wadis in the plains (or rifting zones) is roughly estimated at 200 million cubic meters (MCM) per year, but a large part of it evaporates or recharges the underlying aquifers. Therefore, the regular renewable surface water resources are estimated at 100 MCM per year. At the moment there are 16 dams in operation with total storage capacity of 385 MCM with an average capacity of about 61 MCM. Figure 2.3 shows Wadi Ghan Dam with an average annual storage capacity of about 3.9 MCM (GWA, Libya).

Figure 2.3: Shows Wadi Ghan water Dam with an average annual storage capacity of about 3.9 MCM.

2.4 AQUIFER CONDITIONS AND PALEO ENVIRONMENT

Non-renewable aquifers are commonly described in the literature as paleo aquifers. Theses groundwater aquifers have no appreciable modern recharge. These aquifers generally contain ground water that is captured in the subsurface geological formation; typically, groundwater is non-renewable. Aquifers are hundreds if not thousands (or millions) of years old. Most often found in arid climates, paleo and other non-renewable aquifers are important water resources for many nations. Some of these aquifers are transnational, such as the Nubian Sandstone aquifer underlying Chad, Egypt, Libya and Sudan. Located at depths ranging from a few meters to a few hundred meters, the water in this aquifer is estimated to be as much as 35.000 years old (Sonntag, 1978).

Sonntag et al. (1978) suggested that variations in the isotopic composition of Sahara paleo (fossil) waters are quite similar to those observed in modern European groundwater and pointed to possible commonalities in origin. From west to east and along a 2.000 km transect in central Europe, the isotopic composition (Deuterium isotope) of groundwater varies from δ^2H = -30 ‰ (west) to –70 ‰ (east) (Figure 2.4, Sonntag, 1978). In Figure 2.3 Sonntag (1978) reported that there is a decrease in the heavy isotopic content of paleo Saharan groundwaters from west to the east. They found that paleo waters from western Morocco at the far west are the heaviest (δ^2H = -20‰), and paleo waters from the Western Desert of Egypt (far east) are the lightest (δ^2H = -80 ‰). They also found a progressive decrease in δ^2H values from Morocco

(δ^2H = -20 to -30‰) to Egypt (Algeria δ^2H = -30 to -50 ‰; Tunisia δ^2H = -60 ‰; Libya δ^2H = -70 to -80‰).

These data strongly suggest that North Africa must have been subjected to precipitation during previous wet Pleistocene periods from wet Atlantic air masses as they crossed the Sahara from west to east. Evidence is found in some unconfined aquifers in the Sahara and Sahel that groundwater at the immediate water table is of Holocene age (< 12000 years BP, Fontes et al. 1993). Edmunds and Wright (1979) measured the age of groundwater in the Sirt Basin in east-central Libya and northern Kufra basin using stable and radio-isotopes and determined the recharge history during the Holocene and late Pleistocene periods. They classified the samples into age groups (1.300-3.400 yr. BP) and (500-7.800 yr. BP).

The Hamada Al Hamra Basin of south-west Libya is currently arid with less than 20mm of precipitation per year. However, regionally extensive limestones, sandstones, sands, siltstone deposits show that the Hamada basin previously contained a large paleo lake, indicating that the climate in the past was more humid. The modern climate of the Hamada Al Hamra basin is characterized by high temperatures in the summer months (average maximum of 39 °C in July-September) and marked also with a low temperature in the winter (average 6 °C January).

The radioactive carbon dating (^{14}C) of WJS (Western Jamahiriya System) has shown age differences between regions. In Wadi Ash Shati area the groundwater in deep aquifer (Cambro-Ordovician) showed average ages of 12 to 13 ka. Klitzsch, (1978) and Sonntag et al., (1979) showed that in Sabha area the ages of water in the deep aquifer (Cambro-Ordovician) ranges from 15 to 17 ka. In the shallow aquifer they range from 7.000 to 8.500 yr. BP. The Water in the Tertiary aquifer of Jeffara ranges in ages from 26.000 to 27.000 yr. BP. Water of Hamada Al Hamra (Upper Cretaceous aquifer) ranges in age from 23000 to 30000 yr. BP. Sturchio et al., 2004 have used Krypton-81 and Chlorine-36 to date the groundwater from Nubian Aquifer in the Western Desert of Egypt, which determined the age of groundwater to be as old as one million years.

Groundwater of known age contained in major aquifer systems in the African sedimentary basins enable low-resolution (±1.000 years) characteristics of past climates to be determined, in particular paleo-temperatures. These include air mass origins, humid/arid transitions and rainfall intensity. Results from both northern and southern Africa indicate the predominance of westerly Atlantic airflow during the Late Pleistocene. Greater aridity during the Last

Glacial Maximum (LGM) is recorded over most of Northern Africa by the absence of dated groundwaters (Guendouz et al., 2010).

An intensifying of the African monsoon during the Early Holocene is obviously found from “isotopically light” groundwaters, in particular, over Sudan. Maximum cooling around the LGM of 5-7°C is recorded in the noble gas recharge temperatures from Africa (Fontes, 1991; Edmunds, 1999). Modern recharge can be readily identified from the chemical compositions and isotopic signatures (Cl, $\delta^{18}O$ and Tritium) in the unsaturated zone and in shallow groundwater. The results show the non-renewable nature of many groundwater sources, which are used now across the arid and semi-arid regions of Africa (Edmunds, 1999).

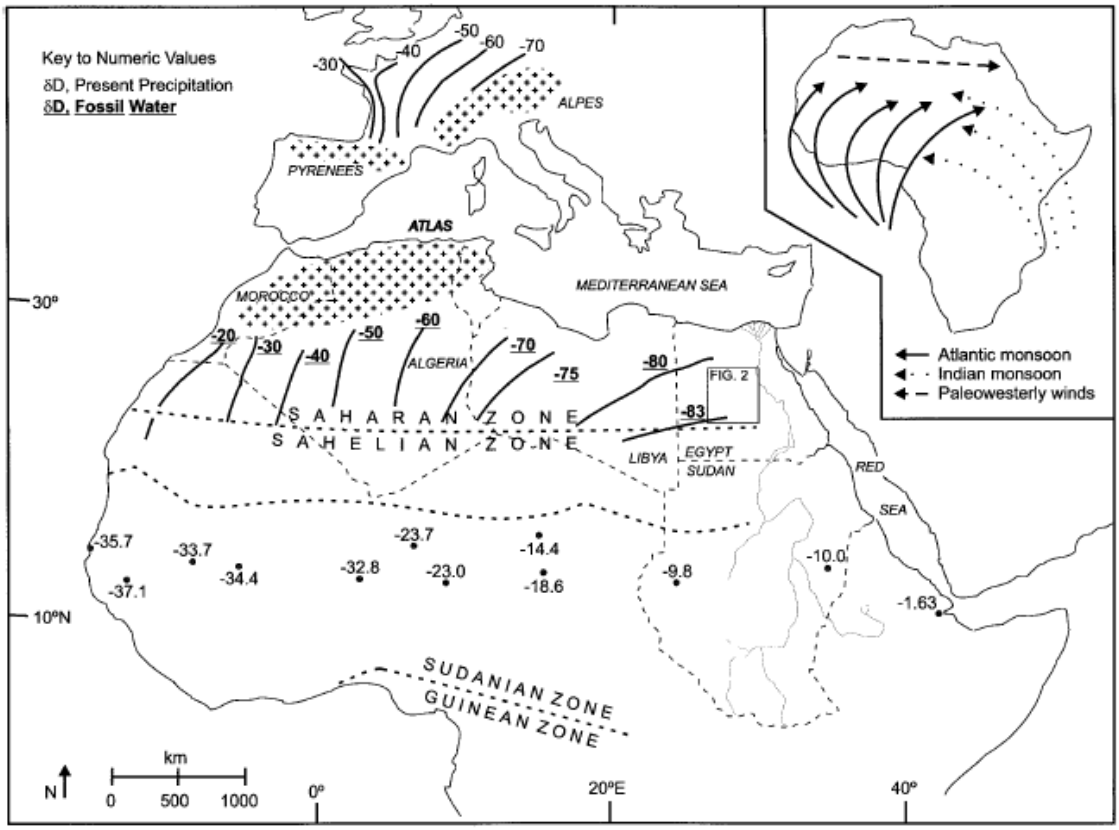

Figure 2.4: Map of the distribution of fossil groundwater in North Africa region and the Sahel countries (variation of the isotope values of Deuterium, δD in ‰, in Sahara Groundwater’s) from Sonntag (1978).

3 GREAT MAN-MADE RIVER PROJECT LIBYA

3.1 MOTIVATION, GOALS AND PERSPECTIVES

Libya is mostly desert and great sand seas with a large volume of paleo groundwater, estimated to exceed 35.000 km^3, and energy (oil). In contrary, limited quantities of renewable fresh water resources are available in coastal regions in the northwest and northeast. The world's largest and most expensive water supply project has been planned, designed and implemented in order to bring fresh water from the deep groundwaters in the southern basins to the people in the northern region.

The purpose of the Great Man-made River Project (GMRP) as it is called, is to carry over 6 million cubic meters of water per day from the groundwater aquifer systems of Sarir and Kufra in the south east and Jabal Hasouna in the south-west of the country. This water is planned to supplement water needs for the coastal areas in the north of the country for domestic and agricultural uses, with about 80% of the water to be allocated for agricultural irrigation.

In 1983, the project was initiated comprising several phases, whereas phase I and phase II being the major components of this project (Fig. 3.1). Phase I of the project covers the eastern part of the country, as water will be conveyed from the Sarir and Tazerbo wellfields to the coastal areas of Benghazi and Sirt. Phase I is already delivering water to coastal reservoirs via 1.850 km of 4 m diameter pipelines. Phase I and III of the project will provide 3.5 million cubic meters (Mm^3) of water per day from wellfields in the south (Kufra, Tazerbo and Sarir) to the eastern coastal belt, which extends from Sirt in the west to Benghazi in the east (GMRP, Libya).

Phase II of the Project will convey water from the Fezzan aquifers in the southwest of the country to the northwest region of greater Tripoli area and the Jeffara Plain. The wellfield area extends over 4.000 square kilometres with total of 440 operating wells and 44 stand-by wells (Fig. 1.1). The phase II main conveyance system consists of over 1.200 km of pipeline, which is part of the Western Jamahiriya System. The pipeline is mainly made of pre-stressed concrete cylindric pipes (PCCP) of 2.4 to 4.0 m diameter.

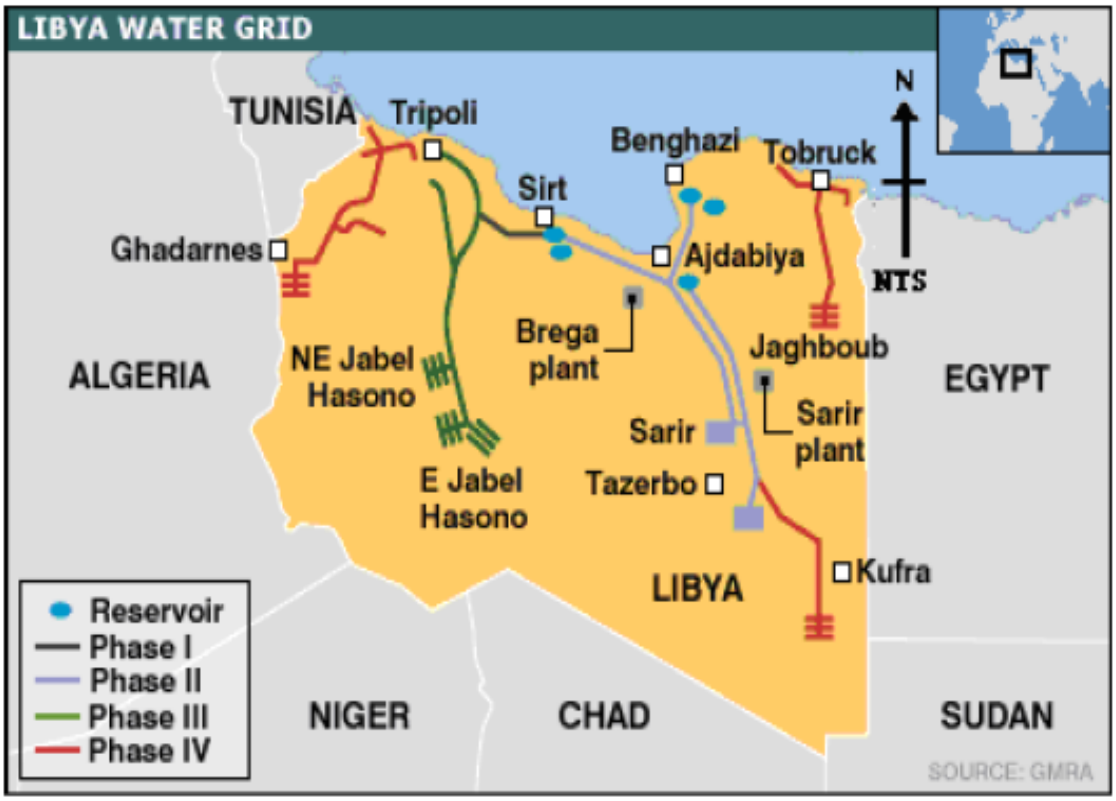

Figure 3.1: Layouts of the Great Man-made River Project and major systems (GMRP, 2004). Source: www.gmmra.org

Phase II represented the Hasouna waterfields (study area), which is planned to convey 2.5 million cubic meters of water from wellfields at East Jabal Hasouna and North East Jabal Hasouna (EJH (W&E), & NEJH (N&S)) to Tarhouna and Tripoli (Fig. 3.1). It extends from Misrata in the east to Zawia in the west (around 300km); (GMRP, Libya). The pipe dimensions, as well as the production water well facility are illustrated in Figures 3.2a and 3.2b. The supplied water is stored in large reservoirs (Man-made Lakes, Fig. 3.3).

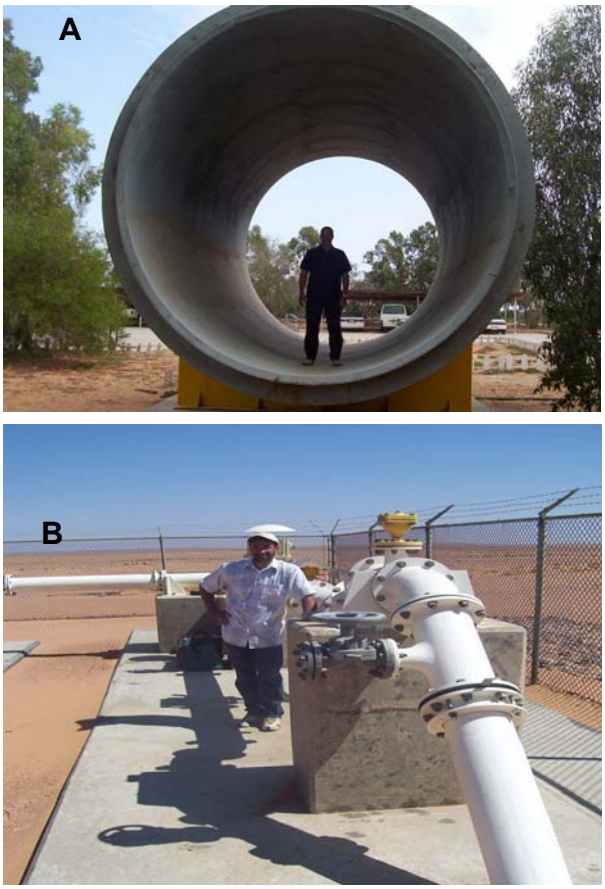

Figure 3.2: (a & b). Pipe lines of great man-made river project (4 meter diameter) and production water well facility.

Figure 3.3: Man-Made Lake, Ommar Al Mochtar water reservoir, with storage capacity of 6 MCM and diameter of about 1 km (GMRA-Phase I).

3.2 WATER RESOURCES MANAGEMENT

The groundwater in Libya is found in five main hydrogeological basins: Jeffara Plain, El Jabal Akhdar, El Hamada El Hamra, Murzuq and Kufra Sarir-Sirt basins (Figure 3.4). The basins in the north region suffer from serve deterioration, with relative recharge from precipitation. Water storage of the basins in the south is not renewable but the hydrogeological basins contain huge volumes of groundwater. According to the water balance of the groundwater basins in Libya, a serious deficit in water supply occurs in the Jeffara Plain basin and moderate deficit in the Jabal El Akhdar basin caused by the concentration of population in north-western Libya (Tripoli capital); (GWA, Libya).

Non-conventional water treatment in the form of desalination covers only a small portion of the domestic and industrial water demands in Libya. Treated sewage is still very limited and is mainly used for irrigation purpose. As for desalinated and treated water (unconventional water), a great number of desalination plants have been built near large municipal centres and industrial complexes. The total amount of desalinated water was 120 million m^3 in 2000 (General Environmental Authority, 2002). A number of treated - sewage water plants are already in operation or planned for the near future. The treated water was estimated to amount to 91 million m^3 in 1990 and increased to 200 million m^3 in 2000 (UNEP, et al., 1996). Figure 3.5 shows the potential water resources in Libya (GWA, Libya).

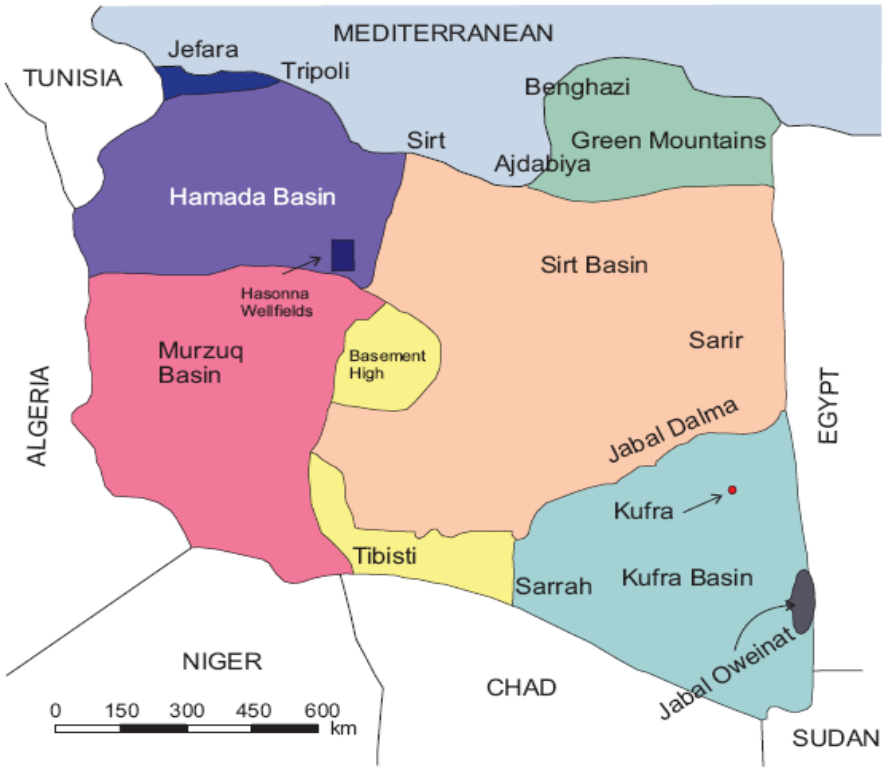

Figure 3.4: Main Groundwater basins in Libya (modified from GMRA, 2002).

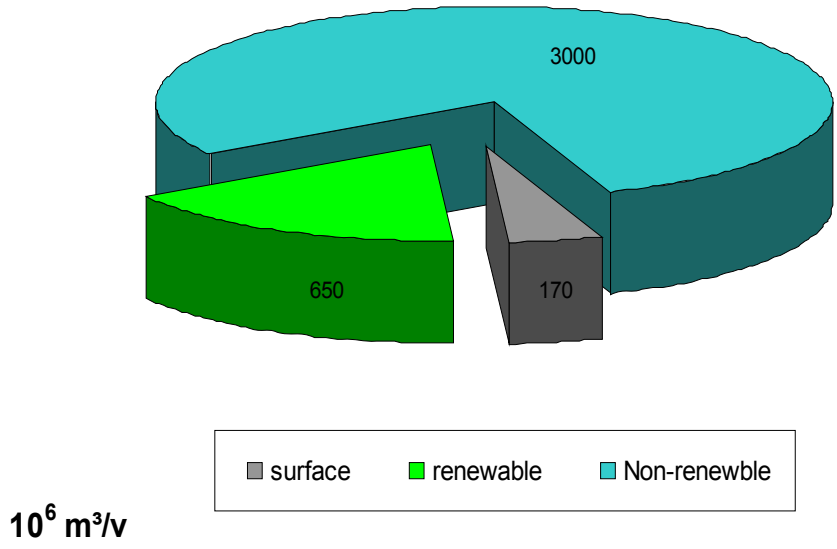

Figure 3.5: Potential water resources in Libya, General Water Authority, 2007)

4 GEOLOGY AND HYDROGEOLOGY SETTING

The geology and hydrogeology information and data used in this current study are referring to Klitzsch (1970); Jurak (1978); Goudarzi (1970); Pallas (1980); Geomath (1990 and 1994); Collomb (1962); Conant and Goudarzi (1964); Massa and Collomb (1960); Tawadros (2001); Freulon (1964); Binsariti et al.(2000); Hea (1971); Dubay (1980); Idrotechnico (1982); the General Water Authority (GWA, Libya), Industrial Research Centre (I.R.C, Libya); El Chair (1984); and GMRP Authority (Libya).

4.1 GEOLOGY OF THE STUDY AREA

The Hamada Al Hamra Basin of NW Libya, where the study area is located, is an intracratonic Paleozoic basin with a thick sequence of clastic rocks deposited during the Paleozoic. These sediments were derived from a Precambrian basement of felsic igneous and metamorphic rocks. Sediments are represented mostly by sandstones and shales. Most clay minerals in the Paleozoic strata were produced from the alteration of feldspar. The Jabal Al Hasouna area is a part of the African Platform, which is characterized by complex tectonic structures and a series of sedimentary packages and depositional sequences.

The Hamada Al Hamra Basin is bordered by the Sirte Basin to the east, the Ghadames Basin to the west, the Gargaf Arch to the south, and the Jeffara (Nafusah) High to the north. The Cambrian-Ordovician sediments are fluvial to shallow marine. In the Hamada Al Hamra Basin, the best-known hydrocarbon fields are the El Hamra, and Al Wafa Fields, with high amounts of hydrocarbon reserves from the Devonian Formation.

The Western Jamahiriya System (WJS) regional geology is characterized by tectonically faulted and folded structures. The structures of Cambro-Ordovician rocks were impaired by the Caledonian Orogeny, which generated a significant discontinuity trend NNE-SSW. The Lower Ordovician sandstone formation lies consistently over the Hasouna Formation. Sandstone and neritic siltstone formations of Middle Ordovician age, and also predominantly marine sandstone formations of Upper Ordovician age are on top of the sequence. The Hasouna area was subjected to continental conditions after marine regression during the Upper Paleocene. Jurak (1978) has classified the Quaternary deposits of the Hasouna area into several types: wadi deposit, eolian deposits, fluvio-eolian deposits, alluvial deposits (fans), wadi terraces and landslides.

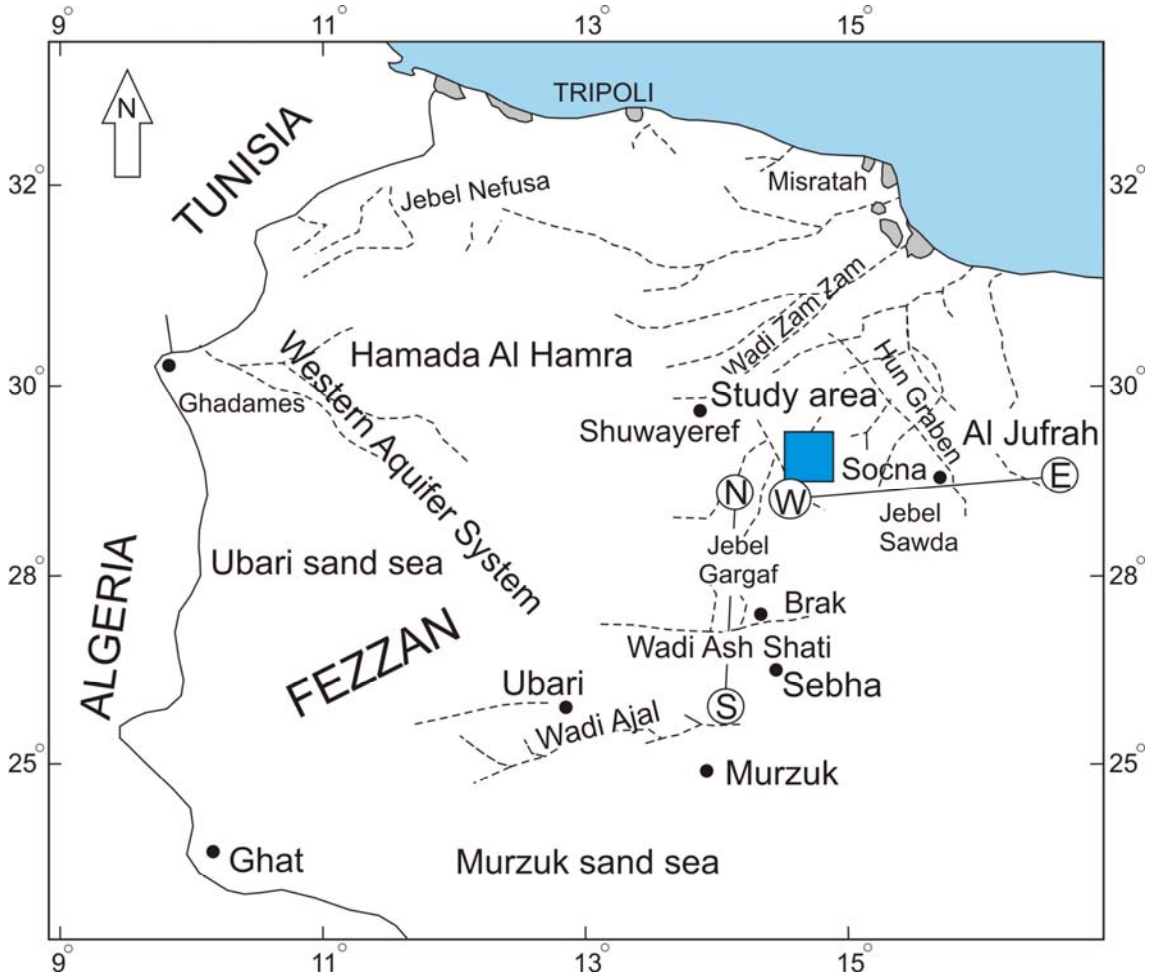

Figure 4.1: Map of the west part of the Libya (Goudarzi, 1970).

There are two geological cross-sections given (viz. south to north and west to east in Fig. 4.1) which can be used to illustrate the major geo-hydrogeological features of the study area. The geology of the Hasouna wellfields region is shown in Figure 4.2. There are two main geological formations within Hasouna study area, the Zimam and Hasouna formations, respectively. In some places in the study area the Zimam formation sediments are covered by basalt lava. The volcanic rocks of Jabal As Swada are Miocene volcanics (Tawadros, 2001). The period of Jabal As Swada volcan activity was considered to be post-Oligocene (Klitzsch, 1970), and Late Oligocene to Middle Miocene (Jurak, 1978) (see Figures 4.2 and 4.3). The Individual stratigraphic units and the production water wells of Hasouna study area (white doted white circles) are shown in Figure 4.4. The Gargaf Uplift (Fig. 4.5), also termed as Gargaf Arch is the major structural feature in the Hasouna study area, which forms the northern boundary of the Murzuq basin (Tawadros, 2001). The Gargaf Uplift has been formed during the Caledonian tectonic cycle (Paleozoic), and is oriented north-northeast to south-southwest. The study area is a part of Jabal Al Hasouna mountain range and is situated at the crossing of these two structural trends (Jurak, 1978).

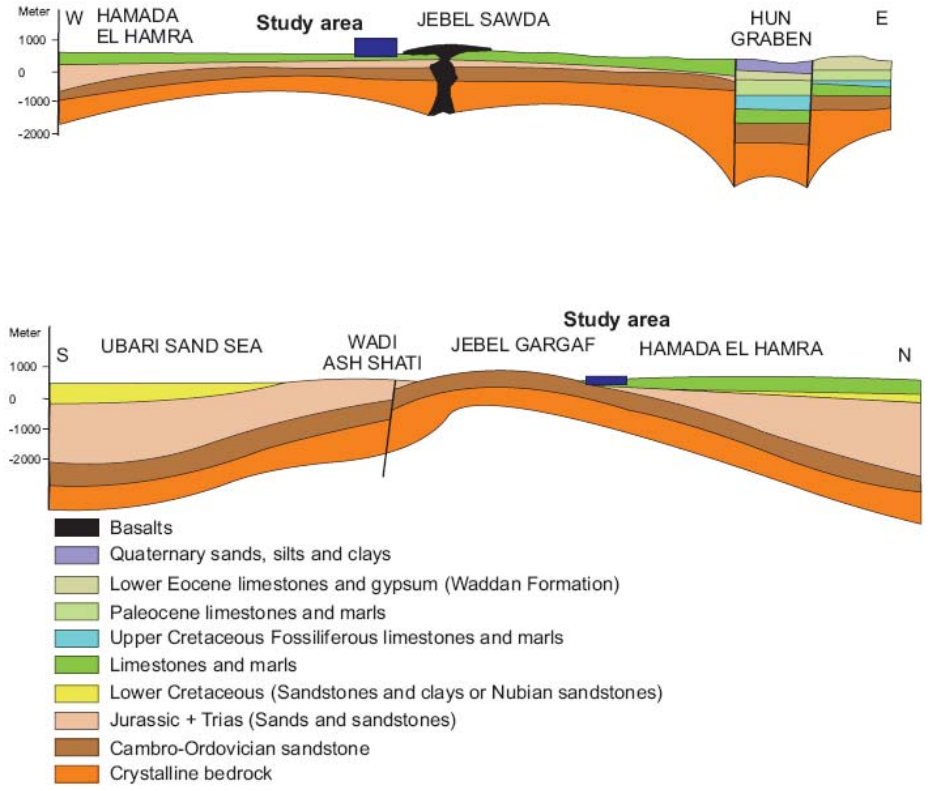

Figure 4.2: Geological cross-sections in and around the study area, (Goudarzi, 1970).

Figure 4.3: Lava flows of basalts of Jabal Aswada (part of study area), geology and major landscape features of the Hasouna study area.

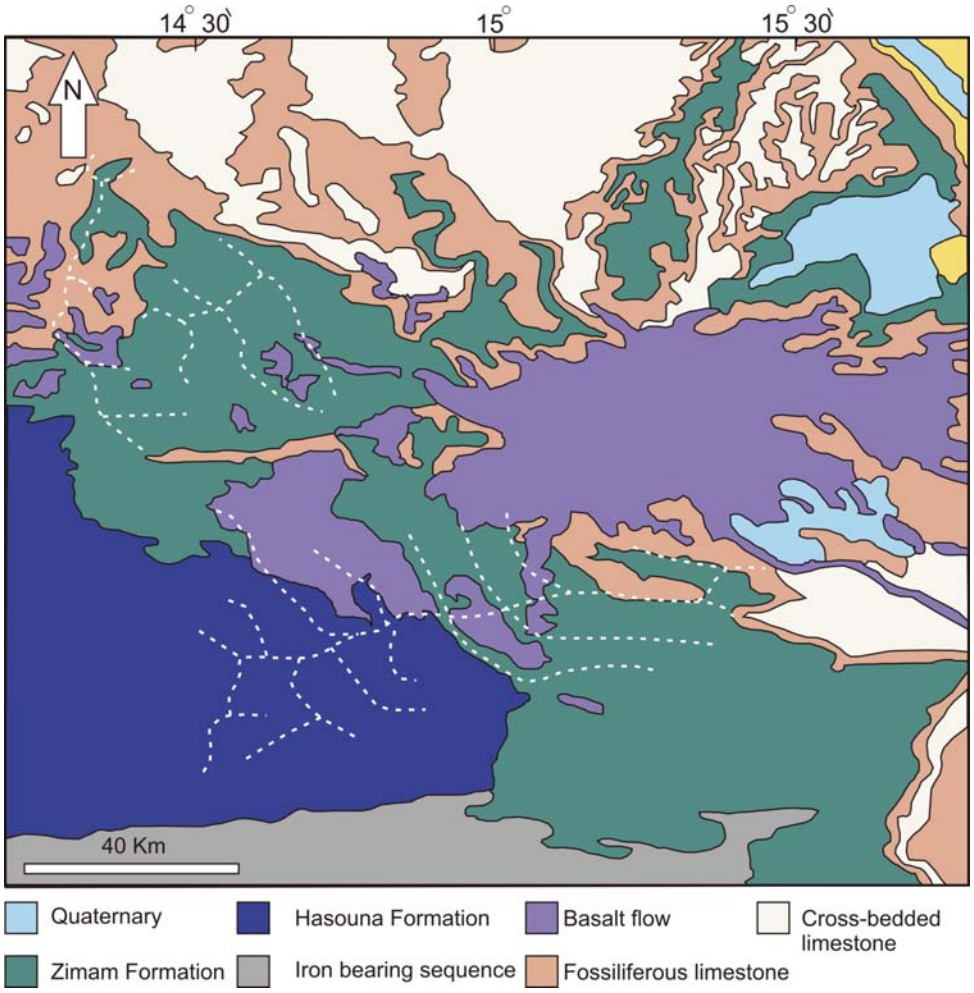

Figure 4.4: Geological map of Hasouna well-fields area (Libya Industrial Research Centre, 1978), the Hasouna water wells are marked in white dots.

The geological and stratigraphical map of the geological basins in the southwest of Libya is shown in Figure 4.5 (El Chair, 1984). The sedimentary and lithological deposits in the basins range from Cambrian to the Quaternary ages (Fig. 4.5). The description of the aquifer systems in the WJS is based on previous modelling of the WJS by Geomath (1994) and the previous hydro-geological studies such as the technical reports prepared by the General Water Authority (GWA, Libya). Another source is the series of explanatory booklets to accompany the regional map sheets of the Geological Map of Libya, which were sponsored and published by the Industrial Research Centre (I.R.C). These booklets include descriptions of the geology, mineral and groundwater resources in each area and have individual authors, for example, Geological Map of Libya (1:250,000), Sheet: Jabal Hasouna (MN 44-16) by Jurak (1978).

4.1.1 HASOUNA SANDSTONE FORMATION

The Gargaf Group which includes the Hasouna Formation in west Libya has Cambrian and Ordovician sediments. The Gargaf Group is extended to include all Cambro-Ordovician rocks in Libya, both in outcrop and in subsurface (Fig. 4.5). The Hasouna Formation is the most extensively developed Lower Paleozoic unit and has been recognized in western, central and eastern Libya (Massa and Collomb, 1960). The Hasouna Formation is composed of cross-bedded, medium to coarse-grained sandstones which are silica cemented with a kaolinite matrix and rare carbonate cement. The sandstones are mostly coarse-grained and feldspatic in the lower part (Collomb, 1962).

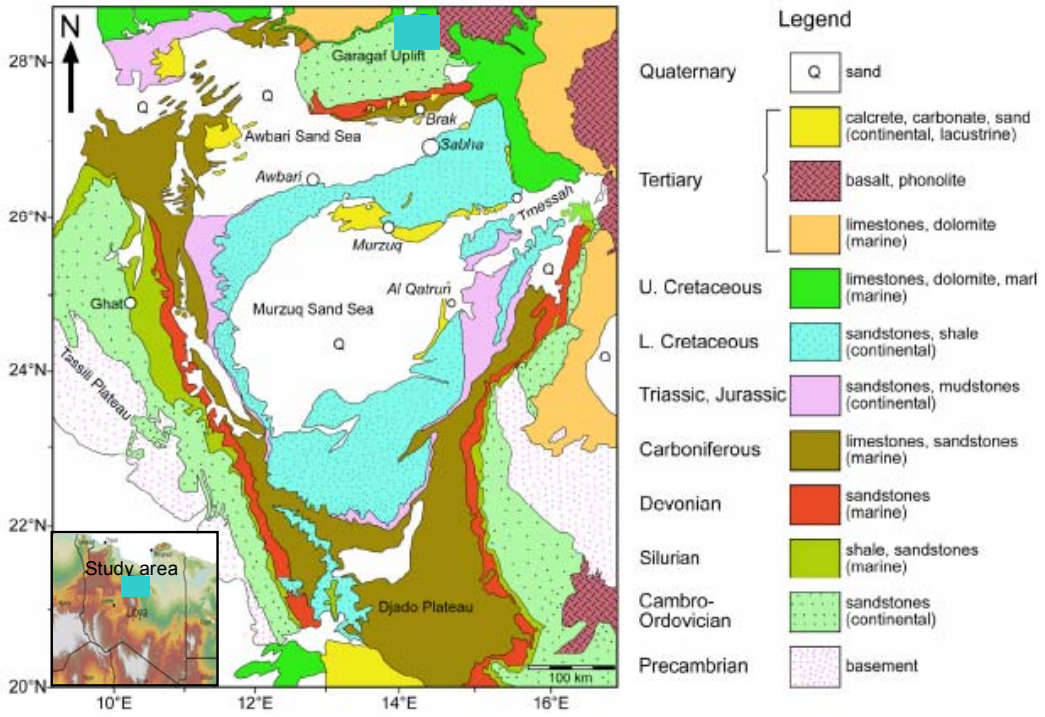

Figure 4.5: Geological map of the basins in the southwest of Libya, showing the main stratigraphical units. Modified from El Chair, (1984).

Freulon (1964) divided the Hasouna Formation in the central Sahara into lower, middle and upper units. The lower unit starts with several meters of basal conglomerates composed of quartz pebbles, quartzite and metamorphic rock fragments, followed by coarse-grained, quartitic, cross-bedded sandstones. The middle unit is about 45 m in thickness and composed of very fine-grained sandstones and silty sandstones, thin-bedded, laminated and rippled with slump structures. The upper unit is about 100 m and consists of fine to medium-grained sandstones, partly coarse grained and conglomeratic, thick-bedded, cross-bedded, friable, and cemented by carbonates. The sand

particles are cemented by silica cement and occasionally by carbonate cement, with kaolinite in the matrix (Tawadros, 2001). Estimates of the total thickness of the Hasouna Formation in the area range from 300 to 800 meter based on examination of the lithology of drill cores, and borehole geophysical logs.

4.1.2 ZIMAM FORMATION (UPPER CRETACEOUS – PALAEOCENE)

Jordi and Lonfat (1963) have classified the Zimam Formation from the base upwards into the (1) Lower Tar Marl, the (2) Socna Mollusc Bed, the (3) Upper Tar Marl and the (4) Had Limestone Member. This Formation represents the last sedimentary cycle of the Hamada Group (Table 4.1). The lithological unit's descriptions of Zimam Formation have been given by Jordi and Lonfat (1963) into:

- The Lower Tar Marl Member contains a marl, yellow calcareous mudstone and shale sequence.
- Socna Mollusc Bed is a unit marked by fossiliferous limestone.
- The Upper Tar Member consists of marls, calcareous mudstone, and shaly intercalations.
- The Had Member consists mainly of calcilutites, calcarenites, dolomitic limestones and marl.

4.2 HYDROGEOLOGY OF WESTERN LIBYAN AQUIFERS SYSTEM (WJS)

4.2.1 INTRODUCTION

The information about the classification of hydrogeology and groundwater aquifers is based on the previous studies and investigations in Libya. The groundwater aquifers and water resources in Libya are located in the major hydro-geological basins (see Figures 3.4 and 4.6).

- Murzuq Basin
- Al Hamada Al Hamra Basin and Jefara Plain (Jabal Hasouna), study area
- AL Kufrah Basin (Nubian Sandstone)
- Sarir and Sirt Basin
- Ghadames Basin
- Jabal Al Akhdar (Cyrenaica Platform)

Table 4.1: Classification of the major Formations describes the main lithological units in the Formations (Jordi and Lonfant, 1963).

System	Group	Formation	Member
Upper Cretaceous	Al Hamada Al Hamra Group	Zimam Formation (Zmam)	Had Limestone Member
			Upper Tar Marl Member
			Socna Mollusc Bed
			Lower Tar Marl Member
		Mizda Formation	Thala Member
			Mazuza Limestone Member
			Tigrinna Marl Member
		Nafusa Formation	Garian Dolomite Member
			Yafran Marl Member
			Ain Tobi Limestone Member

The underground flow of water is mainly from the South to North (east); (Fig. 4.6). Within the whole area, Cambrian to Tertiary sediments overlie Precambrian basement. The Garqaf Uplift (shown in Figs. 4.5 and 4.6) divides the area into two basins: the Hamada Al Hamra basin to the north and the Murzuq basin to the south. The regional groundwater of WJS (Figures 4.1-4.5) extends over an area of about 900.000 km² and is bounded by major faults to the west, north, and east and by a basement outcrop in the south. The Western Jamahiriya System (WJS, Figures 4.1, 4.2 and 4.7) was the subject of the regional investigation by Italian consultants (Idrotechnico, 1982). This study was very comprehensive in scope ranging from remote sensing, geophysics and exploratory drilling for hydrogeology, geochemistry and isotopes.

The results of Idrotechnico represent the hydro-geological modelling study of Wadi Ash Shati-Jufra and Jabal al Hasouna and the extent of fault systems in the area. Tectonic activity has separated the area into the Al Hamada al Hamra Basin and the Murzuq Basin, which lie north and south of the Gargaf Uplift respectively. Alternating cycles of erosion and deposition resulted in a complex layering and interconnection between three aquifers: 1. Upper Aquifer, 2. Middle Aquifer and 3. Lower Aquifer, respectively, and include individual aquifers of different geological age.

The sequence of these aquifers and their main characteristics are detailed in Tables 4.3 and 4.4 together with their area of occurrence (Geomath, 1994). With respect to hydrogeology, it is significant to note the

existence of a continuous 50 to 70 m thick quartzitic unit in the uppermost Cambro-Ordovician succession. This mentioned unit is believed to result from long-lasting pre-Devonian weathering (Hea, 1971; Dubay, 1980) and is also interconnected with the development of confined aquifer conditions in the Cambro-Ordovician aquifer.

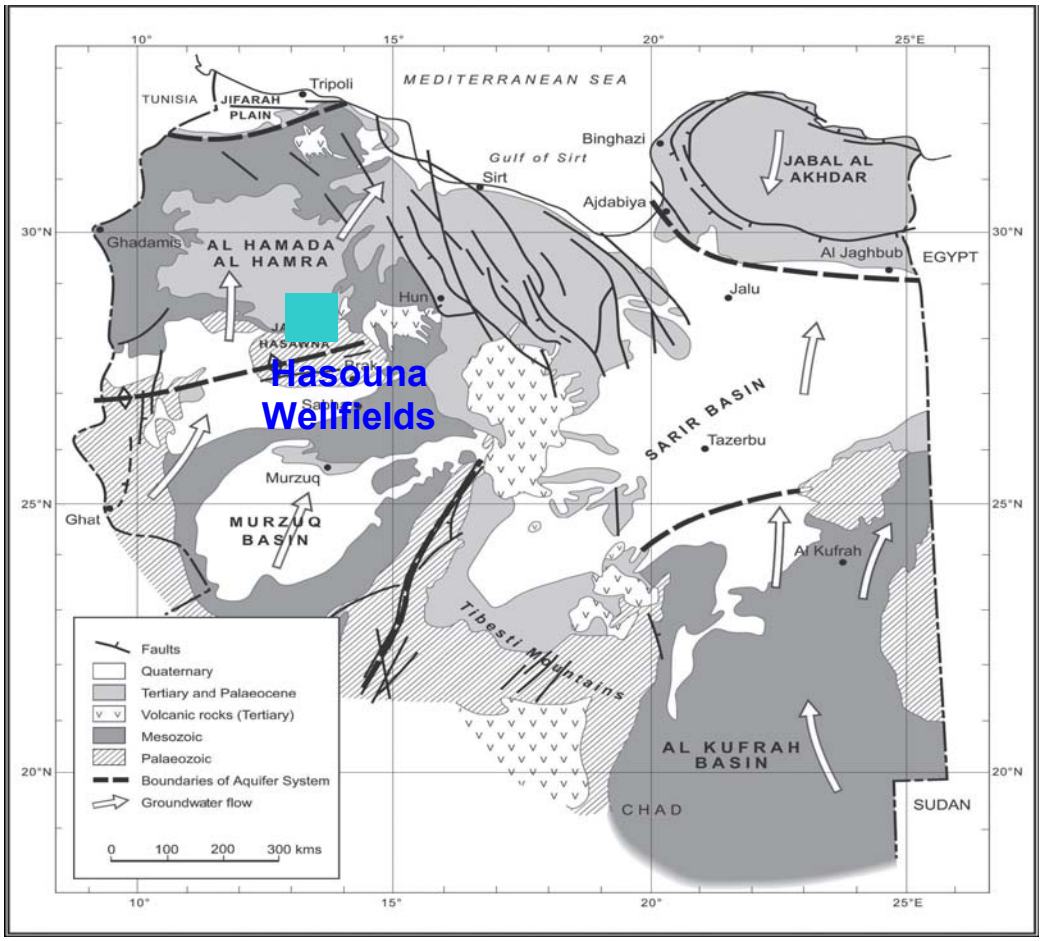

Figure 4.6: Hydro and geological map of sedimentary basins in Libya (Conant and Goudarzi, 1964).

The hydrogeological cross sections of the regional groundwater system (D to H) for this study area are shown in Fig. 4.7. Five hydrogeological cross sections were used to study the hydrogeology of Western Libyan Systems (WJS), which show the different aquifer types around the Hasouna study area.

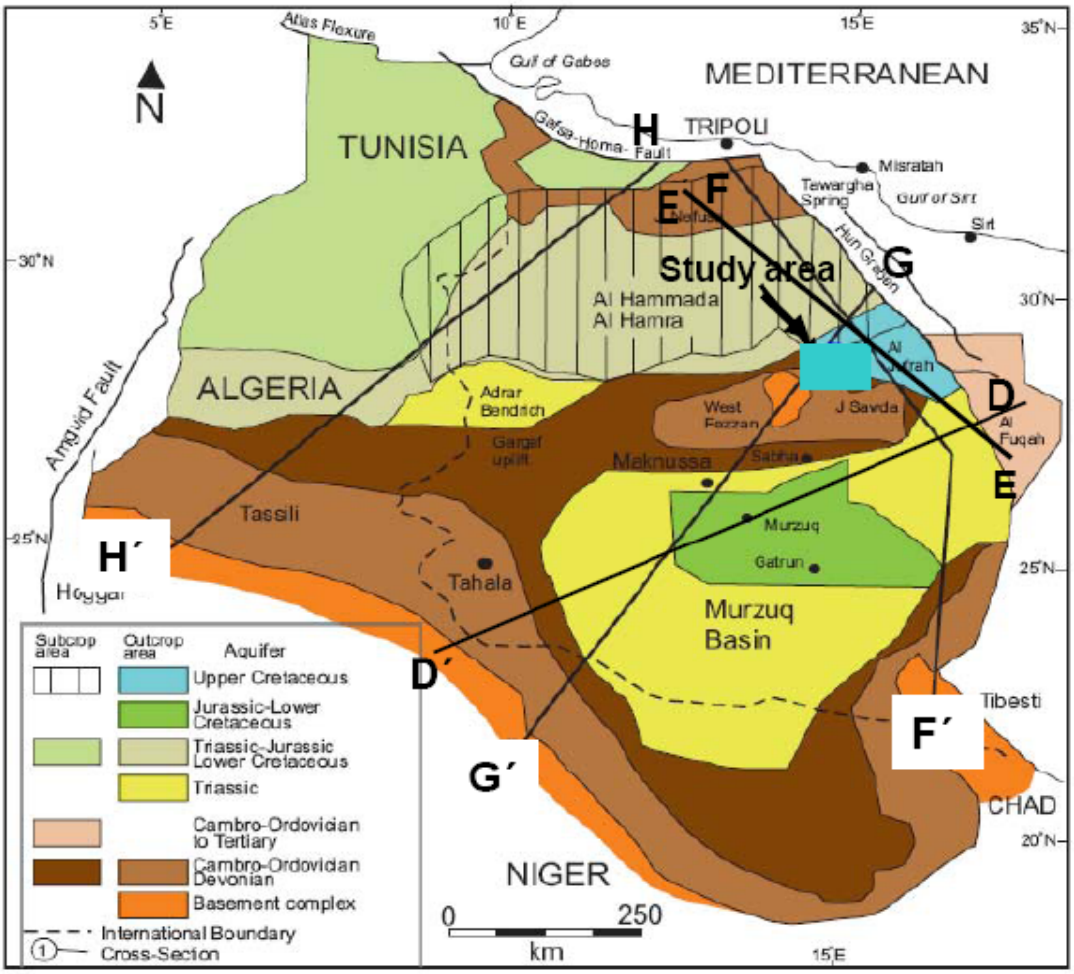

Figure 4.7: Outline map of Western Jamahiriya-System (WJS) and regional groundwater system (Modified from Geomath, 1990). Solid lines D to H represent the cross sections (see Figs. 4.8 and 4.9).

The location of the Hasouna study area is shown in Figs. 4.7 and 4.8 (F-F´, H-H´, and G-G´). The Figure 4.8 shows the distribution of classified groundwater aquifers beneath the study area. The main productive Paleozoic aquifer (Cambrian-Ordovician) sandstone is shown in the cross-section F-F´.

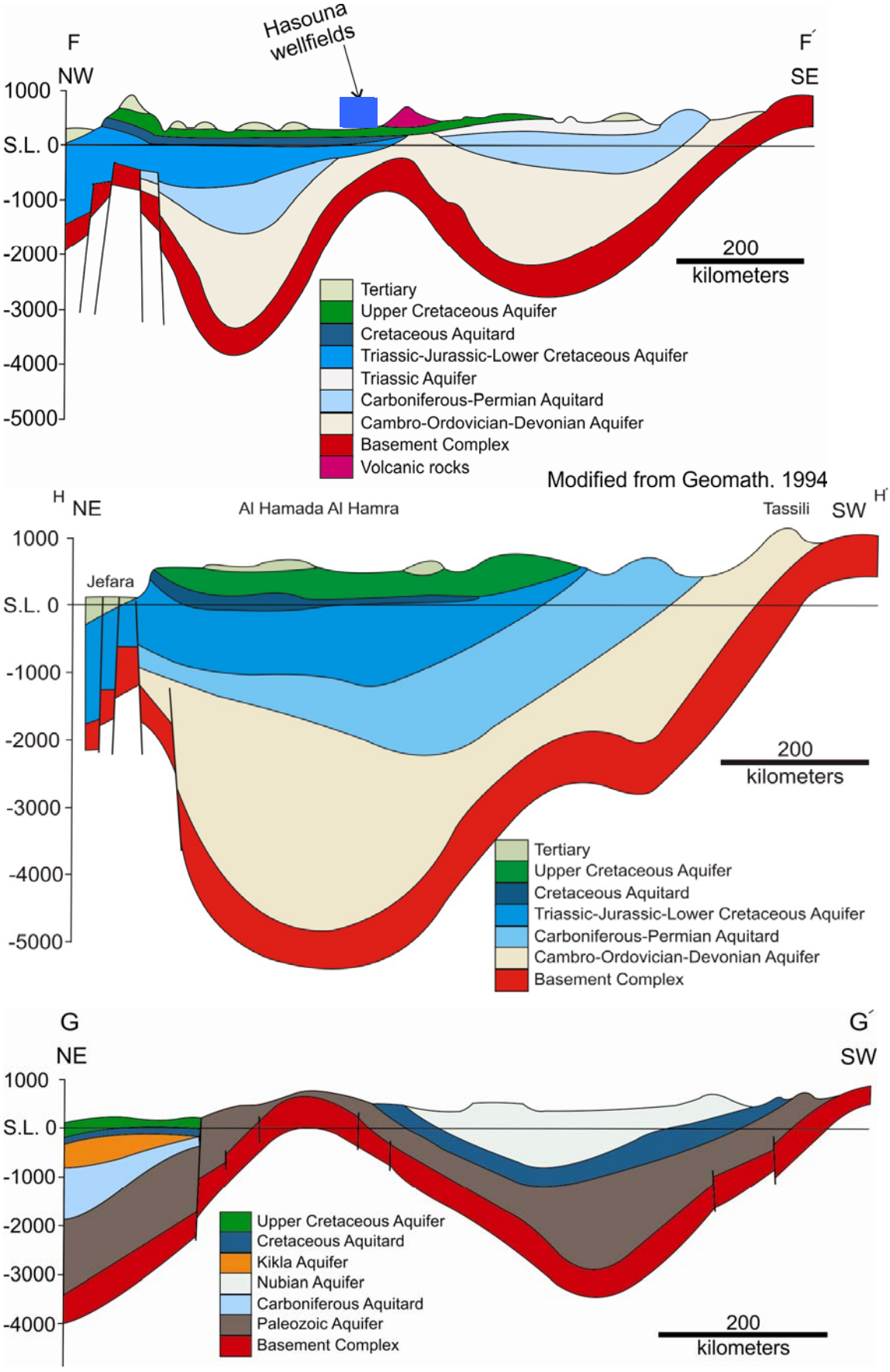

Figure 4.8: Hydrogeological cross-sections F-F´, H-H´, and G-G´of groundwater aquifers of the Hasouna study area (modified from Geomath, 1994).

The Figure 4.9 represents Cross-sections (D-D´ & E-E´) within the Hasouna study area of the regional aquifers system and the main faults.

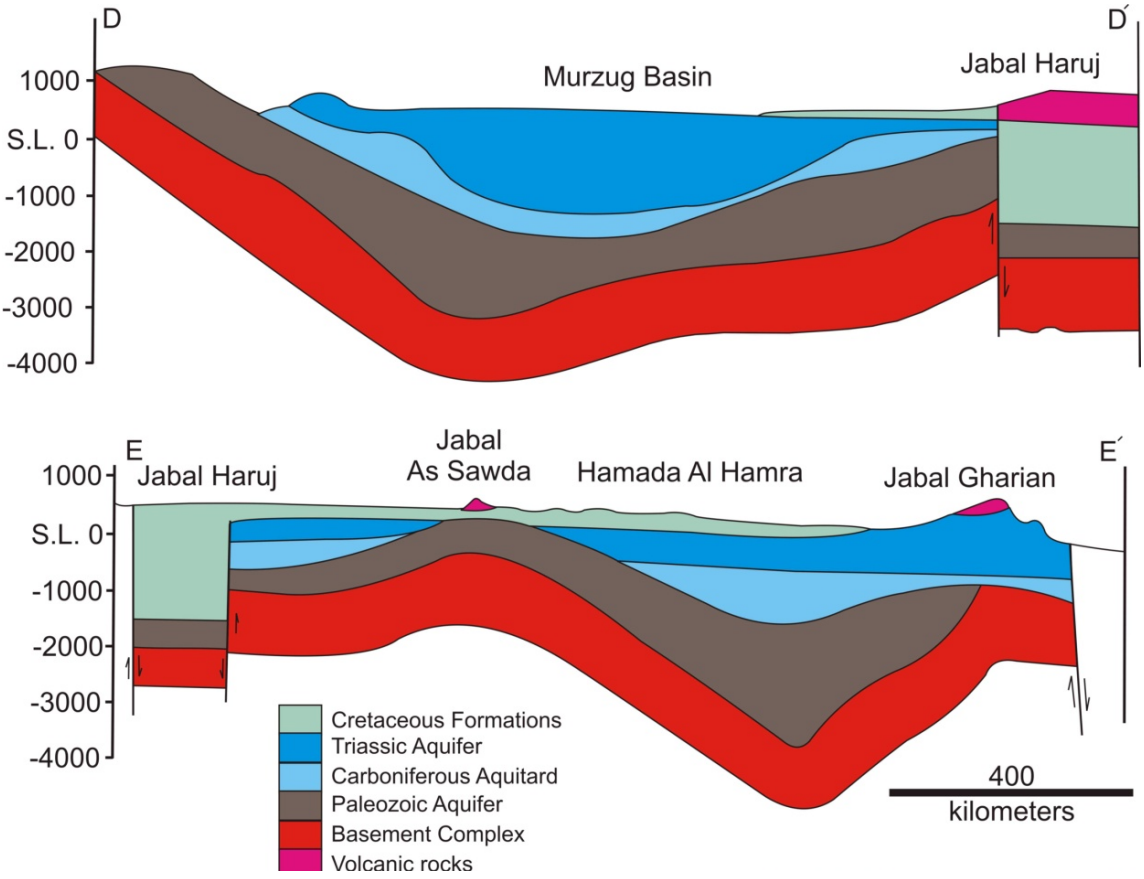

Figure 4.9: Hydrogeological cross-section (D-D´ & E-E´) of groundwater aquifers of the Hasouna study area (modified from Geomath, 1994).

The lithologic units of drill cuttings are reported in Table 4.2. The major litho units, which characterize the study area, are sandstone with different grain sizes, with thin intercalations of clay, limestone and gypsum (Tables 4.2 and 4.3).

Table 4.2: Typical results of core sample description for the well 152/D1, NEJH in the Hasouna area (GMRA).

Depth Interval [m]	Lithological description
0 - 23	Limestone, yellow, reddish, pink, locally with thin intercalations of Clay, yellow and Gypsum, white.
23 - 49	Sandstone, medium grained, subangular-subrounded, weakly to moderately cemented, whitish (95-100%); Sandstone, ferruginous, brick-red (max. 5%).
49 – 82	Sandstone, fine to medium grained, subrounded, moderately cemented, whitish.
82 - 115	Sandstone, medium to coarse grained, subangular-subrounded, moderately to well cemented, whitish (90-95%); Sandstone, ferruginous, reddish-brown (5-10%).
115 - 142	Sandstone, fine to medium grained, subrounded, moderately cemented, white, light brown, yellow (90%); Sandstone, ferruginous, rusty, brick-red (10%).
142 - 192	Sandstone, fine to medium grained, subrounded, moderately cemented, white, yellow, light brown.
192 - 238	Sandstone, medium grained, with local coarse grained variances, subangular to subrounded, moderately cemented, light brown, white (75-80%); Sandstone, ferruginous, reddish-brown (15%), Kaolin, white (5-10%).
238 - 283	Sandstone, medium to coarse grained, subangular to subrounded, moderately cemented, light brown to reddish-brown (85-90%); Sandstone, ferruginous, brick-red (10-15%).
283 - 363	Sandstone, fine grained, with local medium grained variances, subrounded, moderately cemented, white to yellow (90-92%); Sandstone, ferruginous, reddish-brown (5-7%); Kaolin, white (3%).
363 - 425	Sandstone, fine to medium grained, subrounded, moderately cemented, white, grey, yellowish-white (80-88%); Sandstone, ferruginous, dark brown to black (10-15%); Kaolin, white (3%).
425 - 500	Sandstone, medium grained, subangular-subrounded, weakly to moderately cemented, white, grey (92-96%); Sandstone, ferruginous, reddish-brown (3-5%); Kaolin, white (1-3%).

4.2.2 HYDROGEOLOGICAL CLASSIFICATION OF INDIVIDUAL AQUIFERS IN WJS

4.2.2.1 UPPER CRETACEOUS AQUIFER (UC)

In the Hamada Al Hamra and in Al Jufrah area the Upper Cretaceous (UC) aquifer corresponds to the upper aquifer in this region. The water bearing formations consists of fractured dolomitic limestone with marl, shale and gypsum of Late Cretaceous age, (Figures 4.8 and 4.9 and Tables 4.3 and 4.4). This aquifer includes the Mizda, the Tigrinna and Nalut Aquifers as described by Pallas (1980). The thickness of this aquifer ranges from 100 to 250 m. The field transmissivity is low (50 m² /day) except where the limestones are

fractured as it is in the Al Jufrah area, where the transmissivity is high (2.000 m²/day). The storativity ranges from 1.7 10^{-2} up to 2.6 10^{-4} in the confined zones and the specific yield is up to 1.7 10^{-1} in the unconfined areas (Geomath, 1994).

4.2.2.2 CAMBRO-ORDOVICIAN DEVONIAN AQUIFER (COD)

The Cambro-Ordovician Devonian (COD) aquifer occurs in both the Hamada Al Hamra and Murzuq basins and corresponds to the aquifer of the WJS aquifer system. The COD aquifer is considered as the main aquifer within the study area and in the Al Gargaf region. It is equivalent to the Lower Aquifer of the WJS and is named the Hasouna Formation Aquifer. The aquifer consists of fractured sandstone with inter-granular porosity averaging to 20% measured on core samples. This aquifer has a very large lateral extent.

The COD Aquifer is some parts unconfined, but mainly confined. It covers 500 to 1.500 m thick quartzitic continental sandstones, which range in transmissivity between 1.500 and 2.000 m²/day. The storativity is variable, ranges from 2.2 10^{-5} to 2.0 10^{-3} in the confined and semi-confined areas. But in the unconfined zones the specific yield is more uniform, ranging from 2.7 10^{-2} to 6.4 10^{-2} (Geomath, 1994). The change in transmissivity values across the Cambro-Ordovician aquifer in all of Hasouna Wellfields is related to different structures and the presence of clay layers. The average value of transmissivity (pumping) for the Cambro-Ordovician aquifer in all Hasouna Wellfields is 2.088 m^2/day and individual value range from a minimum of 101 m^2/day to a maximum 5.970 m^2/day. The production wells in the Hasouna water-fields in the study area are pumping water from Cambro-Ordovician sandstone aquifer. The Paleozoic aquifer system is the deepest groundwater reservoir occurring in the study area. It consists of Devonian and Cambro-Ordovician sandstone separated by thick layers of lower Silurian shale (Figures 4.8 and 4.9, Tables 4.3 and 4.4).

4.2.2.3 CAMBRO-ORDOVICIAN TO TERTIARY AQUIFER (CO-TE)

The Cambro-Ordovician to Tertiary aquifer occurs in the area east of the Hun Graben-Al Fugha fault. This confined aquifer consists of a 500 to 1.500 m thick sequence of sandstones, fractured dolomite, and limestone with alternating marl, shale and gypsum beds. There are no transmissivity and storativity data for this aquifer available (Figures 4.8 and 4.9, Tables 4.3, and 4.4).

4.2.2.4 ZIMAM AQUIFER

This aquifer is crouched with respect to the major Cambro-Ordovician aquifer, and has poor hydraulic properties as well as high salinity (Binsariti et al.,

2000). Jurak (1978) in his mapping for the Jabal Hasouna Sheet pointed out that the Upper Cretaceous aquifer (Zimam) exists in the northern and north-eastern part of the Jabal Hasouna area (Fig. 4.4). The Zimam Formation has claystones and marls in the lower members, which are layers of relatively low permeability. The Zimam aquifer has heterogeneous sediments such as marly limestone, dolomite, limestone, sandy limestone, siltstone, unconsolidated deposits of sand, gravel, gypsum and anhydrite.

Table 4.3: Groundwater aquifers systems in WJS of Libya (modified from Geomath, 1994).

Aquifers	Al Hammada Al Hamra Basin
Upper aquifer	Upper Cretaceous (UC) fractured set in dolomitic limestone, marl, and gypsum. Thickness: 100-250 m. Where local fracturing occurs, e.g. Al Jefara: Transmissivity 2000 m^2/day
Lower aquifer	Cambro-Orovician-Devonian (COD) quartzitic continental sandstone. Note: The Devonian sandstone and an intervening Silurian shale aquiclude are both eroded in areas of abstraction allowing the COD sandstone to be modelled as a single aquifer. Thickness: 500 – 1400m. Transmissivity: 1500-2000 m^2/day

In the study area, to the east of Jabal Al Hasouna, mapping and exploratory drilling described by Jurak (1978) revealed that the dominant structural elements are faults. The presence of these faults combined with information on water quality variation from the chemical analysis in this study area support the hydraulic connection between the Zimam and Hasouna Aquifers.

Table 4.4: Average of hydraulic parameters in aquifers the Western Jamahiriya system (modified from Geomath, 1994).

Aquifer	Number of data points	Transmissivity [m^2/day]			Storativity		
		Max.	Min.	Mean	Max.	Min.	Mean
UC	6(6)	2590	1650	1948	1.7×10^{-2}	2.6×10^{-4}	1.9×10^{-3}
COD	16(11)	4000	400	2140	3.2×10^{-2}	2.2×10^{-4}	1.3×10^{-3}

Note: UC (Upper Creataceous), and COD (Cambro-Orovician-Devonian)

4.3 AQUIFER CHARACTERISTICS AND GROUNDWATER QUALITY

4.3.1 AQUIFER RECHARGE AND WATER QUALITY

The majority of Libya groundwater resources are confined in paleo aquifers, which were filled thousands of years ago and are under extreme exploitation for daily demands. Groundwater in Libya has been considered as an important source of water supply due to deep aquifers in central Sahara basins with large storage capacity and a low susceptibility to contamination and pollution.

Water quality in the aquifer system of the study area varies from excellent in some wells, with mean value of 1125 mgL^{-1} total dissolved solids (TDS), to moderate with high salinity in some water wells (Table 7.2). These saline water wells interact with the saline Zimam Aquifer. As a result of hydrochemical analysis, the water is generally satisfactory for agricultural purposes but needs some nitrate treatment for drinking use. The water quality values are given in section 7.9.

Former chemical analysis of water samples from these exploratory drilling wells (GMRA, 1995) showed generally good quality for drinking water supply. The total dissolved solids (TDS) range between 434 and 1.500 mgL^{-1}, except in well T 29 (29/89) where the TDS reaches about 3.270 mgL^{-1}. This high salinity in the Hasouna groundwater is assumed to reflect the vertically downward leakage of saline water from the intensively fractured Zimam Aquifer (Binsariti et al., 2000) to the Cambro-Ordovician Aquifer (Hasouna Formation).The concentrations of carbon dioxide are relatively high. According to the data base of the Authority GMRA project, average concentration of CO_2 in all Hasouna waterfields is 16 mgL^{-1} and reached a maximum concentration of 97 mgL^{-1} (Table 9.1). This water with high CO_2 concentrations will attack the metal and concrete of pipelines of GMRA project. To solve this problem, it is important to treat the water directly in Hasouna water fields to remove CO_2. The dissolution of carbonate minerals in groundwater is highly dependent on the concentration of CO_2, which originated either from earth's atmosphere or may have been generated by biological processes (Appelo and Postema, 1996). However, high nitrate concentrations were formerly detected in some wells in the Hasouna study area. Nitrate concentrations exceeding 50 mgL^{-1} NO_3^- have been already recorded from groundwater in the study area of Hasouna wellfields. Therefore, the water in some wells is unsuitable for human consumption without dilution by mixing with water of low nitrate concentration level.

5 FUNDAMENTALS

5.1 NITROGEN

5.1.1 NITROGEN CYCLE

The nitrogen cycle in natural surroundings involves many organic and inorganic compounds. The most common forms of inorganic nitrogen are nitrate (NO_3^-), nitrite (NO_2^-), ammonia (NH_3), ammonium (NH_4^+), and gaseous nitrogen (N_2). The movement and transformation of most important nitrogen compounds through the biosphere can be characterized by the nitrogen cycle depicted in Figure 5.1. The atmosphere acts as a reservoir of nitrogen in the form of N_2 (the atmosphere consists of 79% N_2).

Transformation of nitrogen compounds can occur through several mechanisms, including fixation, ammonification, synthesis, nitrification, and denitrification. Nitrogen fixation process is the conversion of nitrogen by bacteria into ammonia and ammonium. Ammonification refers to the change from organic nitrogen to the ammonium form. In general, ammonification occurs during decomposition of animal and plant tissue and animal fecal matter (US EPA, 1993).

Nitrification occurs through a reaction of ammonium with oxygen via individual microbiological processes according to the reactions (Freeze and Cherry, 1979; Kendall, 1998)

$$2\ NH_4^+ + 3O_2 \rightarrow 2\ NO_2^- + 4\ H^+ + 2\ H_2O \quad (1)$$

$$2\ NO_2^- + O_2 \rightarrow 2\ NO_3^- \quad (2)$$

Denitrification is a microbially facilitated process that reduces nitrate (NO_3^-) to nitrogen gas (N_2), through a series of intermediate reactions (Appelo and Postma 1994). This process is anaerobic and carried out by denitrifying bacteria (e.g. Pseudomonas); (Kendall, 1998). The denitrification reactions are displayed in reactions like:

$$NO_3^- \rightarrow NO_2^- \rightarrow NO \rightarrow N_2O \rightarrow N_{2(g)} \quad (3)$$

The reduction series of nitrate in groundwater can be written as:

$$NO_3^- \rightarrow NO_2^- \rightarrow N_{2(g)} \rightarrow NH_4^+ \quad (4)$$

During denitrification, denitrifying bacteria use organic carbon as energy source and nitrate as an electron acceptor in systems with low levels of oxygen (e.g. Freeze and Cherry, 1979) according to the overall reaction

$$5\ CH_2O + 4NO_3^- + 4H^+ \rightarrow 2\ N_2 + 5\ CO_2 + 7\ H_2O \quad (5)$$

In the natural environment almost all nitrogen found in the soil and subsoil originates from the atmosphere. In water nitrogen may oxidize and occur as nitrate (NO_3^-) or nitrite (NO_2^-). In reduced form nitrogen may appear as ammonium (NH_4^+) circulating in the nitrogen cycle (Matthess 1994).

The main reaction pathways for nitrate from gaseous N_2 are based on the decomposition of ozone, which is generating NO_2^- and NO_3^- according to the equations. NO_2 can be further oxidized by O_3 to NO_3 during the daytime.

In an air mixture containing O_3, NO_2^- and NO_3^-, two main reactions occur (Atktinson, 1997).

$$O_3 + NO \rightarrow O_2 + NO_2^- \quad (6)$$

$$NO_2^- + O_3 \rightarrow NO_3^- + O_2 \quad (7)$$

5.1.2 NITRATE IN GROUNDWATER AND HUMAN HEALTH

Nitrate compounds are very soluble in water and quite mobile in the environment. Thus nitrate is an integral part of the nitrogen cycle in the environment. Studies of effects of nitrate in drinking water for humans have suggested that exposure can have both acute and long-term health effects, like cancer (Ward, 2005).

A high nitrate concentration is a potential human health hazard, especially for infants, by causing methemoglobinemia. Methemoglobinemia, also called "blue baby syndrome" occurs, where the nitrate is converted to nitrite. Nitrate may also interact with organic compounds (secondary amines) to form N-nitrosamines, which are known to cause cancer (Kendall et al., 2007). The excessive amount of nitrate in water resources can potentially have deteriorative effects on both human health and on ecological systems of impacts areas. The World Health Organisation (WHO, 2004) suggests an upper limit value of 50 mgL^{-1} for nitrate.

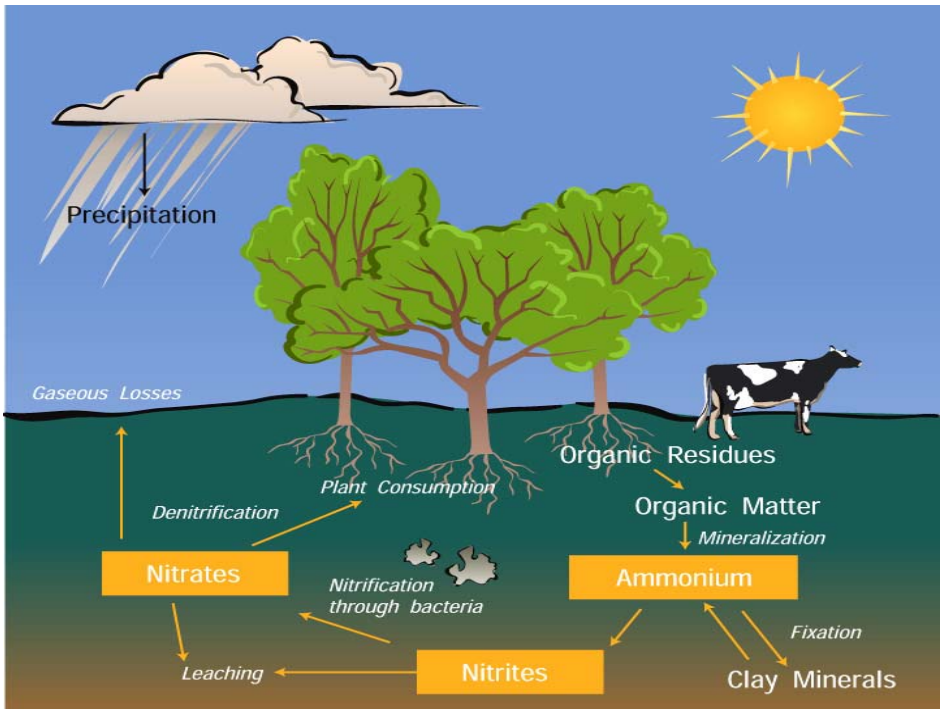

Figure 5.1: Nitrogen cycle shows the nitrogen travel through the living and non-living parts of the earth system, image courtesy UCAR (National Center for Atmospheric, USA).

5.1.3 SOURCE AND ORIGIN OF NITRATE

Nitrate is one of the most widespread groundwater compounds in many countries. Main nitrate sources are from atmosphere, decaying plants and other organic matter, livestock waste, nitrogen based fertilizers, septic tank systems, dissolution of evaporation deposits, and industrial wastewater (Figure 5.1). Accordingly, nitrate in groundwater may result from point sources such as sewage disposal systems and livestock facilities, non-point sources such as fertilized cropland, and agricultural farm activities, or naturally occurring sources of nitrogen.

5.2 SULPHATE

Sulphur is found in groundwater mostly as sulphate anion (SO_4^{2-}) from leaching from gypsum, anhydrite, and other sulphate salts, like kieserite, epsomite etc. from marine and terrestrial evaporates.

Gypsum ($CaSO_4\ 2H_2O$) is one of the most common evaporate minerals occurring in terrestrial, lacustrine and marine sedimentary environments (Waston, 1979). The dissolution of gypsum can be expressed by the reaction

$$CaSO_4\ 2H_2O \rightarrow Ca^{2+} + SO_4^{2-} + 2H_2O \qquad (8)$$

Besides dissolution of sulphate containing minerals, common sources of sulphur are the atmosphere with wet and dry deposition, the admixture of seawater sulphate, and oxidation of pyrite and other sulphide minerals. Thus, sulphate in groundwater has various origins:

1. dissolution of soluble sulphate minerals in sedimentary rocks,

2. oxidation and leaching of sedimentary sulphides (mostly pyrite),

3. directly from the atmosphere and soil, or

4. from anthropogenic sources like from acid rain and organically-bound sulphur (Moncaster et al., 2000).

The SO_4^{2-} concentration in the groundwater may be reduced by precipitation of sulphate containing solids (however mostly high soluble), absorption phenomena, and sulphate reduction by bacteria (e.g. Jorgensen, 1982). The bacteria of the genus Desulfovibrio reduce the sulphate (SO_4^{-2}) according to the reaction

$$2CH_2O + SO_4^{2-} \rightarrow 2HCO_3^- + H_2S \quad (9)$$

The limit of sulphate in potable water is about 250 mgL^{-1}. The average daily intake of sulphate from drinking water, air and food is approximately 500 mgL^{-1}, food being the major source.

The presence of sulphate in drinking water can cause noticeable taste, and very high levels might cause a laxative effect in unaccustomed consumers. No health based guideline value has been derived for sulphate.

5.3 STABLE ISOTOPES

In hydro-geological and geochemical studies distributions of stable isotopes are commonly used to provide information about geochemical evolution, recharge processes, water-rock interaction, and the origin of compounds (Clark and Fritz, 1997; Kendall and McDonell, 1998; Cook and Herczeg, 2000).

Table 5.1 gives the stable isotope ratios used and the respective international standards. The isotopic compositions are expressed as δ-values with respect to the Air, V-SMOW, and V-CD standards for $\delta^{15}N$, $\delta^{18}O$, $\delta^{17}O$, $\delta^{2}H$, and $\delta^{34}S$, respectively.

Table 5.1: Table of main stable isotopic parameters with their international standard.

	Standard	δ value
V-SMOW	Vienna Standard Mean Ocean	$\delta^{18}O$
V-SMOW	Vienna Standard Mean Ocean	$\delta^{2}H$
Air nitrogen	Earth`s atmosphere	$\delta^{15}N$
V-CDT	Vienna Canon Diablo Meteorite	$\delta^{34}S$

5.3.1 DEUTERIUM AND OXYGEN-18 OF WATER

The isotopic composition of hydrogen and oxygen, which are the elements of the water molecules, are variable because their isotopes are fractionated during some chemical and physical processes occurring in nature. Hydrogen has two stable isotopes (^{1}H and ^{2}H), while oxygen has three stable isotopes (^{16}O, ^{17}O, and ^{18}O). The isotopic composition of hydrogen and oxygen are reported in terms of differences of ^{2}H / ^{1}H and ^{18}O / ^{16}O ratios relative to Vienna SMOW (Standard Mean Ocean Water); (Clark and Fritz, 1997), and are expressed as per mil (‰) differences by the following equations:

$$\delta^{2}H_{sample} = \left(\frac{(^{2}H/^{1}H)_{sample}}{(^{2}H/^{1}H)_{VSMOW}} - 1 \right) \times 1000 \text{ ‰ V-SMOW} \quad (10)$$

$$\delta^{18}O_{sample} = \left(\frac{(^{18}O/^{16}O)_{sample}}{(^{18}O/^{16}O)_{VSMOW}} - 1 \right) \times 1000 \text{ ‰ V-SMOW} \quad (11)$$

Positive values of $\delta^{2}H$ and $\delta^{18}O$ in ‰ indicate enrichment of a sample in deuterium ^{2}H and oxygen ^{18}O compared to the standard, while negative values imply depletion of these isotopes in the samples relative to the standard (VSMOW).

The Global Meteoric Water Line (GMWL) was described by Craig (1961), and is commonly used to identify the origin of groundwater recharge. The regression line of GMWL is defined by following equation:

$$\delta^{2}H = 8\ \delta\ ^{18}O + 10 \text{ ‰ VSMOW} \quad (12)$$

The relationship between δ^2H and $\delta^{18}O$ is plotted in Figure 5.2. Thus, the Global Meteoric Water Line provides a useful benchmark against regional or local waters and their isotopic composition. The Libyan Local Meteoric Water Line (LMWL) is based on the spatial isotope data of precipitation, which yielded the following line (IAEA):

$$\delta^2H = 8\ \delta^{18}O + 12‰\ \text{VSMOW} \quad (13)$$

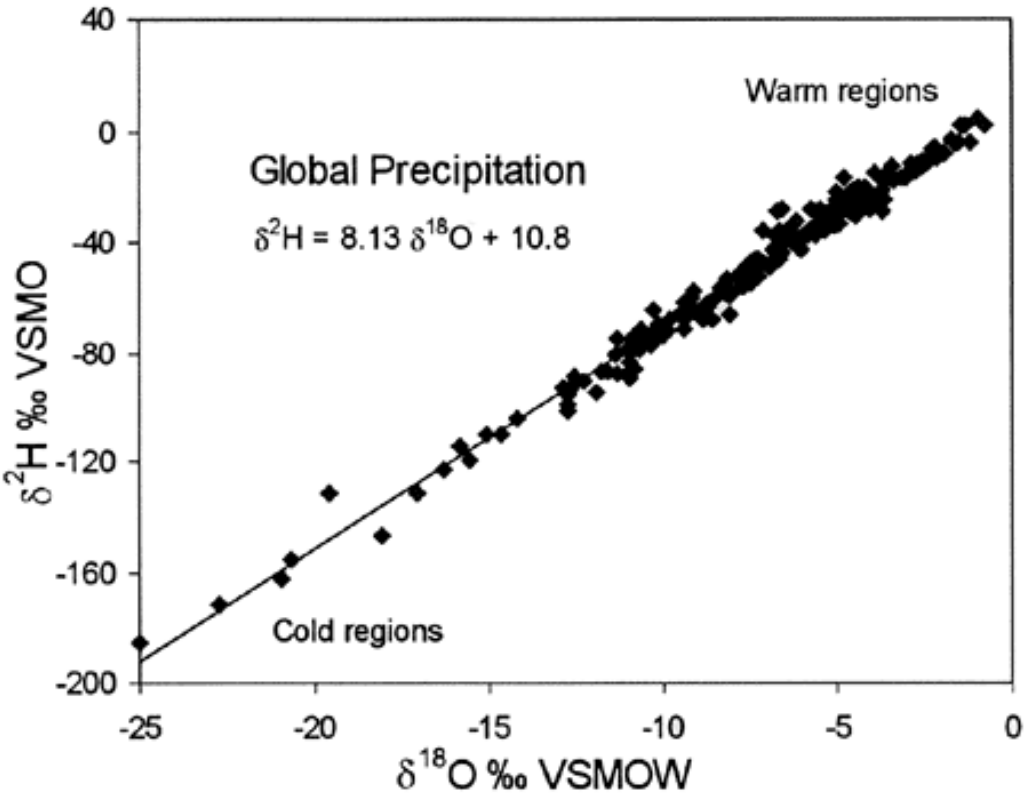

Figure 5.2: The relationship between O and H isotopes gives the GMWL (Clark and Fritz, 1997).

5.3.2 NITROGEN AND OXYGEN ISOTOPES OF DISSOLVED NITRATE

The analysis of both $\delta^{15}N$ and $\delta^{18}O$ of dissolved nitrate provides excellent separation of different nitrate sources (Fig. 5.3). The stable isotopes of nitrogen, ^{15}N and ^{14}N, are often useful in distinguishing sources of nitrogen contamination (Kendall et al., 2007). The isotopic composition of nitrogen is expressed as:

$$\delta^{15}N_{sample} = \left(\frac{(^{15}N/^{14}N)_{sample}}{(^{15}N/^{14}N)_{Air}} - 1 \right) \times 1000\ ‰\ \text{V–Air} \quad (15)$$

Where $^{15}N/^{14}N$ is the ratio of the number of ^{15}N atoms to the number of ^{14}N atoms in the sample or standard. The isotopic composition of the sample is measured relative to the atmospheric nitrogen (AIR) reference (Clark and Fritz, 1997). High nitrate levels in groundwater of semi-arid regions have been observed and documented in different research studies worldwide. The occurrence of nitrate in groundwater is a direct result of natural accumulation during the palaeo recharge processes. However, in semi-arid to arid regions nitrogen losses from the soil zone and accumulation of nitrate in the groundwater can take place naturally without any anthropogenic interference (Tredoux, 1993).

Nitrogen isotope fractionation occurs during several steps in the nitrogen cycle (see Figure 5.1). The usefulness of nitrogen isotopes in water-related studies lies in the fact that certain major potential sources of nitrogen contamination can be distinguished by $\delta^{15}N$ values. Typical $\delta^{15}N$ ranges are given in Table 5.2 for important sources of nitrogen contamination in groundwater (Seiler, 1996).

Table 5.2: Typical $\delta^{15}N$ values for nitrogen contamination in the groundwater (Seiler, 1996).

Potential Contaminant Source	$\delta^{15}N$ [‰]
Commercial fertilizer	-4 to +4
Animal or human waste	> +10
Precipitation	-3
Organic nitrogen in soil	+4 to +9

The use of nitrogen isotopes is well established for identifying nitrate sources, however, this method has some severe limitations due to overlapping signals and changes in the isotopic signal with denitrification within an aquifer (see Fig. 5.3). During microbial denitrification of NO_3^- to N_2 there is also an isotopic fractionation which preferentially utilizes ^{14}N in the conversion to N_2. This leaves the remaining NO_3^- isotopically more enriched in ^{15}N (Fig. 5.3).

The nitrogen isotope ^{15}N signatures may reflect mixing from multiple sources. Therefore, using nitrogen isotope alone for determining sources is often insufficient. To correct this, several studies promote the use of stable isotope of oxygen on nitrate to reduce the ambiguity in source determinations (Wassenaar, 1996). Figure 5.3 shows the relationship between $\delta^{18}O_{nitrate}$ and $\delta^{15}N_{nitrate}$ which can be used to fingerprint nitrate sources (Kendall, 1998). The application of the $\delta^{15}N\text{-}NO_3^-$ and $\delta^{18}O\text{-}NO_3^-$ isotope ratios is a useful technique to differentiate between each possible source, and to identify sources and fate of nitrate in groundwater samples (see Section 8.4).

More recently a triple stable isotope approach using $^{18}O/^{16}O$ and $^{17}O/^{16}O$ signals in NO_3 was successfully applied to discover the contribution of NO_3 from different sources. Interestingly atmospheric NO_3 ($NO_{3,atm}$) is exclusively characterized by a ^{17}O-excess, where non-mass dependent isotope fractionation (NMDF) during the formation of ozone followed by photochemical reactions between atmospheric NO_x and O_3 to NO_3 results in non-zero $\Delta^{17}O_{NO3}$ values ($\Delta^{17}O = \delta^{17}O - 0.52\ \delta^{18}O$; (Michalski et al., 2003; Thiemens, 2006)). Böhlke et al., 1997, for instance, found evidence from $^{15}N/^{14}N$ and $^{18}O/^{16}O$ isotope analyses for atmospheric source of NO_3 for nitrate-rich salts in Atacama (Chile) and Mojave Desert (California). But the atmospheric origin of NO_3 in the Atacama deposits was finally confirmed by pronounced ^{17}O-excesses (Michalski et al., 2004a). Since then, $NO_{3,atm}$ was successfully quantified using ^{17}O-excess for various desert deposits and dissolved NO_3 in

modern groundwater, lakes and wet depositions (Dejwakh et al., 2012; Li et al., 2010; Michalski et al., 2005; Michalski et al., 2004b; Tsunogai et al., 2011; Tsunogai et al., 2010).

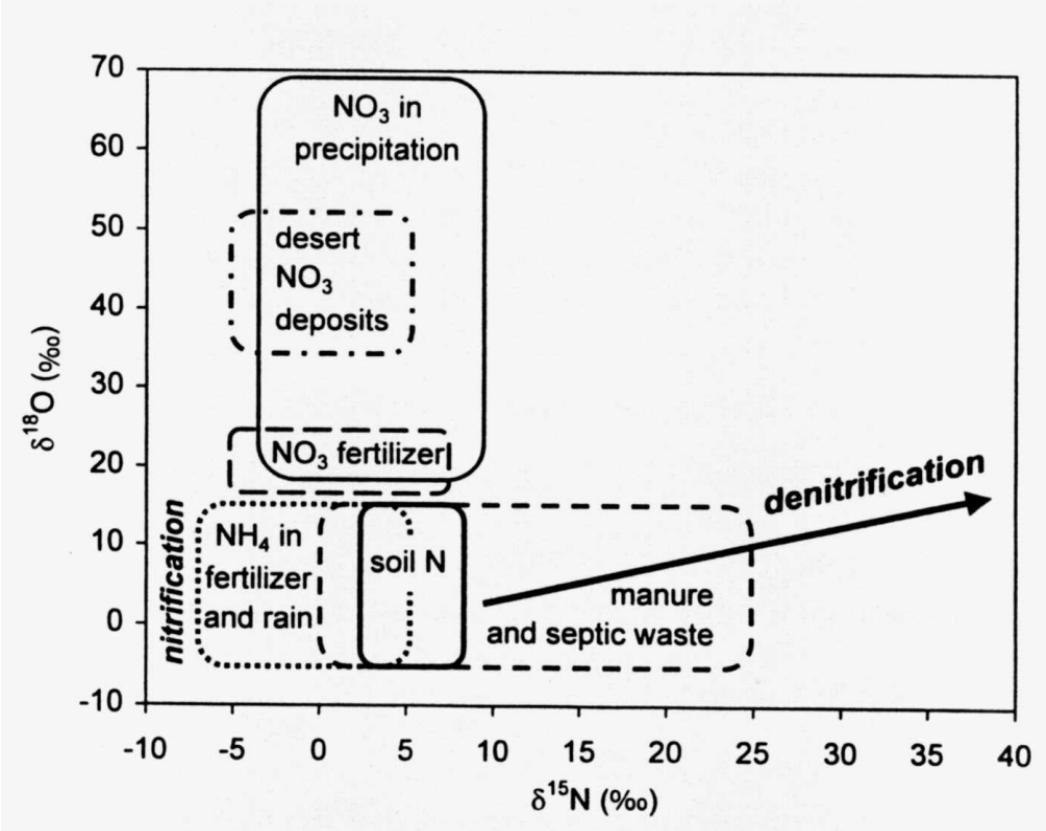

Figure 5.3: Typical isotopic nitrogen and oxygen ranges of nitrate (Kendall, 1998).

5.3.3 SULFUR AND OXYGEN OF DISSOLVED SULPHATE

The stable isotopes of dissolved sulphate $\delta^{34}S$ and $\delta^{18}O$ are commonly used to identify the different sources of sulphate. Sulfur has four stable isotopes: ^{32}S (95.02%), ^{33}S (0.75%), ^{34}S (4.21%), and ^{36}S (0.02%). Stable isotopic compositions are reported as ratios of $^{34}S/\ ^{32}S$ in ‰ relative to the standard (Vienna Canyon Diablo Triolite) V-CDT (Krouse and Coplen, 1997) according to the equation:

$$\delta^{34}S_{sample} = \left(\frac{(^{34}S/^{32}S)_{sample}}{(^{34}S/^{32}S)_{VCDT}} - 1 \right) \times 1000\ ‰\ \text{V–CDT} \qquad (16)$$

The $\delta^{34}S$ values of groundwater are highly variable and depend on the nature of the sulphur inputs to the water. Sulfur has many forms in groundwater, but it is mainly found in the form of sulphates. Some dissolved organic sulphur (DOS), elemental sulphur and from sulfides mineral might also be present in groundwater.

Figure 5.4 shows typical isotope ranges of $\delta^{34}S$ and $\delta^{18}O$ for different sources. Sulphate derived from dissolved evaporates always has positive $\delta^{34}S$ and $\delta^{18}O$ values from +10 to +30‰ and from +12 to 20‰, respectively (Claypool et al., 1980). The commonly accepted $\delta^{34}S$ value of modern seawater sulphate is +20.0‰ (Sasaki, 1972). Mediterranean seawater gave a $\delta^{34}S$ value of +20.5‰ (Nielsen, 1978). The $\delta^{34}S$ values of sulphate in atmospheric deposition in Central Europe vary between 0 and +7‰ and $\delta^{18}O$ values range between +7 and +17‰ (Novak et al., 2001).

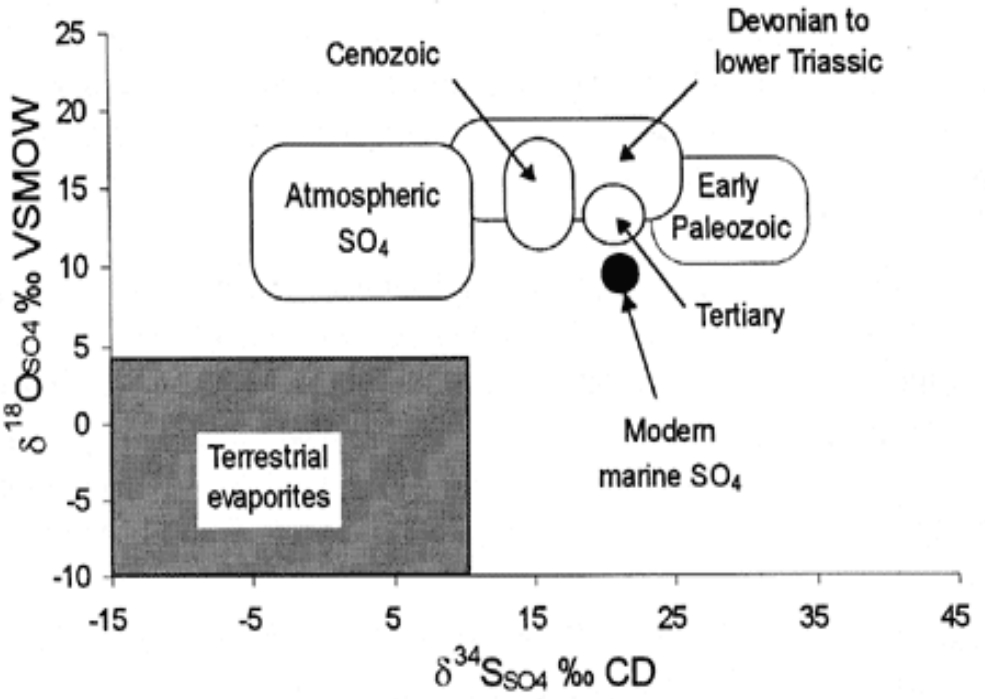

Figure 5.4: Various isotopic sulphur and oxygen ranges in sulphate, (Clark and Fritz, 1997).

6 METHODOLOGY

6.1 SAMPLING CAMPAIGNS

The samplings of groundwater in Hasouna Wellfields were collected along different production groundwater wells. The location of sampling points is illustrated in Fig. 6.1. About 57 water samples were collected for chemical and isotopic analysis (see Tables 12.1 and 12.8). The groundwater sampling was conducted during three sampling campaigns (August, November, and December 2007). To understand the overall distribution of different groundwater ion parameters in the south of the study area of Hasouna water fields, nine groundwater wells in the Wadi Ash Shati study area (see Fig. 12.1 and Tables 12.2 and 12.8 in Appendix (II)) were sampled and analyzed for hydrochemical and isotope parameters. Sampling was performed in September, 2009.

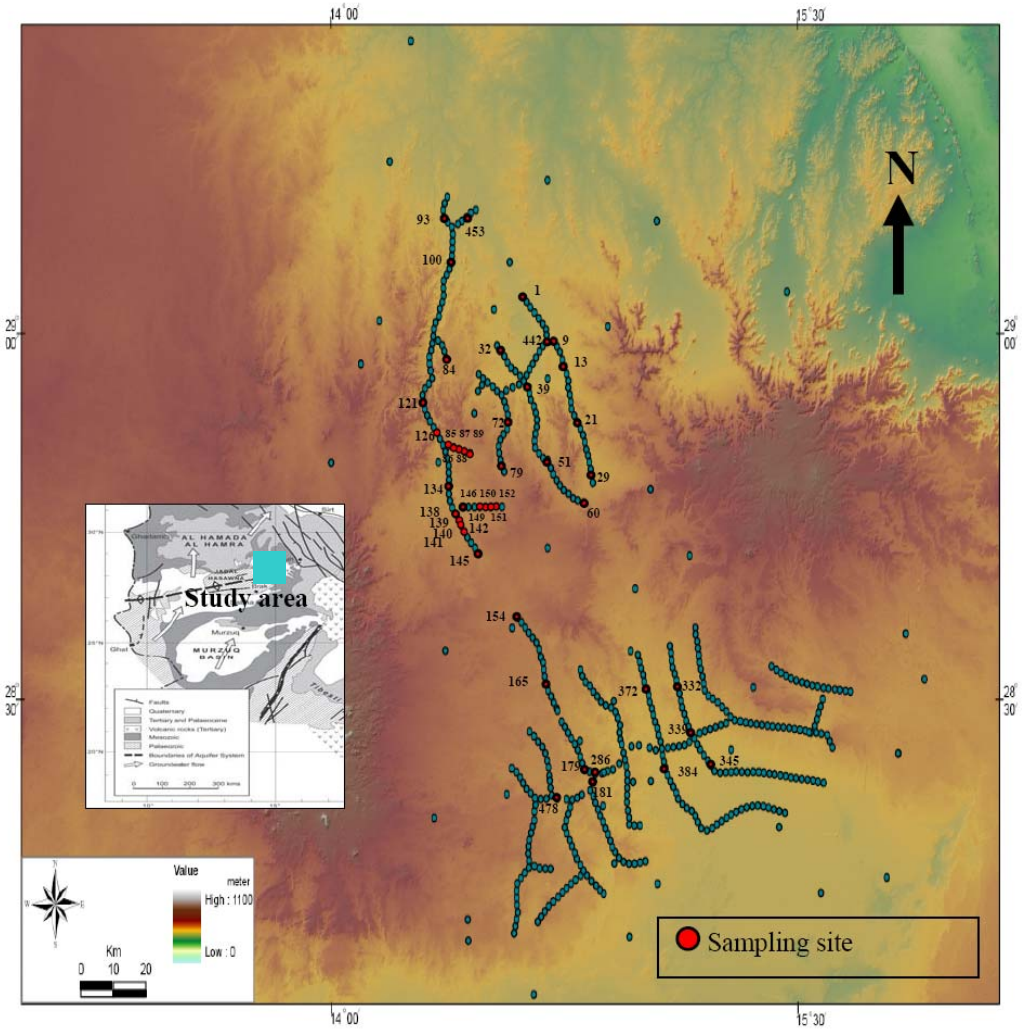

Figure 6.1: Location map of Hasouna water-fields and the layout of the groundwater sampling wells. (Source: GMRA, Libya).

In general, all groundwater samples were filtered in-situ using membranes (0.45µm), transported from Libya to Graz and stored in a fridge for analysis in the hydrochemistry laboratory of the Institute of Applied Geosciences, Graz University of Technology, Austria. Four different types of water samples were taken at each selected well: 50 ml filtered for anion analysis, 100 ml filtered and acidified with 2% HNO_3 for cation and silica analysis, 500 ml filtered for recovery of sulphate as $BaSO_4$ for isotopic analysis, 250 ml for isotope of nitrogen analysis and 500 ml for titration of alkalinity.

6.2 IN SITU PARAMETER

The physico-chemical parameters, electrical conductivity, temperature and pH value were directly determined in the field using a WTW field conductivity meter, model LFT 91 and WTW field pH meter model pH 330 SET. The pH calibration was carried out in the field with pH 4.0, 7.0, and 10.0 standard buffer solutions. In some selected groundwater samples the concentration of dissolved oxygen were also measured in the field.

6.3 ANALYSES OF DISSOLVED COMPONENTS

The cation (e.g. Ca^{2+}, Mg^{2+}, Na^{+}, K^{+}) and silica concentrations of groundwater samples were measured by inductively coupled plasma optical emission spectrometry (Perkin Elmer Optima 330V, ICP-OES, 4300DV) and inductively coupled plasma-mass spectrometry (ICP-MS; Perkin-Elmer Elan 5000). The concentration of anions such as SO_4^{2-}, Cl^{-} and NO_3^{-} were analysed using ion chromatography (IC-Dionex DX 500). The cations and anions were analyzed at the laboratory of the Institute of Applied Geosciences, Graz University of Technology. Alkalinity was determined by titration with diluted HCl. The results of hydrochemical analysis are given in Table 12.1 (Appendix II). The concentrations of major cations, Ca^{2+}, Mg^{2+}, Na^{+}, K^{+}, and major anions, HCO_3^{-}, SO_4^{2-}, Cl^{-}, NO_3^{-} (usually constituting salinity of water), where calculated Total Dissolved Solids contents (TDS, mgL^{-1}) defines water salinity. The Wadi Ash Shati groundwater samples were also analyzed for the major hydrochemical compositions (see Table 12.2 in Appendix (II)).

6.4 HYDROGEOCHMICAL MODELLING

Distribution of dissolved chemical species, charge balance error, saturation indices etc. were calculated using computer code PHREEQC with phreqqc database (Parkhurst and Appelo 1999). The charge balance error (E) calculated from the analyses is an indicator of the dataset reliability. Charge

balance error is calculated as meqL^{-1} units according to the following formula (Freeze and Cherry 1979) and is expressed as a percentage:

$$E(\%) = \frac{\sum(Cations, meq/l) - \sum(Anions, meq/l)}{\sum(Cations, meq/l) + \sum(Anions, meq/l)} * 100 \quad (17)$$

where E of ± 5% can be generally accepted (Appelo and Postma, 1999; Drever, 1997).

The saturation index is obtained according to the reaction

$$SI = \log (IAP/K_{sp}) \quad (18)$$

where IAP denotes the Ion Activity Product and K refers to solubility product. The saturation indices (SI) are expressed exemplarily for calcite by the equation

$$SI_{calcite} = \log \left(\frac{a_{Ca^{2+}} a_{CO_3^{2-}}}{K_{sp(calcite)}} \right) \quad (19)$$

where (Ca^{2+}) and (CO_3^{2-}) are calcium und carbonate activities, respectively, in aqueous solution and $K_{sp(calcite)}$ is the solubility product of calcite. If SI equals zero the water is saturated with respect to calcite. Positive values of SI indicate supersaturation and negative SI values indicate undersaturation with respect to calcite.

P_{CO2} is the theoretical partial pressure of carbon dioxide in equilibrium with the respective water. P_{CO2} values were estimated as follows:

$$Pco_2 = \frac{(H^+) \cdot (HCO_3^-)}{K_H \cdot K_1} \quad (20)$$

where (H^+) and (HCO_3^-) are activities of hydrogen and bicarbonate ions; K_H is the temperature dependent Henry`s Law constant for CO_2 and K_1 (e.g. $10^{-6.35}$ at 25°C) is the first dissociation constant for carbonic acid (e.g. $K_H = 10^{-1.41}$ at 25 °C).

6.5 STABLE ISOTOPE ANALYSIS

In this current study the stable isotopes of the Hasouna groundwater samples were determined and analyzed for the environmental isotopes of $\delta^{18}O_{H2O}$, $\delta^{2}H_{H2O}$, $\delta^{34}S_{sulphate}$ and $\delta^{18}O_{sulphate}$, $\delta^{15}N_{nitrate}$, $\delta^{17}O_{nitrate}$ and $\delta^{18}O_{nitrate}$, see Table 12.8 Appendix II.

6.5.1 DEUTERIUM AND OXYGEN-18 OF WATER

The $\delta^{2}H$ and $\delta^{18}O$ analyses of the water were performed in the laboratory of JOANNEUM RESEARCH CENTER, Institute of Water Resources Management, Hydrogeology and Geophysics in Graz. The isotopes of hydrogen were measured using a Finnigan DELTA plus XP mass spectrometer working in continous flow mode by chromium reduction technique (Morrison et al., 2001). The oxygen isotopic composition was measured with a Finnigan DELTA plus mass spectrometer using the classic CO_2-H_2O equilibrium method (Horita et al., 1989). The $\delta^{18}O$ and $\delta^{2}H$ values of water were given relative to the Vienna Standard Mean Ocean Water (V-SMOW). Measurement precision was better than ±0.1‰ for $\delta^{18}O$ and ±1‰ for $\delta^{2}H$.

6.5.2 $^{34}S/^{32}S$ AND $^{18}O/^{16}O$ SIGNATURES OF SO_4

Procedure for fixation of SO_4^{2-} as $BaSO_4$ was as follows. The solution (0.5l) was, acidified to pH 2.0 - 2.5 with diluted HCl. About 100 g/l $BaCl_2$ solution equals 10% of the sample volume was added (Ba in excess to SO_4^{2-}) and thus SO_4^{2-} was precipitated as $BaSO_4$ quantitatively. The precipitates barium sulphate was separated by a 0.45 µm membrane using a vacuum filtration unit and washed with deionised water. $BaSO_4$ was dried at 110°C and put in filters and combusted at 900 °C to remove residual organic matter and water.

The $BaSO_4$ was split in samples for $\delta^{34}S$ and $\delta^{18}O$ analysis. Isotope analyses were carried out using a Thermo-Finnigan Delta+ gas mass spectrometer coupled to an Eurovector 3000 elemental analyzer (^{34}S) or a Thermo Finnigan TC/EA (^{18}O) via a Thermo Finnigan Conflo II interface at the Leibnitz Institute for Baltic Sea Research, Warnemünde, Germany. The samples are analyzed for isotopes ^{34}S and ^{18}O by mass spectrometry with the standards of NBS127- (+9.3), SO-5 - (+12.4), and SO-6- (-11.2). IAEA intercalibration material was used for mass spectrometric calibration with respect to the V-CDT und V-SMOW scales. Replicate sulfur and oxygen isotope measurements agreed within ±0.3 and ±0.4 ‰, respectively.

6.5.3 $^{15}N/^{14}N$ AND $^{18}O/^{16}O$ SIGNATURES OF NO_3^-

$^{15}N/^{14}N$ and $^{18}O/^{16}O$ isotope ratio analyses were performed by conversion of nitrate to N_2O using the bacterial denitrifier method technique and direct isotope analysis of the N_2O (Casciotti et al., 2002, Kaiser et al., 2007, and Morin et al., 2008); where the isotope values were precisely measured with an analytical error of ±0.03‰ (Savarino et al., 2007).

Further separate samples were taken for isotopic analyses of dissolved NO_3. $\delta^{15}N$ and $\delta^{17}O$-$\delta^{18}O$ are given in respect to atmospheric N_2 and V-SMOW standard, respectively (see details in Appendix I).

7 RESULTS AND INTERPRETATIONS

7.1 INTRODUCTION

In the present study hydrochemical data are used with the main objective to estimate the origin of dissolved nitrate and to provide an insight into hydrochemical evolution of the groundwater in the study area of Hasouna. The hydrochemical data of the 57 groundwater samples from the Hasouna study area and from the Wadi Ash Shati area are summarized in Tables 12.1 and 12.2 (Appendix II).

7.2 QUALITY ANALYSIS CHECKS AND IONIC BALANCE

The accuracy of the analyzed groundwater data of the Hasouna study area are checked by the anion-cation balance. The sum of the charge generated by anions must be balanced by cations. The equi-charged balanced concentrations of the major cations and anions were compared to ensure that these concentrations were within ±5% of each other, using the charge balance error formula ((Freeze and Cherry, 1979) and Appelo & Postma, 2005), see equation (17).

The groundwater samples of the Hasouna study area are within the above error range. The ionic balance of the Hasouna samples ranged from -4.8% to 4.9%, with a mean value of 0.9 % (Table 7.1).

Table 7.1: Ion balance for the analysed groundwater samples in the Hasouna area.

Statistical parameters	Sum of Anions [meqL^{-1}]	Sum of Cations [meqL^{-1}]	Ionic Balance [%]
Max	28.4	29.1	4.9
Min	8.40	9.10	-4.8
Mean	16.6	16.9	0.9

7.3 FIELD PARAMETERS

The pH value of groundwater varied from 6.54 to 7.51 with a mean value of 7.10, indicating that the pH value of groundwater was in near neutral range (Fig. 7.1, a). The dissolved oxygen (O_2) was measured in only 11 groundwater samples, where the values of O_2 ranged from 4.2 to 6.8 mgL^{-1}, with a mean value of 5.4 mgL^{-1} (Table 7.2).

The groundwater varied in temperature from a minimum of 27.2 °C to a maximum of 35.1 °C with a mean temperature of about 30.3 °C (Table 7.2).

The variation of groundwater temperature is plotted in Figure 7.1 (b), where several groundwater wells have a high temperature gradient anomaly. A temperature anomaly may be related to elevated geothermal gradients due magmatic activities (heat flow), and is considered to be of post-Oligocene age (Klitzsch, 1970), which is documented by basalt intrusions in the Jabal Aswada area.

Table 7.2: Statistical analysis of field measurements, Hasouna Water fields.

Statistical Parameter	T [°C]	pH	$O_{2(aq)}$ [mgL^{-1}]	EC [µS/cm]	TDS [mgL^{-1}]	HCO_3 [mgL^{-1}]
Max	35.1	7.51	6.80	2930	1778	277
Min	27.2	6.54	4.21	860	618	144
Mean	30.3	7.10	5.38	1697	1125	183
Median	29.8	7.10	5.35	1713	1134	175
SD	1.94	0.23	0.91	478	290	32.0
n	57	57	11	57	57	57

$O_{2(aq)}$. = Dissolved Oxygen, SD = Standard Deviation, n = number of measured samples.

The measured electrical conductivities (25 °C) are rather high in the groundwater samples ranging from 860 to 2930 µS/cm with a mean value of 1697 µS/cm (Table 7.2). Lowest conductivity was found in well water 165 (860 µS/cm). As for the spatial distribution of high values of conductivity, they were observed in NEJH water field wells of 152, 151, 150 and 126 (see Figure 10.1).

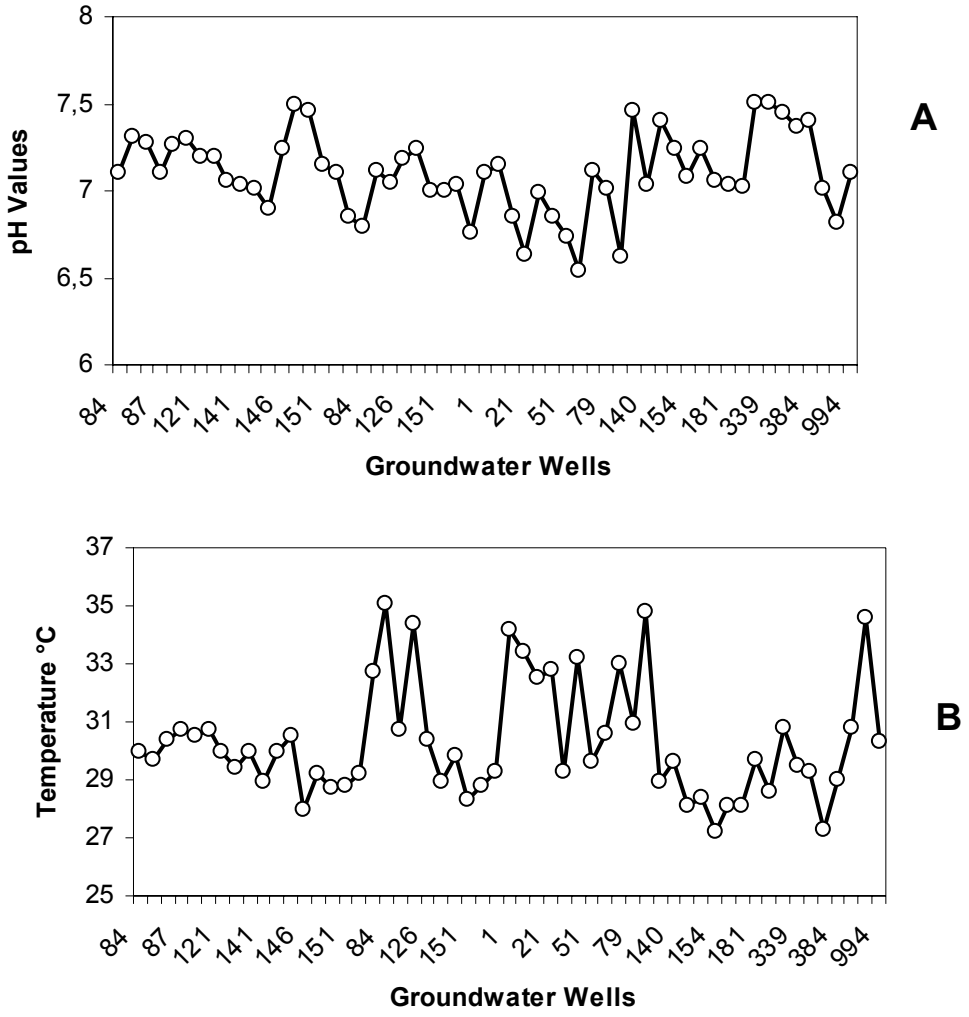

Figure 7.1: (A & B) pH values of collected groundwater and temperature distribution in the Hasouna study area

The range, mean values and standard deviation of physical and alkalinity parameters (temperature, pH, EC, TDS and HCO_3^-) of the Wadi Ash Shati groundwater are shown in Table 7.3.

Table 7.3: Statistical analysis of field measurements in the Wadi Ash Shati groundwater.

Statistical Parameter	T [°C]	pH	EC [µS/cm]	TDS [mgL^{-1}]	HCO_3 [mgL^{-1}]
Max	37.5	6.98	1600	1080	138
Min	32.1	6.40	609	349	94.0
Mean	33.7	6.60	784	487	109
Median	33.1	6.50	710	400	103
SD	1.79	0.21	313	226	17.3
n	9	9	9	9	9

SD = Standard Deviation, n = number of measured samples.

7.4 CONCENTRATION RANGES AND TEMPORAL DISTRIBUTION OF CATIONS AND ANIONS

The concentration range of main cations and anions, of the groundwater are given in Table 7.4. The order of abundance of dissolved cations is $Na^+ > Ca^{2+} > Mg^{2+} > K^+$, with mean values of 189, 119, 32.4 and 5.8 mgL^{-1}, respectively. The order of abundance of dissolved anions is $Cl^- > SO_4^{2-} > HCO_3^-$, > NO_3^- with mean concentrations of 268, 246, 183 and 65.5 mgL^{-1}, respectively. The concentrations of analyzed dissolved ions are presented in Table 12.1 (Appendix II).

Table 7.4: Statistical parameters for the chemical composition of the Hasouna groundwater samples.

Statistical Parameter	Chloride [mgL^{-1}]	Sodium [mgL^{-1}]	Sulphate [mgL^{-1}]	Nitrate [mgL^{-1}]	Calcium [mgL^{-1}]	Magnesium [mgL^{-1}]	Potassium [mgL^{-1}]
Max	533	334	438	114	181	65.1	10.7
Min	68.1	80.0	126	11.1	80.9	15.3	2.20
Mean	268	189	246	65.5	119	32.4	5.80
Median	261	185	259	66.4	119	29.4	5.30
SD	105	64.4	84.3	21.9	26.0	11.2	1.60
n	57	57	57	57	57	57	57

SD: Standard Deviation, n: number of samples

In general, the variations of dominant ions are influenced by the rate of daily production, aquifer characteristics, dissolution processes, and groundwater internal recharge.

The respective minimum and maximum concentrations found in the Hasouna Waterfields study area, indicate large hydrochemical heterogeneity of the groundwater. This is shown in Fig. 7.2 for chloride, nitrate and sulphate concentrations. Fig. 7.2 indicates that these concentrations are positively correlated to each other. In general, chloride, nitrate and sulphate follow similar trends with positively correlated concentrations.

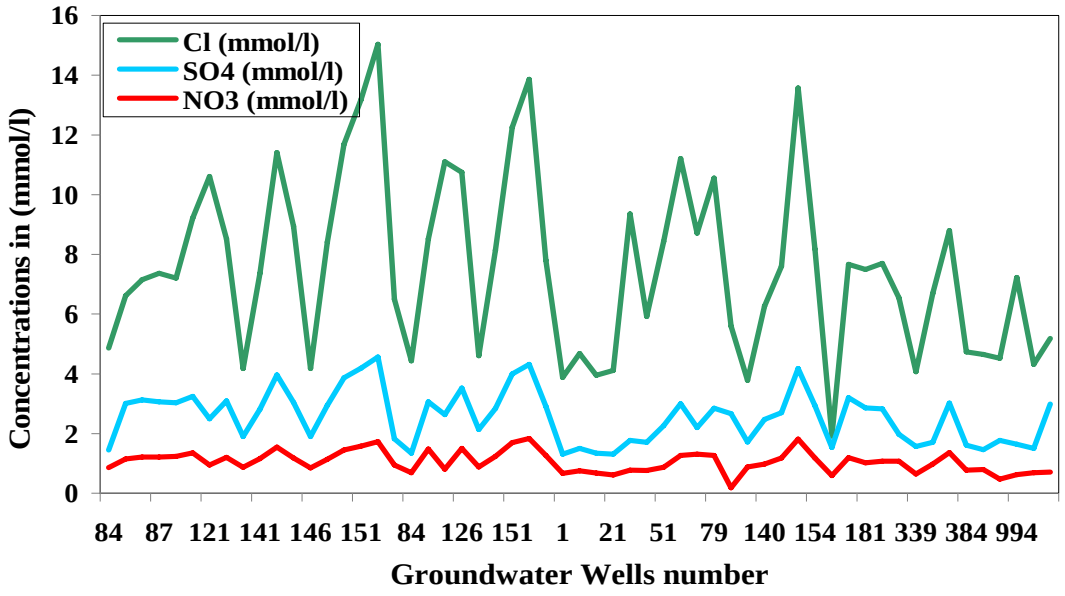

Figure 7.2: Variation of major anions of nitrate, sulphate and chloride concentrations in the Hasouna study area.

Fig. 7.3 displays the evolution of main ion concentrations over time for the three sampling campaigns (August, November, and December 2007) exemplarily for the water well #152. The groundwater well #152 was chosen because of its high ion concentrations. The ions such as nitrate, chloride, sulphate, sodium and calcium displayed small variations with sampling time. The main reason of variability may be related to the daily production rate and internal mixing with downward recharging solutions.

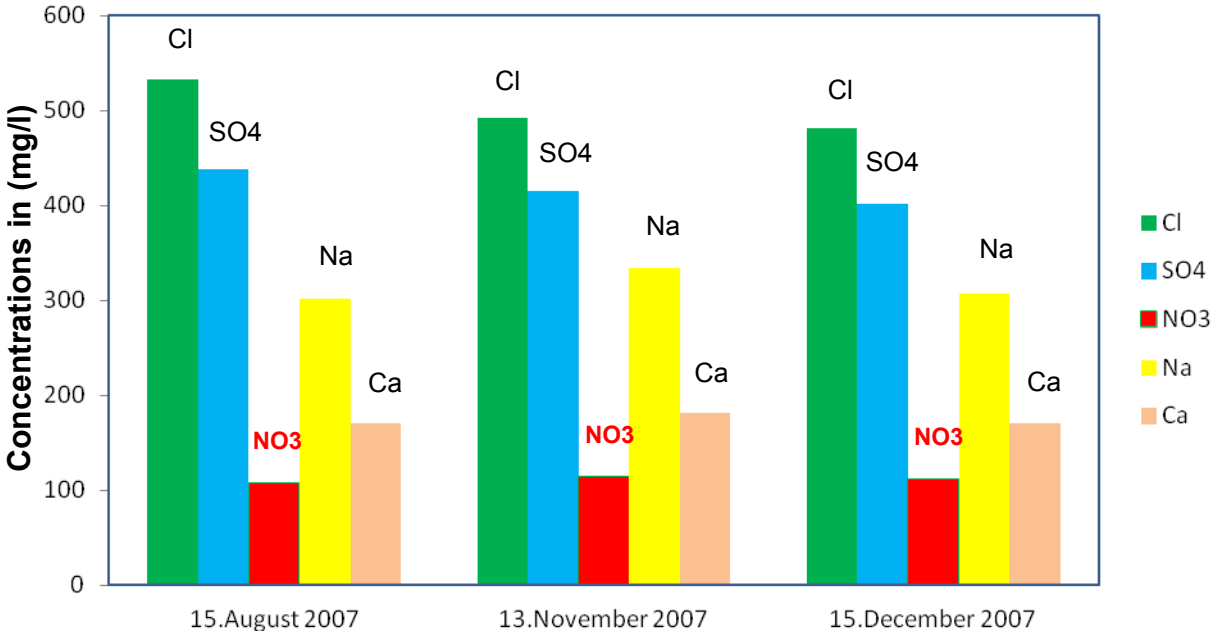

Figure 7.3: Seasonal variation in the major chemical composition of groundwater well 152.

The Figure 7.4 shows the relative concentrations of the cations $Na^{+}+K^{+}$, Ca^{2+}, and Mg^{2+} of groundwater samples. All samples are plotted in the cation ternary plot and lie in the sodium & potassium area. However, sodium concentrations of the Hasouna groundwater are significantly higher than in samples of the Wadi Ash Shati. The samples with the maximum concentration (well #152) and the minimum concentration of Na (well #165) are indicated (Fig. 7.4).

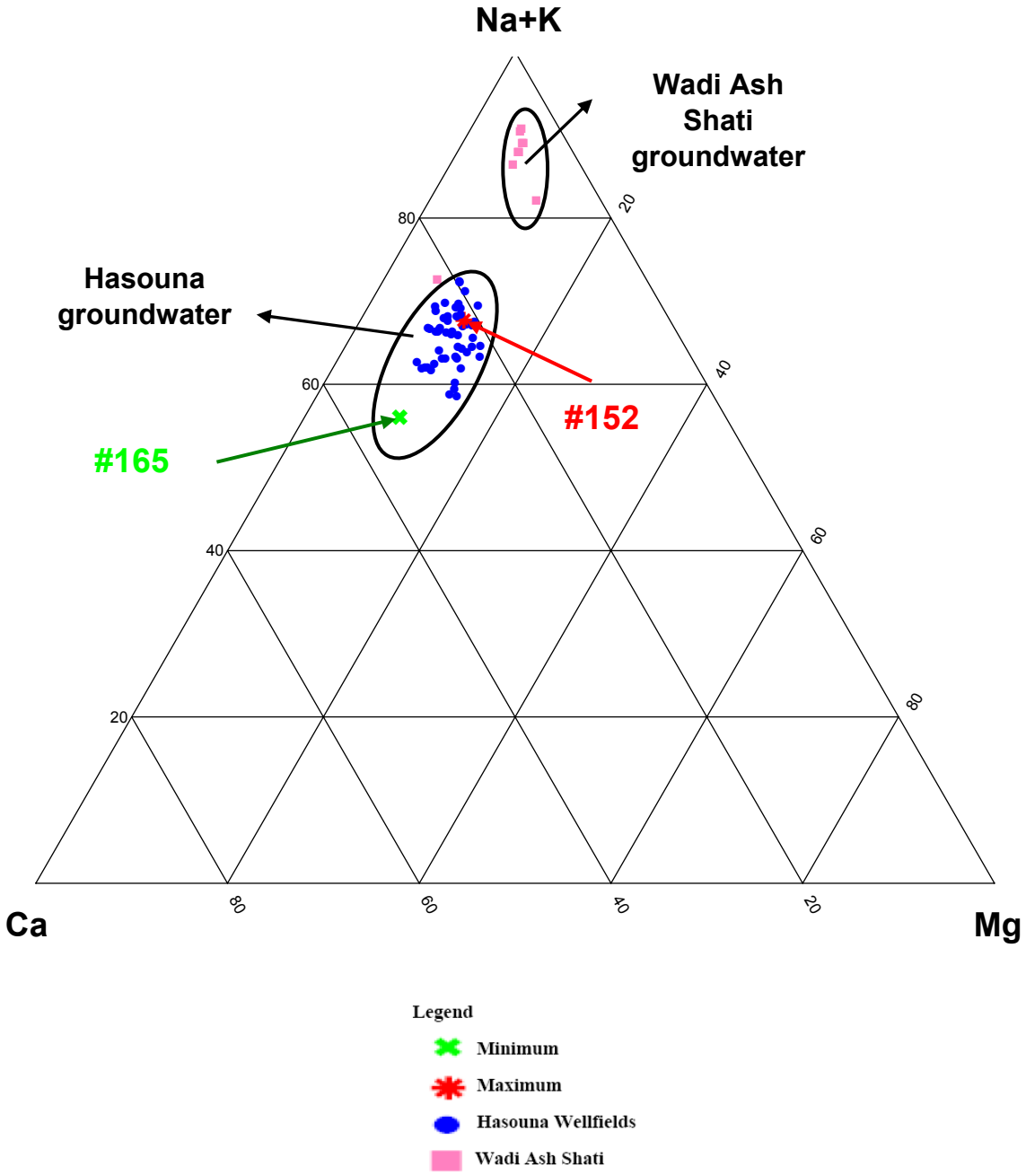

Figure 7.4: Ternary diagram with mol percentage of main cations Ca^{2+}, Mg^{2+} and $Na^{+}+K^{+}$ in the Hasouna study area and Wadi Ash Shati area wells 165 and 152 are indicated as containing lowest and highest concentrations of Na^{+}, Ca^{2+} and Mg^{2+}.

Figure 7.5 shows the relative concentrations of Cl^-, HCO_3^-, and SO_4^{2-} of groundwater samples. The majority of the samples fall in chloride-rich group. The samples with maximum concentration (well #152) and minimum concentration of Cl^- (well #165) are indicated.

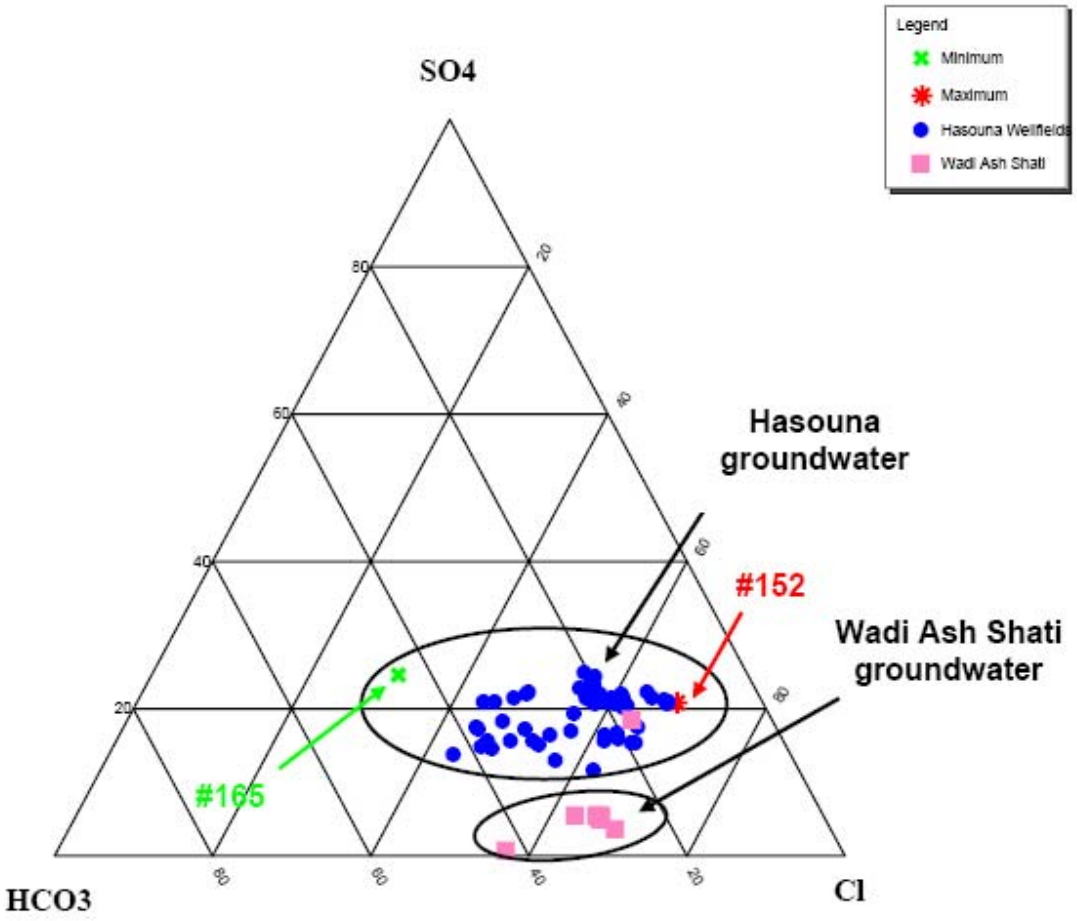

Figure 7.5: Ternary diagram with mole percentage of anions Cl, SO_4 and HCO_3 in the Hasouna study area and Wadi Ash Shati area.

The hydrochemical parameters of the Wadi Ash Shati groundwater were statistically analyzed and the obtained results are summarized in Table 7.5. According to Table 12.2 (Appendix II) it is obvious that the ion compositions of Wadi Ash Shati groundwater show low concentrations in all samples. Nitrate was detected at levels ranging from 0.12 mgL^{-1} to 65 mgL^{-1} with a mean value of 7.7 mgL^{-1}. The water well BH-5 shows elevated nitrate concentrations, which are attributed to the fertilizer contamination in the Mega Agricultural project. While nitrate concentration in most of other samples are low (< 5 mgL^{-1}), see Table 12.2 (Appendix II). The groundwaters generally contain low TDS concentrations (TDS < 1000 mgL^{-1}) with very low sulphate, sodium, and chloride concentrations.

Table 7.5: Statistical parameters for the chemical composition of Wadi Ash Shati groundwater.

Statistical Parameter	Chloride [mgL^{-1}]	Sodium [mgL^{-1}]	Sulphate [mgL^{-1}]	Nitrate [mgL^{-1}]	Calcium [mgL^{-1}]	Magnesium [mgL^{-1}]	Potassium [mgL^{-1}]
Max	287	210	226	65.0	113	17.4	21.7
Min	96.0	69.6	2.80	0.12	8.30	6.50	8.40
Mean	149	108	47.0	7.70	22.6	9.40	18.4
Median	129	97.0	28.0	0.190	10.7	8.80	21.0
SD	54.4	40.0	67.8	21.6	34.0	3.30	5.40
n	9	9	9	9	9	9	9

SD: Standard Deviation, n: number of samples

7.5 SPATIAL DISTRIBUTION

The spatial distributions of major ion concentrations in the Cambro-Ordovician groundwater aquifer of the Hasouna study area are illustrated in Figs. 7.6 and 7.7. The distributions of nitrate, sodium, chloride, sulphate, calcium, magnesium, and bicarbonate ions show similar patterns. Their concentrations (except for bicarbonate) increase in some wells towards the north (NEJHN waterfield). Highest nitrate concentrations are observed around the water well 152 (NEJHN waterfield). The spatial iso-concentration maps for the study area were constructed using ArcGIS. In the south of the study area, in the Wadi Ash Shati area, the distribution of major ion concentration levels is very low (see Table 12.2 in Appendix (II).

The spatial distributions of major ion concentrations in the groundwater of Hasouna show that ion concentrations increase towards the middle of Hasouna water fields. Sodium, calcium, chloride, sulphate, nitrate, and bicarbonate reach their maximum values in the central waterfield, which is close to the so-called Zimam Aquifer (see Figure 10.1).

Sodium concentration varies from 80 to 334 mgL^{-1} with a mean value of 189 mgL^{-1} (Table 7.4). About 40% of the current analyzed samples have sodium content above the guideline limit of 200 mgL^{-1} (WHO, 2004). Regression analyses of sodium concentrations versus those of other major dissolved ions result in best correlation coefficients for Na^+ and TDS (r^2 = 0.93); Na^+ and Cl^- (r^2 = 0.89); Na^+ and Ca^{2+} (r^2 = 0.85); Na^+ and SO_4^{2-} (r^2 = 0.71); Na^+ and Mg^{2+} (r^2 = 0.63); Na^+ and NO_3^- (r^2 = 0.60) (see Table 12.7 (Appendix II)). The distribution of sodium concentration in the study area of Hasouna is shown in Fig. 7.6A. The variation levels of sodium concentration through the Hasouna area display significant anomalies, with a maximum concentration in the northwest and minimum values in the north of the Hasouna waterfield. In

Figure 7.6 the dissolved cations are mostly dominated by Na^+ followed by Ca^{2+} and Mg^{2+}.

The calcium concentration in the study area ranges from 81 to 181 mgL^{-1}, with an overall average of 119 mgL^{-1} (Table 7.4). Comparison of calcium concentration in this current study with other groundwater ions showed a strong and significant positive correlation of Ca^{2+} and TDS (r^2 = 0.88); Ca^{2+} and Na^+ (r^2 = 0.85); Ca^{2+} and Cl^- (r^2 = 0.77); Ca^{2+} and SO_4^{2-} (r^2 = 0.75); (see Table 12.7 in Appendix II). The Hasouna waterfield area shows a local variation in the anomaly of calcium concentration (Fig. 7.6B). Obviously, and in accordance with regression analyses between calcium and sodium, there exists a strong and significant correlation (r^2 = 0.85) between the compositions (see Fig. 7.15).

The concentration of magnesium in the groundwater samples ranged from 15.3 to 65.1 mgL^{-1}, with a mean value of 32.4 mgL^{-1} (Table 7.4). The plots of magnesium concentration versus, chloride (Cl^-), and sodium (Na^+) showed a good positive relationship, with correlation coefficients for; Mg^{2+} and Cl^- (r^2 = 0.65); Mg^{2+} and Na^+ (r^2 = 0.63) (see Table 12.7 in Appendix II). The distribution of magnesium concentration in the study area of the Hasouna is illustrated in the Fig. 7.6C.

The cation potassium usually occurs in natural water in lower concentrations than sodium. Accordingly, the potassium concentrations are ranged between 2.2 $mgL^{-1}$and 10.7 mgL^{-1}, with a mean value of 5.8 mgL^{-1} (Table 7.4). The World Health Organization (WHO, 1998) did not define a guideline for potassium ion in drinking water. The relationship between potassium and major groundwater ions was investigated with the correlation coefficients. The distribution of potassium concentration in the study area of Hasouna is shown in the potassium map in Fig. 7.6D.

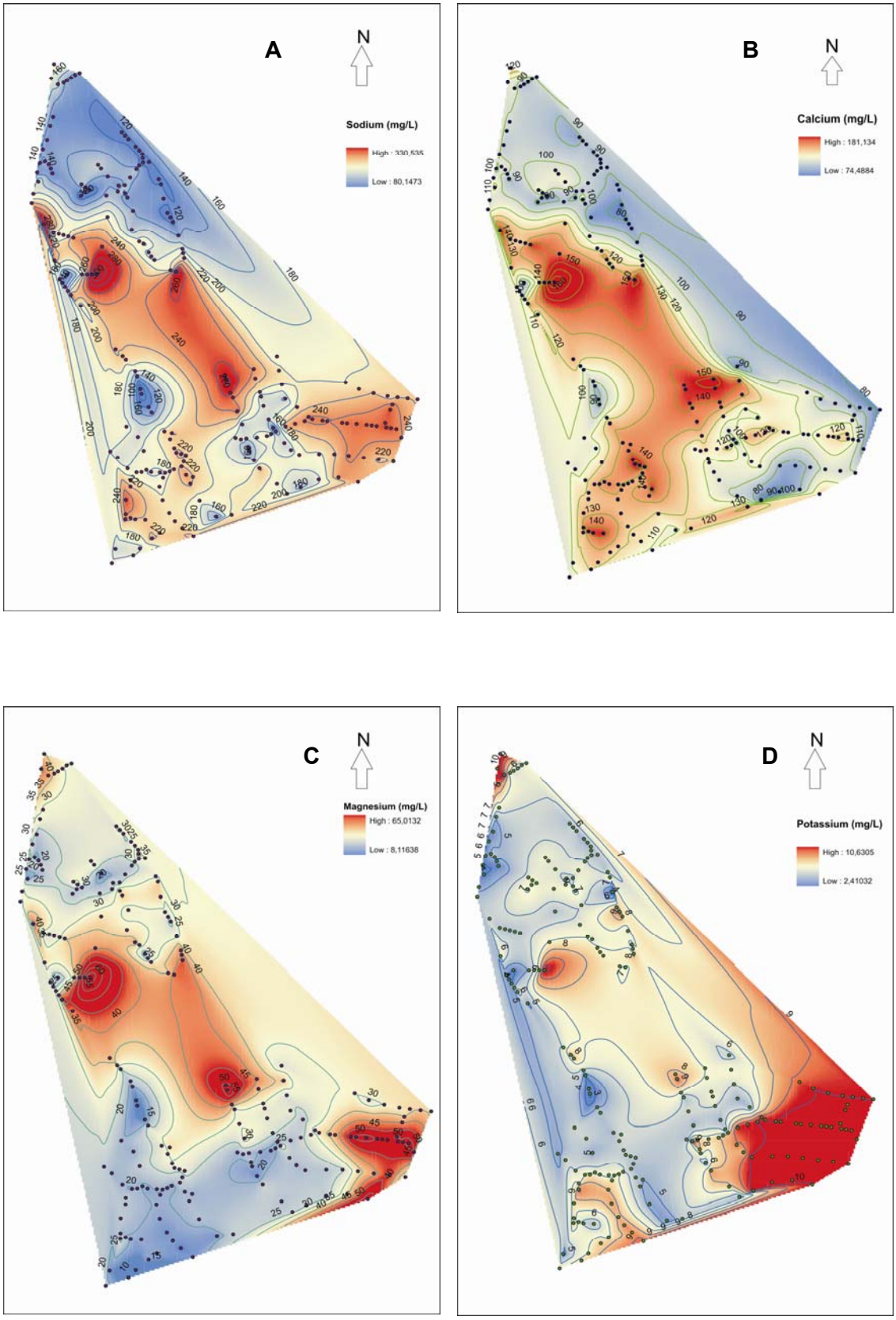

Figure 7.6: Distribution of sodium, calcium, magnesium, and potassium in the groundwater of Hasouna area.

The groundwater in igneous rocks is lightly mineralized; therefore, this groundwater is characterized by high silica concentrations (Hem, 1989). The dissolved form of silicon is commonly termed as silica, which is referring to the oxide SiO_2. The measured dissolved silica concentration in the Hasouna groundwater ranged from 5.2 to 7.3 mgL^{-1}, with a mean value of 6.2 mgL^{-1} (see Table 12.1 in Appendix II).

The distribution of chloride in the groundwater shows extreme differences in chloride content within the study area of Hasouna. The relative chloride concentration ranges from 68 to 533 mgL^{-1}, with a mean value of 268.2 mgL^{-1} (Table 7.4). Such groundwater with very low chloride concentrations shows also very low contents in nitrate, sulphate, calcium and sodium. Figure 7.7A shows the concentrations of chloride in a map of the Hasouna study area. Dissolved anions of the Hasouna groundwater are strongly dominated by SO_4^{2-} and Cl^-, followed by HCO_3^- (Fig. 7.7).

The concentration of sulphate in the groundwater samples of the study area ranges from 125 to 438 mgL^{-1}, with an average of 245.6 mgL^{-1} (Table 7.4). There are variations in the concentration of sulphate, with high sulphate values in the middle of the Hasouna water field, exactly around the water wells numbers 60, 145, 60, 149, 150, 151 and 152. The sulphate distribution in the Hasouna study area has been plotted in the Figure 7.7B.

High concentrations of HCO_3^- were measured in most groundwater samples. The highest bicarbonate alkalinity was 277 $mgL^{-1}$and the lowest analysed groundwater samples value was 150 mgL^{-1} (Table 7.2). The distribution of bicarbonate concentration in the study area of Hasouna is illustrated in the plot 7.7C.

Special focus is given to dissolved nitrate in the groundwater as the concentration of nitrate in the groundwater samples ranged from 11 to 114 mgL^{-1} (Table 7.4). Highest concentration of nitrate of about 114 mgL^{-1} was found in water well 152. Nitrate concentrations increased towards north and in the central waterfields. The spatial distributions of the nitrate concentrations are plotted in the “Nitrate Map” (Fig. 7.7D).

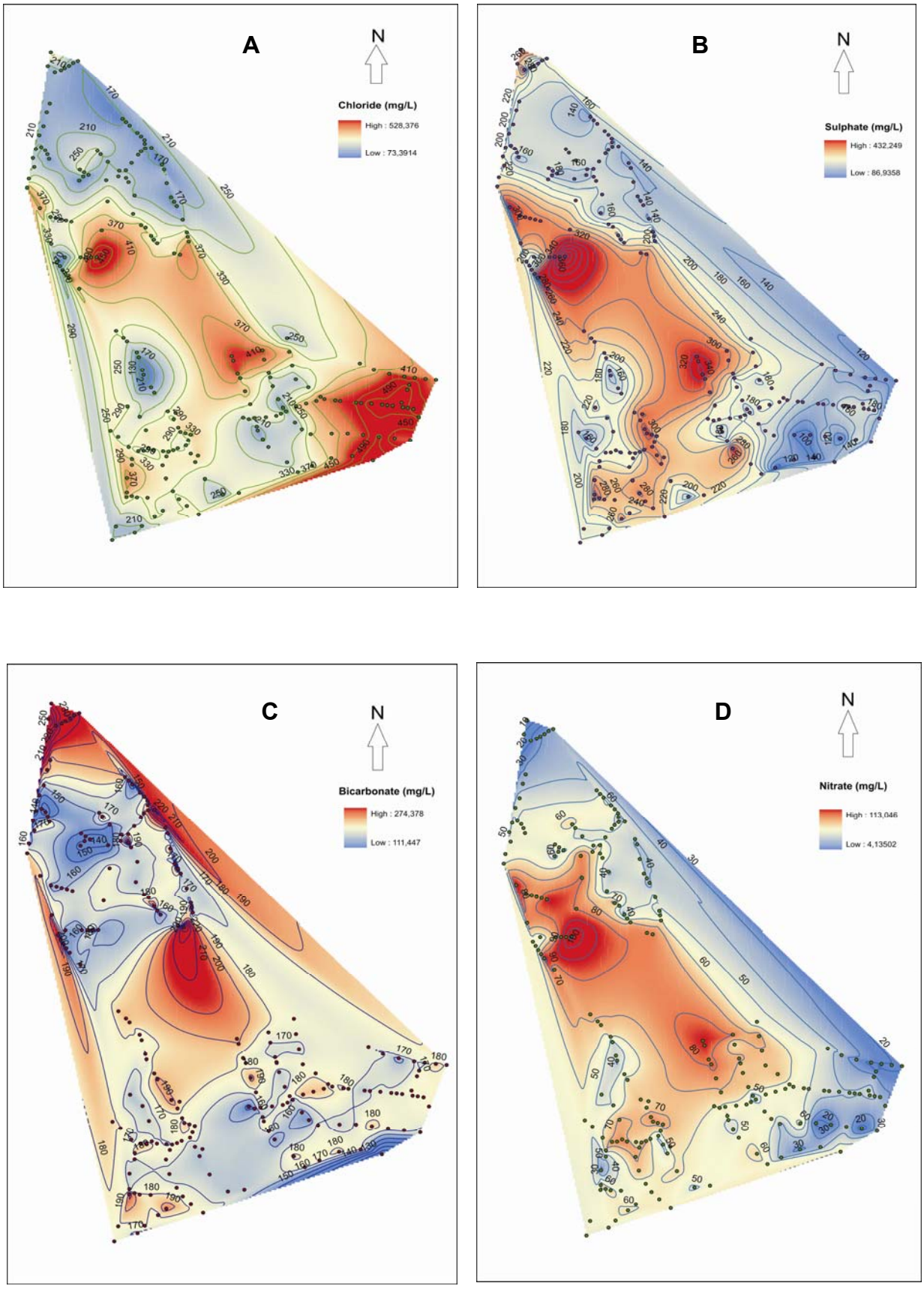

Figure 7.7: Distribution of chloride, sulphate, bicarbonate and nitrate in the groundwater of Hasouna area.

7.6 HYDROGEOCHEMICAL EVOLUTION OF THE GROUNDWATER

The total dissolved solids (TDS) comprise inorganic constituents in the water, mainly sodium, chloride, sulphate, calcium, potassium, magnesium, bicarbonate, nitrate, and silica (Table 12.1 in Appendix II). The majority of groundwater samples have shown TDS values below the maximum permissible limit of 1500 mgL^{-1} (Table 7.2). It is obvious that a strong correlation exists between TDS and EC (Fig. 7.8) values with a significant correlation coefficient ($r^2 = 0.97$).

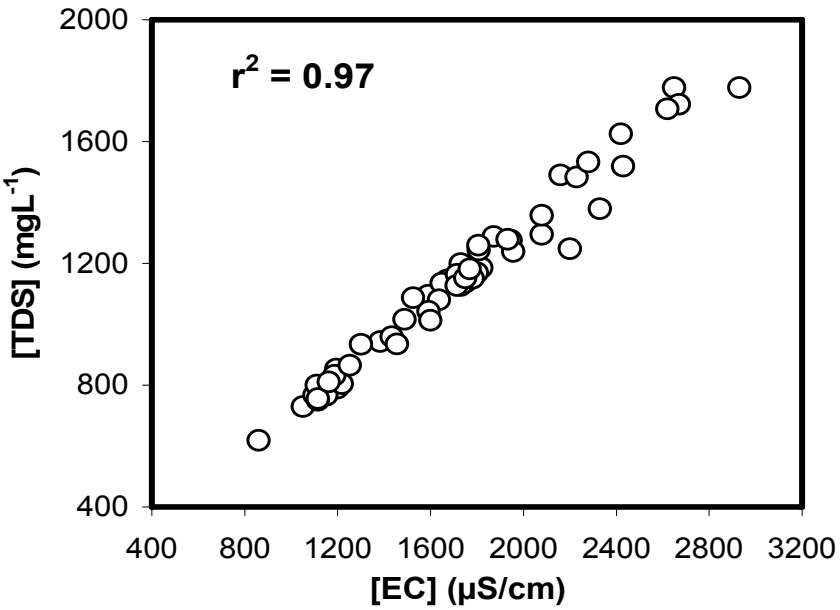

Figure 7.8: Correlation between Electrical conductivity and Total Dissolved Solids of Hasouna water samples.

The existence of high salinity solutions is confirmed by the saline Zimam Aquifer, dissolution process and non-external recharge processes in the Hasouna water fields' area. The Zimam aquifer is characterized by very high TDS, sulphate, chloride, sodium, magnesium, and calcium, (El Baruni et al., 1985). Therefore, the groundwater aquifer of the Hasouna study area may be affected by the salinity of the above Zimam Aquifer as a consequence of fracturing and vertical hydraulic contact. In addition, the nitrate concentrations in the Zimam Aquifer are moderately high according to previous hydrogeological studies; the internal recharge process is related to groundwater movement from south towards north and northeast (see Fig. 4.6).

The different compositions of water types are suggested to be due to the mixtures of water with the saline Zimam Aquifer (or similar solutions). El

Baruni et al., 1985 documented in their paper on the hydrogeology of Ghadamis Basin, that the quality of this water is highly variable, with high mineralization. The levels of TDS vary from 1600 to 6000 mgL^{-1} in Al Hamadah Al Hamra Basin (location of study area) and Ghadamis Basin. The values for salinity (TDS) and nitrate in Zimam Aquifer vary from 2316-6026 mgL^{-1} for TDS and 33-68 mgL^{-1} for nitrate (El Baruni et al., 1985).

The plot of total dissolved solids (TDS) versus chloride, sulphate, sodium and calcium shows good correlation in all groundwater samples of the study area. Obviously, the major ion concnetrations increase positively with TDS values (see Figure 7.9).

Milne-Home and Sahli, 2007 have documented that the Hasouna water fields have maximum groundwater ion concentrations of TDS of 1973 mgL^{-1}, chloride of 600 mgL^{-1}, sulphate of 589.8 mgL^{-1}, nitrate of 133 mgL^{-1}, bicarbonate of 301 mgL^{-1}, calcium of 195.5 mgL^{-1}, magnesium of 68.8 mgL^{-1}, sodium of 429.8 mgL^{-1}, and potassium of 56 mgL^{-1}.

Similar observations were made in the Murzuq Basin in the south of the study area. The maximum ion concentrations of ten groundwater samples were for nitrate about 4.3 mgL^{-1}, for sodium 70 mgL^{-1}, for calcium 25.6 mgL^{-1}, for chloride 125 mgL^{-1}, for sulphate 98 mgL^{-1}, for potassium 20 mgL^{-1}, for TDS 345 mgL^{-1}, and for magnesium 56.4 mgL^{-1}, Shaki and Adeloye (2006).

For simplification the groundwaters of Hasouna area can be characterized by a two endmember mixing approach (see also Appendix I). The first type is a low mineralized and the second type a highly mineralized solution. The spatial distribution and variation of total dissolved solids concentration in the study area of Hasouna is illustrated in the plot 7.10.

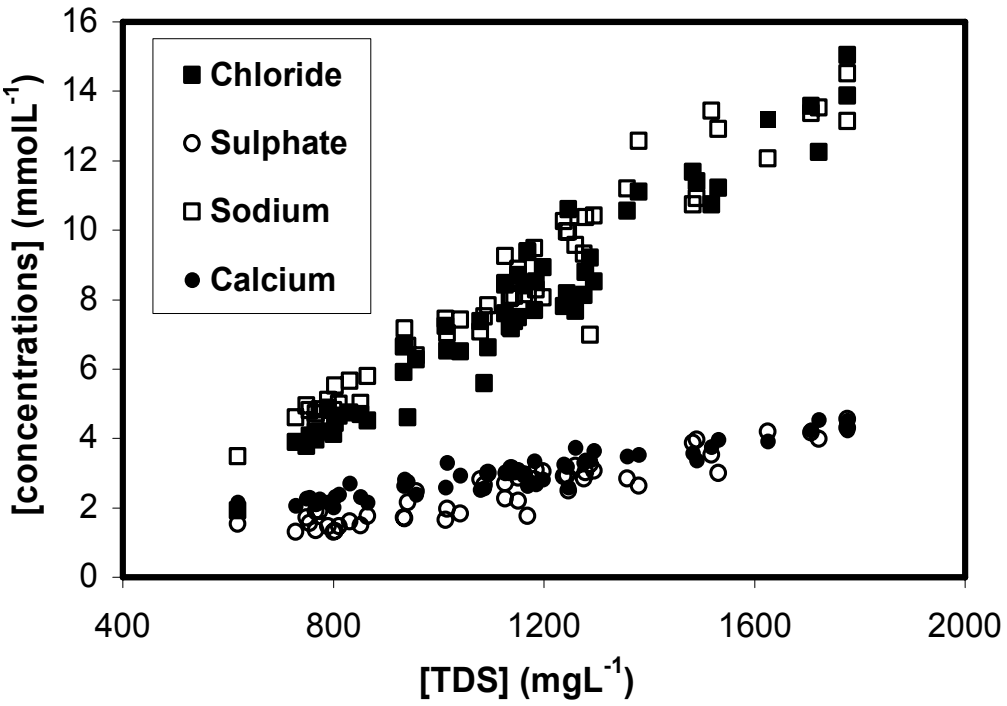

Figure 7.9: Correlation between Total Dissolved Solids (TDS) and the major Ions of Hasouna water area.

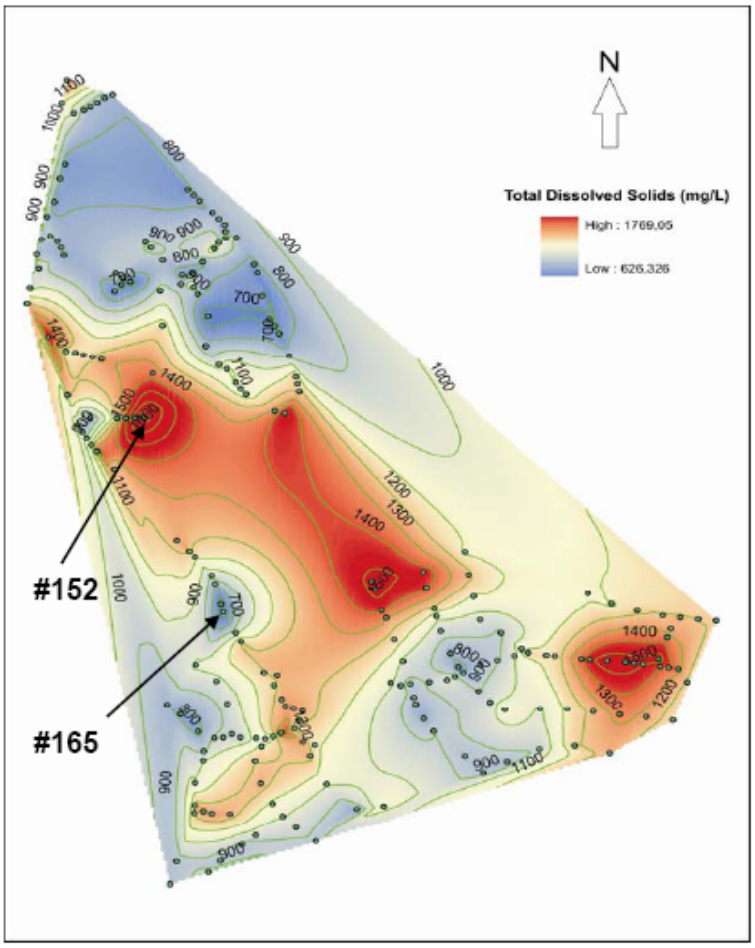

Figure 7.10: Distribution of total dissolved solids in the groundwater of Hasouna area.

The chemical composition of the groundwater from Hasouna wellfield area discussed in Section 7.4 can be used to decipher potential reaction mechanisms and paths by comparison of main dissolved components to each other.

In general, chemical composition of a groundwater is effected by individual occurring dissolution or weathering behaviours of minerals, rather simple ion exchange with the local rocks in the aquifer etc. For instance, the Na/Cl ratio increase (excess sodium) can be caused by the dissolution of sodium silicates like in reaction 21:

$$2NaAlSi_3O_8 + 2CO_2 + 11H_2O \rightarrow Al_2Si_2O_5(OH)_4 + 2Na^+ + 2HCO_3^- + 4Si(OH)_4$$

where weathering of albite is leading to the formation of kaolinite.

Therefore, in Figure 7.11 the Na^+ versus Cl^- concentrations of the groundwaters are plotted. Interestingly, a significant positive correlation between sodium and chloride is obtained (r^2 = 0.89). This positive correlation between sodium and chloride shows a different trend than the evaporation line (see red dashed line in Fig. 7.11). A possibility to interpret the strong correlation of Na^+ and Cl^- concentration may lie in the dissolution of minerals like halite and/or silicates, or proceeding evaporation of a given start solution, respectively.

However, both mechanisms are rather speculative as no halite was found in the study area/aquifer and evaporation would have to result in constant Na/Cl ratios (see evaporation line in Fig. 7.11, which does not fit with chloride and sodium data points; see also section 8.0 for discussion concerning isotopes). The molar ratio of Na^+/Cl^- for Hasouna groundwater samples generally ranges from 0.76 to 1.80, where a Na^+/Cl^- molar ratio above 1 is typically interpreted as reflecting Na^+ released from silicate weathering reactions (Meybeck, 1987).

Alternatively, a simple explanation for the evolution of these groundwaters can be given by assuming mixing of two endmember solutions (groundwater wells #165 and #152).

End member solutions (dashed line) are referred to the lowest (well #165, blue circle) and highest (well #152, red circle) concentration of [Na] and [Cl] ions, respectively.

Mixing solution of the groundwater chemical composition can be obtained according to the equation

$$[\,]_{gw} = x * [\,]_1 + (1-x)\,[\,]_2 \qquad (22)$$

where [ ] denotes the concentrations of the individual groundwater components (e.g. Ca^2, Na^+, Cl^-,..), and x is the fraction of endmember 1 on GW (groundwater).

The mixing line of two endmemeber solutions is given in Fig. 7.11. However, the mixing line between the two solutions (black dashed line) shows a different trend than the evaporation trend line (red dashed line). This confirms that the high salinity of the Hasouna groundwater is attributed to mixing between Zimam and Cambro-Orovician aquifers, and not to evaporation process.The results of this mixing process are discussed in detail in the manuscript in Appendix I).

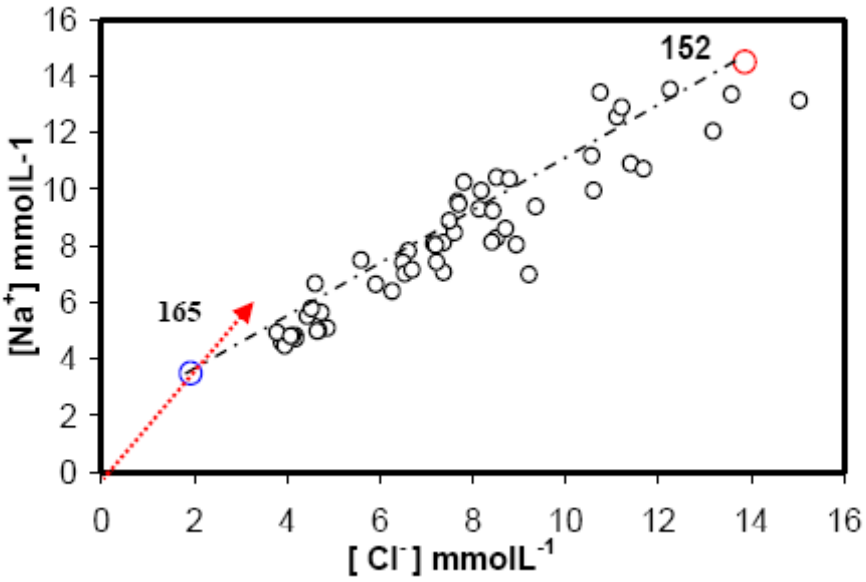

Figure 7.11: Correlation between Chloride and Sodium of Hasouna water samples in mmol/l, the mixing line is given as dashed line (black), and evaporation line is marked as red dashed line.[Na^+] = 0.8901 [Cl^-] + 1.494, (r^2 = 0.89).

The correlation of concentration between calcium versus sodium is illustrated in Fig. 7.12. The plot shows a strong positive relationship with r^2 =0.85. This evolution of solution composition cannot be explained by an evaporation trend too, see red dashed line in Fig. 7.12.

Again the evolution of groundwater composition can be simply explained by the mixing model by using the two endmember solutions (well #165 and #152). The mixing process between the two wells (#165 and #152) is in agreement with high mineralization of most groundwater samples (see Plot 7.12).

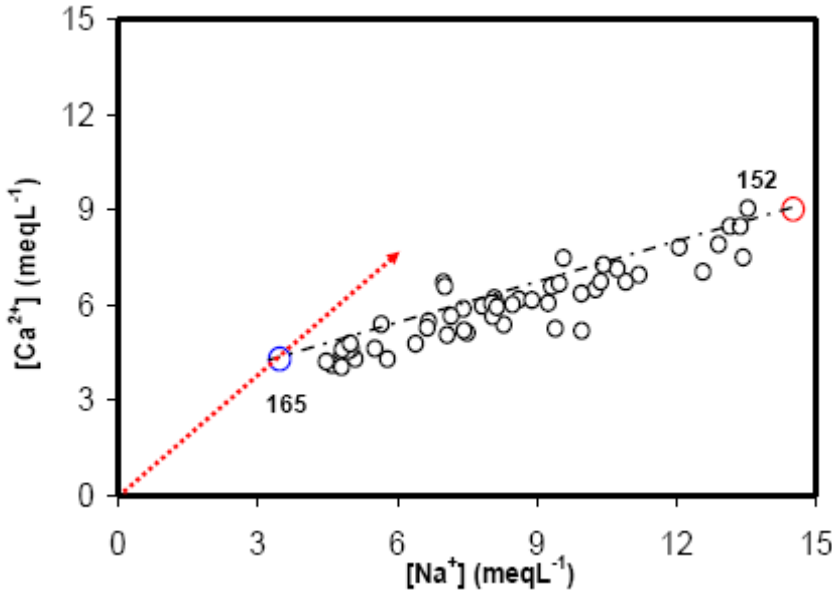

Figure 7.12: Sodium versus calcium relationship of the samples from Hasouna study area, mixing line (dashed line), and evaporation line (red dashed line).

Figure 7.13 shows the relation between Ca^{2+} and SO_4^{2-} in groundwater samples of the Hasouna study area. The increase of calcium concentration is related to an increase of sulphate content. Few samples fall along the 1:1 equiline (Ca^{2+} = SO_4^{2-}), and most of them show excess of calcium over sulphate. Thus Ca^{2+} and SO_4^{2-} seem to be derived from gypsum dissolution, whereas excess calcium shows additional geochemical process like Ca silicate dissolution.

Similarly, an excess of sulphate over calcium in few samples expresses the removal of calcium from the system likely by calcite precipitation. The concentration values of calcium and sulphate do not follow the evaporation trend line (red dashed line in Fig. 7.13).

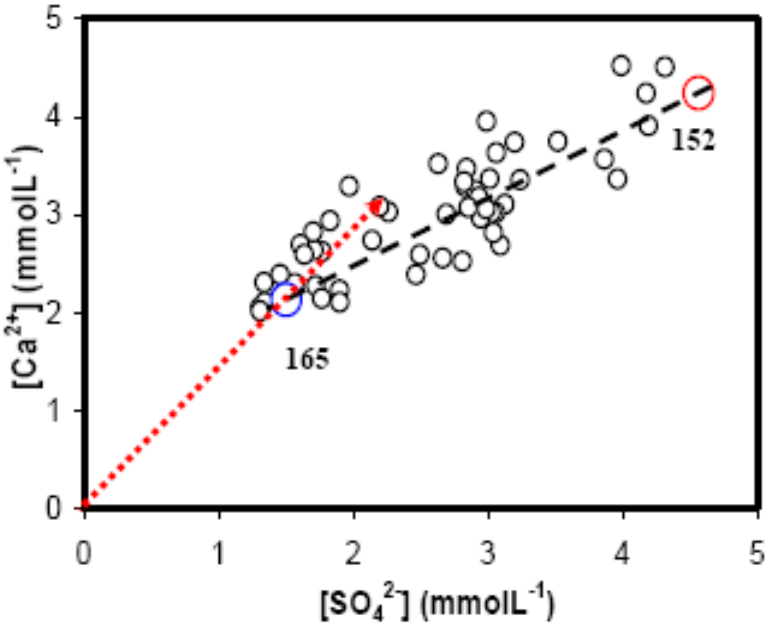

Figure 7.13: Correlation of sulphate (SO_4^{2-}) versus calcium (Ca^{2+}) of the Hasouna study area, where the mixing line is marked as black dashed line, and the evaporation line is marked as red dashed line.

The plot of SO_4^{2-} versus Cl^- concentration shows a positive relationship (r^2 = 0.75) with proportional increase of chloride versus sulphate (Fig. 7.14). Most of groundwater samples follow the solution mixing line (dashed line, low #165 and high #152). The sulphate and chloride concentration do not follow the trend of evaporation line (red dashed line).

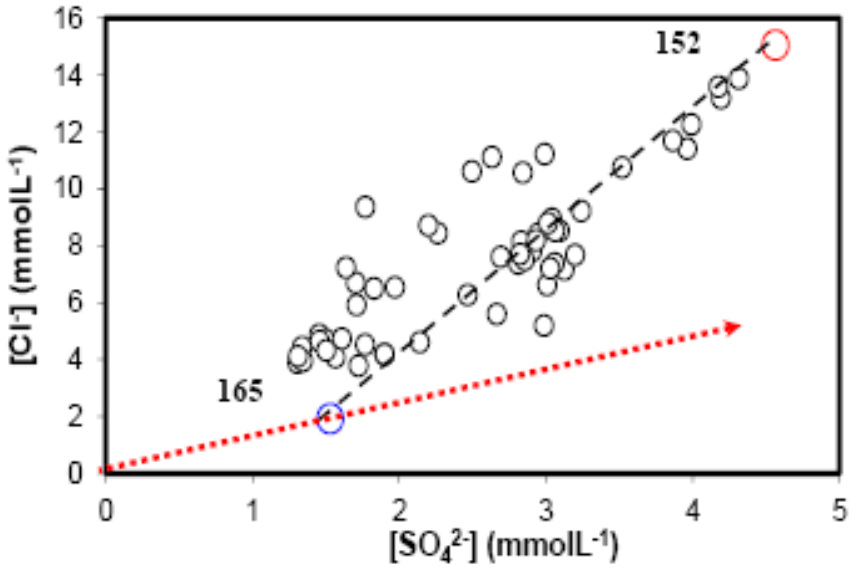

Figure 7.14: Correlation of sulphate (SO_4^{2-}) versus chloride (Cl^-) of the Hasouna study area, where the mixing line is marked as dashed line (black), and the evaporation line in red dashed line.

The relationship between $Ca^{2+} + Mg^{2+}$ ($meqL^{-1}$) and $0.5\ HCO_3^- + SO_4^{2-}$ ($meqL^{-1}$) is plotted in the Figure 7.15. Most samples show that the concentrations of ($Ca^{2+} + Mg^{2+}$) exceed the concentrations of ($0.5HCO_3 + SO_4^{2-}$), which gives an indication of gypsum, anhydrite, calcite and dolomite dissolutions according to the equations (23-25). The solid dashed line again represents the mixing line of the two solutions (wells #165 and #152).

The high correlation between the dissolved ions in the Hasouna groundwater can be explained by the dissolution of gypsum.

$$CaSO_4.2H_2O = Ca^{2+} + SO_4^{2-} + 2H_2O \quad (23)$$

The CO_2-enriched groundwater can dissolve the calcite ($CaCO_3$) according to the reaction

$$CaCO_3 + CO_2 + H_2O = Ca^{2+} + 2HCO_3^- \quad (24)$$

If CO_2 is available, calcite will be dissolved, while degassing may cause a precipitation of calcite.

The dissolution of dolomite in water are presented by the reaction

$$CaMg(CO_3)_2 = Ca^{2+} + Mg^{2+} + 2CO_3^{2-} \quad (25)$$

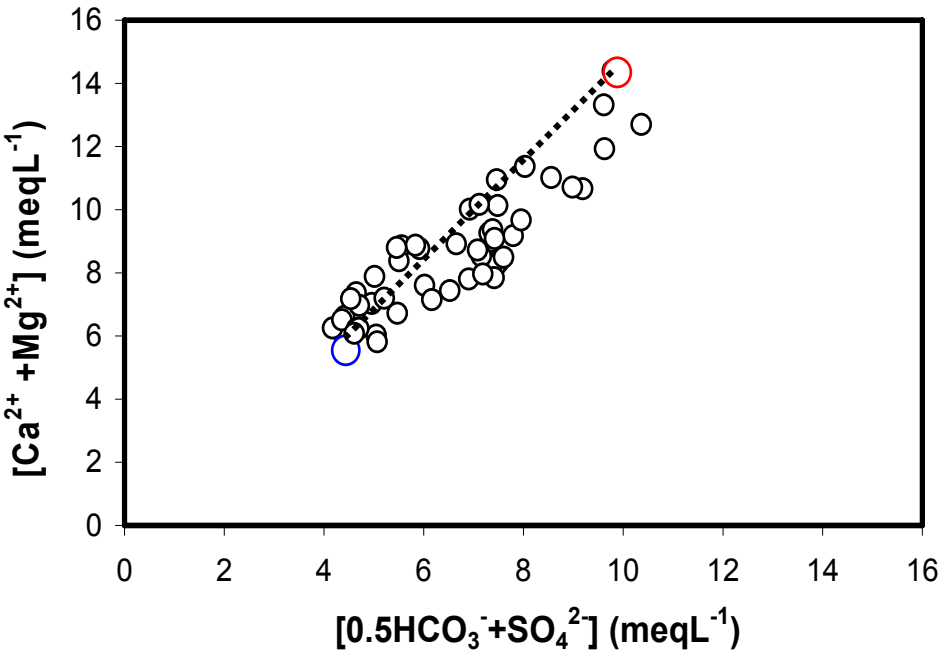

Figure 7.15: Correlation between ([Ca^{2+}] + [Mg^{2+}] (meq/l) and [$0.5HCO_3 + SO_4^{2-}$] of groundwater from the Hasouna study area.

In the Hasouna waterfields dolomite and calcite are probably the main source for magnesium and calcium in the groundwater as the lithology of the study area is dominated by carbonate rocks.

The plot of the dissolved NO_3^- concentration versus the major dissolved ions show positive correlations between the nitrate concentration and Ca^{2+}, Mg^{2+}, Na^+, K^+, Cl^-, and SO_4^{2-} (Figure 7.16).

The investigations and interpretation of this correlation plot of nitrate against the major ions showed that nitrate in the groundwater of the Hasouna study area might be of natural origin, e.g. by the explained mixing model. This issue will be discussed later in details with the help of the nitrogen isotopes technique (^{15}N, ^{17}O, and ^{18}O of nitrate; see also Table 12.8 in Appendix II).

The results of current chemical analysis of groundwater samples in the study area of Hasouna show high nitrate levels in most samples, nitrate values range between 11 and 114 mgL^{-1} with a mean value of 66 mgL^{-1}. This is above the acceptable maximum of 50 mgL^{-1} standard guideline for drinking water (WHO, 2004).

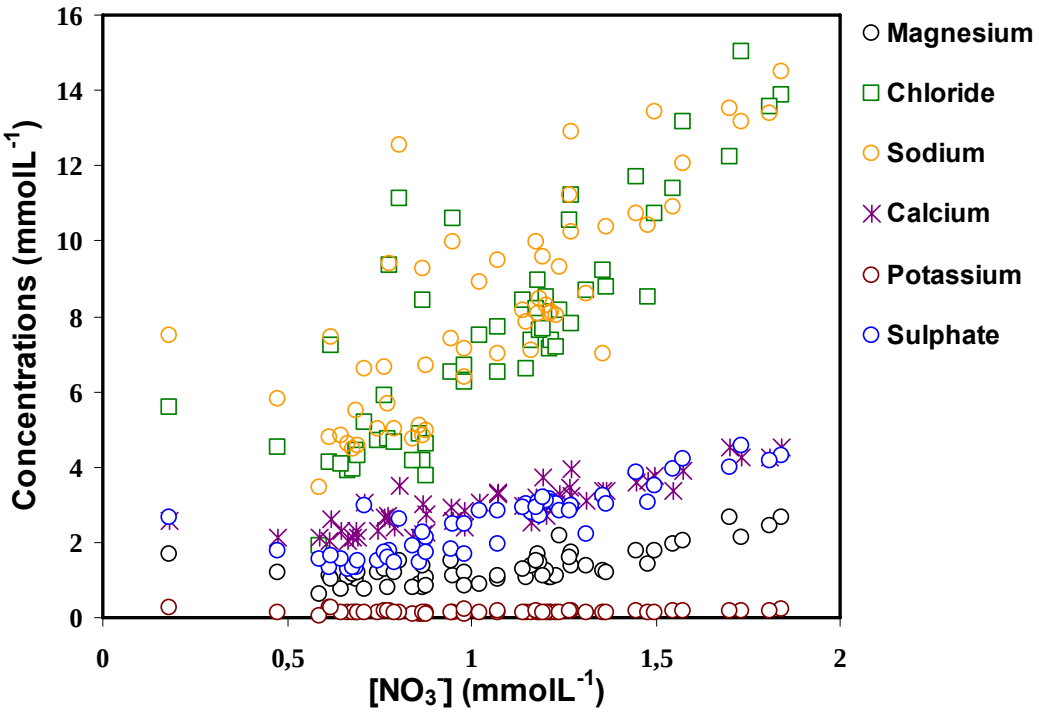

Figure 7.16: Nitrate concentrations versus major ions in the Hasouna study groundwater samples.

The trace element concentrations (mgL^{-1}) in the Hasouna study area are shown in Table 12.4 (Appendix (II). The concentration of **strontium** ranged between 0.95 and 3.5 mgL^{-1}, with a mean value of 1.7 mgL^{-1} (Table 7.6). Concentration of Sr^{2+} was found to be above permissible limit of 0.07 mgL^{-1} (WHO, 1984) in all groundwater samples. The minor and trace elements of Wadi Ash Shati groundwaters are given in Table 12.3 (Appendix II).

For the analyzed groundwater samples there is a significant positive correlation between calcium and strontium (Fig. 7.17), which shows the dependence of calcium and strontium in two separate trends. The relationship between Ca and Sr, which is displayed as two trends, might be related to the mixing with not only two but e.g. an additional and different highly mineralized solution. Thus, two highly mineralized solutions with distinct Sr^{2+} concentrations may exist. Additionally, the mixing line between the two wells (#165 and #152) shows that calcium content increases above this line (Fig. 7.17). The main source of Strontium (Sr^{2+}) probably is the dissolution of carbonates and in particular sulphates.

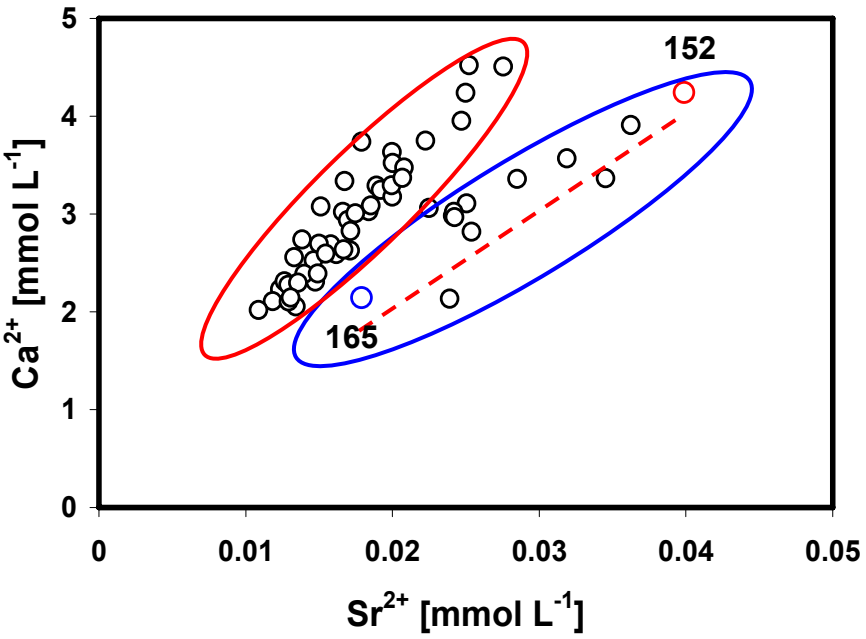

Figure 7.17: Correlation plots of strontium (Sr^{2+}) versus calcium (Ca^{2+}).

According to WHO (2004) standard limit the maximum allowable **iron** (Fe) concentration and the recommended guideline value for drinking water quality is 0.3 mgL^{-1}. The iron concentrations in the Hasouna groundwater above the detection limit were found in 6 samples. Most of the analyzed groundwater samples have iron concentrations below the detectable limit. The concentration of iron in groundwater of the study area varied from 0.01 mgL^{-1} to 0.07 mgL^{-1}, with a mean value of 0.025 mgL^{-1} (Table 7.6). The general concentrations of iron in the study area are very low as compared to the iron concentrations of Wadi Ash Shatti region. Therefore, there are no healths and technical concern or need for treatment need of a groundwater with iron ion contents below 0.3 mgL^{-1}. While, the iron concentration in the Wadi Ash Shati samples ranged from 0.06 to 3.7 mgL^{-1}, with a mean value of 1.9 mgL^{-1} (see Table 12.3 (Appendix II)). Groundwater of Wadi Ash Shati has in the most samples high iron contents. The groundwater in Tazerbo wellfield SSTB (Sarir-

Sirt/Tazerbo-Benghazi) has a high iron concentration, which lies between 1.05 and 4.98 mgL^{-1} (Sahli, 2000).

The elements **nickel** (Ni), and manganese (Mn) is found only in two groundwater samples. Concentrations of most groundwater samples are below the detection limit. Ni and Mn concentrations in the two samples ranged from 0.001 to 0.012 mgL^{-1} and 0.002 to 0.125 mgL^{-1}, respectively, which is within the permissible level of 0.02 (Ni) and 0.5 (Mn) (WHO, 2004). **Chromium** (Cr) concentrations in the Hasouna groundwater samples show low concentrations. Only in 17 of the 55 groundwater samples Cr was detected, where concentration ranged from 0.002 to 0.015 mgL^{-1}, with an average value of 0.005 mgL^{-1} (Table 7.6). **Zinc** (Zn) is a trace element found in water in various concentrations. High amounts of zinc are undesirable in water supply systems because above a threshold of 5 mgL^{-1} a significant number of people can taste zinc, although no hazard to human health exists (HEM, 1985). Zinc values in the 22 groundwater samples ranged from 0.005 to 0.05 mgL^{-1}, with an average value of 0.02 mgL^{-1}, which lie below the permissible limit (Table 7.6).

Boron (B) concentration was detected in only 44 groundwater samples in this current study, which show values below the limit value of 0.5 mgL^{-1} according to WHO (2004) standards. The concentration of boron is ranges from 0.16 mgL^{-1} to 0.43 mgL^{-1}, with a mean value of 0.27 mgL^{-1} (Table 7.6).

Generally, the concentration of **aluminium** (Al) in the current Hasouna study area is low. The Al concentration in the groundwater wells vary from 0.006 to 0.035 mgL^{-1}, with a mean value of 0.012 mgL^{-1} (Table 7.6). The **bromide** (Br) concentrations in the samples of study area range from 0.07 to 0.65 mgL^{-1} with an average value of 0.25 mgL^{-1} (Table 7.6). The bromide values are very low (detected in 41 samples). The **fluoride** (F) concentration in the groundwater of the study area varies from 0.19 to 0.73 mgL^{-1} with average and median values of 0.39 mgL^{-1} and 0.38 mgL^{-1}, respectively (Table 7.6). The fluoride was detected only in 35 groundwater samples. All groundwater samples concentrations are below the minimum required level (1.5 mgL^{-1}) as recommended by the standards (WHO, 2004). The fluoride shows poor correlation with ions of Cl^-, Mg^{2+}, SO_4^{2-}, Na, HCO_3^- and K^+, but a positive good correlation with Li. About 44 samples were analyzed for lithium. Lithium concentration was found in the range from 0.003 to 0.145 mgL^{-1}, with mean value of 0.047 mgL^{-1} (Table 7.6). The results from the Hasouna groundwater analysis indicate that concentrations of lithium are very low and below WHO guideline standard for drinking water limits.

Table 7.6: Statistical analysis of trace elements in the Hasouna groundwater.

Parameter	Fe	Se	Al	Cr	Zn	Mn	Ni	B	Ba	Br	F	Li	Sr
Min	0.013	bld.	0.006	0.002	0.005	0.002	0.001	0.161	0.019	0.067	0.190	0.003	0.950
Max	0.067	0.268	0.035	0.015	0.055	0.125	0.012	0.430	0.055	0.654	0.730	0.145	3.49
Mean	0.025	0.059	0.012	0.005	0.018	0.063	0.006	0.270	0.031	0.253	0.390	0.047	1.69
Median	0.015	0.034	0.008	0.004	0.016	0.063	0.006	0.262	0.029	0.226	0.380	0.047	1.53
SD	0.021	0.068	0.013	0.003	0.011	0.050	0.004	0.112	0.015	0.259	0.220	0.060	1.09
n	6	20	11	17	22	2	2	44	41	41	35	44	55

SD = Standard deviation, n = number of measured samples, Trace elements concentrations in mgL^{-1}.
bld. = below detection limit

7.7 OVERALL CLASSIFICATION OF GROUNDWATERS

Water quality analysis is one of the most important aspects in groundwater studies. The hydrochemical data is used to study the quality of water and its suitability for drinking, agricultural activities and industrial purposes. common Groundwater in the study area of Hasouna Water fields consists the major chemical elements Na^+, K^+, Ca^{2+}, Mg^{2+}, Cl^-, NO_3^-, HCO_3^- and SO_4^{2-}. The hydrochemical parameters of groundwater in the study area play a significant role in classifying and evaluating water quality. For analysis of the hydrochemical groundwater parameters of the Hasouna study area different hydrochemical plots were used to classify the different groundwater types. Therefore, some graphical methods were used to classify and understand the different water groups of groundwater samples from the Hasouna waterfields. The results are presented by means of a Piper diagram. In particular, high concentrations of NO_3^-, SO_4^{2-}, Na^+, Cl^- characterize the groundwater of Hasouna Water fields. The differences of water facies in the same aquifer may be originate from various mechanisms such as mixing, ion exchange, groundwater flow direction, dissolution of gypsum and water exploitation rate. Some wells show more salinity due to the mixing between both aquifers Zimam and Hasouna. The increase of groundwater salinity is supposed to reflect the influence of the Zimam water, ion exchange and the characteristics of the relative aquifer rocks.

The Piper (1944) diagram is used for the geochemical classification of groundwater samples, with concentrations in $meqL^{-1}$ being used for calculation. The Hasouna groundwater samples show a relatively homogeneous distribution of the Water types, while the groundwater of the Wadi Ash Shati area has only one groundwater type (Na-Cl-HCO3). In the cation plot field (triangle on the left) of the Piper diagram (Fig. 7.18), most of the Hasouna samples plot mainly in the no dominant type window which suggests mixed source, while the other samples depict Na+K as the

predominant cation types. However, in the anion plot field (triangle on the right), the majority of the samples plotted in the middle of the diagram which suggest mixed anions (no anions dominant), while few Hasouna samples and all Wadi Ash Shati samples suggests Cl^- as the predominant anion.

Conclusively, in the Hasouna waterfields area the dominant cations are sodium and calcium, while the chloride and sulphate are the dominant anions. This reflects the variation of groundwater properties, where (SO_4^{2-} and Cl^-) exceeds (Na^+ and K^+). The majority of groundwater samples fall in the Na^+, Mg^{2+}, Ca^{2+} facies and Cl^-, SO_4^{2-} facies. Figure 7.18 is a Piper diagram showing the relative chemical composition of groundwater of the Cambro-Ordovician of the Wadi Ash Shati and the Hasouna wellfields. This plot defines the evolution pathway of groundwater chemistry as groundwater with low salinity (TDS = 487 mgL^{-1}) migrates from the region of Wadi Ash Shati in the south to the Hasouna waterfields with an average TDS of 1125 mgL^{-1} (see Tables 7.2 and 7.3). According to hydrochemical facies analysis of groundwater samples in the study area, the facies change from the south at the Wadi Ash Shati (Na-Cl-HCO_3) to the north at the main study area of Hasouna waterfields (Na-Ca-Cl-SO4 and Na-Ca-Cl-SO_4-HCO_3), which reflects the local variability within the mixing zone with Zimam Aquifer (Figs. 7.18 and 10.1)). Concentrations of major ions in both study areas showed significant variation of cations and anions. Binsariti et al., (2000) documented that the hydrochemical facies in the Wadi Ash Shati groundwater changes, when it enters the Hasouna wellfields. This change is a result of mixing with the upper saline aquifer (Zimam), and also from the dissolution of carbonates and gypsum.

The most groundwater types for the Hasouna groundwater are the Na-Ca-Cl-SO4 and Na-Ca-Cl-HCO3-SO4 types, and Na-Cl-HCO3 facies represent the groundwater of Wadi Ash Shati area, where the groundwater samples are characterized by the dominance of $Cl^- + SO_4^{2-}$ over HCO_3^-, and dominance of $Na^+ + Ca^{2+}$ over Mg^{2+}, with relatively high nitrate concentrations in the Hasouna groundwater. The direction of the salinity is consistent with increase in the both EC and TDS concentrations of the Hasouna and Wadi Ash Shati groundwater samples. The geochemical process responsible for this facies evolution is the dissolution of dolomite and gypsum in the water of the Zimam aquifer, where a vertical hydraulic leakage connection between the saline water of Zimam aquifer and water of the Cambro-Ordovician aquifer (Binsariti and Saeed, 2000), therefore the groundwater changed its salinity as it moves northwards (see Fig. 7.18).

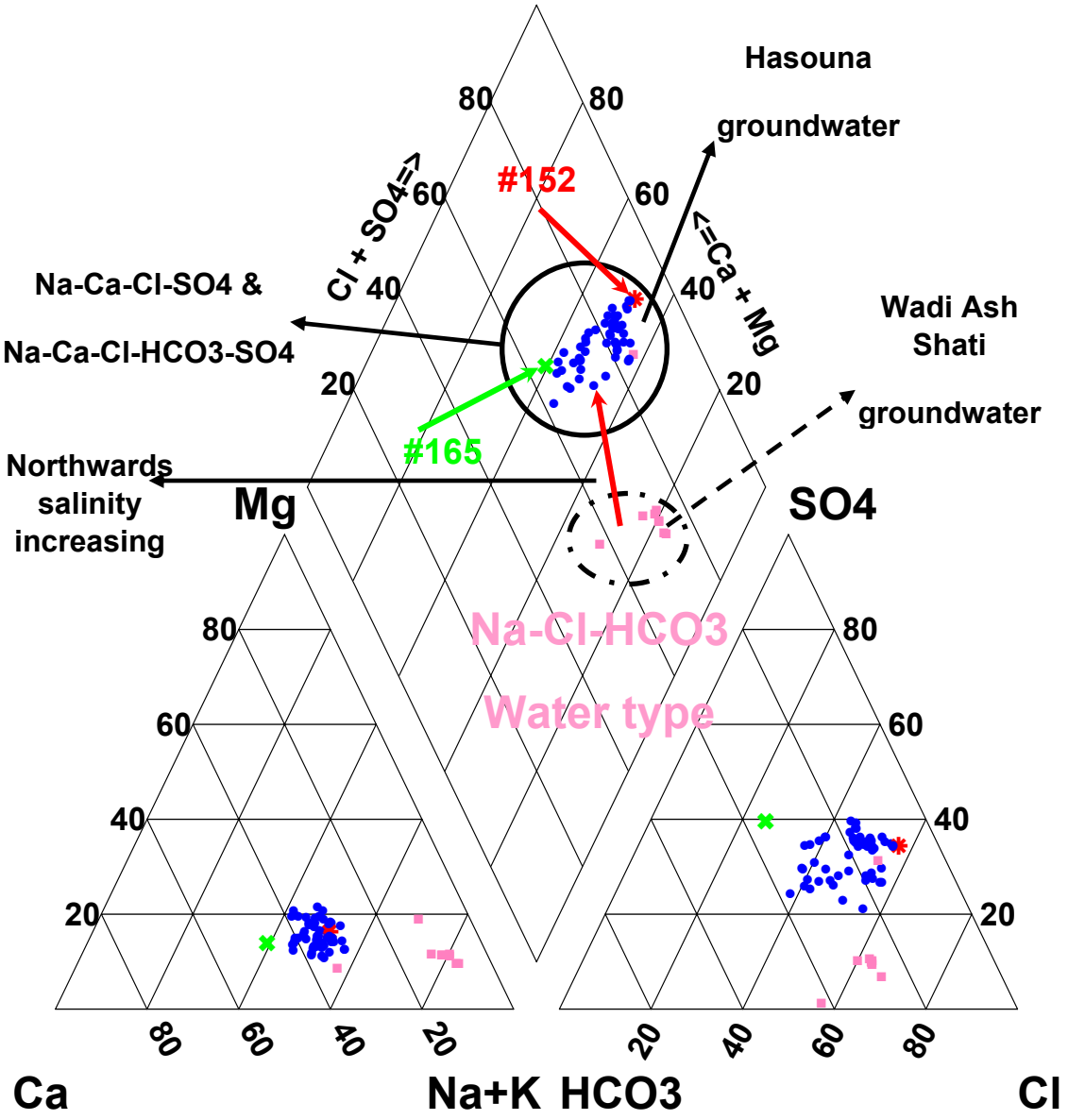

Figure 7.18: Piper diagram showing relative distribution of major cations and anions in the groundwater samples of the Hasouna (●), and Wadi Ash Shati areas (■), water types. Mixing end-members areindicated by wellbore numbers.

As mentioned before in Section 7.5, high nitrate level (114 mgL^{-1}) in the groundwater well (#152) was observed and is associated with increasing in all major ions concentration, while K^{+} and Mg^{2+} have low concentrations, whereas the water well 165 has nitrate concentration of 36.4 mgL^{-1}. In both groundwater wells (#165 and #152) the dominant anion is chloride, sulphate, bicarbonate and nitrate, and among the cations, the order of relative abundance of cations in the Hasouna groundwater is sodium, calcium, magnesium, and potassium (Fig. 7.19).

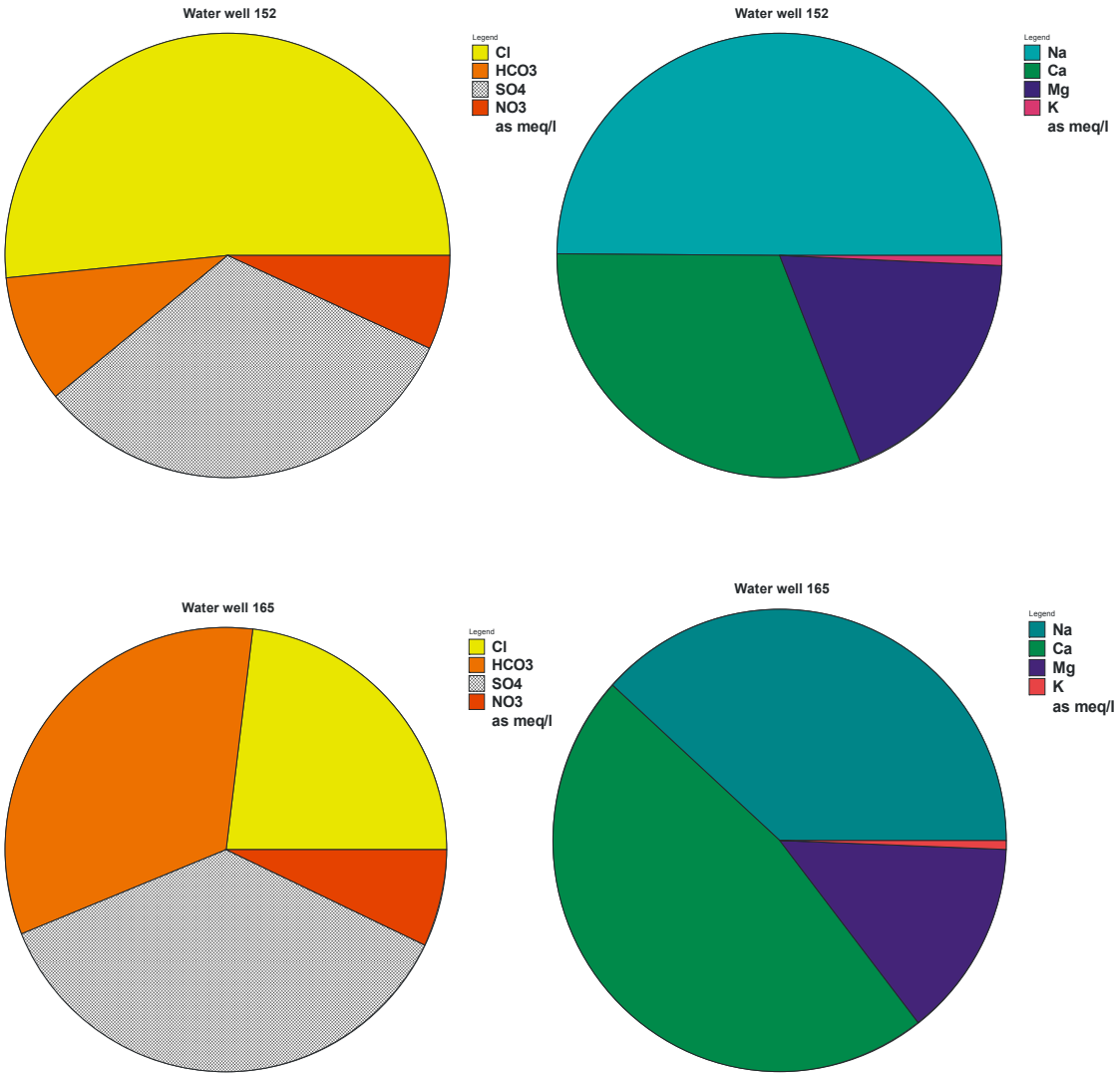

Figure 7.19: Pie diagram showing the relation between the major dissolved ions in two geochemical end members from the Hasouna study area (in meqL^{-}).

7.8 SATURATION INDEX AND HYDROCHEMICAL PROCESSES

Table 7.7 shows the saturation indices (SI) of the minerals, which were calculated on the basis of minimum, maximum, and mean element concentrations of the Hasouna groundwater samples. The saturation indices of all Hasouna groundwater samples are shown in the Table 12.5 (Appendix II). The saturation indices of the carbonate (calcite, and dolomite) and sulphate minerals (gypsum) are displayed in Figures 7.20 and 7.21. Accordingly, all Hasouna groundwater samples are undersaturated with respect to gypsum mineral, ranging from -1.6 to -0.93, with an average value of -1.23 (Table 7.7). The saturation index of gypsum, calcite, dolomite and fluoride is plotted against the concentration of dissolved ions of calcium, magnesium and fluoride (see Figures. 7.20 and 7.21).

The saturation index (SI) of calcite and dolomite in the study area range from -0.52 to +0.37, and -1.2 to +0.45, with a mean value of -0.12, and -0.42, respectively (Table 7.7). Most groundwater samples are undersaturated with respect to calcite and dolomite, some groundwater samples are supersaturated to these minerals, see Table 12.5 (Appendix II).

The saturation indexes of fluoride range from -2.4 to -1.30, with mean values of -1.89 (Table 7.7). The concentration of fluoride in the current study is very low. Therefore, the groundwater is generally undersaturated with respect to fluorite. The saturation index of halite and anhydrite in the Hasouna groundwater ranges from -6.9 to -5.4, and -1.8 to -1.1, with a mean value of -5.98 and -1.43, respectively (Table 7.7).

Thus, the calculated saturation indices indicate that the all groundwaters of the Hasouna waterfields are undersaturated with respect to gypsum, halite, anhydrite, calcite, talc, aragonite, fluoride and dolomite. Few groundwater samples are slightly supersaturated with respect to calcite and aragonite, which is indicating the possibility of precipitation of $CaCO_3$ in the aquifer.

Table 7.7: Saturation Indices (SI) of predominant minerals in the study area waterfields based on minimum, maximum and mean values of the chemical analysis of the Hasouna groundwater using PHREEQC code (Version 2.17.01).

	Calcite	Dolomite	Anhydrite	Gypsum	Halite	Aragonite	Fluorite
Min	-0.5	-1.2	-1.8	-1.6	-6.9	-0.7	-2.4
Max	0.4	0.5	-1.1	-0.9	-5.4	0.2	-1.3
Mean	-0.1	-0.4	-1.4	-1.2	-6.0	-0.3	-1.9

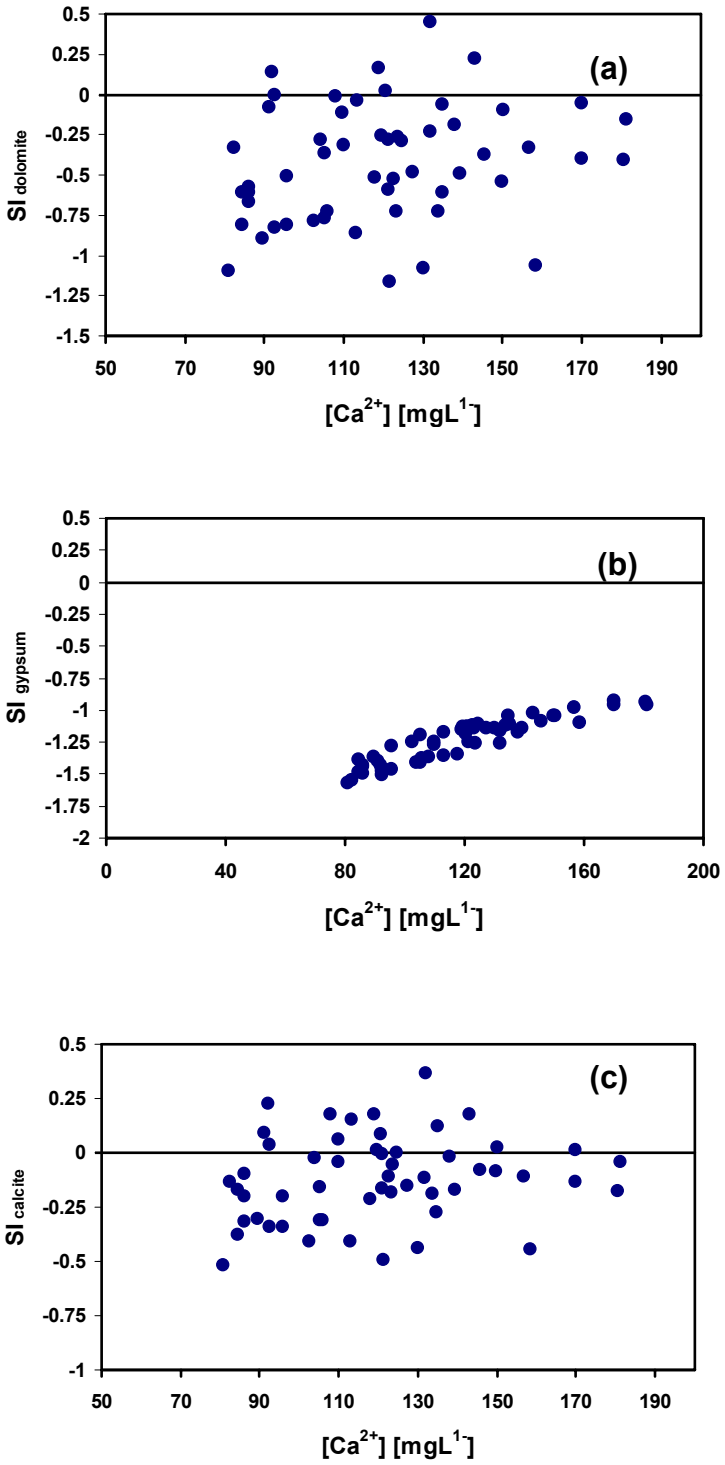

Figure 7.20: Correlation of Ca^{2+} concentrations versus saturation indices of dolomite, gypsum, and calcite.

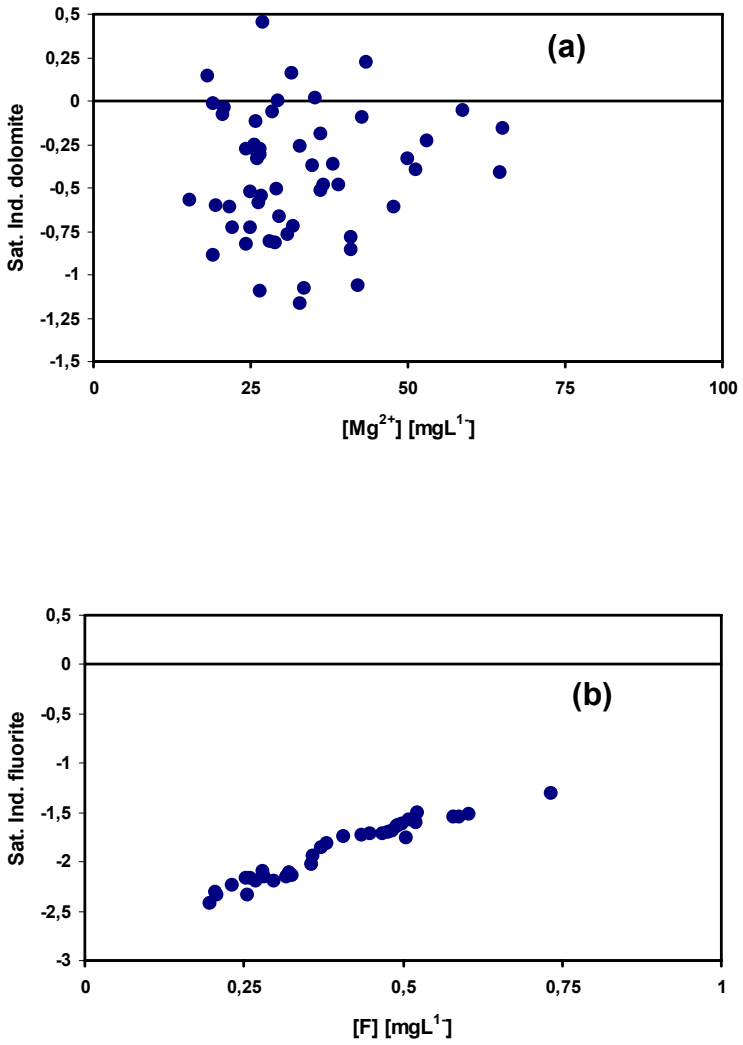

Figure 7.21: Correlations of Mg^{2+}, and F^- concentrations versus saturation indices of dolomite, and fluorite.

7.9 GROUNDWATER QUALITY AND ITS SUITABILITY FOR DRINKING AND AGRICULTURAL USE

7.9.1 GROUNDWATER QUALITY FOR AGRICULTURAL USE

Groundwater in Libya is used not only for domestic and industrial purposes, but also for irrigation of farms and mega agricultural projects. The analyzed groundwater samples data in this current study have been used for the evolution of groundwater quality of drinking water and irrigation. The water for drinking and irrigation purposes must meet very well the recommended

standards of physical, chemical and biological categories (WHO, 2004). The water of this project is planned for about 80% for use in agriculture, 18% for drinking water supply demand and 2% for industry. For this reasons, it is important to evaluate the groundwater quality and its suitability for drinking and irrigations uses. The suitability of the Hasouna water-fields for irrigation is regulated by a sequence of values based on the total dissolved solids (TDS), salinity, sodium percentage content (SSP %Na), water hardness (TH) and sodium hazard (SAR). All these parameters influence the quality of groundwater and produce hazard effects in the water of study area. The water quality parameters are discussed in details in this section. The results of all parameters are listed in Table 12.6 (Appendix II).

7.9.1.1 GROUNDWATER HARDNESS

Water hardness is the sum of the calcium and magnesium ions, which can precipitate as solid phase from water. Hardness is expressed in $meqL^{-1}$ or mgL^{-1} $CaCO_3$ or in hardness degrees. One degree German hardness (°dH) equals 17.8 $mgL^{-1}CaCO_3$ (Appelo & Postma 1994). There is no health-risk guideline standard for the hardness in drinking water (WHO, 2004). The main source of the high total hardness values is the high concentration of calcium and magnesium in groundwater aquifer matrix.

The total water hardness (TH) is expressed as equivalent of $CaCO_3$ and calculated with the following formula: $TH = 2.497\ [Ca^{2+}\ (mgL^{-1})] + 4.118\ [Mg^{2+}\ (mgL^{-1})]$, Fournier 1981. The hardness degree of water is classified on the basis of water hardness, which is listed in the Table 7.8 (Sewyer and McCarty, 1967).

Table 7.8: Classification of water hardness (Sewyer and McCarty, 1967).

Hardness range $[mgL^{-1}]$ of $CaCO_3$	Water classification
0 - 75	soft
75 - 150	Moderately hard
150 - 300	Hard
> 300	Very hard

The total hardness of the groundwater samples in the Hasouna study area ranges from a minimum of 277.6 mgL^{-1} as $CaCO_3$, to a maximum of 720.6

mgL^{-1} as $CaCO_3$, with a mean value of 434 mgL^{-1} (Table 7.9). This value belongs to the fourth category with very hard water (see Table 7.8). The calculated values of total hardness show a variation in hardness over the waterfields (see Table 12.6 in Appendix II).

7.9.1.2 SODIUM HAZARD (SAR)

The big problem of high sodium levels is its effect on the soil parameters. Calculation of sodium hazard is an important parameter for investigating the suitability of Hasouna groundwater for irrigation purposes. High values of SAR mean that sodium in the water may replace calcium and magnesium ions in the soil, potentially causing damage to the soil structure (LIoyd et al., 1985). The Sodium hazard is typically expressed as sodium adsorption ratio (SAR). It is calculated from sodium, calcium and magnesium concentrations in water using the formula (USSLS, 1954):

$$SAR = \frac{[Na^{+}]}{\sqrt{\frac{[Ca^{2+} + Mg^{2+}]}{2}}}, \quad (26)$$

where cations are expressed in meq/l.

In the classification of water samples based on USSL sodium hazard (SAR), water with SAR values less than 10 is considered excellent, 10-18 as good, 18-26 as fair and above 26 is unsuitable for irrigation use (USSLS).

Table 7.9: Statistical measures of groundwater hazards in Hasouna the study area.

Parameters	Magnesium Hazard (MH) [%]	Sodium Percentage (NA) [%]	Sodium Hazard (SAR)	Total hardness (TH)	Soluble Sodium (SSP) [%]
Max	39.9	57.6	5.70	721	57.6
Min	22.6	38.9	2.08	278	38.9
Mean	30.7	48.7	3.94	434	48.6
Median	30.5	49.6	3.96	425	49.2
SD	4.75	3.90	0.930	104	3.90
n	57	57	57	57	57

SD = Standard deviation, n = number of measured samples.

From the calculated value, the sodium hazard values range between 2.08 and 5.72%. Accordingly the SAR values in the Hasouna study are classified as excellent in the category for irrigation use with no concern about soil damage. The SAR values are shown in the Table 7.9. The classification of the Hasouna groundwater for irrigation use can also be determined by plotting of the salinity versus SAR values (Wilcox and Durum, 1967). The Wilcox diagram expresses the relationship between the sodium (SAR) and salinity / (EC, 25 °C) hazards and therefore represents the effect of both hazards on groundwater for irrigation use.

The data of the Hasouna and Wadi Ash Shati groundwaters is plotted in salinity diagram 7.22. This plot confirms for the majority Hasouna groundwater low sodium hazard and high salinity hazard, where few samples show medium sodium hazard with very high salinity hazard (Fig. 7.22).

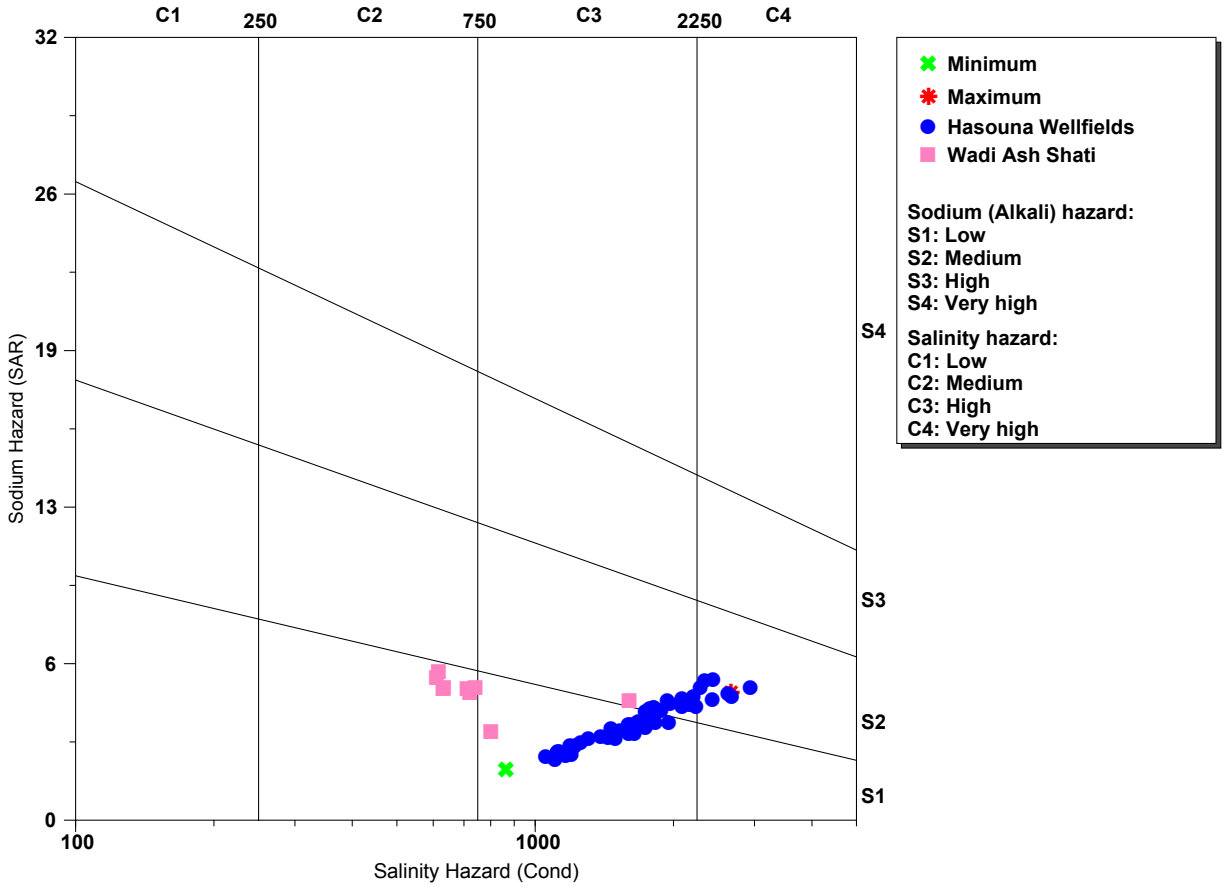

Figure 7.22: Classification of the Hasouna and Wadi Ash Shati groundwaters for irrigation proposes (Wilcox and Durum, 1967).

7.9.1.3 MAGNESIUM HAZARD (MH)

The magnesium and calcium ions are important for plant growth, while they are associated to soil destruction. The classification of groundwater samples is calculated using the relation of Szabolcs and Darab (1964), which is based on magnesium hazard (MH) value for irrigation water, which is given below:

$$\text{MH} = \left(\frac{[Mg^{2+}]}{[Ca^{2+} + Mg^{2+}]} \right) \times 100 , \qquad (27)$$

where values of Ca^{2+} and Mg^{2+} concentrations are in $meqL^{-1}$

MH > 50 is considered harmful and unsuitable for irrigation use.

MH < 50. is classified as not harmful for irrigation.

The calculated magnesium hazard in this current study ranges from 22.6 to 39.9%, with a mean value of 22.6% (Table 7.9). These MH values of the groundwater samples in the Hasouna study area indicate that the groundwater is safe and suitable for irrigation (Fig. 7.23 and Table 7.9).

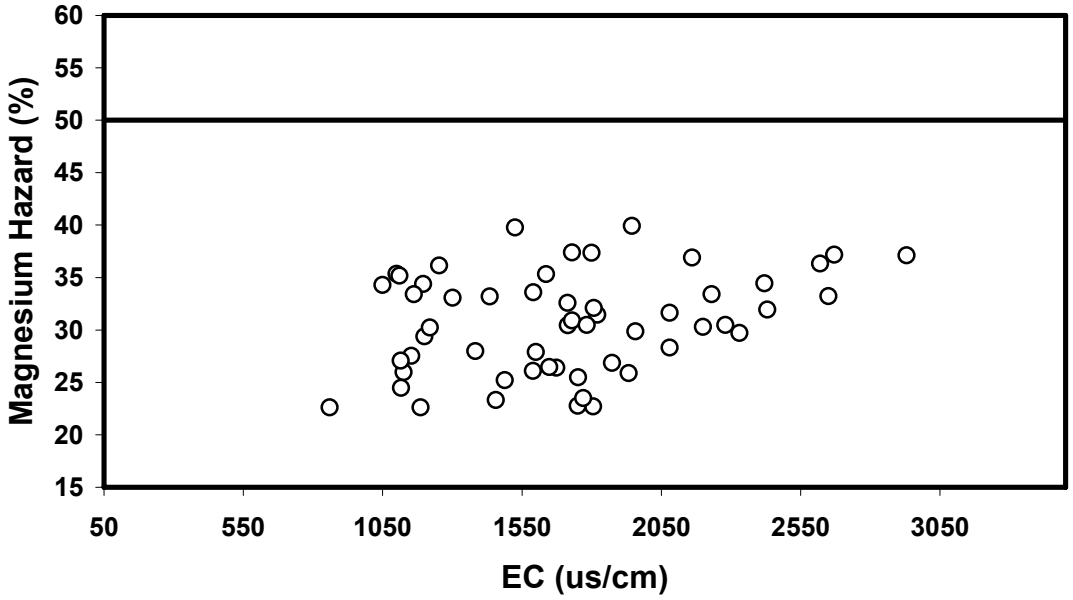

Figure 7.23: Correlation between the measured electrical conductivity (EC, 25 °C) and magnesium hazard (MH) in the groundwater.

7.9.1.4 SOLUBLE SODIUM PERCENTAGE (SSP, % NA)

Soluble sodium percentage (SSP) is an estimation of the sodium hazard of irrigation water like SAR. Wilcox (1955) has proposed classification scheme for the range of soluble sodium percentage (SSP) for irrigation waters. The SSP was calculated by using following formula (Todd, 1980):

$$\text{SSP (\% Na)} = \frac{[Na^{+} + K^{+}]}{[Ca^{2+} + Mg^{2+} + Na^{+} + K^{+}]} * 100 \qquad (28)$$

where the ionic concentrations are in $meqL^{-1}$.

The values of calculated SSP were classified based on the Todd classification (1980); see Table 7.10. The calculated SSP values in this current study range from 38.9% to 57.6%, with mean value of 48.7%. This indicates permissible quality of the Hasouna water for irrigation. About 16 groundwater samples in the study area have %Na concentrations of more than 50%; this groundwater must be mixed with water from other wells to be suitable for irrigation purposes. Therefore, the groundwater of the Hasouna study area is generally suitable for irrigation uses. The SSP values are shown in the Table 7.9. Based on calculated values of SAR, % Na and Magnesium hazard the groundwater of the Hasouna study area is good to permissible irrigation water quality.

Table 7.10: Classification of water for irrigation based on SSP, Todd (1980).

Water Class	SSP [%]	EC [µs/cm]
Excellent	< 20	> 250
Good	20-40	250-750
Permissible	40-60	750-2000
Doubtful	60-80	2000-3000
Unsuitable	> 80	> 3000

7.9.2 GROUNDWATER QUALITY FOR DRINKING USE

The analyzed 57 groundwater samples in the Hasouna study area are characterized by high ion concentrations. Therefore, it is necessary to mix the water wells with high ions values with wells having low ion concentrations. This mixing of water is done directly on site to reach the optimal water quality for drinking standards (Hasouna 00). The average chemical composition is summarised in the Table 7.11. This Table shows the average physical and chemical parameters of the analyzed 57 groundwater samples and mixing water wells (Hasouna 00) in comparison with the Milne-Home and Sahli (2007), and the international World Health Organisation Standards (WHO, 2004) for drinking water use. Correlation and comparisons are presented in Table 7.11. Groundwater suitability for domestic purposes was studied and correlated using the WHO Standards so that the groundwater in a few samples was suitable for domestic purposes in Table 7.11, and Table 12.6 in Appendix II. Groundwater pH is around neutral with pH values ranged from 6.54 to 7.51, with an average pH value of 7.10, which is within the permissible limit (WHO, 2004). The general arrangement of dominance of cations is $Na^+ > Ca^{2+} > Mg^{2+} > K^+$ and for anion $Cl^- > SO_4^{2-} > HCO_3 > NO_3^-$. The Total Dissolved Solids (TDS) values in the current study range from 618 to 1777.5 mgL^{-1}, with a mean value of 1134 mgL^{-1}. The groundwater of the Hasouna waterfields characterized by high salinity (TDS), high nitrate and classified as hard water.

Table 7.11: Correlation between different groundwater parameters in comparison with others study and standard, bld: below limit of detection.

Water Parameters	Concentrations			
	Mean values of current study	Milne-Home and Sahli (2007)	Standard WHO (2004)	Mixing water (Hasouna- 00) Current study (2012)
pH value	7.10	7.17	6.5-9.5	7.10
T [°C]	30.3	30.5	-	30.3
TDS [mgL^{-1}]	1134	1039	1000	1013
EC [µS/cm]	1712	1600	-	1600
NO_3 [mgL^{-1}]	66.3	53.6	50.0	38.4
Cl [mgL^{-1}]	272	297	250	256
SO_4 [mgL^{-1}]	246	210	500	157
HCO_3 [mgL^{-1}]	183	170	-	236
Na [mgL^{-1}]	191	188	200	171
Ca [mgL^{-1}]	120	114	-	104
Mg [mgL^{-1}]	33.0	28.0	-	24.4
K [mgL^{-1}]	10.7	8.44	-	10.2
Total Hardness	434.	400	-	360
Li [mgL^{-1}]	0.047	-	0.	0.011
F [mgL^{-1}]	0.39	0.78	1.50	0.27
As [mgL^{-1}]	bld.	bld.	0.01	bld.
Mn [mgL^{-1}]	0.060	0.010	0.400	bld.
Pb [mgL^{-1}]	bld.	bld.	0.010	bld.
Zn [mgL^{-1}]	0.018	0.020	0.030	0.016

The result of the hydrochemical analysis for trace elements (Fe, Zn, Pb, Mn, As, F, Li, Cd, Al, Cr, Ba) show that all Hasouna groundwater samples have very low concentrations, and in many samples are below the detection limits (see Table 7.6). This results support the argument that all named trace elements bear no health hazards in the Hasouna groundwater.

To meet nitrate concentration limits in the groundwater (< 50 mgL^{-1}, NO_3^-), it is important to use the cheaper method of mixing or dilution, i.e. to mix water from low nitrate wells with that from with high levels. Mixing currently is only applied method in the Hasouna waterfields. The product of this dilution process is represented in the Table 7.12 of the water well mixing (Hasouna 00). Therefore, the results of this easy dilution process deliver groundwater with low nitrate concentration of 38 mgL^{-1} and TDS mean value of 1013 mgL^{-1}

(Table 7.12), which is the optimum for water supply from Hasouna waterfields area to consumption at the supply station in Tripoli. The water from this well with this quality is transported via pipeline to Tripoli city for drinking purpose.

Table 7.12: Physical and chemical parameters of mixing process in the groundwater of Hasouna 00.

Water Well ID	pH	T [°C]	EC [µs/cm]	TDS	NO_3^-	Cl^-	SO_4^{2-}	HCO_3^-	Na^+	Ca^{2+}	Mg^{2+}	K^+
Hasouna 00	**7.1**	**30.3**	**1600**	**1013**	**38**	**256**	**157**	**236**	**171**	**104**	**24**	**11**

Note: values of total dissolved solids, nitrate, chloride, sulphate, bicarbonate, sodium, calcium, magnesium and potassium are in [mgL^{-1}].

.

8 APPLICATION OF ENVIRONMENTAL ISOTOPE PROXIES

A big series of groundwater chemical data and isotopic signatures that include oxygen in water and sulphates ($\delta^{18}O_{H2O}$, $\delta^{18}O_{SO4}$), H ($\delta^{2}H_{H2O}$), and S ($\delta^{34}S_{SO4}$) is used. This whole data set is applied to assess the origin of groundwater in aquifers systems in the study area. The analyzed isotopic data of groundwater samples of the Hasouna waterfields are given in Table 12.8 (Appendix II).

8.1 DEUTERIUM AND OXYGEN ISOTOPES

The groundwater in many hydrogeological basins in Sahara and Sahel regions in northern Africa and in the arid zones of Middle East have low $\delta^{18}O_{H2O}$ and $\delta^{2}H$, and deuterium-excess values (d ≤ 10‰) relative to modern precipitation in these regions (Deuterium-excess > 16‰; Sonntag et al., 1978; Gat, 1981; Sultan et al., 1997; Clark and Fritz, 1997). The interpretation of the previous isotopes studies in the west and southwest region parts of Libya, which has characterised the deep Libya Sahara groundwater as paleo-water with a recharge during periods of higher humidity during the Late Pleistocene (Klitzsch, 1976, 1977; Gonfiantini, 1977; Sonntag et.al., 1978, 1979). The previous isotope work of Sonntag et al. (1978, 1979) shows that groundwater in the Libya Sahara region, which represents paleo (fossil) water, in their $\delta^{18}O_{H2O}$ and $\delta^{2}H$ contents correspond to today's central European water (Fig. 8.2).

In arid regions of the Middle East and northern Africa the major regional aquifer system, such as Damam Formation and Umm Er Rhaduma aquifers in the Saudi Arabian peninsula; aquifer systems of Nubian sandstone and Continental Interclaire in north Africa; have turned out to contain paleowaters, recharged mainly during earlier pluvial times. This is proven by a wide range of isotope field investigations led by the IAEA in its program of technical cooperation in these regions (IAEA, 1980).

Water recharge in the Sahara during the humid periods is depleted in heavy isotopes, and has a d-excess less than 10 ‰ (Rozanski, 1985; Rozanski et al., 1993). The depleted isotopic content shows lower temperatures during recharge. Lower temperatures induce variation in air saturation and thus an increase in the amount of precipitation. At humid conditions the massifs of the central Sahara could have controlled the global atmospheric circulation as the Alps are doing presently. The isotopic data of the North Sahara palaeowaters have been interpreted in terms of westward drift of Atlantic air masses over North Africa (Sonntag et al., 1978), with a continental gradient, which has the

same order of magnitude compared to that of the modern winter precipitation over Northern and Central Europe (Rozanski, 1985). In the Grand Ergs, Sirte and in Kufra oasis in Libya, the isotopic evidence indicates large-scale of recharge corresponding to humid - pluvial phases (Edmunds and Wright, 1979; Salem et al., 1980).

Deuterium excess (d-excess) was defined by Dansgaard (1964) as $d = \delta^2H - 8\ \delta^{18}O$. The d-excess describes the conditions that lead to isotope fractionation between water and vapor during primary evaporation of the oceans (Dansgaard, 1964). Any deviation from a slope of 8 on the plot diagram of the relationship between $\delta^{18}O$ and δ^2H may indicates evaporation, mixing between different water groups, or water-rock interactions. Also, the d-excess values are varying significantly from one region to another (Dansgaard, 1964). Paleowaters are often characterized by relatively small d-excess values (Yurtsever & Araguas Araguas, 1993).

Some selected groundwater samples from the current study of Hasouna waterfields have been analyzed for stable isotopes of oxygen and hydrogen. The $\delta^{18}O$ values vary from -10.1 ‰ to -8.8 ‰ with a mean value of -9.5 ‰ and from -64.6 ‰ to -73.5 ‰ for δ^2H with a mean value of -70.0 ‰ (see Table 12.8 in Appendix II). These values correlate very well with the analyzed isotope data of Salem et al. (1980) in the study area, who measured the values of $\delta^{18}O$ (-9.58 ‰, and -9.88 ‰) and δ^2H (-69.0 ‰, and -72.7 ‰) with ^{14}C ages of 10 400 ±5700, and 12 300 ±5900 years BP.

The variation of isotopic compositions of the analyzed Hasouna groundwater samples is small (see Table 12.8 in Appendix II). The stable isotope values are plotting below the GMWL (Global Meteoric Water Line); (left side) on the δ^2H versus $\delta^{18}O$ diagram (Fig. 8.1), indicating probably a paleo recharge effect with origin during previous cooler climatics periods.

The groundwater from the Hasouna study area in this study is depleted in deuterium in a comparison with the water from Tripoli area with recent recharge (Fig. 8.1), with d-excess mean values around 6 ‰, which indicates that these groundwaters are paleo groundwaters of meteoric origin recharged at cooler periods (Pulvial time). During the late Pleistocene time, the recharged water in the Sahara region is depleted in heavy isotopes relative to modern precipitation, and has d-excess values lower than 10 ‰ (Rozanski, 1985; Rozanski et al., 1993). The heavy isotope depletion was also documented for groundwater recharged during the early Holocene, which reflects humid periods (Rozanski, 1985). The groundwaters of the Paleozoic Cambro-Ordovician aquifer from the Hasouna water area are isotopically much heavier than the isotope data of Wadi Ash Shati area (see Fig. 8.2). This

fact is due to the different climate conditions during the recharge time of the paleo groundwater and altitude effects.

In the Fig. 8.1 the Hasouna isotopes samples ($\delta^{18}O$ and $\delta^{2}H$); (**o**), and the isotope samples of groundwater of Wadi Ash Shati area in the south of the Hasouna study area are plotted (**o**). The isotope values of groundwater wells from the area Tripoli are also plotted (**o**). The isotopic composition of Tripoli samples falls on or close to the GMWL, which indicates that these waters are meteoric origin with recharge by modern local precipitation (Fig. 8.1).

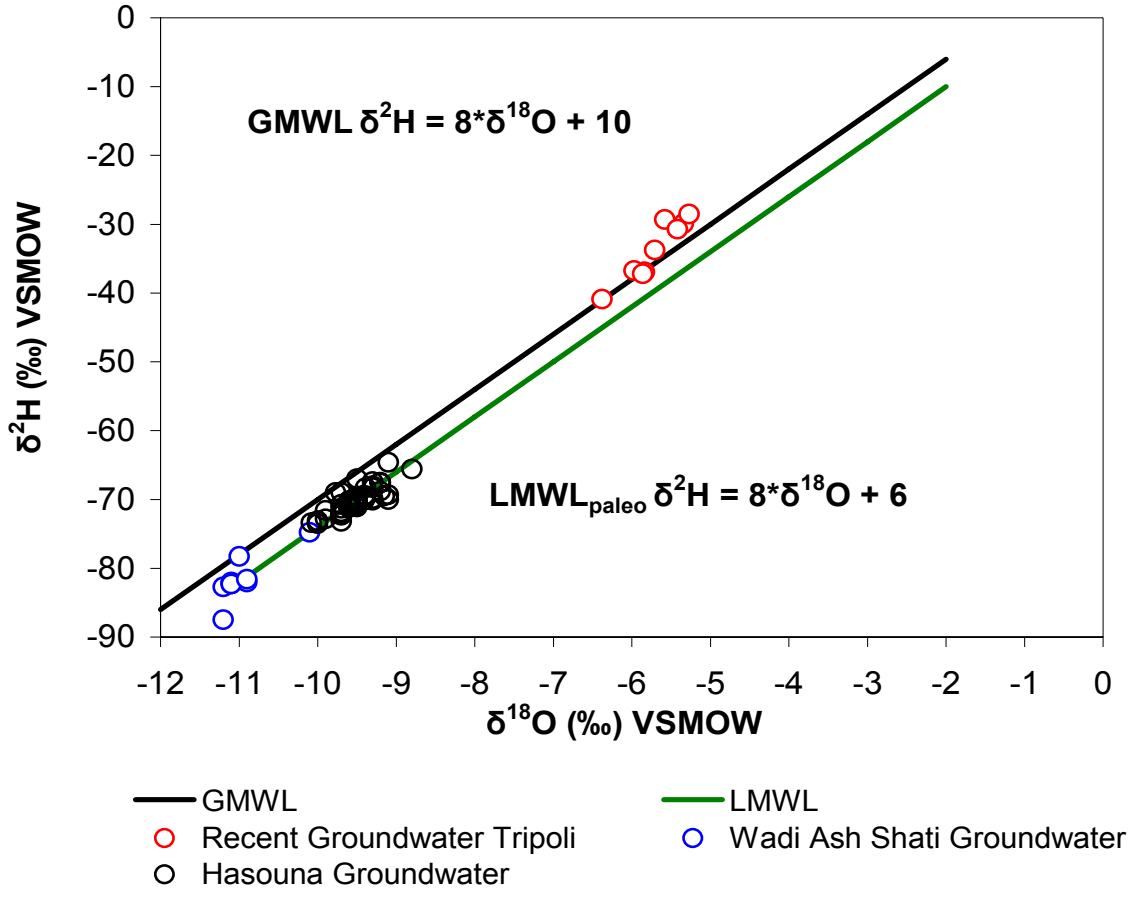

Figure 8.1: Correlations of $\delta^{18}O$ and $\delta^{2}H$ for groundwater from the Hasouna waterfields with plot of global meteoric water line (GMWL, solid black line), and local line for paleo water (solid green line); as wells samples of the Wadi Ash Shati and Tripoli.

Based on the comparison of the results of $\delta^{18}O$ and $\delta^{2}H$ values with the paleo (fossil) groundwater of northern Sahara (Sonntag et al., 1978), the isotope values of oxygen and hydrogen for the Hasouna groundwater were plotted vs. the paleo Saharian groundwater in south Libya (Fig. 8.2). The Hasouna samples fit well to former results for paleo groundwater from Murzuq Basin groundwater. Thus the deep groundwater of Cambro-Ordovician Hasouna aquifer in the study area has a paleometeoric origin (see Fig. 8.2), and the depleted signatures of the stable isotopes of oxygen and hydrogen in these Hasouna groundwaters correspond to recharge during a cooler period than present day climatic conditions.

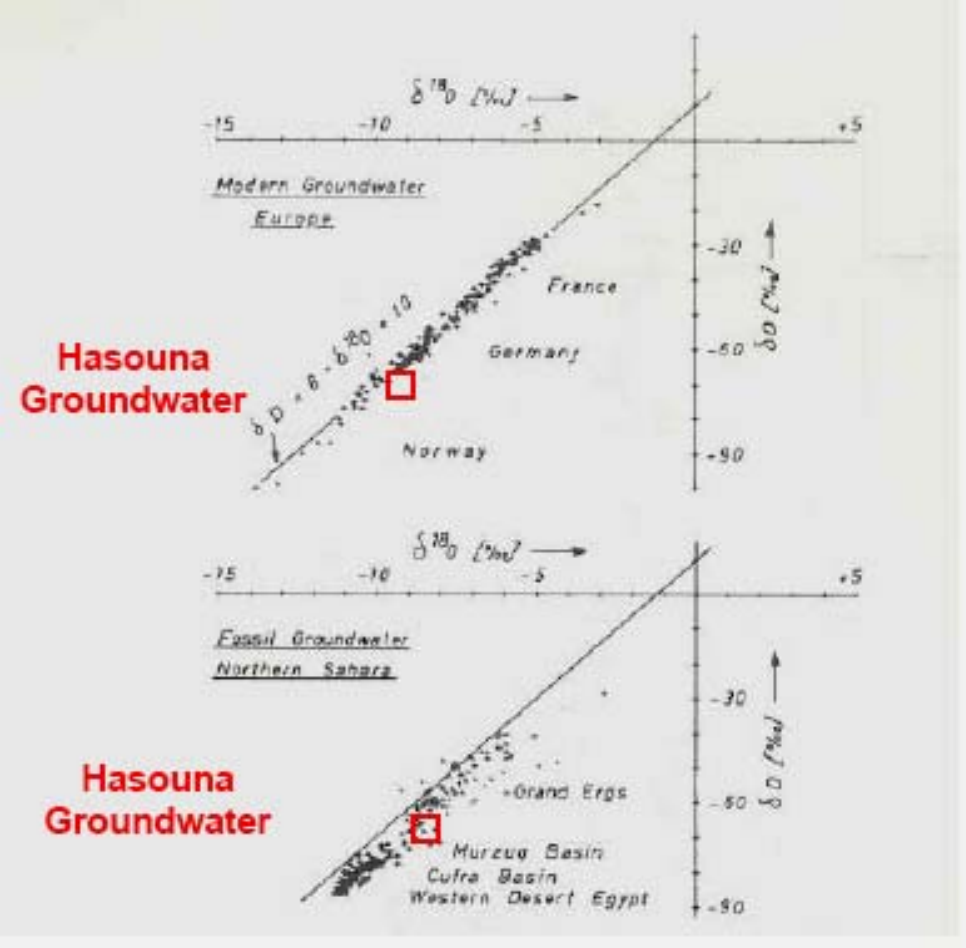

Figure 8.2: $\delta^{2}H$ versus $\delta^{18}O$ diagram of modern European and fossil Saharian groundwater (data of Gonfiantini., et al, 1974). The Hasouna isotope samples mean values (are presented in the plot (red square).

8.2 SULPHUR AND OXYGEN ISOTOPES OF GROUND WATER SAMPLES

Groundwater samples were collected for stable isotope analysis on dissolved sulphate from 11 wells in Hasouna study area. Possible sulphur sources comprise atmospheric contribution (precipitation and dry depositions), volcanic sources, marine sources, mineral (gypsum and anhydrite) or rock contribution and biological contributions (Fritz et al. 1994).

Groundwater of the Hasouna waterfields contains dissolved sulphate in the range from 126 to 438 mgL^{-1} with a mean value of 245 mgL^{-1} (Table 7.4). The isotopes signature $\delta^{34}S$ of dissolved sulphate ranges from 9.0 ‰ to 11.1‰ with a mean value of 10.3 ‰, whereas the values of $\delta^{18}O$ for dissolved sulphate range from 9.2 ‰ to 11.7 ‰ with a mean value of 10.4 ‰, (see Table 12.8 in Appendix II). The plot of $\delta^{34}S_{sulphate}$ versus $\delta^{18}O_{sulphate}$ of dissolved sulphate reflects the behaviour of the Hasouna groundwater in the aquifer. The values of sulphate isotope groundwater samples show small variation.

The high sulphate level in the groundwater from Hasouna aquifer is mainly attributed to sulphate from marine evaporates (Permian). The sulphur isotopic signatures of the groundwater are suggested to be generated from Permian geological units (dissolution of Permian marine sulphate) (see also Appendix I for further discussion).

8.3 NITRATE AND NITROGEN ISOTOPES

To determine the origin of nitrate in Hasouna groundwater, about 28 groundwater samples were collected for $\delta^{15}N$ and $\delta^{18}O$ analysis of nitrate. Some groundwater samples were selected for nitrogen isotopes $\delta^{15}N_{nitrate}$, $\delta^{17}O_{nitrate}$ and $\delta^{18}O_{nitrate}$ based on moderate and high nitrate concentrations in the Hasouna study area. The measured $\delta^{15}N$, $\delta^{18}O$ and $\delta^{17}O$ values of nitrate in Hasouna groundwater are summarized in Table 12.8 in Appendix (II).

In the Hasouna studied area, $\delta^{15}N_{nitrate}$ ranged from +6.6 ‰ to +9.2 ‰ with a mean value of +8 ‰, and the $\delta^{18}O_{nitrat}$ ranged between +5.0 ‰ and +20.0 ‰, with mean value of +11.73 ‰, where the values of isotope $\delta^{17}O_{nitrate}$ varied from +2.8 ‰ to +15.6 ‰, with mean value of +8.6 ‰, while $\Delta^{17}O$ ranged from +0.5 ‰ to +5.1 ‰, with mean value of +2.63 ‰ (see Table 12.8 in Appendix II).

High level (114 mgL^{-1}, Table 7.4) of dissolved nitrate in this study is analyzed and interpreted on the basis of previous studies of Böhlke et al. (1997), Michaliski et al., 2003, 2004a, 2004b, and Thiemens, 2006. Böhlke et al., 1997, which studied the atmospheric deposition source of nitrate in Atacama and Mojave Desert.

The source of nitrate accumulation from atmospheric deposition in Atacama Desert in Chile was documented and confirmed by using mass-independent oxygen isotopic fractionation (Michalski, 2004a); (Figs. 8.3a and b). In dry seasons $NO_{3\ atm}^{-}$ accumulates on plants and soil surface in the Devil Canyon watershed (Fig. 8.3c) and in rainy seasons the accumulated nitrate leaches rapidly into water in the shallow groundwater (Michalski, 2004b).

The analyzed distribution of oxygen isotopes of the Hasouna samples for dissolved nitrate are plotted in diagrams of Michalski, 2004a, to understand and identify the origin of high nitrate levels in the Hasouna study area. The isotope values (^{17}O, ^{18}O, $\Delta^{17}O$) show a clear atmospheric trend, (see Figure 8.3). The red rectangle represents the range in $\delta^{17}O$, $\Delta^{17}O$ and $\delta^{18}O$ values of dissolved nitrate.

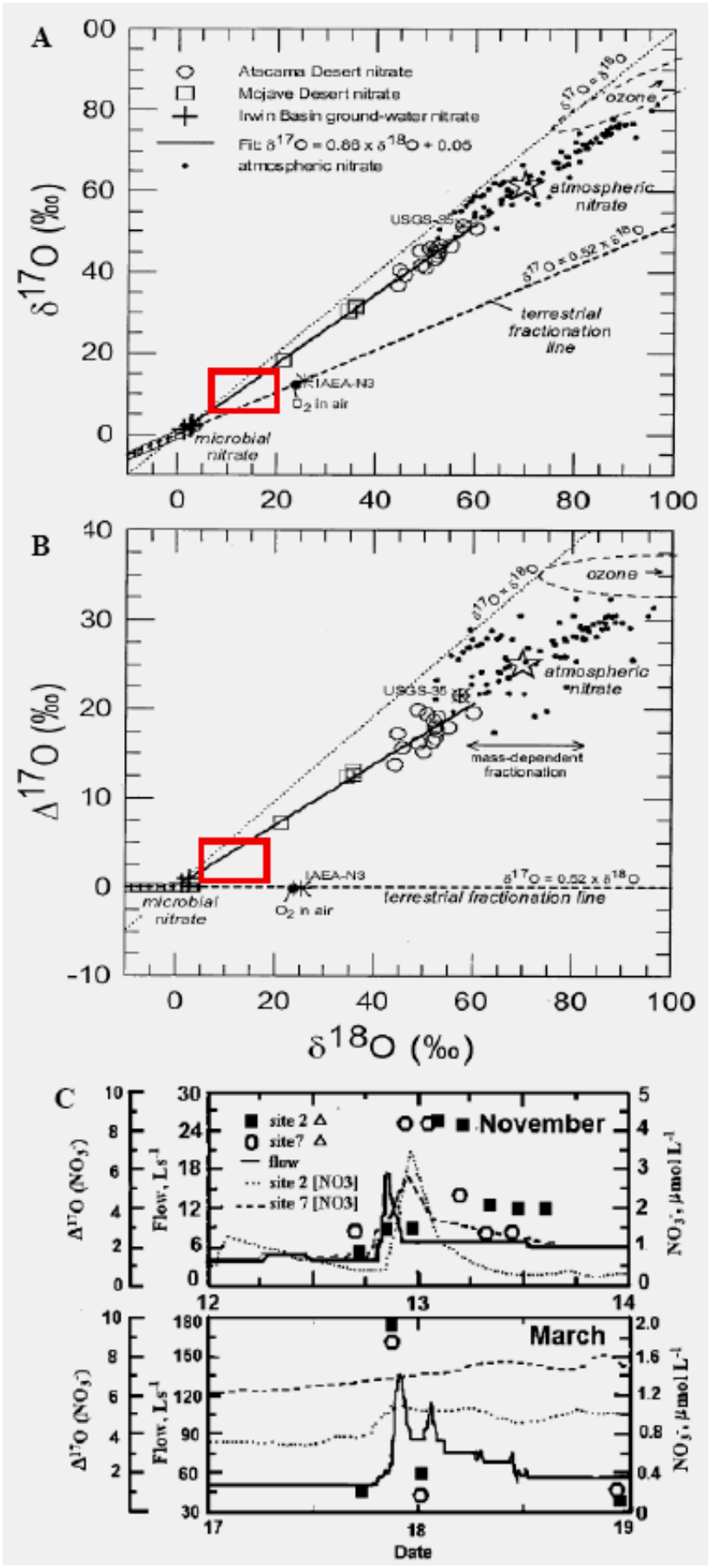
A
Atacama Desert nitrate
Mojave Desert nitrate
Irwin Basin ground-water nitrate
Fit: δ17O = 0.88 x δ18O + 0.05
atmospheric nitrate
δ17O = δ18O
ozone
atmospheric nitrate
USGS-35
δ17O = 0.52 x δ18O
terrestrial fractionation line
IAEA-N3
O2 in air
microbial nitrate
δ17O (‰)
B
ozone
atmospheric nitrate
USGS-35
mass-dependent fractionation
IAEA-N3
O2 in air
δ17O = 0.52 x δ18O
terrestrial fractionation line
microbial nitrate
Δ17O (‰)
δ18O (‰)
C
site 2
site7
flow
site 2 [NO3]
site 7 [NO3]
November
March
Δ17O (NO3-)
Flow, Ls-1
NO3-, μmol L-1
Date

Figure 8.3 (previous page): Nitrate O isotopic variations in samples of Atacama Desert caliche-type salts, Mojave Desert caliche-type salts, and Mojave Desert (Irwin Basin) groundwater nitrate:
(A) $\delta^{17}O$ versus $\delta^{18}O$; $\Delta^{17}O$ versus $\delta^{18}O$. Data shown for comparison include atmospheric nitrate in rain and aerosols from California and Antarctica (Michalski et al., 2003 unpublished data) and isotopic reference materials IAEA-N3 and USGS35 (Michalski et al., 2002; Böhlke et al., 2003). The terrestrial fractionation line indicates the trajectory followed by mass-dependent isotopic variations.
(B) The $\Delta^{17}O$ versus $\delta^{18}O$ plot (b) emphasizes the effects of mass-dependent fractionations (horizontal vectors) that are less obvious in the $\delta^{17}O$/ $\delta^{18}O$ plot.
(C) Streamflow hydrograph for Devil Canyon (solid line), stream NO_3^- concentration for site 2 (dotted line) and site 7 (dashed line), and $\Delta^{17}O$ variations for site 2 (■) and site 7 (○) during November and March rainstorms in the Devil Canyon watershed. The November storm was preceded by an 8 month dry period. The March storm came at the end of the rainy season. The Hasouna oxygen isotopes values for dissolved nitrate were plotted in the Michalski et al., 2004a plot, which are marked with red square symbol (□).

The high nitrate concentration was studied by Vogel et al., 1981 in the Kalahari Desert region, where they documented that nitrate concentrations are of natural origin. The triple-oxygen isotope plot shows the mass-independent anomaly concept. In this plot mass-dependent fractionation (MDF) for nitrate value can be approximately calculated by the relation: $\delta^{17}O = 0.52*\delta^{18}O$ (Michalski et al., 2002); (Fig. 8.4).

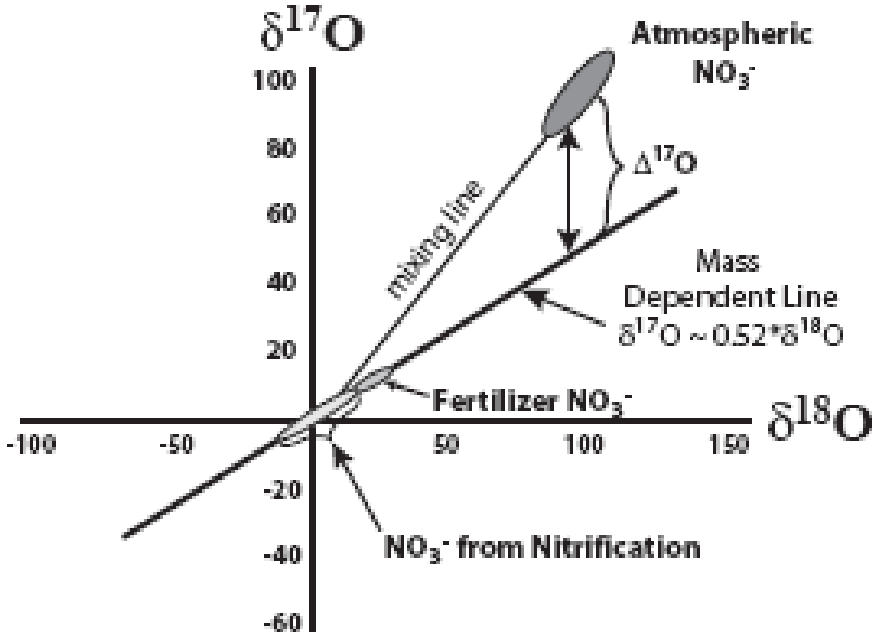

Figure 8.4: Schematic relationship between $\delta^{18}O$ and $\delta^{17}O$ values of dissolved nitrate (Modified from Michalski et al., 2002).

The correlation of $\delta^{15}N_{nitrate}$ versus $\delta^{18}O_{nitrat}$ shows that the distribution of isotope values has no denitrification trend (Fig. 8.5a). This nonlinear relationship confirms the exclusion of denitrification process in the Hasouna groundwater samples (Fig. 8.5a). The measured $\delta^{15}N_{NO3}$ and $\delta^{18}O_{NO3}$ values of dissolved nitrate are nearly within the range of microbial originated NO_3 e.g. by nitrification in soils, where $^{18}O/^{16}O$ is incorporated apparently from H_2O and O_2, and $^{15}N/^{14}N$ is derived from organic matter.

The relationship between $\delta^{18}O$ and $\delta^{17}O$ isotopes values in the Figure 8.5b shows strong correlation (r^2 = 0.94), which represents an atmospheric deposition trend of the oxygen isotope signature.

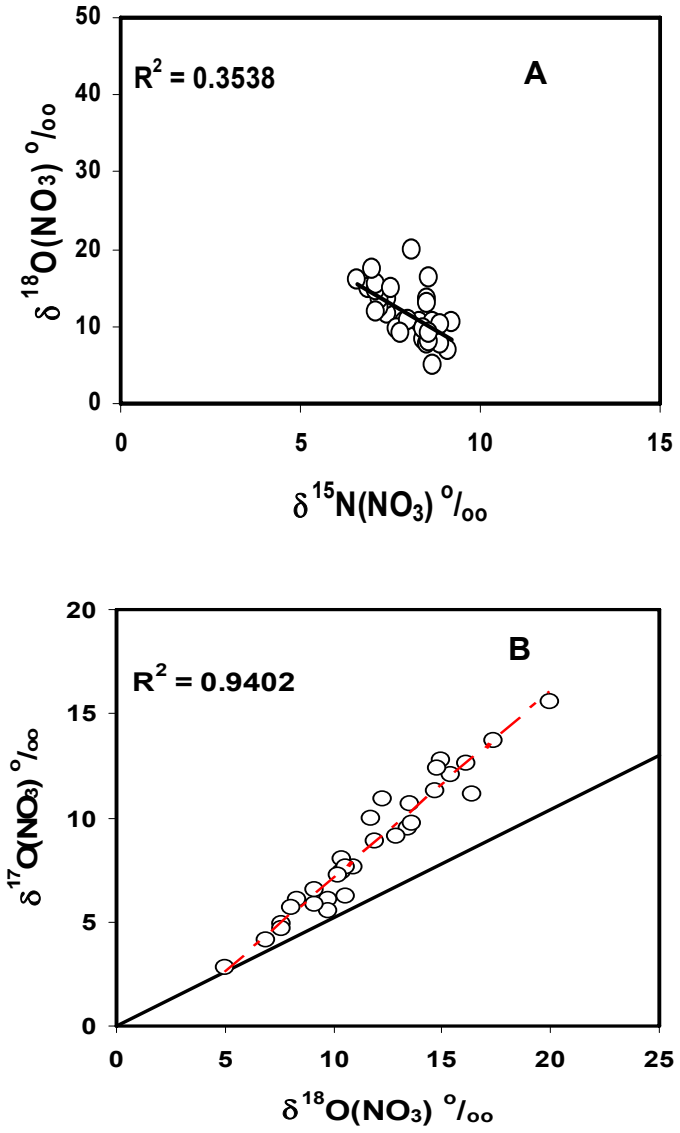

Figure 8.5: a) Correlation of $\delta^{15}N_{nitrate}$ versus $\delta^{18}O_{nitrate}$, b) $\delta^{15}N_{nitrate}$ vs. $\delta^{17}O_{nitrate}$, Mass dependent line (solid line) is defined by the relation: $\delta^{17}O=0.52*\delta^{18}O$ (Michalski et al., 2002).

For a better characterization of sources and origin of high nitrate levels in the Hasouna groundwater samples, the measured nitrogen isotopes data for nitrate ($\delta^{15}N$ and $\delta^{18}O$) were compared to measured nitrogen isotopes of (Milne-Home and Sahli, 2007), which show small differences.

The isotopes values in Figs. 8.6a and c show high $\delta^{15}N_{nitrate}$ values with decrease of NO_3^- values, whereas $\delta^{18}O_{nitrate}$ shows a linearly increasing trend with the concentrations of nitrate. These trends in Figures 8.6a and c exclude the occurrence of denitrification processes in the Hasouna groundwater samples. In the Figs. 8.6b and d the correlation between $1/(NO_3^-)$ in Lmg^{-1} versus $\delta^{15}N_{nitrate}$ and $\delta^{18}O_{nitrate}$ is displayed.

The interpretation of nitrogen isotopes (^{15}N, ^{17}O and ^{18}O) is given in detail in Appendix (I). In the following main conclusions are given:

The origin of high nitrate concentration in the groundwater samples of the Hasouna area is attributed to humid periods, which are characterized by high precipitation accompanied by flood events, and in dry periods with accumulation of nitrate in solid surfaces. In rainy periods the deposited nitrate is flushed out and infiltrated rapidly into the soil layers and into shallow aquifers of the study area. The results of this leaching process are an increase in the concentrations of dissolved ions and salinity of the Hasouna ground waters.

Thus by far more accurate and precise information about the origin of NO_3^- is obtained by analysing both $\delta^{17}O_{NO3}$ and $\delta^{18}O_{NO3}$ values. Surprisingly, all Hasouna paleo groundwaters measured here exhibit a positive ^{17}O-excess up to $\Delta^{17}O_{NO3} \approx 5\ ^{o}/_{oo}$ which is attributed to MIF during conversion of atmospheric NO_x and O_3 to $NO_{3(atm)}$ (Table 12.8 in Appendix II; (Kendall and Doctor, 2004; Michalski et al., 2004a; Thiemens, 2001)).

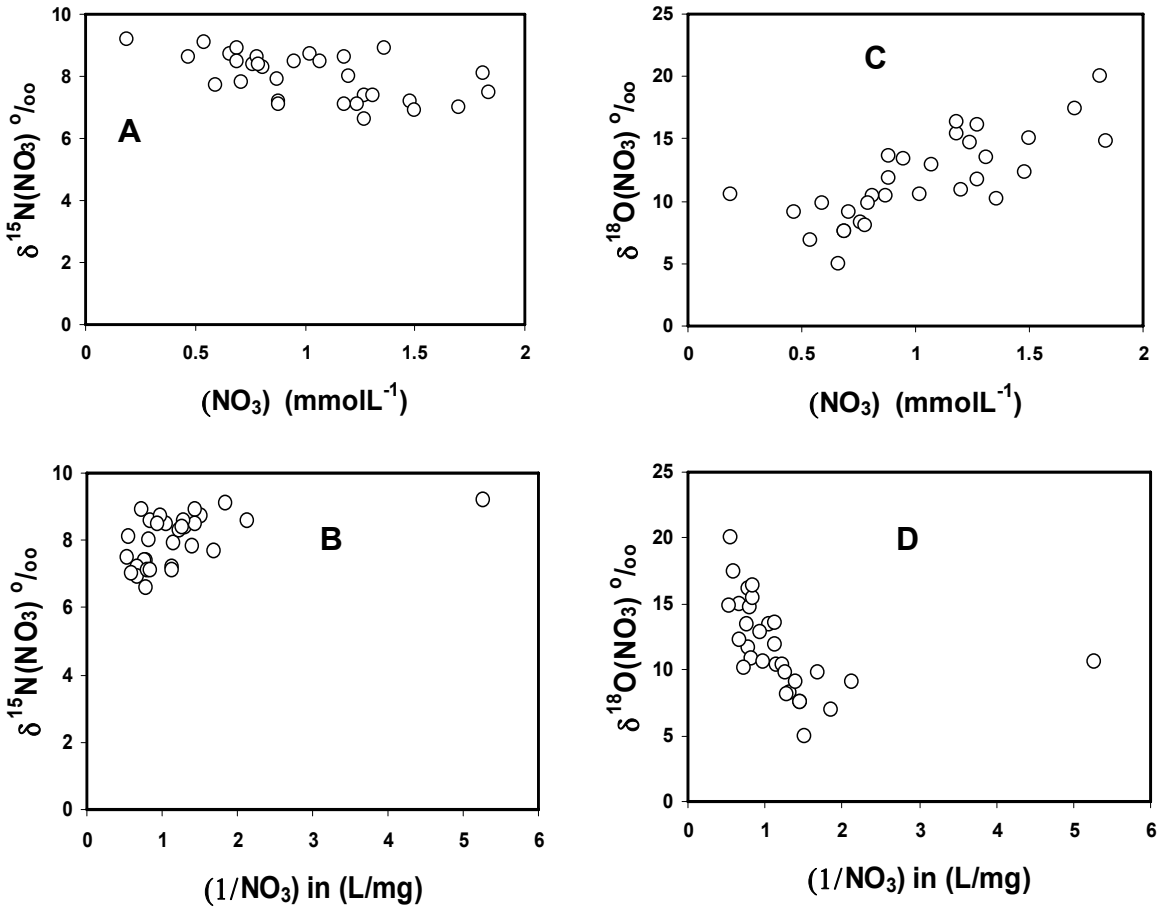

Figure 8.6: Correlation between the isotopes $\delta^{15}N_{nitrate}$ versus $\delta^{18}O_{nitrat}$ versus dissolved nitrate (NO_3^-), and 1/[NO_3^-] in L/mg.

9 EVALUATION OF THE HYDROCHEMICAL AND GEOPHYSICAL DATABASE OF LIBYAN GREAT MAN-MADE RIVER PROJECT

9.1 EVALUATION OF HYDROCHEMICAL DATABASE

This current study is based on analyses of the hydrochemical and geophysical database of Great Man-made River Project (GMRA). It includes the groundwater hydrochemistry of all wells in Hasouna waterfields area. This database contains parameters such as: pH, T, electric conductivity, TDS, cations (Na^+, Ca^{2+}, Mg^{2+}, and K^+), anions (NO_3^-, SO_4^{2-}, Cl^-, and HCO_3^-). The investigations also contain the analysis of petrophysical and geophysical data (as logging data) of some groundwater wells of the Hasouna study area. The purpose of this groundwater database review is to provide a background for the major distribution of groundwater ion-concentrations within the study area and the analysis of geophysical and petrophysical logdata. We expect that reviewing the hydrochemistry data of main ions will help to understand the sources of high ion concentrations in groundwater wells (NO_3^-, Cl^-, SO_4^{2-}, and Na^+). The hydrochemical composition of groundwater samples from GMRPA database is summarized in Tables 9.1 and 9.2. Statistical relevant parameters were calculated to evaluate and study hydrochemical and physical properties by comparing the range of measured values of different groundwater parameters. In the Hasouna groundwater the physico-chemical parameters show considerable variation in their concentrations (see Tables 9.1 and 9.2). The pH in the Hasouna waterfields samples varies from 6.29 to 8.49, with mean value of 7.12. All evaluated samples are within the recommended standard limit (7.0-8.5) for human demands. The groundwater temperature (T) of groundwater samples range between 14.4 and 42.5 °C, with an average value of 30.57°. Hasouna groundwater samples are characterized in general by a high temperature anomaly. Carbon dioxide content varies from 0.40 to 60.2 mgL^{-1} with a mean value of 16.3 mgL^{-1}.

Additionally, the Hasouna groundwater has high CO_2 contents, which means an increase in the dissolution processes of carbonate rocks in aquifers. The dissolved oxygen rises up to 14.4 mgL^{-1} with an average value of 4.9 mgL^{-1}. Therefore, denitrification processes with high oxygen concentration levels can be rather excluded. The total dissolved solids (TDS) range from 439 to 2815 mgL^{-1}, with a mean value of 1040 mgL^{-1}. Generally, the Hasouna groundwater shows high mineralization. The electrical conductivity values (EC) vary from 675 to 4330 µs/cm, with a mean value of 1703 µs/cm. Regarding the analyzed physical parameters, groundwater of the Hasouna has high salinity, and most

of groundwater samples have values higher than the recommended limits (WHO, 2004). All physical statistical parameters are presented in Table 9.1.

Table 9.1: Descriptive statistical of groundwater analyzed sampled database.

Statistical parameters	pH	T [°C]	CO_2 [mgL^{-1}]	DO [mgL^{-1}]	TDS [mgL^{-1}]	EC [µs/cm]
Max	8.49	42.5	60.2	14.4	2815	4330
Min	6.29	14.4	0.40	bld.	439	675
Mean	7.19	30.6	16.3	4.90	1041	1703
Median	7.21	30.1	12.9	5.30	1003	1603
SD	0.29	2.75	9.80	1.67	295	516
n	515	513	513	498	446	515

Temperature (T), Carbon dioxide (CO_2), Dissolved Oxygen (DO), total dissolved solids (TDS), and electrical conductivity (EC), SD: Standard deviation and n: samples numbers.
bld. = below detection limit

The nitrate (NO_3^-) values ranges from 1.0 to 133.3 mgL^{-1}, with a mean value of 52.6 mgL^{-1} (see Table 9.2). The majority of groundwater samples in the database (GMRA, 1996) presented higher values than the recommended concentration level for human consumption (50 mgL^{-1}; WHO, 2004). Consequently, the high levels of nitrate in groundwater of Hasouna waterfields are of major concern for human health, although mixing the water from wells with low nitrate levels with waters of high nitrate contents is under consideration. This might be only the optimal procedure for the management of the nitrate issue in the Hasouna area. Bicarbonate (HCO_3^-) levels range from 98.8 to 318 mgL^{-1}, with a mean value of 116.6 mgL^{-1}. The contents of calcium (Ca^{2+}) and magnesium (Mg^{2+}) in groundwater samples range from 17 to 400 mg/l and 6.4 to 143 mgL^{-1}, with mean values of 116.6 mgL^{-1} and 29.8 mgL^{-1}, respectively. The Hasouna groundwater samples generally show high calcium and magnesium values, with a high variation in actual levels. The sodium (Na^+) ion concentrations in the Hasouna water show wide variation from a minimum of 42 mgL^{-1} to a maximum of 382 mgL^{-1}, with a value of 191 mgL^{-1} on average. The chloride (Cl^-) concentration ranges from 77 mgL^{-1} to 609 mgL^{-1}, while sulphate (SO_4^{2}) ranges from 70 mgL^{-1} to 465 mgL^{-1}, with mean values of 298.6 $mgL^{-1}$and 229 mgL^{-1}, respectively. The major groundwater ions as nitrate, bicarbonate, calcium, magnesium, sodium, chloride and sulphate show high concentrations in the most groundwater of Hasouna waterfields, which are higher than the recommended standards (WHO, 2004). The evaluated hydrochemical data of major ions are presented in the Table 9.2.

Table 9.2: Summery statistical parameters of groundwater ions concentration in the Hasouna waterfields.

Statistical Parameters	NO_3 [mgL^{-1}]	HCO_3 [mgL^{-1}]	Ca [mgL^{-1}]	Mg [mgL^{-1}]	Na [mgL^{-1}]	Cl [mgL^{-1}]	SO_4 [mgL^{-1}]
Max	133	318	400	143	382.7	609	465
Min	1.00	98.8	17.0	6.40	42.1	77.0	70.0
Mean	52.6	171	117	29.9	191.3	299	229
Median	54.0	170	119	26.9	193	284	221
SD	20.6	171	30.8	13.6	49.0	105	76.9
n	446	502	445	444	446	445	436

There are wide ranges of ion concentrations and variations within the Hasouna groundwater chemistry, which suggests that the hydrochemical parameters have been controlled by the hydro-geological characteristics, as there are: groundwater flow, mixing from Zimam aquifer, dissolution processes, geological faults and fractures between the water wells of the study area. Clearly, the evaluation of the hydrochemical database of the groundwater shows a significant increase in the degree of groundwater mineralization in the direction of groundwater flow (from south to north), where also an extreme high concentration anomaly is found close to middle of Hasouna water fields in the mixing Zone (see Fig. 10.1) between the saline Zimam aquifer and Cambrian Ordovician Paleozoic Hasouna aquifer. Within the mixing zone in water fields became the Hasouna groundwater more salinity.

9.2 EVALUATION OF GEOPHYSICAL DATABASE

Based on the available information's data of tectonics, stratigraphy, hydro-geology, and geophysics in the study area, the most relevant geological formations, tectonics events, and lithology boundaries were described and constructed. Groundwater well numbers, Upper Tar member, Hassawnah (Hasouna) Formation, groundwater level (GWL), and geological faults are displayed and shown in Figures 9.1a and b. Jurak (1978) documented the existence of several structural faults around the exploration well T29 (29/89),. This well has located in middle of Hasouna waterfields and has high salinity contents, chloride 1127 mgL^{-1}, nitrate 123 mgL^{-1} and sulphate 661 mg/l (Fig. 10.1). The industrial Research Centre (IRC, 1978) confirmed the existence of various faults close to the water wells 125 and 126 in the Hasouna waterfields area.

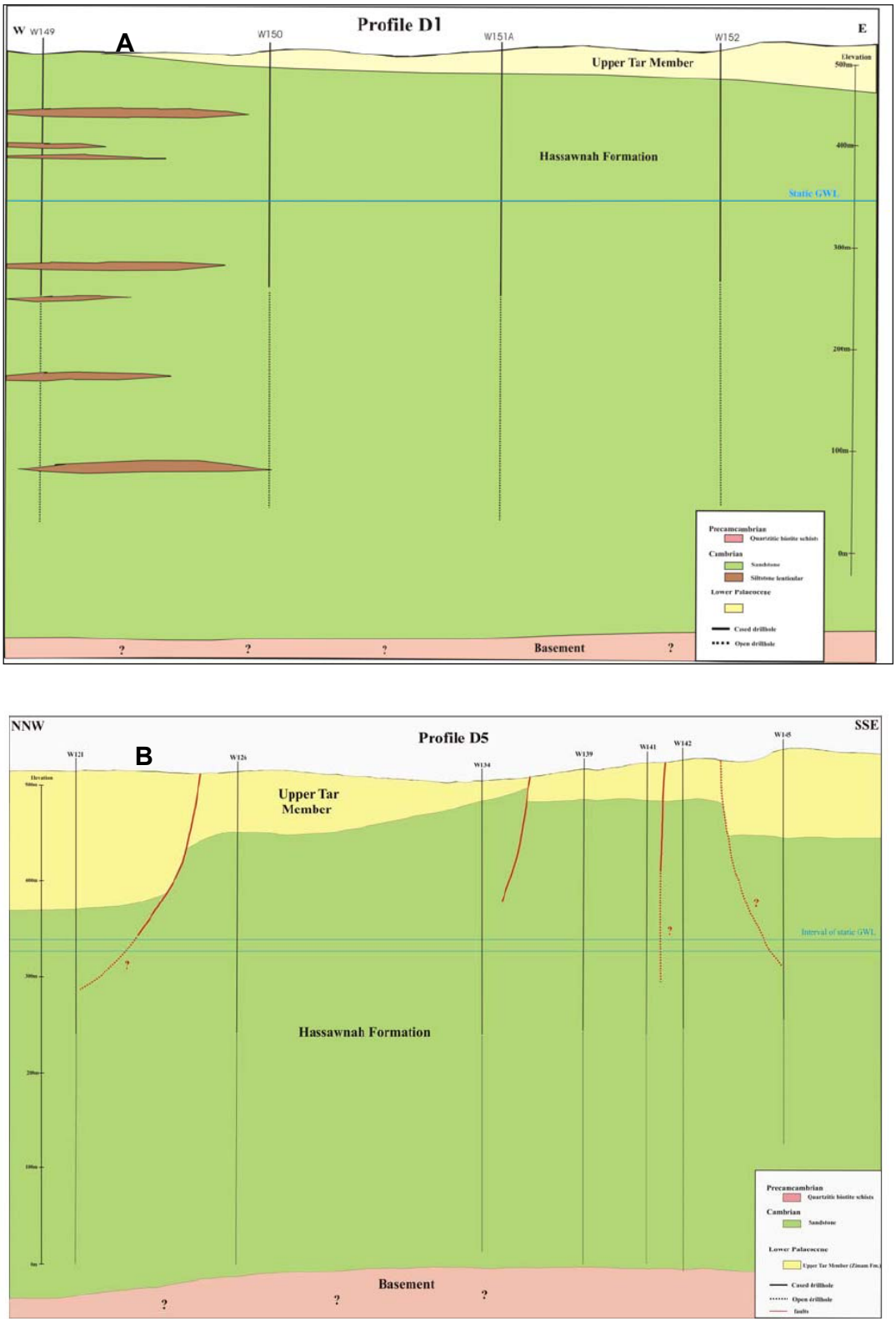

Figure 9.1: a) profile 1, E-W-trending. Siltstones are only reported in one well, but the continuation of the lenses towards the E is supposable. b) NNW-SSE-trending, distribution of the faults within the basement are the result of interpretation. (Source: J. Amtmann, and H. Pölzl, 2008).

In the Plot 9.2 shows the correlation of Gamma ray log between the groundwater wells 121, 126, 85, 134 and well 139. It shows clearly the presence of several faults between water wells. This correlation result is confirmed the before mentioned results of Jurak (1978) and IRC (1978).

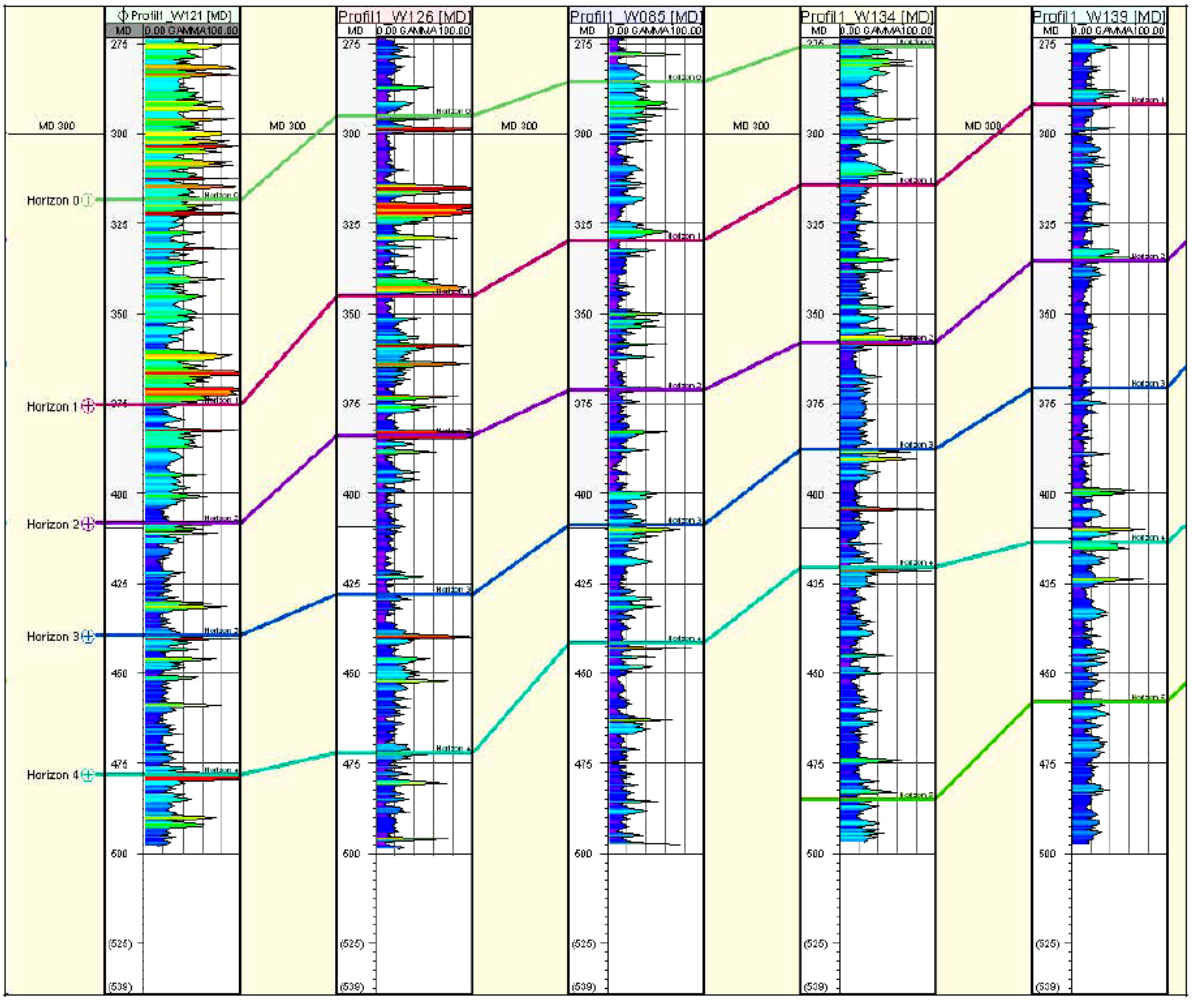

Figure 9.2: Correlation plot on a part of Profile 1 on base of the Gamma ray data. (Source: J. Amtmann, and H. Pölzl, 2008).

10 SUMMARY, CONCLUSION AND RECOMMENDATIONS

10.1 SUMMARY AND CONCLUSION

This thesis uses a hydrochemical and isotopic approach (^{18}O and ^{2}H for water, ^{15}N, ^{17}O and ^{18}O for nitrate, ^{34}S and ^{18}O for sulphate) to identify the origin of high nitrate concentration and other groundwater ions; and to reconstruct paleo environmental conditions during recharge of Saharan groundwater (Hasouna groundwater), see Table 12.8 in Appendix II.

The study area is located in the desert of an arid and semi-arid region, which characterized by very low actual precipitation (less than 30 mm annually) and high temperature (GWA, Libya). Under such conditions the recharge and renewing abilities for groundwater are absent.

Therefore, the only recharge is attributed to the groundwater intern migration flow e.g. from the south to north in the study area (see Fig. 4.6). The occurrence of geological faults, fractures and Zimam aquifer characteristics share the responsibility for the mixing process and the connection between of two aquifers (Zimam and Cambro Ordovician), and the groundwater directional flow (from South to North and North-east) (see Figures. 4.6 and 10.1).

The results of the analyzed physico-chemical parameters of the Hasouna groundwater shows neutral pH values (pH = 7.1), with a mean groundwater temperature value of 30°C (see Table 7.2). In the groundwater of the study area the relative abundance of dissolved cations and anions is in the order of $Na^{+} > Ca^{2+} > Mg^{2+} > K^{+} > Sr^{2+}$ and $Cl^{-} > SO_4^{2-} > HCO_3^{-} > NO_3^{-}$, respectively (see Table 7.4 and Fig. 7.16).

The big concern regarding drinking groundwater quality of the Hasouna is related to high nitrate concentrations in most water wells. For this reasons this groundwater must be diluted directly in waterfields to meet optimized recommended level for nitrate. High nitrate concentration was found in most groundwater wells of the Hasouna study area (> 50 mg L^{-1}), the highest nitrate concentration trend in the Hasouna waterfields area was found in this study, level (114 mgL^{-1}) was observed in the groundwater well #152 (Fig. 7.3). The standard limit of nitrate concentration in groundwater is 50 mgL^{-1} (WHO, 2004).

The vertical contact between the Zimam aquifer (upper aquifer) and Cambro-Orodovician aquifer (lower aquifer) within the Mixing Zone (Fig. 10.1) influences the groundwater hydrochemistry and isotope behaviour. The concentrations of dissolved ions of the groundwater (NO_3^{-}, Cl^{-}, Na^{+}, SO_4^{2-}, Ca^{2+}, and Mg^{2+}) are high within the mixing zone in the study area. Both El-

Baruni et al. (1985) and Binsariti and Saeed (2000) have documented the frequently occurring vertical hydraulic leakage within the mixing zone of Zimam aquifer, close to the middle of the Hasouna waterfields (see Fig. 10.1).

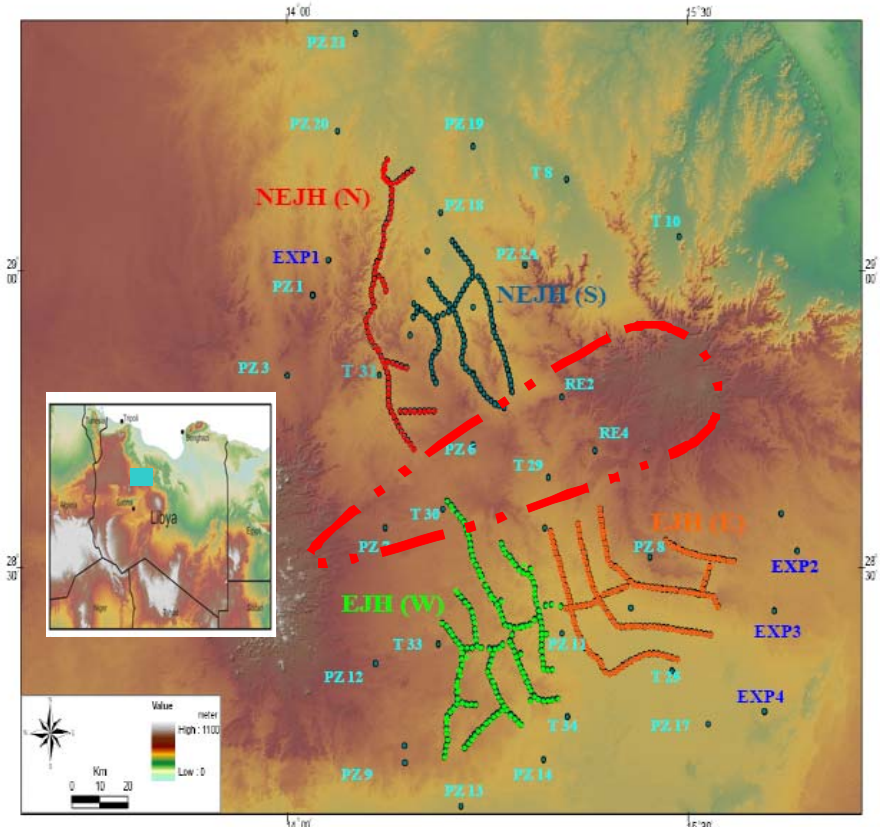

Figure 10.1: Location map of study area. Expected mixing zone in the middle of Hasouna waterfields area is marked with dashed red line.

The groundwater quality is checked for public consumption and irrigation usage. Generally, water quality is worst in some individual water wells. All values of trace elements are within the recommended standard (see Table 7.6). The dissolved ions show positive correlation relationships between the analyzed groundwater ions and can be followed by a simple mixing approach. The spatial distributions of major ions concentrations in the Hasouna study area are presented in the Figures 7.6, 7.7 and 7.10. Chloride, nitrate, sodium, sulphate and calcium show maxima towards the middle of Hasouna waterfields as a result of mixing with water from the saline Zimam Aquifer. The groundwaters are moderately undersaturated with respect to sulphate minerals (gypsum and anhydrite) indicating the possibility of their dissolution through water-rock interaction. This is consistent with the lithology of the study area, which comprises mainly sandstone, dolomite and sulphate rocks. The results of analyses on the isotopic composition of the Hasouna deep groundwater show paleo (fossil) origin. Deuterium (δ^2H) and oxygen ($\delta^{18}O$) isotopic data indicate that the groundwaters were recharged under cooler climatic conditions. These waters of Hasouna are depleted in isotope values (δ

^{18}O and $\delta\ ^{2}H$), with low d-excess, and show no evidence of evaporation trend (Table 12.8, Appendix II). This suggests that these waters are recharged under humid conditions (Fig. 10.2). Moreover, the isotopic composition of deep groundwater samples is slightly different to each other, indicating the possibility of different recharge periods and inhomogeneous character of the Hasouna aquifer. The values of oxygen and hydrogen isotope distributions plot closely and fit well to the previous isotopes study of Sonntag et al. (1978) see Figs. 8.2 and 10.2. An evaporation trend is not valid for both, solution chemistry and $\delta^{2}H_{H2O}$-$\delta^{18}O_{H2O}$ relationship. However from the isotopic composition of the groundwater a local Paleo Meteoric Water Line can be estimated: $\delta^{2}H_{H2O}$ = 8.0 $\delta^{18}O_{H2O}$ + 6.3 (Fig. 8.1). Low d-excess and low isotope values clearly indicate that the groundwater in the Hasouna basin was recharged under paleo climate conditions.

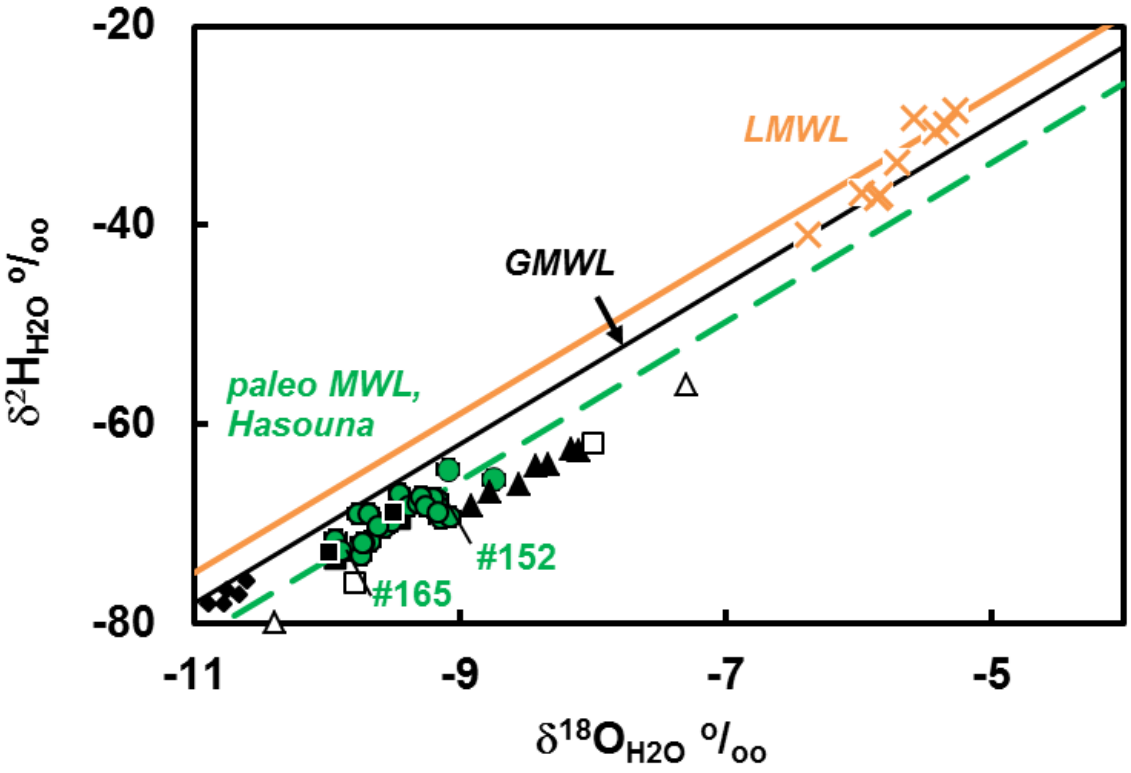

Figure 10.2 (previous page): Stable hydrogen and oxygen isotopic composition of groundwater from North Africa. Paleo groundwater displays lower stable isotope values and an elevated d-excess compared to modern precipitation which indicates recharge under cooler and more humid climate conditions versus modern climate conditions. The analytic inaccuracies lay within the size of the symbols. ●: Hasouna, Libya (this study); ■: Hasouna, Libya, isotopic range(Milne-Home and Sahli, 2007); □: Murzuq Basin, Libya, isotopic range (Sonntag et al., 1978); Δ: Arab Jamahiriya, Libya (Srdoč et al., 1980); ▲: South Tunisia (Abid et al., 2012); ♦: Wadi Ash Shati Valley, Libya (Salem et al., 1980). x: Groundwater recharged by modern precipitation close to Tripoli (own data). GMWL: Global Meteoric Water Line ($\delta^{2}H = 8\ \delta^{18}O + 10$; (Craig, 1961)). LMWL: Local Meteoric Water Line for Sfax metereological station, southern Tunisia (yellow line: $\delta^{2}H = 8\ \delta^{18}O + 13$; (Abid et al., 2012). Paleo MWL: Paleo Meteoric Water Line estimated from isotopic data of the present study by least square method (dashed green line: $\delta^{2}H = 8\ \delta^{18}O + 6.3$).

Some selected groundwater samples in the Hasouna area were analyzed for N and O isotope ratios of dissolved nitrate (^{17}O, ^{18}O, ^{16}O, ^{15}N, ^{14}N). The results univocally verify that $\Delta^{17}O_{NO3}$ values survived up to thousands of years and can be still used to estimate $NO_{3,atm}$ proportion (atmospheric nitrate) of total dissolved NO_3^- during ancient recharge. Accordingly for water management issues of Saharan groundwater from Hasouna wellfields elevated NO_3^- concentrations have to be considered as a long-lasting challenge as NO_3^- content within the aquifer is predetermined by paleo recharge conditions.

The positive correlation between $\Delta^{17}O_{NO3}$ values and NO_3^- concentrations unveils past alternating arid and humid periods. In arid periods a continuous dry deposition and accumulation of atmospheric NO_3^- at plant or soil surfaces occurred. Humid periods result in high amounts of precipitation including flood events which washed out the accumulated $NO_{3,atm}$ and were rapidly infiltrated through the subsurface to recharge the Saharan paleo groundwater of Hasouna area. The use of $\Delta^{17}O_{NO3}$ values provides information about the origin of NO_3^- deposition; it is a powerful and robust tool to trace the sources on nitrate in groundwater. Therefore, $\Delta^{17}O_{NO3}$ values are used as a tracer of conserved $NO_3^-{}_{atm}$.

This ^{17}O-excess ($\Delta^{17}O_{NO3}$) shows clearly that in the present Saharan groundwater up to 20 mol% (see Table 12.8 in Appendix II) of the dissolved NO_3^- is originated from the atmosphere with the rest NO_3^- comes from microbial sources. Isotope signatures of NO_3^- and H_2O reveal paleo recharge of the Hasouna Saharan groundwater under cool and humid paleoclimate conditions without significant evaporation, but with flooding events from periodic of heavy rainfall and rapid infiltration.

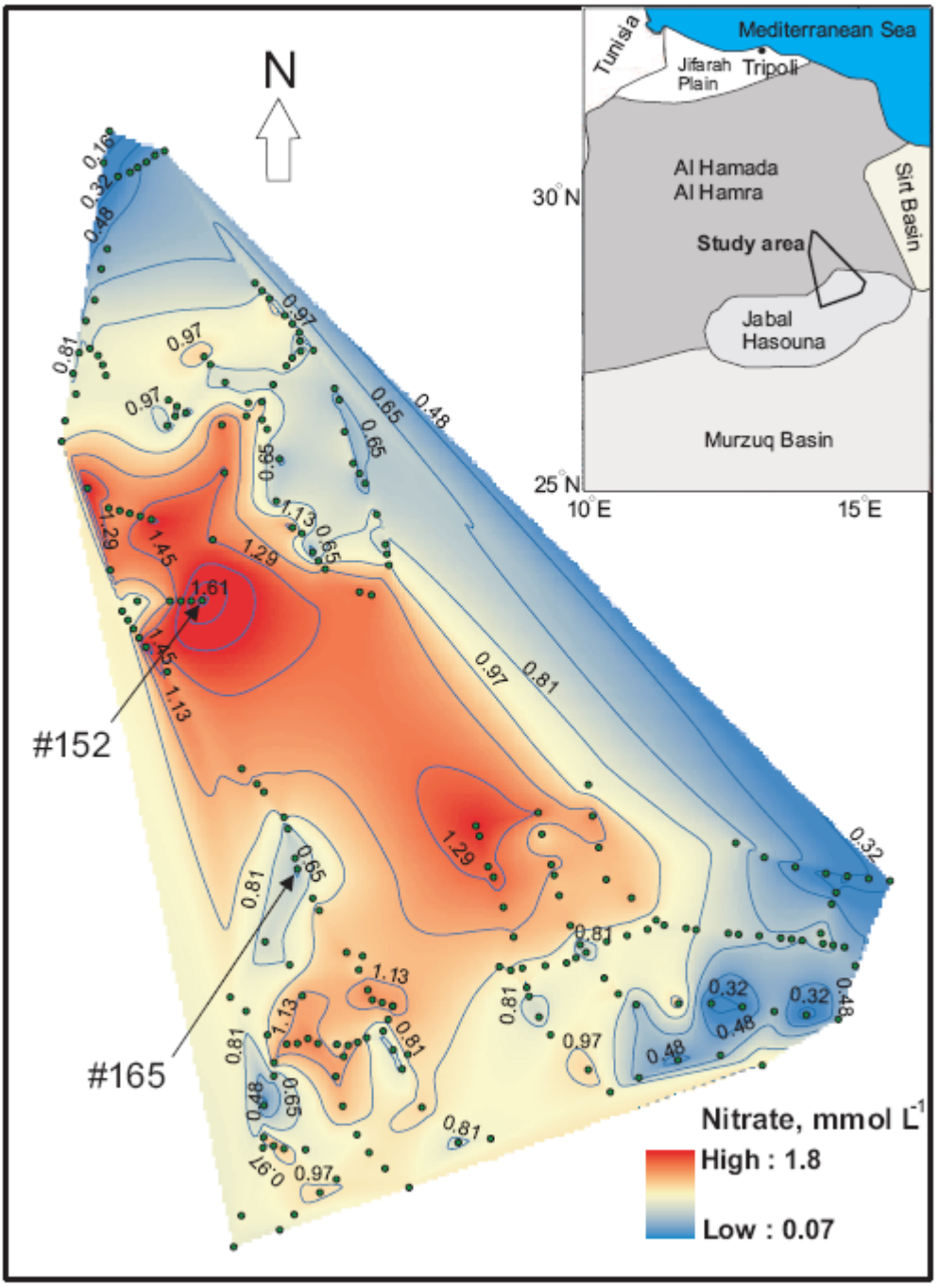

Figure 10.3: Spatial distribution map of nitrate in the Hasouna groundwater waterfields, nitrate contour map shows the maxima anomaly of nitrate in the middle of waterfields, and the end-members mixing solutions with low concentration in water well 165, and with high concentration in water well 152.

10.2 RECOMMENDATIONS

Libyan groundwater quality should be monitored regularly. Therefore, the groundwater samples from all water wells should be analyzed several times a year. High nitrate levels affect the use of groundwater as drinking water. Therefore, the nitrate limits should be measured continuously with using on-line sensors for some selected water wells. It is recommended to establish a long-term spatial/temporal monitoring layout to measure continuously the concentrations of nitrate in the Hasouna waterfields. The physic-chemical properties of water such as pH, temperature, dissolved oxygen and DIC content should be additionally and continuously measured in each water-well. In order to better define the extent and the dimensions of salinity of Hasouna groundwater (middle of waterfields), it is recommended that priority has to be given to analyze the chemical composition of the groundwater wells of the "mixing zone", viz. the wells 152, 151, 150, 149, 146, 138, 141, 145, 154, 165, 60, 30, 80, T29, REG29 (T29), PZ6, T30, PZ7, RE2, 326, 369 and RE4 (see Figure 10.1).

It is further recommended, that the above-mentioned kind of research work might be further extended to the neighbouring towns around the Hasouna waterfields in Libya. Subjects have to include water quality and balance estimation, hydrochemical studies with special emphasis on trace elements and environmental isotope investigations. Isotopic signatures for nitrogen and oxygen (^{15}N, ^{17}O, and ^{18}O), stable isotopes for water (^{18}O, ^{2}H), and sulphur isotopes (^{34}S and ^{18}O) for dissolved sulphate must be assessed from certain selected groundwater wells to understand their origin and fate.

More work is also needed in evaluating aquifer characteristics in areas of intense tectonic fracturing and large-scale faults. According to previous studies, the Hasouna area contains major tectonic fracture elements which lead to vertical hydraulic contacts between the Upper aquifer (Zimam, saline aquifer) and the Lower aquifer of the Hasouna sandstone Formation (Cambro-Ordovician Paleozoic; Elbaruni et al., 1985; Binsariti et al., 2000 and Milhne-Home and Sahli., 2007). The salinity of the Zimam aquifer needs to be studied carefully. To solve the issue and get more information about these hydraulic contacts in the mixing zone area, drilling of some selected exploration and observations wells, and also installation of piezometers are needed to explore the stratigraphy, lithology, and chemistry in the Zimam aquifer. Drilling core samples of these wells must be examined on mineralogical and lithological contents. In the mixing zone; rocks and soil samples should be collected and analyzed in the laboratory for mineralogy and chemical composition. Accordingly, soil profiles must be excavated at certain sites of the Hasouna

waterfields, in particular within the mixing zone, i.e. the zone between NEJH(N&S), and EJH(W&E) (see Fig. 10.2).

A long-term plan should be implemented for a sustainable, controlled exploitation of groundwater. A responsible office for strategy and management of related activities must provide information to the Libyan government and water Authority. Furthermore, it is recommended to establish a demand management to considerably lower the demand for water and to reduce the decline of aquifer levels. Managing demand includes detecting the decline of water levels, water quality, controlling groundwater abstraction, pumping and production rates, and improving irrigation techniques.

The tectonic problems, distribution of major faults, depth and thickness of different lithological units, and geometry of bedrock structure in the Hasouna study area must be studied and mapped by using hydro-geological approaches and geophysical methods.

In order to avoid heavy water abstraction and over-exploitation of the groundwater resources in the Hasouna area, it is important to develop a management policy and strategies for all the water resources throughout Libya. These policies and strategy include: the reduction and control of water consumption for both, the agriculturural sector and public consumptions, as well as the reuse of waste water. In the long term, the improvement of old desalination plants along the Libyan coast and construction of new plants with advanced technology is considered necessary to mitigate the deficits in fresh water supply, and thereby reducing the daily pumping rate at Hasouna waterfields.

It is suggested to implement the renewable energy technologies with using solar and wind energies to produce electricity for groundwater wells pumping systems. As Libya is located within a climatically arid area, with limited water resources and groundwater recharge, it is also highly recommended to solve the problems of water loss and evaporation in the mega storage water reservoirs in Sirte and Slug, as part of the Great Man-made River Project.

11 REFERENCES

Abid, K., Dulinski, M., Ammar, F. H., Rozanski, K. & Zouari, K., 2012. Deciphering interaction of regional aquifers in Southern Tunisia using hydrochemistry and isotopic tools. Applied Geochemistry 27, 44-55.

Al-Idrissi et al., 1996. Libya: Country Report to the FAO International conference on plant genetic resources (Leipzig, 1996), Tripoli.

Appelo, C.A.J. & Postma, D., 1994. Geochemistry, groundwater and pollution. A.A. Ballema Publisher, Rotterdam.

Appelo, C.A.J. & Postma, D., 1996. Geochemistry, groundwater and pollution. Balkema, Rotterdam.

Appelo, C.A.J. & Postma, D.,1999. Geochemistry, groundwater and pollution. Rotterdam: Balkema-Publisher.

Appelo, C.A.J. & Postma, D., 2005. Geochemistry, groundwater and pollution, 2nd. Edn. Balkema-Leiden.

Atkinson, R., Baulch, D.L., Cox., R. A., Hampson, Jr R.F., Kerr, J. A. and Troe, J., 1997. Evaluated kinetic and photochemical data for atmospheric chemistry. Journal of Physical and Chemical Reference Data, Supplement VI, 26, 1329-1499.

Barr, F. T. and Weegar, A. A., 1972. Stratigraphic Nomenclature of the Sirt Basin, Libya. Petrol. Explor. Soc. Libya, p. 179.

Benfield, A.C. and Wright, E.P., 1981. Post-Eocene sedimentation in the eastern Sirte Basin. In: The Geology of Libya, Salem, M. and Busrewil, M. (eds.), Academic Press, London, pp. 463-469.

Binsariti, A. A. and Said. F. A., 2000. Groundwater Salinity Variation in the Cambro-Ordovician Aquifer of Jabal al Hasouna, Great Man-Made River Project, Libya. Exploration in Murzuq Basin, (eds) Sola, and Worsley. Elsevier Science, B. V., pp. 1-16.

Böhlke, J. K. Ericksen, G. E., and Revesz, K., 1997. Stable isotope evidence for an atmospheric origin of desert nitrate deposits in northern Chile and southern California, U.S.A. Chemical Geology 136, 135-152.

Casciotti, K. L., Sigman, D. M., Hastings, M. G., Böhlke, J. K. & Hilkert, A., 2002. Measurement of the oxygen isotopic composition of nitrate in seawater and freshwater using the denitrifier method. Analytical Chemistry 74, 4905-4912.

Clark, I. D. and Fritz, P., 1997. Environmental Isotopes in Hydrology. CRC Press, 352 pp.

Claypool et al., 1980. The age curves of sulphur and oxygen isotopes in marine sulphate and their mutural interpretation. Chemical Geology, 28,199-260.

Collomb, G. R., 1962. Etude Geologique du Jebel Fezzan et de sa bordure Paleozique. Notes et Memoiries, No.1, Compagnie Francaise des Petroles 35p. Paris.

Cook P. and Herczeg A.L. (eds.), 2000. Environmental Tracers in Subsurface Hydrology, Kluwer Academic, Norwell, MA.

Craig, H., 1961. Isotopic variations in meteoric waters. Science 133, 1702-1703.

Dejwakh, N. R., Meixner, T., Michalski, G., and McIntosh, J., 2012. Using O-17 to Investigate Nitrate Sources and Sinks in a Semi-Arid Groundwater System. Environ. Sci. Technol. 46, 745-751.

Dansgaard, W., 1964. Stable isotopes in precipitation. Tellus 16, 436-467.

Drever, J.I., 1997. The Geochemistry of Natural Waters. Third ed. Prentice Hall, USA.

Dubay, L., 1980. Groundwater in Wadi Ash Shati Fazzan: A case history of resource Development. In: The Geology of Libya, Salem, M.J. and Busrewil, M.T., (eds). Academic Press, London, II, pp. 611-627.

Drake, N.A., El-Hawat, A.S., Turner, P., Armitage, S.J., Salem, M.J., White, K.H., McLaren, S., 2008. Palaeohydrology of the Fazzan Basin and surrounding regions: The last 7Â million years. Palaeogeography, Palaeoclimatology, Palaeoecology 263, 131-145.

Edmunds, W. M. & Wright, E. P., 1979. Groundwater recharge and palaeoclimate in the Sirte and Kufra basins, Libya. J. Hydrol. 40, 215-241.

Edmunds, W.M., Fellman, E.& Goni, I.B., 1999. Lakes, groundwater and palaeohydrology in the Sahel of NE Nigeria: evidence from hydrogeochemistry. Journal of the Geological Society, London 156: 345-355.

Edmunds, W. M., 2006. Libya's Saharan Groundwater: Occurrence, Origins and Outlook In (eds.: Mattingly, D. McLaren, S. Savage, E.) The Libyan Desert: Natural Resources and Cultural Heritage. Society of Libyan Studies Monograph 6, Chapter 4, 45-64.

El-Baruni, S. S., El-Futasi, R. H., and Maaruf, A. M., 1985. Hydrology of Ghadamis Basin, NW Libya. In the Geology of Libya, Libyan Arab Jamahiriya, Tripoli, pp. 269 – 290.

El Chair, M.N., 1984. Zur Hydrogeology, Hydrochemie und Isotopenzusammensetzung der Grundwässer des Murzuq-Beckens, Fezann/Libyen. Unpublished Dissertation Naturwissenschaften Fakultät Universität, Tübingen, Germany, 214 pp.

El Maryme, A.M., 1994. Hydrology and hydrogeochemistry of the Al Kufra Basin, Libya, in Project Report-Grad. Dip. Eng., (Unpubl.), University of Technology, Sydney, pp. 138.

Freeze, R.A. and Cherry, J.A., 1979. Groundwater, Prentice-Hall, Inc., Englewood Cliffs, New Jersey, 604 p.

Fontes, J.Ch., Gasse, F., Andrews, J.N., Edmunds, W.M., Guerre, A. & Travi, Y., 1991. Palaeorecharge by the Niger River (Mali) deduced from groundwater chemistry. Water Resources Research 27: 199-214.

Fontes, J.Ch., Gasse, F., Andrews, J.N., 1993. Climatic conditions of Holocene groundwater recharge in the Sahel zone of Africa. In: Isotope Techniques in the Study of Past and Current Environmental Changes in the Hydrosphere and the Atmosphere. IAEA-SM-329/59, International Atomic Energy Agency, Vienna.

Fournier, R.O., 1981. Application of water Geochemistry to Geothermal exploration and reservoirs enginnering in L. Rybach and L.J.P. Muffler, eds., Geothermal Systems, Principles and Case Histories, Wiley, New york,p. 109-143.

Fritz, P., Frape, S.K., Drimmie, R.J., Appleyard, E.C. and Hattori K., 1994. Sulfate in brines in the crystalline rocks of Canadian Shields. Geochim. Cosmochim. Acta, 58: 57-65.

Geomath, 1994. Phase II- Western Jamahiriya System: hydrogeological modelling of aquifers and wellfields, in Final Report for Great Man-Made River Authority (GMRA), Brown and Root Ltd (ed.), (Unpubl).

Guendouz, A., Moulla, A. S., Edmunds, W. M., Shand, P., Poole, J., Zouari, K., and Mamou, A., 1998. Palaeoclimatic information contained in groundwaters of the Grand Erg Oriental, north Africa. Isotope techniques in the study of environmental change. Proceedings of a IAEA symposium, Vienna, 555-571.

Great Man Made River Authority (GMRA), Libya. http://www.gmmra.org

Goudarzi, G.H., 1970. Geology and Mineral Resources of Libya – a Reconnaissance. U.S. Geol. Survey, Proc. Pap.660, Washington D.C.

Hea, J.P., 1971. Petrography of Paleozoic-Mesozoic sandstones of the Southern Sirte Basin, Libya. In Symposium on the Geology of Libya, C. Gray (Ed.). Fac. Sci. Univ. Libya, Tripoli, 107-125.

Heaton, T.H.E., Talma, A.S. & Vogel, J.C., 1983. Origin and history of nitrate in confined groundwater in the Western Kalahari. Journal of Hydrology 62: 243-262.

Heaton, T.H.E., 1984. Source of the nitrate in phreatic groundwater in the Western Kalahari. J. Hydrol., 67: 249-259.

Heaton, T. H.E., 1986. Isotope studies of nitrogen pollution in the hydrosphere and atmosphere: a review: Chemical Geology, v.59, pp. 87-102.

Hem, J. D., 1992. Study and interpretation of chemical characteristics of natural water (3d ed.): US Geological Survey Water Supply Paper 2254, 263p.

Hoefs, J., 2001. Stable Isotope Geochemistry, 4th ed.: Springer, 201 p.

Horita, J., Ueda, A., Mizukami, K., and Takatori, I., 1989. Automatic Î´D and Î´18O analyses of multi-water samples using H2- and CO2-water equilibration methods with a common equilibration set-up. Applied Radiation and Isotopes 40, 801-805.

International Atomic Energy Agency, 1980. Arid-zone hydrology: Investigations with isotope techniques. IAEA, Vienna.

Idrotecneco, 1982. Hydrogeological Study of Wadi Ash Shati, Al Jeffara and Jabal Fazzan area. Rept. To Secretariat of Agricultural Reclamation and Land Development, Socialist Peopl's Libyan Arab Jamahiriya, 8 Vols.

Industrial Research Centre (IRC), 1978. Geological Map of Libya, Jabal Al Hasouna Sheet, NH33-14, Tripoli.

IMBGMBH Consulting Engineers, 1980. Regional geology and hydrogeology of the Fezzan Basin. Final Report, Part III—Hydrogeological Study. Secretariat of agrarian reform and land reclamation, Tripoli, Libya.

Kaiser, J., Hastings, M. G., Houlton, B. Z., Röckmann, T. & Sigman, D. M., 2007. Triple oxygen isotope analysis of nitrate using the denitrifier method and thermal decomposition of N2O. Analytical Chemistry 79, 599-607.

Kendall, C., 1998. Tracing nitrogen sources and cycling in catchments. In: Isotope tracers in catchment hydrology (Eds.: Kendall C. and McDonnell J.J.) Chapter 16, 519-576.

Kendall, C., Doctor, D.H., 2004. Stable Isotope Applications in Hydrologic Studies in: Drever, J.I. (Ed.), Treatise on Geochemistry - Surface and Groundwater, weathering and soils pp. 319 - 364.

Kendall, C., Elliott, E.M., Wankel, SD., 2007. Tracing anthropogenic inputs of nitrogen to ecosystems, in ecology and environmental science, Blackwell publishing, Eds, Michener, R. & Lajtha, K., p. 375-449.

Klitzsch, E., 1970. Die Strukturgeschichte der Zentralsahara. Neue Erkenntnisse zum Bau und zur Paläogeographie winw Taffellands. Geologische Rundschau, 59, 459-527.

Klitzsch, E., 1978. Stratigraphic section from type ares of Silurian and Devonian strata at western Murzuk Basin Libya. In: Geology, Archaeology and Prehistory of the southern Fezzan, Libya, W.H. Kanes ED. Petrol. Explor. Soc. Libya, Tripoli, 11th Ann. Field Conf., pp.83-90.

Kohl, D.H., Shearer, G.B., and Commoner, B., 1971. Fertilizer nitrogen contribution to nitrate in surface water in a corn belt watershed: Science, v. 174, pp. 1331-1334.

Krouse, H. R., and Coplen, T. B., 1997. Reporting of relative sulfur isotope-ratio data: Pure and Applied Chemistry, v. 69, p. 293-295.

Lloyd, J. W. and Heathcote, J.A., 1985. Natural Inorganic Hydrochemistry in Relation to Groundwater. Oxford Press Oxford. 296 pp, UK.

Li, Y.H., Qin, Y., Liu, F., Hou, K.J., Wan, D.F., 2010. Discovery of mass independent oxygen isotopic compositions in superscale nitrate mineral deposits from Turpan-Hami Basin, Xinjiang, China and its significance. Acta Geol. Sin.-Engl. Ed. 84, 1514-1519.

Massa, D. and Collomb, G.R., 1960. Observations nouvelles sur la region d Aouinet Ouenine et du Djebel Fezzan (Libye). -XXI.Internat. Geol. Congress Norden, Section, v. 12, pp. 65-73, Kopenhagen.

Martyn, D., 1992. Climates of the world, PWN-Polish Scientific Publishers, Warszawa, Poland.

Meybeck, M., 1987. Global chemical weathering of surficial rocks estimated from river dissolved loads. American Journal of Science, 287 (5), 401-428.

Michalski, G., Savarino J. Böhlke J. K. and Thiemens, M., 2002. Determination of total oxygen isotopic composition of nitrate and calibration of a $\Delta^{17}O$ nitrate reference material. Anal. Chem. 74, 4989-4993.

Michalski, G., Scott, Z., Kabiling, M., and Thiemens, M. H., 2003. First measurements and modeling of Î”^{17}O in atmospheric nitrate. Geophysical Research Letters 30, 14-1.

Michalski, G., Bohlke, J. K., and Thiemens, M., 2004a. Long term atmospheric deposition as the source of nitrate and other salts in the Atacama Desert, Chile: New evidence from mass-independent oxygen isotopic compositions. Geochim. Cosmochim. Acta 68, 4023-4038.

Michalski, G., Meixner, T., Fenn, M., Hernandez, L., Sirulnik, A., Allen, E., and Thiemens, M., 2004b. Tracing Atmospheric Nitrate Deposition in a Complex Semiarid Ecosystem Using Î”17O. Environmental Science and Technology 38, 2175-2181.

Michalski, G., Bockheim, J.G., Kendall, C., Thiemens, M., 2005. Isotopic composition of Antarctic Dry Valley nitrate: Implications for NO(y) sources and cycling in Antarctica. Geophysical Research Letters 32, 4.

Milne-Home, W. A. and Sahli, N. I. M., 2007. Application of 15N isotopes to management of groundwater quality Hasouna wellfields, Great man-made river project, Libyan Arabjamahiriya IAEA-CN-151/63, 487-494.

Moncaster, S. J., Bottrell, S. H., Tellam, J. H., Lloyd, J. W. & Konhauser, K. O., 2000. Migration and attenuation of agrochemical pollutants: insights from isotopic analysis of groundwater sulphate. J. Contam. Hydrol. 43. 147-163.

Morin, S. et al. Tracing the origin and fate of NOx in the arctic atmosphere using stable isotopes in nitrate. Science 322, 730-732 (2008).

N.C. Sturchio et al., 2004. Geophys. Res. Lett. (31) L05503, doi: 10.1029/2003GL019234.

Nielsen, H., 1978. Sulfur isotopes. In : K.-H. Wedepohl (Editor), Handbook of Geochemistry. Springer, Berlin, pp. 16B1-16B40.

Novak, M., Bottrell, H. S. and Prechova, E., 2001. Sulfur isotope inventories of atmospheric depositions, spruce forest floor and living Sphagnum along a NW-SE transect across Europe. Biogeochem. 53, 23-50.

Jurak L. 1978. Geological Map of Libya, 1: 250,000, Sheet Jabal Al Hasouna (NH33-14), Industrial Research Centre, Tripoli.

Jordi, H. A. and F. Lonfat, Stratigraphic subdivision and problems in Upper Cretaceous-Lower Tertiary Deposits in Northwestern Libya, Rev. Inst. Fran. Petrole, 18, 1428–1436, 1963.

Pallas, P. 1980. Water resources of the Socialist People's Libyan Arab Jamahiriya. In: The Geology of Libya, Vol. II. Academic Press, London, pp. 539 – 594.

Parkhurst, D.L. and Appelo, A.A.J.,1999. Users guide to PhreeqC (version 2) A computer program for speciation, batch-reaction, one dimensional transport, and inverse geochemical modeling U.S. Geo. Survey, water-resource invest., 99-4259.

Pim, R.H. and Binsariti, A., 1994. The Libyan Great Man-made River Project. Paper 2. The water resource. Proceedings Institution of Civil Engineers Waters, Marititime & Energy 106: 123-145

Piper, A.M., 1944. A graphic procedure in the geochemical interpretation of water analysis. –Trans. Am. Geophy. Union 25: 914-928.

Pizzi, G., del Guidice, C., Pizzi, U., Salem, O., El Sonni, A., Binsariti, A., Lloyd, J.W. and Moorwood, H., 1999. Modelling of the western Jamahiriya Aquifer System Paper presented at the International Conference on Regional Aquifer Systems in Arid Zones: Managing Non-Renewable Resources, Tripoli, Libya, 20-24, 20 pp.

Plummer, L.N., 1984. Geochemical modelling: A comparison of forward and inverse methods, in Hitchon, B., and Wallick, E.I., eds., First Canadian/American Conference on Hydrogeology, Practical Applications of Ground Water Geochemistry: Worthington, Ohio, National Water Well Association, p. 149-177.

Rozanski, K., 1985. Deuterium and oxygen-18 in European groundwaters-links to atmospheric circulation in the past. Chemical Geology 52, 349-363.

Rubino, J.-L., Blanpied, C., 2000. Sedimentology and sequence stratigraphy of the Devonian to lowermost Carboniferous succession on the Gargaf Uplift (Murzuk Basin, Libya). In: Sola, M.A., Worsly, D. (Eds.), Geological Exploration in Murzuq Basin. Elsevier Science, pp. 321–348.

Salem, O., Visser, J.H., Dray, M. & Gonfiantini, R., 1980. Groundwater flow patterns in the western Libyan Arab Jamahiriya evaluated from isotopic data. Arid Zone Hydrology: Investigations with isotope techniques, 165-179. IAEA, Vienna.

Sasaki, A., 1972. Variations in sulphur isotopic compositions of oceanic sulphate. 24th IGC, Sect. 10, pp.342-345.

Savarino, J., Kaiser, J., Morin, S., Sigman, D. M. & Thiemens, M. H., 2007. Nitrogen and oxygen isotopic constraints on the origin of atmospheric nitrate in coastal Antarctica. Atmos. Chem. Phys. 7, 1925-1945.

Sawyer, C. N., and Mc Carty, P. L., 1967. Chemistry for Sanitary Engineers, and classification of naturally soft and naturally hard waters to sources and hardness of their water supplies., J. Hyg.

Schroeder, H. A., 1960. Relation between hardness of water and death rates from certain chronic and degenerative diseases in the United States, J. Chron disease, 12: 586-591.

Shaki, A.J. Adeloye, 2002. Evaluation of Quantity and quality of irrigation water at Gadwa irrigation project in Murzuq basin, southwest Libya, School of the Built Environment, Heriot-Watt University, Riccarton, Edinburgh EH144AS, UK.

Schult, A. and H. Soffel, 1973. Paleomagnetism of Tertiary basalts from Libya, Geophys. J. R. Astron. Soc., 40, 491–499, London.

Seiler, R.L., 1996. Methods for identifying sources of nitrogen contamination of groundwater in valleys in Washoe Country, Nevada: U.S. Geological Survey Open-File Report 96-461, 29p.

Srdoč, D. et al., 1980. Isotope investigations as a tool for regional hydrogeological studies in the Libyan Arab Jamahiriya. IAEA-AG-158/11, 153-164.

Sonntag, C., Klitzsch, E., Löhnert, E. P., El-Shazly, E. M., Münnich, K. O., Junghans, C., Thorweihe, U., Weistroffer, K., and Swailem, F. M., 1978. Paleoclimatic information from deuterium and oxygen-18 in carbon-14 dated north Saharan groundwaters, IAEA-SM-228/28, 569–581.

Szabolcs, I. and Darab, C., 1964. The influence of irrigation water of sodium carbonate content of soils. In: Proceddings of 8th international congress of ISSS, Transaction II, pp 803-812.

Tawadros, E., 2001. Geology of Egypt and Libya, 480 pp., A. A. Balkema, Rotterdam.

Thiemens, M.H., 2006. History and applications of mass-independent isotope effects. Annual Review of Earth and Planetary Sciences, Palo Alto, pp. 217-262.

Tsunogai, U., Daita, S., Komatsu, D.D., Nakagawa, F., Tanaka, A., 2011. Quantifying nitrate dynamics in an oligotrophic lake using Delta O-17. Biogeosciences 8, 687-702.

Tsunogai, U., Komatsu, D.D., Daita, S., Kazemi, G.A., Nakagawa, F., Noguchi, I., Zhang, J., 2010. Tracing the fate of atmospheric nitrate deposited onto a forest ecosystem in Eastern Asia using Delta O-17. Atmos. Chem. Phys. 10, 1809-1820.

U.S. Salinity Laboratory Staff (USSLS), 1954. Diagnosis and improvement of Saline and alkali soils. U.S. Department of Agriculture Handbook 60, 160p.

Todd, D.K., 1980. Groundwater hydrology (Third Edition): John Wiley and Sons, New York, 533 p.

US EPA., 1993. Manuel: Nitrogen Control, EPA/625/R-93/010, Office of Water, Washinton, D.C., September.

Vogel, J.C., Talma, A.S. and Heaton, T.H.E., 1981. Gaseous nitrogen as evidence for dentrification in groundwater. J. Hydrol., 50: 191-200.

Watson, A., 1979. Gypsum crusts in deserts. J. Arid Environ. **2**, 3-20.

Wilcox, L. V., 1955. Classification and Use of irrigation Waters, U.S.A. Salinity lab. Circulation. No. 969.

Wilcox, L. V., and Durum, W. H., 1967. Quality of irrigation water: American Society of Agronomy, Agronomy Series, chapter 9.

World Health Organisation (WHO), 1993. Guidelines for drinking water quality. Revision of the 1984 guidelines. Final task group meeting. Geneva, 21-25 September 1992.

World Health Organisation (WHO), 1998. Guidelines for drinking-water quality, 2nd ed. Appendum to Vol. 2. Health criteria and other supporting information. Geneva, World Health Organization: 64-80

World Health Organisation (WHO), 2004. Guidelines for drinking water quality. Recommendations. Geneva: World Health Organization.

Wright, E.P., Benfield, A.C., Edmunds, W.M. and Kitching, R., 1982. Hydrogeology of the Kufra and Sirte basins, eastern Libya. Quarterly Journal of Engineering Geology London 15: 83-103.

12 APPENDIX

12.1 APPENDIX I

The following manuscript dealing with "**Tracing atmospheric nitrate in paleo groundwater of Saharan desert using ^{17}O-excess**" of the Hasouna study area has been submitted for publication.

Tracing atmospheric nitrate in paleo groundwater of Saharan desert using its ^{17}O-excess

Martin Dietzel[1*], Albrecht Leis[2], Rashid Abdalla[1], Joel Savarino[3,4], Samuel Morin[5], Michael E. Böttcher[6,7], and Stephan Köhler[1,8]

[1]Graz University of Technology, Institute of Applied Geosciences, Rechbauerstrasse 12, A-8010 Graz, Austria, email: martin.dietzel@tugraz.at, [2] Joanneum Research, Institute of Water Resources Management, Graz, Austria, [3]CNRS, Institut National des Sciences de l'Univers, France, email: joel.savarino@lgge.obs.ujf-grenoble.fr, [4]Laboratoire de Glaciologie et de Géophysique de l'Environnement, Université Joseph Fourier, Grenoble, France, [5]Météo-France - CNRS, CNRM-GAME URA 1357, CEN, Grenoble, France, email: samuel.morin@meteo.fr, [6]Max Planck Institute for Marine Microbiology, Bremen, Germany, [7]present address: Leibniz Institute for Baltic Sea Research, Warnemünde, Germany, email: michael.boettcher@io-warnemuende.de, [8]present address: Department of Aquatic Sciences and Assessment, Swedish University of Agricultural Sciences, Uppsala, Sweden, email: Stephan.Kohler@slu.se.

*Corresponding author

Phone: 0043-316-8736360, Fax: 0043-316-8736876

Abstract

Saharan paleo groundwater from Hasouna wellfield in Libya contains up to 1.8 mM of nitrate with a highly disputed origin. Herein we discover for the first time that, surprisingly, pristine ^{17}O-excess in NO_3 ($\Delta^{17}O_{NO3}$ = $\delta^{17}O_{NO3}$ - 0.52 $\delta^{18}O_{NO3}$) is well preserved in the ancient groundwater reservoir. ^{17}O-excess provides an excellent tracer of atmospheric NO_3 which is caused by the interaction of ozone with NO_x via photochemical reactions coupled with a non-mass dependent isotope fractionation. Our $\Delta^{17}O_{NO3}$ analyses from 0.4 to 5.0 $^{o}/_{oo}$ expose up to 20 mol% of NO_3 originated from the Earth`s atmosphere besides microbial NO_3. From combined elemental data and isotope signals of NO_3 ($\delta^{15}N$, $\delta^{18}O$ and $\delta^{17}O$), SO_4 ($\delta^{34}S$ and $\delta^{18}O$) and H_2O ($\delta^{2}H$ and $\delta^{18}O$) we clearly discover paleo recharge of Saharan groundwater under cool and humid paleoclimate conditions without significant evaporation, but with flood events from periodic heavy precipitation and instantaneous infiltration. The range of ion concentrations and isotope values is revealed by a mixing approach using the lowest and highest mineralized groundwater as endmembers.

1. Introduction

The accumulation of nitrate in groundwater is a well known and world wide occurring phenomenon (Clark and Fritz, 1997; Kendall, 1998). Individual NO_3 sources and mechanisms for its accumulation depend strongly on the environmental conditions during recharge, infiltration and aquifer storage. Discovering the source of NO_3 for Saharan groundwater in Libya is highly challenging as recharge is negligible at present arid conditions (Edmunds, 2006). High NO_3 concentrations of paleo groundwater from Hasouna area (Libya) are monitored for several years, but its origin is still hotly debated (El-Baruni et al., 1985; Milne-Home and Sahli, 2007).

Libyan paleo groundwater is part of the Nubian Sandstone Aquifer System, which had been recharged at about 30 ±10 and 10 ±3 ka BP based on ^{14}C dating (Edmunds et al., 2003; Edmunds and Wright, 1979; Guendouz et al., 1998; Milne-Home and Sahli, 2007; Sonntag et al., 1978). Although individual epochs for humidity and groundwater recharge periods are still disputed, Pleistocene and Holocene cover lettehumid periods in northern Africa are verified by paleo climate records from (i) lacustrine fresh-water sediments (Rognon, 1987), (ii) wadi river systems (Kuper and Kröpalin, 2006), (iii) travertine (Carrara et al., 1998), (iv) paleobotanic investigations (Doherty et al., 2000), (v) rock art dating and varnish-coating of petroglyphs (Dietzel et al., 2008), and (vi) dating of aragonitic molluscs shells (Blackwell et al., 2012).

The source of dissolved NO_3 in groundwater is commonly attributed to (i) anthropogenic origin, including leaching of fertilisers or animal waste, (ii) dissolution of evaporate deposits, (iii) leaching of organic or inorganic nitrogen from soils and (iv) atmospheric deposition. vidence for NO_3 origin is traditionally obtained by measuring $^{15}N/^{14}N$ and $^{18}O/^{16}O$ ratios (Amberger and

Schmidt, 1987; Kendall, 1998). From respective $\delta^{15}N$ and $\delta^{18}O$ signatures the NO_3 provenances can be evaluated and by considering changes in NO_3 concentration reaction mechanisms like denitrification were deduced based on mass dependent isotope fractionation (MDF) (Kendall, 1998). However pristine isotope ratios may be overprinted during nitrogen conversion processes in soils and within the aquifer (e.g. by (de)nitrification (Xue et al., 2009)).

More recently a triple stable isotope approach using $^{18}O/^{16}O$ and $^{17}O/^{16}O$ signals in NO_3 was successfully applied to discover the contribution of NO_3 from different sources. Interestingly atmospheric NO_3 ($NO_{3,atm}$) is exclusively characterized by a ^{17}O-excess, where non-mass dependent isotope fractionation (NMDF) during the formation of ozone followed by photochemical reactions between atmospheric NO_x and O_3 to NO_3 results in non-zero $\Delta^{17}O_{NO3}$ values ($\Delta^{17}O = \delta^{17}O - 0.52\ \delta^{18}O$; (Michalski et al., 2003; Thiemens, 2006)). Böhlke et al. (1997), for instance, found evidence from $^{15}N/^{14}N$ and $^{18}O/^{16}O$ isotope analyses for atmospheric source of NO_3 for nitrate-rich salts in Atacama (Chile) and Mojave Desert (California). But the atmospheric origin of NO_3 in the Atacama deposits was finally confirmed by pronounced ^{17}O-excesses (Michalski et al., 2004a). Since then $NO_{3,atm}$ was successfully quantified using ^{17}O-excess for various desert deposits and dissolved NO_3 in modern groundwater, lakes and wet depositions (Dejwakh et al., 2012; Li et al., 2010; Michalski et al., 2005; Michalski et al., 2004b; Tsunogai et al., 2011; Tsunogai et al., 2010).

The goal of the present study is to discover the origin of NO_3 in Saharan paleo groundwater by using $^{15}N/^{14}N$ ratios and triple stable isotopes of oxygen. As Hasouna groundwater (Libya) was recharged under paleo environmental conditions and no recent agriculture activities exist in the study area, anthropogenic source of NO_3 can be ruled out, but natural provenances are yet not discovered and quantified. Herein we analysed Hasouna groundwater with special regards on both (i) the origin of NO_3 and (ii) the reconstruction of ancient recharge and climate conditions by using a multi elemental-isotopic approach.

2. Study area

The Hasouna wellfield is located about 700 km south of Tripoli (Libya) within the so-called Cambro-Ordovician Sandstone Aquifer System (Fig.1). The latter system comprises one of the world's largest aquifer for paleo groundwater. The aquifer mostly consists of fractured sandstone ranging from ≈ 500 to 1500 m thickness with thin beds of marine limestone and marl. The sandstone itself is mostly referred to quartzitic sandstone, but occasionally carbonate cement occurs. In the study area the main Cambro-Ordovician Sandstone aquifer is overlain by a shallow carbonate aquifer with a basal aquitard, predominantly composed of marly limestone, clay and shale.

Freshwater in the study area of Jabal Hasouna was discovered during oil exploration in the 1960s (Edmunds, 2006). However groundwater was sampled from wells which were installed through the so-called Great Man-made River Project to bring up to ≈ 6 Mm^3 fresh water per day to the Mediterranean coast for water supply issues (Salem, 1992). The spacing of a total of 484 wells is ≈ 1.5 km with individual discharges of ≈ 50 L s^{-1} covering ≈ 4000 km^2 (Binsariti and Saeed, 2000). Sampling of Hasouna groundwater was carried out at 28 wells (see # coding and sampling sites in Tab.1 and Fig.1, respectively).

3. Methodology

Chemical composition

Temperature and pH of groundwaters were measured in the field. Sampled solutions were filtered in situ (0.45 µm cellulose acetate membrane), partly acidified, and stored in PE and gas-tight glass vessels for Lab analyses. Anions and alkalinity were measured by ion chromatography and potentiometric titration, respectively. In the acidified solutions (2% HNO_3) cations were analysed by ICP-OES. Calculation of saturation index with respect to calcite ($SI_{calcite}$) was done by using the computer code PHREEQC (Parkhurst and Appelo, 1999) with the phreeqc.dat database.

Stable isotopes

Additional samples were gathered for analyzing $^2H/H$ and $^{18}O/^{16}O$ distribution in H_2O. The isotopes of hydrogen were measured using a Finnigan DELTA plus XP mass spectrometer working in continuous flow mode by chromium reduction technique (Morrison et al., 2001). The oxygen isotopic composition was measured with a Finnigan DELTA plus mass spectrometer using the classic CO_2-H_2O equilibrium method (Horita et al., 1989). Respective δ^2H_{H2O} and $\delta^{18}O_{H2O}$ values are given relative to the Vienna Mean Ocean Water (VSMOW). $\delta^{34}S$ and $\delta^{18}O$ values of dissolved sulphate were measured on $BaSO_4$ that was precipitated by the addition of dissolved barium chloride into acidified sample solutions. The solids were analysed using a Thermo Delta+ mass spectrometer at MPI-MM Bremen (Böttcher et al., 2001; Kornexl et al., 1999) and are referred to the VCDT and VSMOW scales, respectively. Separate samples were taken for isotope analyses of dissolved NO_3. Analyses were carried out by using the bacterial denitrifier technique in combination with the N_2O decomposition method (Casciotti et al., 2002; Kaiser et al., 2007; Morin et al., 2008), where the above isotope values have been precisely measured with an analytical error of ±0.03 ‰ (Savarino et al., 2007). $\delta^{15}N$ and $\delta^{17}O/\delta^{18}O$ of NO_3 are given with respect to atmospheric N_2 and VSMOW standard, respectively.

4. Ion content and mixing approach

The sampled Hasouna groundwaters display near neutral pH conditions (pH = 7.0 ±0.5) at slightly elevated temperatures from 27 to 35°C. Dissolved cations and anions occur in the quantitative sequences of Na > Ca > Mg > K > Sr and Cl > HCO_3 > SO_4 > NO_3, respectively. The chemical composition of the groundwater fulfils the limits for drinking water, except for nitrate. In ≈ 85 % of the analysed Hasouna groundwater the maximum contaminant level (MCL) of the World Health Organization (WHO, 2004) for NO_3 in drinking water of 0.71 mM is exceeded (Tab.1).

Na and Cl concentrations correlate strongly and as solutions #165 and #152 bracket the full observed range, their chemical composition is used for a mixing approach (solid green line in Fig.2a). An evaporation trend for #165 to reach composition of #152 does not fit with the measured data (dotted arrow). Analogous relationships are found for all dissolved compounds (e.g. Ca versus NO_3 in Fig.2b). Thus intermediate solution chemistry can be best followed by mixing of the above two end-member solutions. This is also valid if a decrease of Ca concentration through calcite precipitation ($SI_{calcite}$ = 0) is considered, which may be induced by evaporation (solid arrow in Fig.2b).

5. Origin of water and climate record

The δ^2H_{H2O} and $\delta^{18}O_{H2O}$ values of the analysed Saharan groundwater typically fall below the modern Global and Local Meteoric Water Line (LMWL is given for Sfex, southern Tunisia; Fig.3). Our isotope data fit well with former results for paleo groundwater from Hasouna, Murzuq Basin, Wadi Ash Shati Valley, Arab Jamahiriya in Libya and paleo groundwater from southern Tunisia (Abid et al., 2012; Milne-Home and Sahli, 2007; Salem et al., 1980; Sonntag et al., 1978; Srdoč et al., 1980). The lower deuterium excess (d-excess = δ^2H - 8 $\delta^{18}O$) for paleo groundwater of 5 ±2 $^o/_{oo}$ compared to that of modern precipitation (12 ±2 $^o/_{oo}$) is caused by decreasing moisture deficit (increase in relative humidity) of the air above sea water during evaporation (Sonntag et al., 1978). As air moisture deficit is mostly positive related to temperature, lower paleo temperature vs. modern terms can be suggested from lower d-excess (Kendall and Doctor, 2004). In accordance with the overall shift of Saharan paleo groundwater to low δ^2H_{H2O} and $\delta^{18}O_{H2O}$ values compared to apparent local precipitation (in Sfex and Tripoli, Fig.3) it can be reasonably assumed that the Hasouna groundwater was recharged under past climate which was cooler and much more humid compared to the modern situation (Clark and Fritz, 1997; Edmunds, 2006). In analogy to the above mentioned mixing approach an evaporation effect for Hasouna paleo groundwater, e.g. subsequent to precipitation or during infiltration, can be ruled out as the slope of the regression line for isotope data fits with that of the MWLs (Craig, 1961; Kendall and Doctor, 2004).

6. Origin of nitrate

Our measured $\delta^{15}N_{NO3}$ and $\delta^{18}O_{NO3}$ values of dissolved nitrate are almost within the range of microbial originated NO_3 e.g. by nitrification in soils, where $^{18}O/^{16}O$ is incorporated from apparent H_2O and O_2 and $^{15}N/^{14}N$ is derived from organic matter (Fig.4). In modern groundwater it has been observed, that the isotope composition of NO_3 might be modified within pyrite-bearing aquifers by microbial NO_3 reduction via oxidation of the iron sulfides which is identified by a characteristic lowering in the sulfur and oxygen isotope pair of dissolved SO_4(Zhang et al., 2012). Analysed $\delta\ ^{34}S_{SO4}$ and $\delta\ ^{18}O_{SO4}$ values of 10.5 ±1.5 and 11.4 ±2.4 $^{o}/_{oo}$ (n = 14) for our Hasouna groundwaters are rather constant considering the observed wide range in SO_4 concentrations from 0.9 to 2.6 mM and do not correlate with the NO_3 content which adumbrates insignificance of an overprint by microbal NO_3 reduction. However a pronounced trend to higher $\delta^{18}O_{NO3}$ and lower $\delta^{15}N_{NO3}$ values is obvious for elevated NO_3 concentrations (solid green arrow in Fig.4). This trend cannot be followed by assuming e.g. denitrification (dashed arrow), but may be explained by an impact of NO_3 from desert depositions. $\delta\ ^{15}N_{NO3}$ data of desert NO_3 deposition are close to 0 $^{o}/_{oo}$, the atmospheric value, and the range of $\delta^{18}O_{NO3}$ values may indicate supply of atmospheric nitrate. Although a NO_3 load in the Saharan groundwater from the atmosphere might be suggested from $\delta^{15}N_{NO3}$ and $\delta^{18}O_{NO3}$ values, it has to be kept in mind that these values may vary by complex isotope alteration and fractionation effects.

By far more accurate and precise informations about the origin of NO_3 are obtained by analysing both $\delta^{17}O_{NO3}$ and $\delta^{18}O_{NO3}$ values. Surprisingly all Hasouna paleo groundwaters measured here exhibit a positive ^{17}O-excess up to $\Delta^{17}O_{NO3} \approx 5\ ^{o}/_{oo}$ which is attributed to NMDF during conversion of atmospheric NO_x and O_3 to $NO_{3(atm)}$ (Tab.1; (Kendall and Doctor, 2004; Michalski et al., 2004a; Thiemens, 2001)). In Fig.5a the ^{17}O-excess versus the traditional $\delta^{18}O_{NO3}$ value is displayed. A potential secondary (de)nitrification or reduction impact can be followed by a shift parallel to the terrestrial fractionation trend (horizontal arrows indicate MDF effect). In contrast the $\Delta^{17}O_{NO3}$ value behave conservatively. Thus the deviation from the correlation of isotope data in Fig.5a can be reasonable explained by MDF effects. Although different environmental conditions have to be considered for the given isotope data of NO_3 in Fig.5a, an overall relationship with a slope of 0.342 is obtained from least square method, which fits well with the $\Delta^{17}O_{NO3}$ end-member, the atmospheric photochemical NO_3 (Michalski et al., 2004a). Briefly the formation of $NO_{3,atm}$ is based on the most important oxidants in the atmosphere O_3 (Seinfeld and Pandis, 1998). Individual lifetime of excited O_3 isotopologues during formation depends on molecule symmetry and isotope substitution, which results in a NMDF for O_3 (Gao and Marcus, 2001; Savarino, 2000). The respective $\Delta^{17}O$ of atmospheric NO_3, gained from the conversion of atmospheric NO_x and O_3, can be followed by three major reaction pathways involving NO_2, O_3, OH and H_2O (Michalski et al., 2003). The proportion of $NO_{3,atm}$ for the former reaction paths and corresponding

precipitation rates can be obtained from global climate models, which finally results in $\Delta^{17}O_{NO3,atm}$ of about 25 ‰ , a value well corroborated by atmospheric observations (Michalski et al., 2003; Morin et al., 2008). In contrast microbial induced nitrification in soils results in $\Delta^{17}O_{NO3,soil}$ = 0 ‰ and potential denitrification is leaving the $\Delta^{17}O$ unaltered. As NO_3 does not exchange oxygen isotopes with water directly, the ^{17}O-excess is a highly conserved tracer for $NO_{3,atm}$ and is a more robust proxy compared to $\delta^{18}O_{NO3}$ values (Michalski et al., 2004a). Considering both, microbial and atmospheric NO_3, the individual ^{17}O excesses of dissolved NO_3 of the analysed Saharan groundwater yield in proportions from 1.6 up to 20.0% for atmospheric origin ($xNO_{3,atm}$ in Tab.1).

7. Implications for paleo climate conditions during precipitation

In analogy to ion concentrations a mixing approach considering the end-member solutions #165 and #152 is also valid for the ^{17}O-excess in Hasouna paleo groundwater which is displayed by a linear correlation of $\Delta^{17}O_{NO3}$ versus 1/[NO_3^-] in Fig.5b. Thus elevated $NO_{3,atm}$ proportions are obtained at highest total NO_3 concentrations (e.g. #152). Such elevated $NO_{3,atm}$ proportions can be reasonably explained by an impact of flood events as shown by Michalski et al. (2004b) from monitored values during storm events in Devil Canyon watershed (southern California, USA). $\Delta^{17}O_{NO3}$ maximum values are caused by a sudden wash out of dry deposition of atmospheric NO_3 which was accumulated through rather long-lasting arid conditions on plant or soil surfaces. Wash out during storm flow periods and flood events enhances mobilization of NO_3 and corresponding NO_3 concentration in groundwater as reported by Chiwa et al. (2010) for a small forested watershed.

Accordingly for the present case it is reasonably predicted that dry periods had been alternated with heavy precipitation and flood events, where infiltration of solutions occurred leaving the ^{17}O-excess of NO_3 preserved. Preserved $\Delta^{17}O_{NO3}$ > 0 ‰ obviously indicates that $NO_{3,atm}$ did not undergo complete biological processing as time for infiltration through soil horizons was limited (Michalski et al., 2004b). Limited NO_3-biotic interaction periods are also documented by the uniform sufur and oxygen isotope composition of SO_4 and in particular by $\delta^{18}O_{NO3}$ values which change in the direction to atmospheric NO_3 at elevated NO_3^- concentrations, opposite to what would be expected to occur during (de)nitrification (Fig.4). Interestingly elevated intensity of cyclic storm and flood events are referred to relatively warmer paleo climate conditions (see #152 versus #165 in Figs. 3 and 2, respectively).

8. Conclusions

Here we used an integrated hydrogeochemical and isotope approach to identify the origin of NO_3 and to reconstruct paleo environmental conditions during the recharge of Saharan groundwater (Hasouna, Libya). High NO_3 concentrations are common features of paleo groundwater not only in North Africa but also in other arid and semi-arid areas (Edmunds, 2006). As the source of NO_3 in paleo groundwater is still under debate, we applied the outstanding feature of $\Delta^{17}O_{NO3}$ values to trace atmospheric NO_3 as the respective ^{17}O-excess is not being affected by terrestrial fractionation processes (MDF), e.g. induced by (de)nitrification or assimilation (Kendall and Doctor, 2004). Our ^{17}O-excess data clearly discover that in the present Saharan groundwater up to 20 mol% of the dissolved NO_3 is originated from the atmosphere with the remaining NO_3 being due to microbial sources. To our knowledge it is herein the first study, where ^{17}O-excess of NO_3 is measured in paleo groundwater. Our results thus univocal verify that $\Delta^{17}O_{NO3}$ values survived up to thousands of years and can be still used to estimate $NO_{3,atm}$ proportion of total dissolved NO_3 during anchient recharge. Accordingly for water management issues of Saharan groundwater from Hasouna wellfields elevated NO_3 concentrations have to be considered as a long-lasting challenge as NO_3 content within the aquifer is predetermined by paleo recharge conditions.

The analysed individual composition and also isotope signals of NO_3 and H_2O of Hasouna groundwater can be followed by a simple mixing of two end-member solutions: The lowest (#165) and highest mineralized solutions (#152) with NO_3 concentration of 0.5 and 1.8 mM, respectively. The assumption of end-member solutions sounds highly reasonable as paleo groundwater with a huge variability in salinity is regionally documented. For instance for the so-called Zimam aquifer with enhanced salinities and elevated NO_3 concentration up to 1.1 mM ((El-Baruni et al., 1985); located close to #152) a significant leakage to the underlying Cambro-Ordovician sandstone aquifer through fractures in limestone and dolomite is postulated (Binsariti and Saeed, 2000).

An evaporation trend is reflected by neither solution chemistry nor the $\delta\,^{2}H_{H2O}$-$\delta^{18}O_{H2O}$ relationship. However from the isotopic composition of the groundwater a local Paleo Meteoric Water Line can be estimated: $\delta\,^{2}H_{H2O} = 8.0\,\delta^{18}O_{H2O} + 6.3$ (Fig.2). Low d-excess as well as low $\delta^{2}H_{H2O}$ and $\delta^{18}O_{H2O}$ values clearly indicate that the groundwater in the Hasouna basin was recharged under cooler and more humid climate compared to the present conditions. Positive correlation between $\Delta^{17}O_{NO3}$ values and NO_3 concentrations discover past alternating arid and humid periods. In arid periods a continuous dry deposition and accumulation of atmospheric NO_3 at plant or soil surfaces occurred. Humid periods yield in high amounts of precipitation or even flood event which washed out the accumulated $NO_{3,atm}$ and were rapidly infiltrated through the subsurface to recharge the Saharan paleo groundwater of Hasouna area. Accordingly^{17}O-excess in NO_3 provides a

robust and powerful tool within a multi proxy approach (i) to trace the origin of NO_3 in paleo groundwater reservoirs and (ii) to reconstruct the paleo recharge and climate conditions during the formation of deep paleo groundwater of the Saharan desert.

Acknowledgements

We wish to thank the General Water Authority (Tripoli, Libya) and in particular Omar Salem for the permission to collect groundwater samples from Hasouna wellfield area and for administrative arrangements. Support from the Authority of the Great Man-made-River Project in Tripoli and from Christian Schmid (Leoben, Austria) in respect to logistics and field work is greatly appreciated. This work was financially supported by the Graz University of Technology (Austria) scientific grant program.

References

Abid, K., Dulinski, M., Ammar, F.H., Rozanski, K., Zouari, K. (2012) Deciphering interaction of regional aquifers in Southern Tunisia using hydrochemistry and isotopic tools. Applied Geochemistry 27, 44-55.

Amberger, A., Schmidt, H.L. (1987) Natürliche Isotopengehalte von Nitrat als Indikatoren für dessen Herkunft. Geochim. Cosmochim. Acta 51, 2699-2705.

Binsariti, A., Saeed, F.S. (2000). Groundwater salinity variations in the Cambro-Ordovician aquifer of eastern Jabal al Hasawnah, the great man-made river project, Libya in: Sola, M.A., Worsley, D. (Eds.), Geological Exploration in Murzuq Basin pp. 1-16.

Blackwell, B.A.B., Skinner, A.R., Mashriqi, F., Deely, A.E., Long, R.A., Gong, J.J.J., Kleindienst, M.R., Smith, J.R. (2012) Challenges in Constraining Pluvial Events and Hominin Activity: Examples of ESR Dating Molluscs from the Western Desert, Egypt. Quaternary Geochronology 10, 430-435.

Böhlke, J.K., Ericksen, G.E., Revesz, K. (1997) Stable isotope evidence for an atmospheric origin of desert nitrate deposits in northern Chile and southern California, U.S.A. Chemical Geology 136, 135-152.

Böttcher, M.E., Thamdrup, B., Vennemann, T.W. (2001) Oxygen and sulfur isotope fractionation during anaerobic bacterial disproportionation of elemental sulfur. Geochim. Cosmochim. Acta 65, 1601-1609.

Carrara, C., Cremaschi, M., Quinif, Y. (1998). The travertine deposits in the Tadrart Acacus (Libyan Sahara); nature and age, in: Cremaschi, M., Di Lernia, S. (Eds.), Wadi Teshuinat - Palaeoenvironment and Prehistory in South-western Fezzan (Libyan Sahara) C.N.R. Quaderni di Geodinamica Alpina e Quaternaria, pp. 59-66.

Casciotti, K.L., Sigman, D.M., Hastings, M.G., Böhlke, J.K., Hilkert, A. (2002) Measurement of the oxygen isotopic composition of nitrate in seawater and freshwater using the denitrifier method. Analytical Chemistry 74, 4905-4912.

Chiwa, M., Ide, J., Maruno, R., Higashi, N., Otsuki, K. (2010) Effects of storm flow samplings on the evaluation of inorganic nitrogen and sulfate budgets in a small forested watershed. Hydrol. Process. 24, 631-640.

Clark, I.D., Fritz, P. (1997) Environmental Isotopes in Hydrology. CRC Press.

Craig, H. (1961) Isotopic variations in meteoric waters. Science 133, 1702-1703.

Dejwakh, N.R., Meixner, T., Michalski, G., McIntosh, J. (2012) Using O-17 to investigate nitrate sources and sinks in a semi-arid groundwater system. Environ. Sci. Technol. 46, 745-751.

Dietzel, M., Kolmer, H., Pölt, P., Simic, S. (2008) Desert varnish and petroglyphs on sandstone - Geochemical composition and climate changes from Pleistocene to Holocene (Libya). Geochemistry 68, 31-43.

Doherty, R., Kutzbach, J., Foley, J., Pollard, D. (2000) Fully coupled climate/dynamical vegetation model simulations over Northern Africa during the mid-Holocene. Climate Dynamics 16, 561-573.

Edmunds, W.M. (2006). Libya's Saharan Groundwater: Occurrence, Origins and Outlook, in: Mattingly, D., McLaren, S., Savage, E. (Eds.), The Libyan Desert: Natural Resources and Cultural Heritage Society of Libyan Studies Monograph, pp. 45-64.

Edmunds, W.M., Dodo, A., Djoret, D., Gasse, F., Gaye, C.B., Goni, I.B., Travi, Y., Zouari, K., Zuppi, G.M. (2003). Groundwater as an archive of climatic and environmental change, in: Battarbee, R.W., F., G., Stickly, C.E. (Eds.), Past Climate Variability through Europe and Africa, Developments in Paleoenviromental Research Kluwer Dordrecht, pp. 279-306.

Edmunds, W.M., Wright, E.P. (1979) Groundwater recharge and palaeoclimate in the Sirte and Kufra basins, Libya. Journal of Hydrology 40, 215-241.

El-Baruni, S.S., El-Futasi, R.H., Maaruf, A.M. (1985). Hydrology of Ghadamis Basin, NW Libya, Geology of Libya, Libyan Arab Jamahiriya, Tripoli, pp. 269-290.

Gao, Y.Q., Marcus, R.A. (2001) Strange and unconventional isotope effects in ozone formation. Science 293, 259-263.

Guendouz, A., Moulla, A.S., Edmunds, W.M., Shand, P., Poole, J., Zouari, K., Mamou, A. (1998). Palaeoclimatic information contained in groundwaters of the Grand Erg Oriental, north Africa, Isotope techniques in the study of environmental change IAEA Vienna, pp. 555-571.

Horita, J., Ueda, A., Mizukami, K., Takatori, I. (1989) Automatic dD and $d^{18}O$ analyses of multi-water samples using H_2- and CO_2-water equilibration methods with a common equilibration set-up. Applied Radiation and Isotopes 40, 801-805.

Kaiser, J., Hastings, M.G., Houlton, B.Z., Röckmann, T., Sigman, D.M. (2007) Triple oxygen isotope analysis of nitrate using the denitrifier method and thermal decomposition of N2O. Analytical Chemistry 79, 599-607.

Kendall, C. (1998). Tracing nitrogen sources and cycling in catchments, in: Kendall, C., McDonnell, J.J. (Eds.), Isotope tracers in catchment hydrology, pp. 519-576.

Kendall, C., Doctor, D.H. (2004). Stable Isotope Applications in Hydrologic Studies in: Drever, J.I. (Ed.), Treatise on Geochemistry - Surface and Groundwater, weathering and soils pp. 319 - 364.

Kornexl, B.E., Gehre, M., Hofling, R., Werner, R.A. (1999) On-line delta O-18 measurement of organic and inorganic substances. Rapid Communications in Mass Spectrometry 13, 1685-1693.

Kuper, R., Kröpalin, S. (2006) Climate-controlled holocene occupation in the Sahara: Motor of Africa's evolution. Science 313, 803-807.

Li, Y.H., Qin, Y., Liu, F., Hou, K.J., Wan, D.F. (2010) Discovery of mass independent oxygen isotopic compositions in superscale nitrate mineral deposits from Turpan-Hami Basin, Xinjiang, China and its significance. Acta Geol. Sin.-Engl. Ed. 84, 1514-1519.

Michalski, G., Bockheim, J.G., Kendall, C., Thiemens, M. (2005) Isotopic composition of Antarctic Dry Valley nitrate: Implications for NO(y) sources and cycling in Antarctica. Geophysical Research Letters 32, 4.

Michalski, G., Bohlke, J.K., Thiemens, M. (2004a) Long term atmospheric deposition as the source of nitrate and other salts in the Atacama Desert, Chile: New evidence from mass-independent oxygen isotopic compositions. Geochim. Cosmochim. Acta 68, 4023-4038.

Michalski, G., Meixner, T., Fenn, M., Hernandez, L., Sirulnik, A., Allen, E., Thiemens, M. (2004b) Tracing Atmospheric Nitrate Deposition in a Complex Semiarid Ecosystem Using $D^{17}O$. Environmental Science and Technology 38, 2175-2181.

Michalski, G., Scott, Z., Kabiling, M., Thiemens, M.H. (2003) First measurements and modeling of $D^{17}O$ in atmospheric nitrate. Geophysical Research Letters 30, 14-11.

Milne-Home, W.A., Sahli, N.I.M. (2007) Application of ^{15}N isotopes to management of groundwater quality Hasouna wellfields, Great man-made river project, Libyan Arabjamahiriya IAEA-CN-151/63, 487-494.

Morin, S., Savarino, J., Frey, M.M., Yan, N., Bekki, S., Bottenheim, J.W., Martins, J.M.F. (2008) Tracing the origin and fate of NOx in the arctic atmosphere using stable isotopes in nitrate. Science 322, 730-732.

Morrison, J., Brockwell, T., Merren, T., Fourel, F., Phillips, A.M. (2001) On-line high-precision stable hydrogen isotopic analyses on nanoliter water samples. Analytical Chemistry 73, 3570-3575.

Parkhurst, D.L., Appelo, C.A.J. (1999) User`s guide to PHREEQC (version 2); a computer program for speciation, batch-reaction, one-dimensional transport,

and inverse geochemical calculations. Water-Resources Investigations U.S. Geol. Sur., 312.

Rognon, P. (1987) Late quaternary climatic reconstruction for the maghreb (North Africa). Palaeogeography, Palaeoclimatology, Palaeoecology 58, 11-34.

Salem, O. (1992) The great manmade river project: A partial solution to Libya`s future water supply. International Journal of Water Resources Development 8, 270-278.

Salem, O., Visser, J.H., Dray, M., Gonfiantini, R. (1980) Groundwater flow patterns in the Western Libyan Arab Jamahiriya evaluated from isotopic data. IAEA-AG-158/12, 165-178.

Savarino, J. (2000) Laboratory oxygen isotopic study of sulfur(IV) oxidation: Origin of the mass-independent oxygen isotopic anomaly in atmospheric sulfates and sulfate mineral deposits on Earth. Journal of Geophysical Research D: Atmospheres 105, 29079-29088.

Savarino, J., Kaiser, J., Morin, S., Sigman, D.M., Thiemens, M.H. (2007) Nitrogen and oxygen isotopic constraints on the origin of atmospheric nitrate in coastal Antarctica. Atmos. Chem. Phys. 7, 1925-1945.

Seinfeld, J.H., Pandis, S.N. (1998) Atmospheric chemistry and physics: From air ollution to climate change. Wiley, New York.

Sonntag, C., Klitzsch, E., Löhnert, E.P., El-Shazly, E.M., Münnich, K.O., Junghans, C., Thorweihe, U., Weistroffer, K., Swailem, F.M. (1978) Paleoclimatic information from deuterium and oxygen-18 in carbon-14 dated north Saharan groundwaters. IAEA-SM-228/28, 569–581.

Srdoč, D., Sliepčević, A., Obelić, B., Horvatinčić, N., Moser, H., Stichler, W. (1980) Isotope investigations as a tool for regional hydrogeological studies in the Libyan Arab Jamahiriya. IAEA-AG-158/11, 153-164.

Thiemens, M.H. (2001) Atmospheric science: The mass-independent ozone isotope effect. Science 293, 226.

Thiemens, M.H. (2006). History and applications of mass-independent isotope effects. Annual Review of Earth and Planetary Sciences, Palo Alto, pp. 217-262.

Tsunogai, U., Daita, S., Komatsu, D.D., Nakagawa, F., Tanaka, A. (2011) Quantifying nitrate dynamics in an oligotrophic lake using Delta O-17. Biogeosciences 8, 687-702.

Tsunogai, U., Komatsu, D.D., Daita, S., Kazemi, G.A., Nakagawa, F., Noguchi, I., Zhang, J. (2010) Tracing the fate of atmospheric nitrate deposited onto a

forest ecosystem in Eastern Asia using Delta O-17. Atmos. Chem. Phys. 10, 1809-1820.

WHO (2004) Guidelines for drinking water quality. Geneva: World Health Organization.

Xue, D., Botte, J., De Baets, B., Accoe, F., Nestler, A., Taylor, P., Van Cleemput, O., Berglund, M., Boeckx, P. (2009) Present limitations and future prospects of stable isotope methods for nitrate source identification in surface- and groundwater. Water Research 43, 1159-1170.

Zhang, Y.C., Slomp, C.P., Broers, H.P., Bostick, B., Passier, H.F., Bottcher, M.E., Omoregie, E.O., Lloyd, J.R., Polya, D.A., Van Cappellen, P. (2012) Isotopic and microbiological signatures of pyrite-driven denitrification in a sandy aquifer. Chemical Geology 300, 123-132.

Captions of Table and Figures

Table 1. Composition of Saharan paleo groundwater from wells of Hasouna area (Libya).

No.: well number (see Fig.1). T: Temperature in °C. $[NO_3^-]$: Nitrate concentrations are given in mM. $\delta^{18}O_{H2O}$ and $\delta^{2}H_{H2O}$ values of the groundwater are given in $^{o}/_{oo}$ (VSMOW). $\delta^{15}N_{NO3}$, $\delta^{18}O_{NO3}$, and $\Delta^{17}O_{NO3}$ values of dissolved NO_3 are given in $^{o}/_{oo}$ relative to AIR and VSMOW standard, respectively. $xNO_{3,atm}$: proportions of dissolved NO_3 from atmospheric origin.

No.	T	pH	$[NO_3^-]$	$\delta^{18}O_{H2O}$	$\delta^{2}H_{H2O}$	$\delta^{15}N_{NO3}$	$\delta^{18}O_{NO3}$	$\delta^{17}O_{NO3}$	$\Delta^{17}O_{NO3}$	$xNO_{3,atm}$
13	33.0	6.66	0.54	-9.75	-73.2	9.1	6.9	4.1	0.5	2.0
32	33.2	6.85	0.76	-9.68	-71.8	8.4	8.3	6.1	1.8	7.1
39	32.7	6.85	0.95	-9.72	-72.0	8.5	13.4	9.5	2.5	10.1
51	29.6	6.74	0.87	-9.17	-67.6	7.9	10.4	8.0	2.6	10.4
60	30.6	6.54	1.27	-8.75	-65.6	7.4	11.7	10.0	3.9	15.7
72	33.0	7.12	1.31	-9.46	-67.0	7.4	13.5	10.7	3.7	14.7
84	35.1	6.79	0.69	-9.77	-69.0	8.9	7.6	4.9	0.9	3.8
89	30.7	7.11	1.48	-9.51	-69.5	7.2	12.3	10.9	4.5	18.0
100	29.9	7.08	0.69	n.a.	n.a.	8.5	7.6	4.7	0.7	3.0
121	34.4	7.05	0.81	-9.39	-68.3	8.3	10.4	7.4	2.0	8.0
126	30.4	7.18	1.50	-9.15	-69.5	6.9	15.0	12.8	5.0	20.0
134	29.3	6.76	1.27	-9.58	-70.4	6.6	16.1	12.6	4.2	16.9
138	28.9	7.24	0.88	-9.94	-71.6	7.2	13.6	9.7	2.6	10.5
139	28.9	7.46	0.88	-9.97	-73.1	7.1	11.9	8.9	2.7	10.8
145	29.8	7.00	1.24	-9.52	-69.8	7.1	14.7	11.3	3.7	14.6
149	28.1	7.40	1.18	-9.69	-69.0	7.1	15.4	12.1	4.1	16.4
151	28.3	7.00	1.70	-9.32	-68.0	7.0	17.4	13.7	4.7	18.6
152	28.8	7.03	1.84	-9.20	-67.5	7.5	14.8	12.4	4.7	18.8
154	27.2	7.08	1.18	-9.30	-67.4	8.6	16.4	11.1	2.6	10.3
165	28.1	7.24	0.59	-9.90	-72.8	7.7	9.8	6.1	1.0	4.0
179	28.1	7.06	1.20	-9.26	-68.3	8.0	10.9	7.6	1.9	7.7
181	29.7	7.03	1.02	-9.08	-69.3	8.7	10.6	7.6	2.1	8.4
286	28.6	7.02	1.07	-9.17	-68.8	8.5	12.9	9.1	2.4	9.6
372	27.3	7.37	1.36	-9.09	-64.6	8.9	10.2	7.2	1.9	7.6
384	29.0	7.40	0.78	n.a.	n.a.	8.6	8.1	5.7	1.5	6.0
442	30.8	7.01	0.79	-9.74	-72.0	8.4	9.8	5.5	0.4	1.6
453	34.6	6.82	0.47	-9.62	-70.3	8.6	9.1	5.8	1.1	4.3
478	29.8	7.01	0.71	n.a.	n.a.	7.8	9.1	6.5	1.8	7.1

n.a.: not analysed

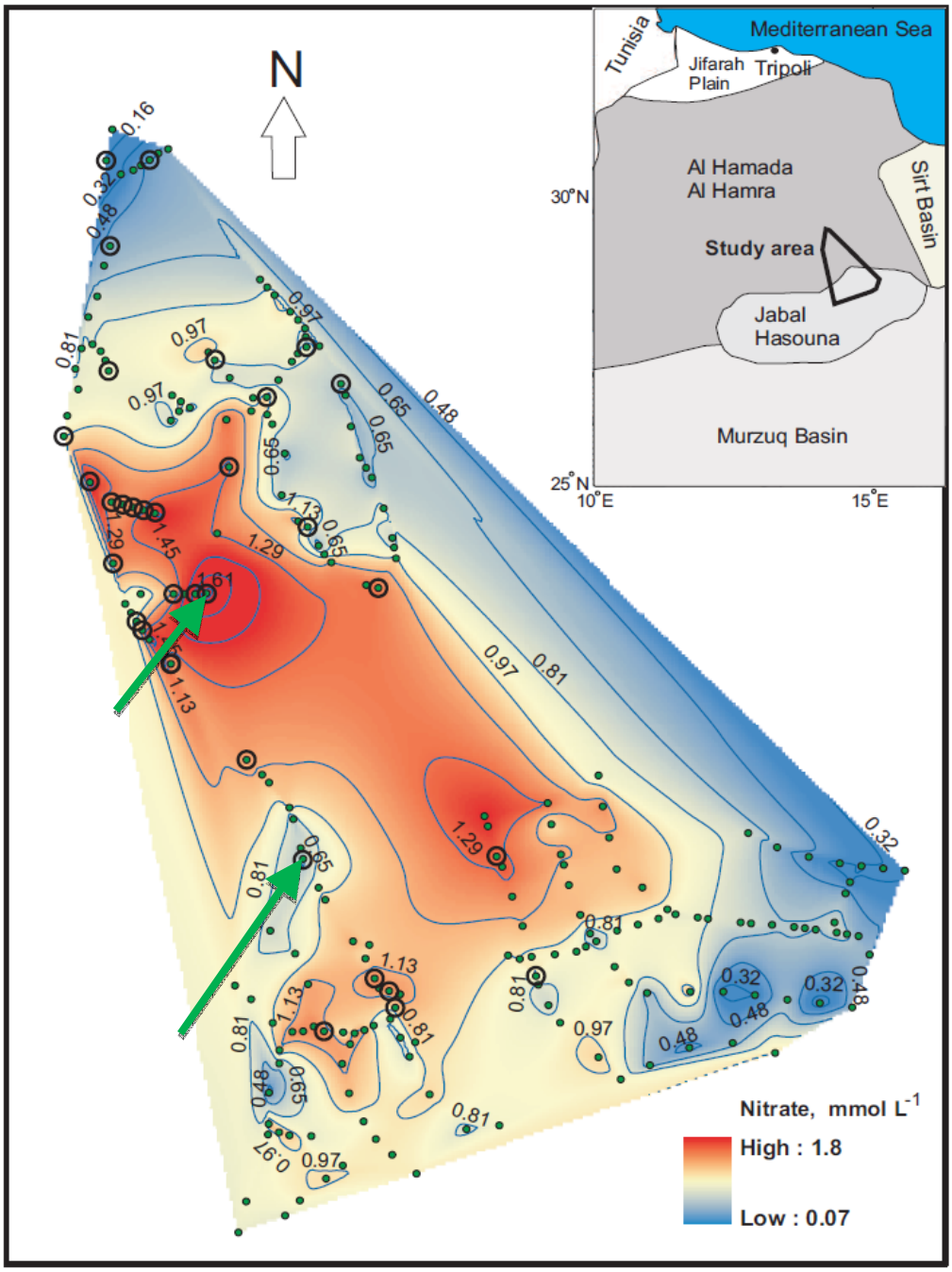

Fig. 1 Sampling sites (□) and distribution of nitrate in paleo groundwater from Hasouna, Libya. Isolines are obtained from a total of 57 NO_3 analyses of paleo groundwater from wells (●).

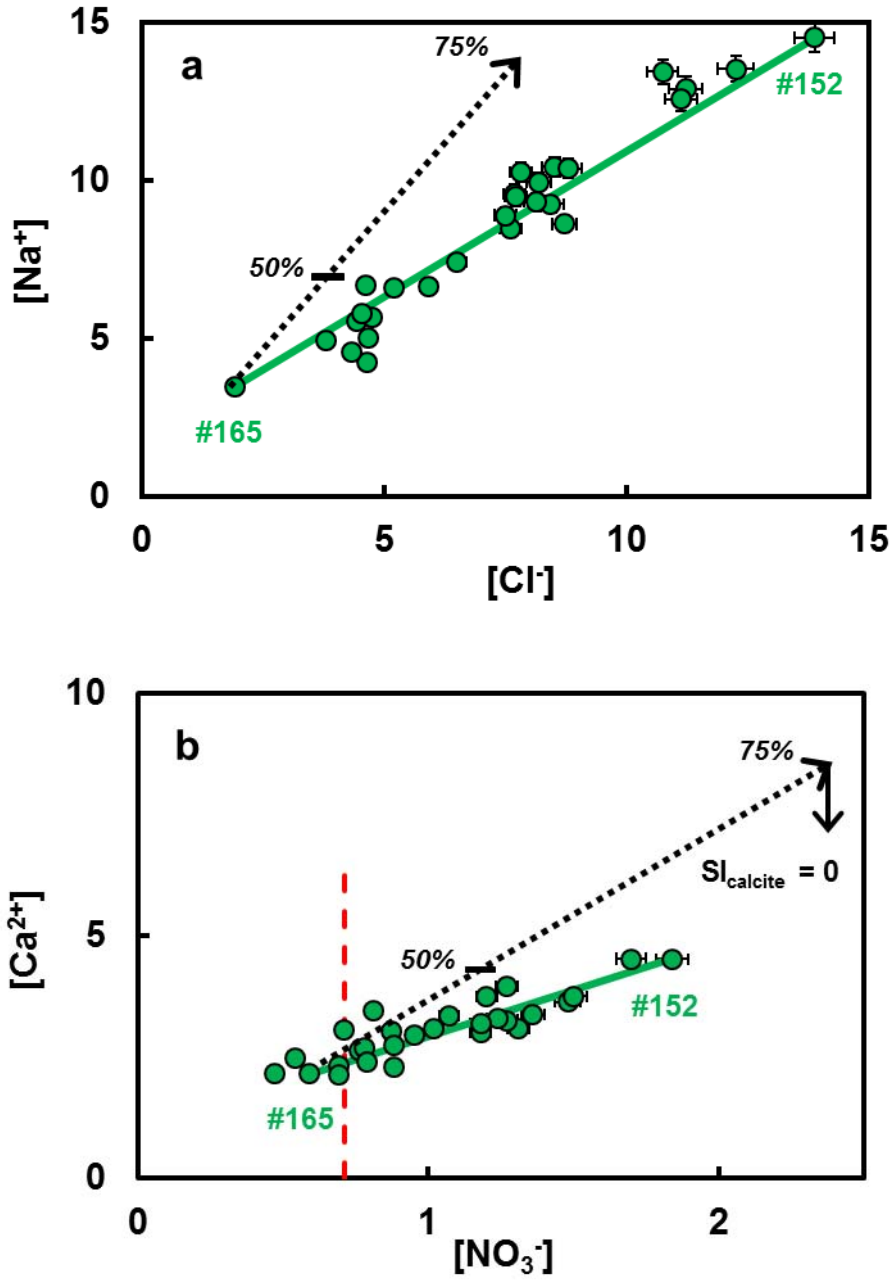

Fig. 2 Chemical composition of groundwater from Hasouna, Libya. a: Na versus Cl concentration. b: Ca versus NO_3 concentration. Values are given in mM. Solid green lines: Mixing between end-member solutions #165 and #152 with lowest and highest ion concentrations, respectively. Dotted arrows: Chemical trend for evaporation of solution #165, where 50 and 75% denote ion concentrations at respective loss of H_2O by evaporation. Solid arrow: Decrease of Ca concentration by considering calcite precipitation to reach $SI_{calcite}$ = 0. Dashed red line: MCL for NO_3 in drinking water according to WHO (WHO, 2004).

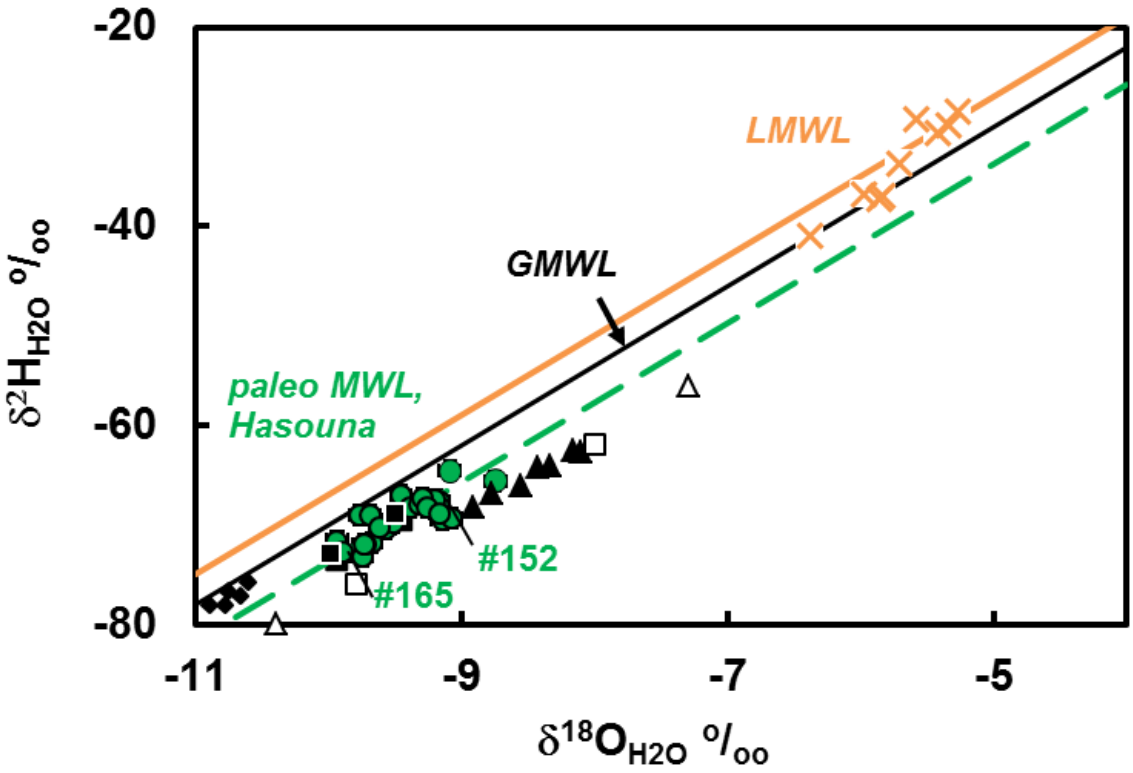

Fig. 3 Stable hydrogen and oxygen isotopic composition of groundwater from North Africa. Paleo groundwater displays lower stable isotope values and an elevated d-excess compared to modern precipitation which indicates recharge under cooler and more humid climate conditions versus modern climate conditions. The analytic inaccuracies lay within the size of the symbols. ●: Hasouna, Libya (this study); ■: Hasouna, Libya, isotopic range(Milne-Home and Sahli, 2007); □: Murzuq Basin, Libya, isotopic range (Sonntag et al., 1978); Δ: Arab Jamahiriya, Libya (Srdoč et al., 1980);▲: South Tunisia (Abid et al., 2012); ♦: Wadi Ash Shati Valley, Libya (Salem et al., 1980). x: Groundwater recharged by modern precipitation close to Tripoli (own data). GMWL: Global Meteoric Water Line ($\delta^2H = 8\ \delta^{18}O + 10$; (Craig, 1961)). LMWL: Local Meteoric Water Line for Sfax metereological station, southern Tunisia (yellow line: $\delta^2H = 8\ \delta^{18}O + 13$; (Abid et al., 2012). Paleo MWL: Paleo Meteoric Water Line estimated from isotopic data of the present study by least square method (dashed green line: $\delta^2H = 8\ \delta^{18}O + 6.3$).

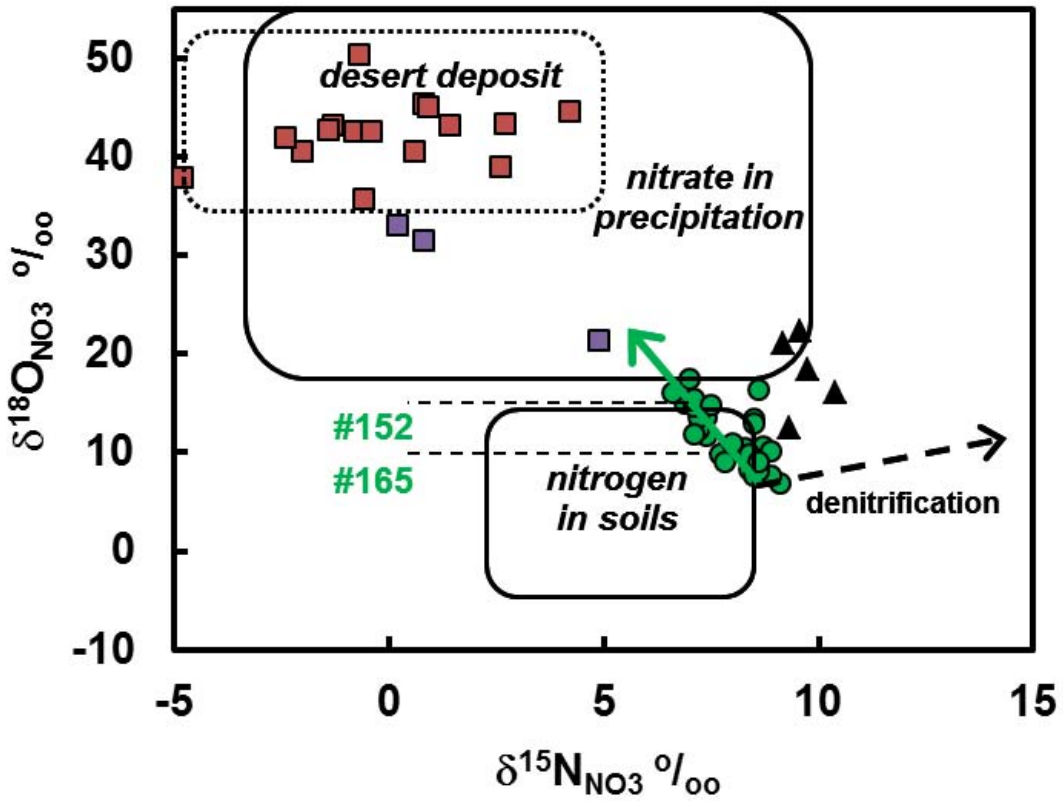

Fig. 4 $^{8}O/^{16}O$ versus $^{15}N/^{14}N$ distribution in nitrate (adapted from Kendall, 1998). $\delta^{18}O_{NO3}$ and $\delta^{15}N_{NO3}$ values are referred to the VSMOW and atmospheric N_2 standard, respectively. The analytic inaccuracies lay within the size of the symbols.
●: Hasouna groundwater (this study), where the solid green arrow displays increase in NO_3 concentration; ▲: Hasouna groundwater (Milne-Home and Sahli, 2007); ■ and ■: NO_3-rich deposit of Atacama (Chile) and Mojave desert (California), respectively (Böhlke et al., 1997).

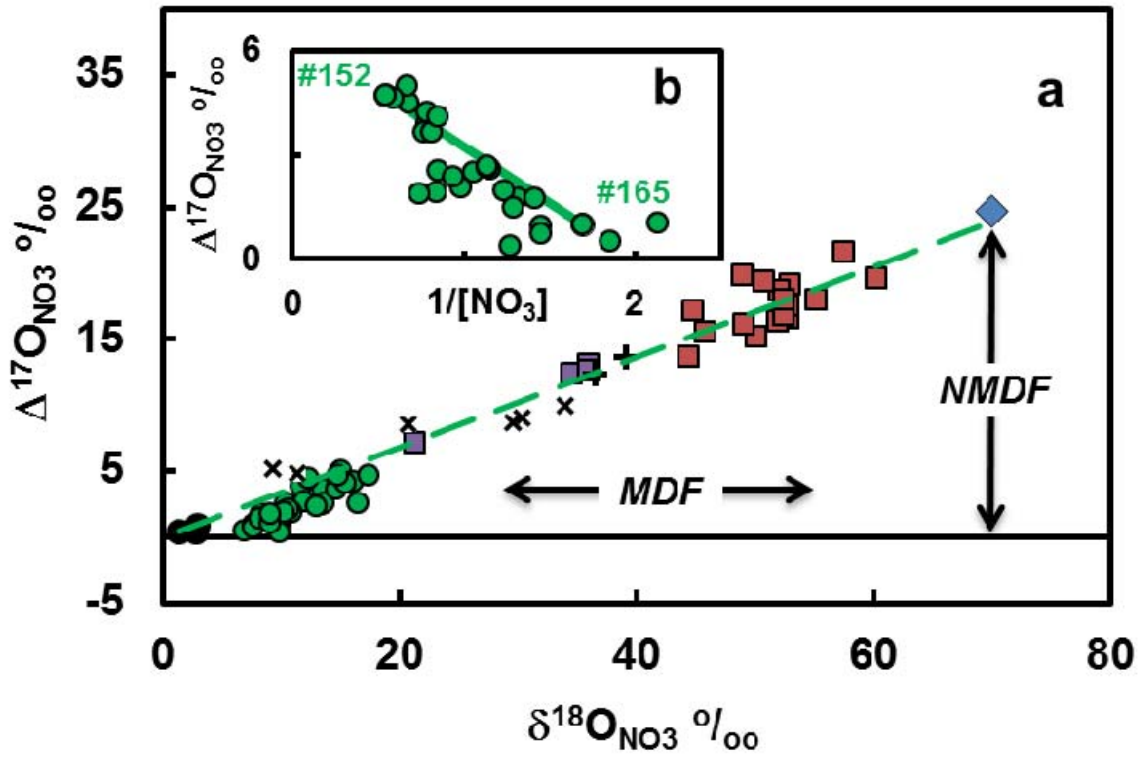

Fig. 5 ^{17}O excess ($\Delta^{17}O_{NO3}$) versus $\delta^{18}O_{NO3}$ and nitrate content. a: Isotope values are related to the VSMOW standard. The analytic inaccuracies lay within the size of the symbols. ●: Hasouna groundwater, Libya (this study); ■ and ■: NO_3-rich deposit of Atacama (Chile) and Mojave desert (California), respectively (Michalski et al., 2004a). ●: Groundwater from Mojave desert (Michalski et al., 2004a). **x**: Stream water from San Gorgonio and Devil Canyon at storm flow event (California; Michalski et al., 2004b). **+**: NO_3-rich deposit of Kumutag (China; Li et al., 2010); ♦: Atmospheric photochemical NO_3 (Michalski et al., 2004a). Solid horizontal line: Terrestrial fractionation line considering MDF. Dashed green line: Regression line for all given data ($\Delta^{17}O_{NO3} = 0.342\ \delta^{18}O_{NO3}$; $R^2 = 0.978$).
b: Mixing approach for #165 and #152 end-member solutions where ^{17}O excess of dissolved NO_3 can be followed by inverse NO_3 concentration (mM) with a straight line.

12.2 APPENDIX II

Data of Groundwater chemistry and isotope results of the Hasouna Study area

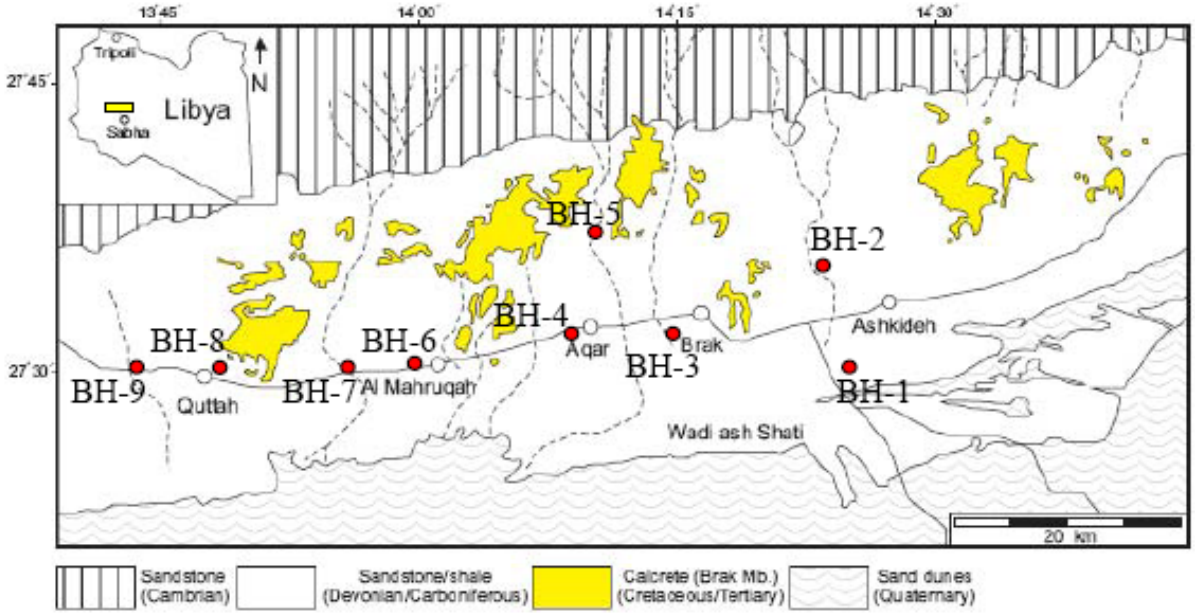

Figure 12.1: Location map of the Wadi Ash Shati study area and the groundwater sampling points (red circles).

Table 12.1: Physical and chemical parameters of groundwater in the Hasouna study area. TDS= total dissolved solids, EC= electrical conductivity [µs/cm], DO= dissolved oxygen, all groundwater compositions are in mgL^{-1}. n.a: not analysed.

No.	Well No.	Sampling Date	T [°C]	TDS	EC	pH	DO	Cl	SO_4	NO_3	Ca	K
1	84	15.08.2007	30.0	790	1200	7.10	6.50	173	140	53.4	86.1	4.00
2	85	15.08.2007	29.7	1094	1590	7.31	n.a.	234	289	71.2	120	5.30
3	86	15.08.2007	30.4	1139	1752	7.28	n.a.	254	300	75.2	125	5.30
4	87	15.08.2007	30.7	1145	1673	7.10	n.a.	261	294	75.5	121	5.40
5	88	15.08.2007	30.5	1135	1648	7.26	n.a.	255	291	76.3	121	5.20
6	89	15.08.2007	30.7	1288	1873	7.30	n.a.	327	311	84.0	135	5.60
7	121	15.08.2007	30.0	1248	2200	7.20	6.80	376	240	58.9	104	4.10
8	134	15.08.2007	29.4	1185	1820	7.20	n.a.	302	297	74.7	108	5.40
9	139	15.08.2007	30.0	774	1125	7.06	n.a.	148	182	53.8	89.5	3.60
10	141	15.08.2007	28.9	1080	1637	7.04	n.a.	261	270	72.0	101	4.40
11	142	15.08.2007	30.0	1491	2160	7.01	n.a.	404	381	95.9	135	6.60
12	145	15.08.2007	30.5	1199	1730	6.90	n.a.	317	292	73.2	113	4.70
13	146	15.08.2007	28.0	767	1153	7.24	n.a.	148	183	52.3	84.5	3.80
14	149	15.08.2007	29.2	1164	1715	7.49	n.a.	298	283	70.6	119	5.10
15	150	15.08.2007	28.7	1483	2230	7.46	n.a.	414	371	89.9	143	6.20
16	151	15.08.2007	28.8	1626	2420	7.15	n.a.	467	403	97.7	157	6.90
17	152	15.08.2007	29.2	1778	2650	7.10	n.a.	533	439	107	170	7.40
18	39	13.11.2007	32.7	1042	1591	6.85	4.26	230	176	58.8	118	5.80
19	84	13.11.2007	35.1	804	1219	6.79	4.21	157	129	42.6	92.6	5.30
20	89	13.11.2007	30.7	1295	2080	7.11	5.48	302	294	91.7	146	5.50
21	121	13.11.2007	34.4	1380	2330	7.05	6.45	394	253	50.0	141	4.80
22	126	13.11.2007	30.4	1519	2430	7.18	5.35	381	338	93.0	150	5.70
23	138	13.11.2007	28.9	942	1383	7.24	4.62	163	206	54.4	110	4.40
24	145	13.11.2007	29.8	1276	1945	7.00	n.a.	289	272	76.9	132	5.00
25	151	13.11.2007	28.3	1722	2670	7.00	5.72	434	383	106	181	6.80
26	152	13.11.2007	28.8	1777	2930	7.03	5.03	492	415	114	181	8.30
27	134	13.11.2007	29.3	1239	1957	6.76	4.76	277	279	78.7	130	6.80
28	1	15.12.2007	34.2	729	1050	7.10	n.a.	138	126	41.3	82.3	5.20
29	9	15.12.2007	33.4	852	1195	7.15	n.a.	166	144	46.3	92.5	5.40
30	13	13.12.2007	32.5	767	1100	6.85	n.a.	140	129	42.1	84.4	5.30
31	21	15.12.2007	32.8	800	1110	6.63	n.a.	146	126	38.2	80.9	10.2
32	29	15.12.2007	29.3	1169	1800	6.99	n.a.	332	170	48.2	105	6.10
33	32	13.12.2007	33.2	934	1301	6.85	n.a.	210	164	47.3	106	6.10
34	51	13.12.2007	29.6	1126	1730	6.74	n.a.	299	217	53.8	121	5.80
35	60	13.12.2007	30.6	1532	2280	6.54	n.a.	398	287	78.9	159	6.70
36	72	15.12.2007	33.0	1151	1782	7.12	n.a.	309	211	81.3	124	5.30
37	79	15.12.2007	30.9	1358	2080	7.01	n.a.	374	273	78.6	139	7.10
38	93	15.12.2007	34.8	1087	1525	6.62	n.a.	198	256	11.1	103	10.6
39	139	15.12.2007	28.9	750	1115	7.46	n.a.	134	166	54.3	91.2	3.60
40	140	15.08.2007	29.6	958	1434	7.04	n.a.	222	237	60.8	95.7	3.90
41	149	15.12.2007	28.1	1127	1713	7.40	n.a.	270	259	73.4	121	5.20
42	152	15.12.2007	28.4	1707	2620	7.24	n.a.	481	401	112	170	7.30
43	154	14.12.2007	27.2	1244	1808	7.08	n.a.	290	282	73.0	127	6.10
44	165	14.12.2007	28.1	618	860	7.24	n.a.	68.1	147	36.4	86.0	2.30
45	179	14.12.2007	28.1	1260	1806	7.06	n.a.	272	307	74.1	150	5.30
46	181	14.12.2007	29.7	1152	1750	7.03	n.a.	266	274	63.5	123	4.90
47	286	14.12.2007	28.6	1182	1770	7.02	n.a.	273	271	66.4	134	5.20
48	332	16.12.2007	30.8	1016	1488	7.51	n.a.	230	186	66.4	132	6.90
49	339	16.12.2007	29.5	756	1116	7.51	n.a.	145	150	40.1	92.1	5.10
50	345	16.12.2007	29.3	935	1456	7.45	n.a.	237	164	60.8	113	8.00
51	372	16.12.2007	27.3	1279	1933	7.37	n.a.	312	290	84.6	135	5.10
52	384	16.12.2007	29.0	832	1186	7.40	n.a.	168	155	48.1	108	7.40
53	442	13.12.2007	30.8	811	1162	7.01	n.a.	165	140	49.2	95.8	5.10
54	453	15.12.2007	34.6	865	1253	6.82	n.a.	160	170	29.4	86.0	5.60
55	Has 00	18.12.2007	30.3	1013	1600	7.10	n.a.	256	157	38.5	104	10.7
56	100	13.11.2007	29.9	771	1201	7.10	n.a.	153	144	42.8	85.5	5.30
57	478	13.11.2007	29.8	971	1400	7.00	n.a.	184	287	44.1	123	4.50

Table 12.1 (continued)

No.	Well No.	Sampling Date	Mg	Na	SiO_2	Sr	HCO_3
1	84	15.08.2007	21.7	117	6.95	1.09	180
2	85	15.08.2007	25.6	180	6.56	2.11	154
3	86	15.08.2007	25.8	186	6.21	2.20	153
4	87	15.08.2007	26.3	187	5.93	1.46	161
5	88	15.08.2007	26.4	185	6.12	2.12	160
6	89	15.08.2007	30.0	161	6.13	2.50	161
7	121	15.08.2007	26.5	229	6.08	1.42	187
8	134	15.08.2007	25.0	191	5.24	1.38	150
9	139	15.08.2007	19.0	111	6.19	1.08	153
10	141	15.08.2007	30.9	163	5.83	1.28	157
11	142	15.08.2007	47.9	251	6.23	3.03	154
12	145	15.08.2007	40.9	185	6.04	2.23	158
13	146	15.08.2007	19.5	109	6.06	1.04	155
14	149	15.08.2007	31.6	187	6.30	2.12	154
15	150	15.08.2007	43.5	247	6.15	2.79	153
16	151	15.08.2007	49.9	277	6.22	3.18	151
17	152	15.08.2007	51.3	302	6.41	3.49	151
18	39	13.11.2007	36.1	171	6.35	1.49	232
19	84	13.11.2007	24.4	127	6.54	1.11	212
20	89	13.11.2007	34.9	240	6.81	1.75	166
21	121	13.11.2007	36.2	289	6.23	1.76	202
22	126	13.11.2007	42.8	309	5.82	1.95	185
23	138	13.11.2007	25.9	153	5.82	1.21	212
24	145	13.11.2007	53.1	214	6.13	1.66	220
25	151	13.11.2007	65.1	311	5.96	2.21	220
26	152	13.11.2007	64.7	334	6.73	2.41	153
27	134	13.11.2007	33.6	236	5.89	1.68	183
28	1	15.12.2007	26.0	106	6.72	1.18	190
29	9	15.12.2007	29.4	115	6.30	1.29	239
30	13	13.12.2007	28.0	103	6.10	1.13	204
31	21	15.12.2007	26.6	110	6.30	0.950	248
32	29	15.12.2007	38.1	216	5.67	1.50	240
33	32	13.12.2007	31.7	153	7.10	1.46	195
34	51	13.12.2007	33.0	213	5.87	1.61	170
35	60	13.12.2007	42.1	297	6.26	2.17	250
36	72	15.12.2007	32.9	198	5.97	1.63	175
37	79	15.12.2007	39.1	257	5.84	1.82	175
38	93	15.12.2007	41.0	172	7.31	1.17	277
39	139	15.12.2007	20.5	114	5.93	1.13	153
40	140	15.08.2007	28.9	147	5.71	1.23	150
41	149	15.12.2007	35.3	195	5.82	1.53	155
42	152	15.12.2007	58.8	307	5.94	2.19	154
43	154	14.12.2007	36.6	226	6.52	1.75	185
44	165	14.12.2007	15.3	79.8	7.23	0.919	168
45	179	14.12.2007	26.7	220	6.23	1.57	190
46	181	14.12.2007	22.0	204	5.85	1.33	180
47	286	14.12.2007	24.9	218	6.14	1.47	175
48	332	16.12.2007	27.0	161	7.04	1.75	185
49	339	16.12.2007	18.1	111	6.29	1.19	180
50	345	16.12.2007	20.9	165	6.58	1.50	151
51	372	16.12.2007	28.6	238	6.64	1.81	170
52	384	16.12.2007	19.2	130	6.62	1.32	182
53	442	13.12.2007	29.2	115	6.14	1.31	198
54	453	15.12.2007	29.5	133	6.66	1.15	236
55	Has 00	18.12.2007	24.4	171	6.42	1.35	236
56	100	13.11.2007	28.9	105	6.30	2.09	192
57	478	13.11.2007	18.7	152	6.30	1.97	144

Table 12.2: Physical and Chemical groundwater parameters of samples in the Wadi Ash Shati area (concentrations are given in mgL^{-1}, T = temperature [°C], TDS = total dissolved solids and EC= electrical conductivity [µs/cm].

Well ID	Locations	T	TDS	EC	pH	Na	Cl	SO_4	NO_3	Ca	K	Mg	HCO_3
BH-1	Ashkedah	33.1	349	800	6.80	69.6	96.1	2.80	0.60	10.7	8.40	10.8	125
BH-2	Ghira	32.1	487	720	6.90	109	151	34.5	2.15	17.1	21.2	9.70	130
BH-3	Al Afia	32.6	436	740	6.40	103	150	20.6	0.12	13.2	21.7	8.80	103
BH-4	Agar	33.5	443	710	6.55	103	144	29.1	0.66	12.9	21.7	8.90	106
BH-5	Dabwat	37.5	1080	1600	6.98	210	287	226	65.4	113	9.40	17.4	138
BH-6	Mahrouga	34.3	400	631	6.52	93.9	129	27.3	0.16	9.90	21.1	7.90	95.2
BH-7	Chazan	32.6	397	630	6.50	93.7	128	27.0	0.14	9.70	21.2	8.10	94.0
BH-8	Aloun	35.7	398	609	6.42	93.4	126	29.0	0.19	8.70	20.3	6.50	95.2
BH-9	Guttah	32.5	397	615	6.53	97.2	128	28.2	0.15	8.30	21.0	6.70	94.0

Table 12.3: Minor and trace element concentrations in the groundwater of Wadi Ash Shati area. All values in mgL^{-1}, n.a.: not analysed and bld: below limit of detection.

Well ID	Locations	Sr	Li	F	Br	Fe	Mn	Zn	Al	Ni	NH_4
BH-1	Ashkedah	0.410	0.010	0.40	1.19	2.20	0.380	0.090	0.600	0.056	0.39
BH-2	Ghira	0.330	n.a.	0.38	0.97	0.100	0.970	0.004	2.15	0.003	0.01
BH-3	Al Afia	0.300	0.010	0.33	1.07	2.60	0.270	0.003	0.120	0.001	0.37
BH-4	Agar	0.270	n.a.	0.30	0.91	2.30	0.240	0.071	0.660	0.003	0.10
BH-5	Dabwat	1.40	0.040	0.53	0.60	0.100	bld.	0.014	65.4	bld.	0.09
BH-6	Mahrouga	0.230	n.a.	0.30	0.90	2.60	0.260	0.002	0.160	bld.	0.35
BH-7	Chazan	0.240	0.010	0.33	0.90	2.30	0.250	0.001	0.140	bld.	0.50
BH-8	Aloun	0.210	n.a.	0.34	0.81	3.70	0.430	0.066	0.190	bld.	0.05
BH-9	Guttah	0.180	0.030	0.38	0.89	1.40	0.360	0.002	0.150	bld.	0.22

Table 12.4: Results of trace elements analysis of the Hasouna groundwater samples (concentrations are given in mg L^{-1}, n= samples numbers, and bld.: below limit of detection).

No.	Well ID	Sampling Date	F	Br	Li	Mn	Ni	Al	Ba	B	Cr	Sr	Se	Zn	Fe
1	84	15.8.2007	bld	0.32	0.012	bld	0.001	bld	0.048	0.195	0.004	1.09	0.03	bld	bld
2	85	15.8.2007	bld	0.14	0.036	bld	bld	bld	0.027	0.271	0.006	2.11	0.031	0.006	bld
3	86	15.8.2007	bld	0.14	0.035	bld	bld	bld	0.028	0.252	0.005	2.19	0.031	0.014	bld
4	87	15.8.2007	bld	0.17	0.039	bld	bld	bld	0.028	0.238	0.006	1.46	0.033	0.013	bld
5	88	15.8.2007	bld	bld	0.045	bld	bld	bld	0.024	0.246	0.004	2.12	0.038	0.005	bld
6	89	15.8.2007	bld	bld	0.065	bld	bld	bld	0.027	0.250	0.005	2.49	0.036	0.005	bld
7	121	15.8.2007	bld	0.65	0.013	bld	0.012	bld	0.040	0.212	0.005	1.42	0.034	bld	bld
8	134	15.8.2007	0.49	bld	0.056	0.002	bld	bld	0.022	0.238	0.003	1.38	0.033	0.013	bld
9	139	15.8.2007	0.59	0.11	0.046	bld	bld	0.006	0.029	0.242	bld	1.08	0.032	bld	bld
10	141	15.8.2007	0.58	bld	0.062	bld	bld	0.009	0.023	0.331	0.003	1.28	0.029	bld	bld
11	142	15.8.2007	bld	bld	0.088	bld	bld	0.008	0.020	0.425	0.004	3.03	0	0.028	bld
12	145	15.8.2007	bld	0.15	0.085	bld	bld	0.006	0.022	0.331	0.002	2.22	0.034	0.005	bld
13	146	15.8.2007	bld	0.12	0.047	bld	bld	0.012	0.025	0.238	0.003	1.04	0.03	bld	bld
14	149	15.8.2007	bld	0.15	0.074	bld	bld	0.007	0.031	0.248	0.003	2.12	0.04	bld	bld
15	150	15.8.2007	bld	bld	0.099	bld	bld	0.008	0.028	0.300	0.004	2.79	0.038	bld	bld
16	151	15.8.2007	bld	bld	0.122	bld	bld	0.007	0.023	0.324	0.004	3.17	0.036	bld	bld
17	152	15.8.2007	bld	bld	0.145	bld	bld	0.007	0.023	0.298	0.005	3.50	0.045	bld	bld
18	39	13.11.2007	0.47	0.31	bld	bld	bld	bld	bld	bld	bld	1.48	bld	bld	bld
19	84	13.11.2007	0.32	0.31	bld	bld	bld	bld	bld	bld	bld	1.11	bld	bld	bld
20	89	13.11.2007	0.51	0.27	bld	bld	bld	bld	bld	bld	bld	1.75	bld	bld	bld
21	121	13.11.2007	0.36	0.67	bld	bld	bld	bld	bld	bld	bld	1.75	bld	bld	bld
22	126	13.11.2007	0.37	0.32	bld	bld	bld	bld	bld	bld	bld	1.95	bld	bld	bld
23	138	13.11.2007	0.49	0.12	bld	bld	bld	bld	bld	bld	bld	1.21	bld	bld	bld
24	145	13.11.2007	0.73	0.16	bld	bld	bld	bld	bld	bld	bld	1.66	bld	bld	bld
25	151	13.11.2007	0.52	0.22	bld	bld	bld	bld	bld	bld	bld	2.21	bld	bld	bld
26	152	13.11.2007	0.41	0.25	bld	bld	bld	bld	bld	0.432	bld	2.41	bld	bld	bld
27	134	13.11.2007	0.44	0.26	0.044	0.125	bld	bld	bld	0.302	bld	1.68	bld	0.011	bld
28	1	15.12.2007	0.26	0.21	0.013	bld	bld	bld	0.023	0.330	bld	1.17	bld	0.021	bld
29	9	15.12.2007	0.36	0.23	0.022	bld	bld	bld	bld	bld	bld	1.29	bld	0.016	bld
30	13	13.12.2007	0.29	0.23	0.029	bld	bld	bld	0.029	0.251	bld	1.13	bld	0.025	0.027
31	21	15.12.2007	0.51	0.24	0.036	bld	bld	bld	bld	bld	bld	0.950	bld	0.037	bld
32	29	15.12.2007	0.60	0.34	0.056	bld	bld	bld	bld	bld	bld	1.50	0.268	0.018	bld
33	32	13.12.2007	bld	bld	0.010	bld	bld	bld	0.047	0.182	bld	1.46	bld	bld	bld
34	51	13.12.2007	bld	bld	0.065	bld	bld	bld	0.041	0.161	bld	1.61	bld	bld	0.067
35	60	13.12.2007	bld	bld	0.068	bld	bld	bld	0.045	0.168	bld	2.16	bld	bld	0.014
36	72	15.12.2007	0.48	0.34	0.055	bld	bld	bld	0.055	0.209	bld	1.63	bld	bld	bld
37	79	15.12.2007	0.45	0.29	0.073	bld	bld	0.032	0.039	0.252	bld	1.82	bld	bld	0.013
38	93	15.12.2007	0.32	0.30	0.028	bld	bld	bld	bld	0.346	bld	1.17	bld	bld	bld
39	139	15.12.2007	0.48	0.11	0.033	bld	bld	bld	0.030	0.245	bld	1.13	bld	bld	bld
40	140	15.8.2007	bld	bld	0.037	bld	bld	bld	0.031	0.273	bld	1.27	bld	bld	bld
41	149	15.12.2007	0.49	0.15	0.051	bld	bld	bld	0.034	0.262	bld	1.53	bld	bld	bld
42	152	15.12.2007	0.38	0.20	0.085	bld	bld	bld	0.025	0.287	bld	2.19	bld	bld	bld
43	154	14.12.2007	bld	bld	0.103	bld	bld	bld	0.022	0.187	bld	1.75	bld	bld	bld
44	165	14.12.2007	0.52	0.07	0.068	bld	bld	bld	0.019	0.162	bld	1.57	bld	bld	bld
45	179	14.12.2007	0.21	0.19	0.022	bld	bld	bld	0.025	0.162	bld	1.57	bld	bld	bld
46	181	14.12.2007	0.19	0.19	0.019	bld	bld	bld	0.032	0.263	bld	1.32	bld	0.027	0.014
47	286	14.12.2007	0.23	0.22	0.020	bld	bld	0.035	0.033	0.334	bld	1.47	bld	0.019	bld
48	332	16.12.2007	0.25	0.25	0.013	bld	bld	bld	0.049	0.283	bld	1.75	bld	0.018	bld
49	339	16.12.2007	0.28	0.17	bld	bld	bld	bld	0.029	0.280	bld	1.19	bld	0.012	bld
50	345	16.12.2007	0.26	0.46	bld	bld	bld	bld	0.036	0.323	0.015	1.50	0.197	0.02	bld
51	372	16.12.2007	0.21	0.26	0.018	bld	bld	bld	0.024	0.280	bld	1.80	bld	0.015	bld
52	384	16.12.2007	0.28	0.18	0.003	bld	bld	bld	0.047	0.270	bld	1.30	0.171	0.055	0.016
53	442	13.12.2007	bld	bld	0.018	bld	bld	bld	0.039	0.160	bld	1.31	bld	bld	bld
54	453	15.12.2007	0.33	0.27	0.015	bld	bld	bld	0.019	0.297	bld	1.15	bld	bld	bld
55	Has 00	18.12.2007	0.27	0.65	0.012	bld	bld	bld	0.039	0.430	bld	1.35	bld	0.017	bld
n			35	41	44	2	2	11	41	44	17	55	20	22	6

Table 12.5: The calculated saturation indexes values of the Hasouna samples, (n.a.: not analysed).

Well ID	Sampling Date	SI (Anhydrite)	SI (Aragonite)	SI (Gypsum)	SI (Calcite)	SI (Dolomite)	SI (Fluorite)	SI (Talc)	SI (Halite)
84	15.08.2007	-1.69	-0.34	-1.49	-0.20	-0.61	n.a.	-3.92	-6.31
85	15.08.2007	-1.33	-0.13	-1.13	0.01	-0.26	n.a.	-2.76	-6.01
86	15.08.2007	-1.30	-0.14	-1.11	0.00	-0.29	n.a.	-2.97	-5.96
87	15.08.2007	-1.32	-0.30	-1.13	-0.16	-0.59	n.a.	-4.06	-5.95
88	15.08.2007	-1.32	-0.15	-1.13	-0.01	-0.28	n.a.	-3.06	-5.97
89	15.08.2007	-1.28	-0.22	-1.09	-0.08	-0.38	-1.58	-3.42	-5.79
121	15.08.2007	-1.45	-0.18	-1.25	-0.04	-0.31	n.a.	-3.46	-5.72
134	15.08.2007	-1.32	-0.25	-1.12	-0.11	-0.52	-1.63	-3.89	-5.88
139	15.08.2007	-1.56	-0.45	-1.37	-0.31	-0.89	-1.55	-4.58	-6.40
141	15.08.2007	-1.40	-0.45	-1.20	-0.31	-0.77	-1.55	-4.42	-6.00
142	15.08.2007	-1.24	-0.42	-1.04	-0.28	-0.61	n.a.	-3.91	-5.65
145	15.08.2007	-1.37	-0.55	-1.18	-0.41	-0.86	n.a.	-4.68	-5.87
146	15.08.2007	-1.59	-0.31	-1.39	-0.17	-0.61	n.a.	-3.72	-6.41
149	15.08.2007	-1.36	0.04	-1.15	0.18	0.16	n.a.	-1.54	-5.89
150	15.08.2007	-1.23	0.04	-1.02	0.18	0.22	n.a.	-1.49	-5.64
151	15.08.2007	-1.18	-0.25	-0.98	-0.11	-0.33	n.a.	-3.16	-5.54
152	15.08.2007	-1.13	-0.27	-0.93	-0.13	-0.40	n.a.	-3.37	-5.45
39	13.11.2007	-1.53	-0.35	-1.34	-0.21	-0.51	-1.71	-4.72	-6.04
84	13.11.2007	-1.68	-0.48	-1.51	-0.34	-0.83	-2.11	-5.20	-6.33
121	13.11.2007	-1.35	-0.16	-1.18	-0.02	-0.19	-1.94	-3.48	-5.60
126	13.11.2007	-1.25	-0.11	-1.05	0.03	-0.09	-1.86	-3.09	-5.58
138	13.11.2007	-1.48	-0.08	-1.28	0.06	-0.12	-1.64	-3.38	-6.23
145	13.11.2007	-1.37	-0.25	-1.17	-0.11	-0.23	-1.30	-3.79	-5.85
151	13.11.2007	-1.17	-0.19	-0.96	-0.05	-0.16	-1.51	-3.84	-5.53
152	13.11.2007	-1.14	-0.31	-0.94	-0.17	-0.41	-1.74	-3.42	-5.45
134	13.11.2007	-1.34	-0.58	-1.14	-0.44	-1.08	-1.73	-5.94	-5.83
1	15.12.2007	-1.73	-0.27	-1.55	-0.13	-0.34	-2.34	-3.28	-6.46
9	15.12.2007	-1.66	-0.10	-1.48	0.03	0.00	-2.02	-3.07	-6.35
13	13.12.2007	-1.67	-0.51	-1.49	-0.38	-0.81	-2.20	-5.06	-6.42
21	15.12.2007	-1.75	-0.66	-1.57	-0.52	-1.10	-1.75	-6.34	-6.42
29	15.12.2007	-1.61	-0.30	-1.41	-0.16	-0.36	-1.51	-4.38	-5.78
32	13.12.2007	-1.56	-0.45	-1.38	-0.31	-0.72	n.a.	-4.61	-6.13
51	13.12.2007	-1.45	-0.64	-1.25	-0.50	-1.17	n.a.	-6.00	-5.83
60	13.12.2007	-1.29	-0.59	-1.09	-0.45	-1.07	n.a.	-6.77	-5.58
72	15.12.2007	-1.44	-0.19	-1.26	-0.06	-0.26	-1.70	-3.34	-5.86
79	15.12.2007	-1.34	-0.31	-1.14	-0.17	-0.49	-1.71	-4.10	-5.67
93	15.12.2007	-1.42	-0.55	-1.25	-0.41	-0.79	-2.15	-5.54	-6.11
139	15.12.2007	-1.60	-0.05	-1.40	0.09	-0.08	-1.69	-2.25	-6.43
140	15.08.2007	-1.48	-0.48	-1.28	-0.34	-0.81	n.a.	-4.41	-6.11
149	15.12.2007	-1.39	-0.05	-1.18	0.09	0.02	-1.62	-2.16	-5.91
152	15.12.2007	-1.17	-0.13	-0.96	0.01	-0.06	-1.81	-2.54	-5.49
154	14.12.2007	-1.35	-0.30	-1.14	-0.15	-0.48	n.a.	-3.97	-5.81
165	14.12.2007	-1.64	-0.24	-1.43	-0.10	-0.57	-1.61	-3.91	-6.87
179	14.12.2007	-1.25	-0.23	-1.04	-0.09	-0.55	-2.30	-4.50	-5.86
181	14.12.2007	-1.34	-0.33	-1.14	-0.19	-0.73	-2.43	-4.83	-5.90
286	14.12.2007	-1.33	-0.33	-1.12	-0.19	-0.73	-2.24	-4.76	-5.86
332	16.12.2007	-1.45	0.23	-1.26	0.37	0.45	-2.17	-1.17	-6.06
339	16.12.2007	-1.63	0.09	-1.43	0.23	0.14	-2.15	-1.94	-6.41
345	16.12.2007	-1.55	0.01	-1.35	0.15	-0.04	-2.17	-2.10	-6.03
372	16.12.2007	-1.32	-0.02	-1.11	0.12	-0.07	-2.34	-2.52	-5.77
384	16.12.2007	-1.57	0.03	-1.37	0.17	-0.02	-2.10	-2.51	-6.28
442	13.12.2007	-1.66	-0.34	-1.47	-0.20	-0.51	n.a.	-4.22	-6.35
453	15.12.2007	-1.61	-0.46	-1.44	-0.32	-0.67	-2.15	-4.84	-6.30
Has 00	18.12.2007	-1.60	-0.17	-1.41	-0.03	-0.28	-2.19	-3.94	-5.99

Table 12.6: Results of calcuations of groundwater quality in the Hasouna waterfields.

Well ID	Sampling Date	Magnesium Hazard [%]	Sodium Percentage [%]	Sodium Hazard [%]	Total Hardness
84	15.08.2007	29	46	3	305
85	15.08.2007	26	50	4	404
86	15.08.2007	26	50	4	417
87	15.08.2007	26	50	4	411
88	15.08.2007	27	50	4	411
89	15.08.2007	27	44	3	459
121	15.08.2007	30	58	5	387
134	15.08.2007	32	52	4	430
139	15.08.2007	26	45	3	302
141	15.08.2007	35	48	4	401
142	15.08.2007	37	51	5	534
145	15.08.2007	37	48	4	451
146	15.08.2007	28	45	3	291
149	15.08.2007	31	49	4	427
150	15.08.2007	33	50	5	536
151	15.08.2007	35	51	5	597
152	15.08.2007	33	51	5	636
39	13.11.2007	34	46	4	443
84	13.11.2007	30	46	3	332
89	13.11.2007	28	51	5	507
121	13.11.2007	30	56	6	486
126	13.11.2007	32	55	6	551
138	13.11.2007	28	47	3	381
145	13.11.2007	40	46	4	548
151	13.11.2007	37	49	5	721
152	13.11.2007	37	51	5	718
134	13.11.2007	30	53	5	463
1	15.12.2007	34	43	3	313
9	15.12.2007	34	42	3	352
13	13.12.2007	35	41	3	326
21	15.12.2007	35	45	3	312
29	15.12.2007	37	53	5	420
32	13.12.2007	33	46	3	395
51	13.12.2007	31	52	4	439
60	13.12.2007	31	54	5	569
72	15.12.2007	31	50	4	444
79	15.12.2007	32	53	5	509
93	15.12.2007	40	48	4	425
139	15.12.2007	27	45	3	312
140	15.08.2007	33	48	3	358
149	15.12.2007	33	49	4	447
152	15.12.2007	36	50	5	667
154	14.12.2007	32	52	5	469
165	14.12.2007	23	39	2	278
179	14.12.2007	23	50	4	484
181	14.12.2007	23	53	5	399
286	14.12.2007	24	52	5	437
332	16.12.2007	25	45	3	441
339	16.12.2007	25	45	3	305
345	16.12.2007	23	50	4	369
372	16.12.2007	26	54	5	455
384	16.12.2007	23	46	3	349
442	13.12.2007	33	42	3	359
453	15.12.2007	36	47	3	336
Has 00	18.12.2007	28	52	4	360

Table 12.7: Correlation coefficients of groundwater parameter in the study area.

	EC	TDS	pH	Cl	Na	SO_4	HCO_3	Ca	Mg	K	NO_3	Sr
EC	1.000	0.97	0.0016	0.95	0.95	0.77	0.026	0.84	0.67	0.10	0.69	0.50
TDS		1.000	0.0047	0.95	0.94	0.84	0.026	0.88	0.70	0.113	0.72	0.58
pH			1.000	0.0002	0.009	0.006	0.33	0.001	0.05	0.08	0.048	0.02
Cl				1.000	0.8904	0.75	0.044	0.77	0.65	0.11	0.67	0.58
Na					1.000	0.70	0.011	0.85	0.63	0.10	0.62	0.43
SO_4						1.000	0.167	0.75	0.5	0.03	0.73	0.63
HCO_3							1.000	0.04	0.006	0.17	0.24	0.144
Ca								1.000	0.55	0.09	0.72	0.53
Mg									1.000	0.15	0.46	0.41
K										1.000	0.004	0.03
NO_3											1.000	0.53
Sr												1.000

Table 12.8: Isotopic composition of groundwater from wells in the Hasouna area, $\delta^{15}N$, $\delta^{18}O$, and $\delta^{17}O$ values of dissolved NO_3^- are given in $^o/_{oo}$ related to atmospheric nitrogen (AIR) reference. $\Delta^{17}O$ and $xNO_{3(atm)}$: proportion of dissolved NO_3^- which is originated from atmospheric nitrogen. Groundwater samples from Tripoli area and Wadi Ash Shati waters were also represented in this table, (n.a.: not analysed).

Well No.	Sampling Date	$\delta^{18}O_{H2O}$ ‰ VSMOW	$\delta^{2}H_{H2O}$ ‰ VSMOW	$\delta^{32}S_{sulphate}$ ‰ VCDT	$\delta^{18}O_{sulphate}$ ‰ VSMOW	$\delta^{15}N$ ‰ AIR	$\delta^{18}O$ ‰ AIR	$\delta^{17}O$ ‰ AIR	$\Delta^{17}O$	$xNO_{3(atm)}$
84	15.8.2007	n.a.	n.a.	n.a.	n.a.	n.a.	n.a.	n.a.	n.a.	n.a.
85	15.8.2007	-9.4	-70.0	n.a.	n.a.	n.a.	n.a.	n.a.	n.a.	n.a.
86	15.8.2007	-9.5	-70.1	n.a.	n.a.	n.a.	n.a.	n.a.	n.a.	n.a.
87	15.8.2007	-9.5	-70.7	n.a.	n.a.	n.a.	n.a.	n.a.	n.a.	n.a.
88	15.8.2007	-9.6	-70.8	n.a.	n.a.	n.a.	n.a.	n.a.	n.a.	n.a.
89	15.8.2007	n.a.	n.a.	n.a.	n.a.	n.a.	n.a.	n.a.	n.a.	n.a.
121	15.8.2007	-9.4	-69.4	n.a.	n.a.	n.a.	n.a.	n.a.	n.a.	n.a.
134	15.8.2007	-9.6	-71.2	n.a.	n.a.	n.a.	n.a.	n.a.	n.a.	n.a.
139	15.8.2007	-10.1	-73.4	n.a.	n.a.	n.a.	n.a.	n.a.	n.a.	n.a.
141	15.8.2007	-9.5	-70.5	n.a.	n.a.	n.a.	n.a.	n.a.	n.a.	n.a.
142	15.8.2007	-9.3	-69.9	n.a.	n.a.	n.a.	n.a.	n.a.	n.a.	n.a.
145	15.8.2007	n.a.	n.a.	n.a.	n.a.	n.a.	n.a.	n.a.	n.a.	n.a.
146	15.8.2007	-10.0	-73.5	n.a.	n.a.	n.a.	n.a.	n.a.	n.a.	n.a.
149	15.8.2007	-9.7	-72.3	n.a.	n.a.	n.a.	n.a.	n.a.	n.a.	n.a.
150	15.8.2007	-9.3	-70.1	n.a.	n.a.	n.a.	n.a.	n.a.	n.a.	n.a.
151	15.8.2007	n.a.	n.a.	n.a.	n.a.	n.a.	n.a.	n.a.	n.a.	n.a.
152	15.8.2007	-9.1	-70.0	n.a.	n.a.	n.a.	n.a.	n.a.	n.a.	n.a.
13	13.11.2007	-9.7	-73.2	n.a.	n.a.	9.1	6.9	4.1	0.5	2.0
39	13.11.2007	-9.7	-72.0	9.0	9.0	8.5	13.4	9.5	2.5	10.1
84	13.11.2007	-9.8	-69.0	9.6	9.4	8.9	7.6	4.9	0.9	3.8
89	13.11.2007	-9.5	-69.5	10.9	11.7	7.2	12.3	10.9	4.5	18.0
121	13.11.2007	-9.4	-68.3	9.3	9.2	8.3	10.4	7.4	2.2	8.0
126	13.11.2007	-9.2	-69.5	11.0	11.3	6.9	15.0	12.8	5.0	20.0
138	13.11.2007	-9.9	-71.6	11.1	10.3	7.2	13.6	9.7	2.6	10.5
145	13.11.2007	-9.5	-69.8	10.3	9.6	7.1	14.7	11.3	3.7	14.6
151	13.11.2007	-9.3	-68.0	10.1	10.6	7.0	17.4	13.7	4.7	18.6
152	13.11.2007	n.a.	n.a.	10.2	10.6	7.5	14.8	12.4	4.8	17.6
134	13.11.2007	-9.6	-70.4	11.0	11.2	6.6	16.1	12.6	4.2	16.9
1	15.12.2007	-9.6	-70.2	n.a.	n.a.	n.a.	n.a.	n.a.	n.a.	n.a.
9	15.12.2007	-9.7	-71.3	n.a.	n.a.	n.a.	n.a.	n.a.	n.a.	n.a.
13	13.12.2007	-9.7	-70.7	n.a.	n.a.	n.a.	n.a.	n.a.	n.a.	n.a.
21	15.12.2007	-9.7	-72.2	n.a.	n.a.	n.a.	n.a.	n.a.	n.a.	n.a.
29	15.12.2007	-9.5	-70.7	n.a.	n.a.	n.a.	n.a.	n.a.	n.a.	n.a.
32	13.12.2007	-9.7	-71.8	n.a.	n.a.	8.4	8.3	6.1	1.8	7.1
51	13.12.2007	-9.2	-67.6	n.a.	n.a.	7.9	10.4	8.0	2.6	10.4
60	13.12.2007	-8.8	-65.6	n.a.	n.a.	7.4	11.7	10.0	3.9	15.7
72	15.12.2007	-9.5	-67.0	n.a.	n.a.	7.4	13.5	10.7	3.7	14.7
79	15.12.2007	-9.4	-69.7	n.a.	n.a.	n.a.	n.a.	n.a.	n.a.	n.a.
93	15.12.2007	-9.5	-71.1	n.a.	n.a.	9.2	10.6	6.2	0.9	3.3
139	15.12.2007	-10.0	-73.1	n.a.	n.a.	7.1	11.9	8.9	2.8	10.4
149	15.12.2007	-9.7	-69.0	n.a.	n.a.	7.1	15.4	12.1	4.1	16.4
152	15.12.2007	-9.2	-67.5	n.a.	n.a.	7.5	14.8	12.4	4.7	18.8
154	14.12.2007	-9.3	-67.4	n.a.	n.a.	8.6	16.4	11.1	2.6	10.3
165	14.12.2007	-9.9	-72.8	n.a.	n.a.	7.7	9.8	6.1	1.0	4.0
179	14.12.2007	-9.3	-68.3	n.a.	10.5	8.0	10.9	7.6	1.9	7.7
181	14.12.2007	-9.1	-69.3	n.a.	n.a.	8.7	10.6	7.6	2.1	8.4
286	14.12.2007	-9.2	-68.8	n.a.	n.a.	8.5	12.9	9.1	2.4	9.6
372	16.12.2007	-9.1	-64.6	n.a.	n.a.	8.9	10.2	7.2	1.9	7.6
384	16.12.2007	n.a.	n.a.	n.a.	n.a.	8.6	8.1	5.7	1.5	6.0
442	13.12.2007	-9.7	-72.0	n.a.	n.a.	8.4	9.8	5.5	0.4	1.6
453	15.12.2007	-9.6	-70.3	n.a.	n.a.	8.6	9.1	5.8	1.1	4.3
478	13.11.2007	n.a.	n.a.	n.a.	n.a.	7.8	9.1	6.5	1.8	7.1
100	13.11.2007	n.a.	n.a.	n.a.	n.a.	8.5	7.6	4.7	0.7	3.0
Ash Shati 1	17.9.2009	-11.0	-78.3	n.a.	n.a.	n.a.	n.a.	n.a.	n.a.	n.a.
Ash Shati2	17.9.2009	-11.2	-82.7	n.a.	n.a.	n.a.	n.a.	n.a.	n.a.	n.a.
Ash Shati 3	17.9.2009	-11.1	-82.3	n.a.	n.a.	n.a.	n.a.	n.a.	n.a.	n.a.
Ash Shati 4	17.9.2009	-11.1	-82.0	n.a.	n.a.	n.a.	n.a.	n.a.	n.a.	n.a.
Ash Shati 5	17.9.2009	-10.1	-74.8	n.a.	n.a.	n.a.	n.a.	n.a.	n.a.	n.a.
Ash Shati 6	17.9.2009	-10.9	-82.0	n.a.	n.a.	n.a.	n.a.	n.a.	n.a.	n.a.
Ash Shati 7	17.9.2009	-11.1	-82.3	n.a.	n.a.	n.a.	n.a.	n.a.	n.a.	n.a.
Ash Shati 8	17.9.2009	-11.2	-87.5	n.a.	n.a.	n.a.	n.a.	n.a.	n.a.	n.a.
Ash Shati 9	17.9.2009	-10.9	-81.6	n.a.	n.a.	n.a.	n.a.	n.a.	n.a.	n.a.
Tripoli 31	17.9.2009	-6.4	-42.4	n.a.	n.a.	n.a.	n.a.	n.a.	n.a.	n.a.
Tripoli 32	17.9.2009	-5.1	-33.9	n.a.	n.a.	n.a.	n.a.	n.a.	n.a.	n.a.
Tripoli 33	17.9.2009	-5.9	-35.5	n.a.	n.a.	n.a.	n.a.	n.a.	n.a.	n.a.
Tripoli 34	17.9.2009	-5.4	-30.5	n.a.	n.a.	n.a.	n.a.	n.a.	n.a.	n.a.
Tripoli 35	17.9.2009	-4.7	-29.2	n.a.	n.a.	n.a.	n.a.	n.a.	n.a.	n.a.
Tripoli 36	17.9.2009	-5.1	-32.4	n.a.	n.a.	n.a.	n.a.	n.a.	n.a.	n.a.
Tripoli 38	17.9.2009	-5.7	-33.5	n.a.	n.a.	n.a.	n.a.	n.a.	n.a.	n.a.
Tripoli 39	17.9.2009	-5.7	-36.0	n.a.	n.a.	n.a.	n.a.	n.a.	n.a.	n.a.
Tripoli 40	17.9.2009	-5.6	-34.9	n.a.	n.a.	n.a.	n.a.	n.a.	n.a.	n.a.

12.3 LIST OF ABSTRACTS AND PUBLICATIONS

Abdalla, R., Leis, A., Dietzel, M., Köhler, S.J., Böttcher, M.E., Savarino, J, Morin, S. Hydrochemical and isotopic characterisation of deep groundwater reservoirs in the Sahara desert. EGU General Assembly 2009, held 19-24 April, 2009 in Vienna, Austria http://meetings.copernicus.org/egu2009, p.8958.

Leis, A., Dietzel, M., **Abdalla, R.,** Savarino, J., Böttcher, M.E., Köhler, S. J.: Tracing the origin of nitrate accumulation in deep groundwater reservoir in the Sahara desert using mass dependent and non-mass-dependent isotopic signatures. EGU General Assembly 2010, held 2-7 May, 2010 in Vienna, Austria, p.10932.

Abdalla, R., Rinder, T., Dietzel, M., Leis, A.: Seawater Intrusion and groundwater quality of the coastal area in Tripoli region, Libya. – In: EGU (2010), p. 11911.

Abdalla, R., Rinder, T., Dietzel, M., Leis, A.: Quality of groundwater in the shallow and deep aquifers of the Gefara Plain, Tripoli region, Libya. – In: Groundwater Quality Sustainability, Extended Abstracts (2010), p. 2182.

Rinder, T., Dietzel, M., Spatzenberger, J., **Abdalla, R**.: Calcium carbonate cementation of unconsolidated materials - An experimental approach. – in: EGU 2010. (2010), p. 12395.

Martin Dietzel, Albrecht Leis, **Rashid Abdalla**, Joel Savarino, Samuel Morin, Michael E. Böttcher, and Stephan Köhler, 2012: Tracing atmospheric nitrate in paleo groundwater of Saharan desert using its ^{17}O-excess (review), Journal Geochim. Cosmochim. Acta.